UNIVERSITAT POLITÈCNICA
DE CATALUNYA
BARCELONATECH

Ph.D. in Electronic Engineering

Design and Characterization of Wearable Antenna Sensors for Healthcare Applications

Doctoral thesis by
Mariam El Gharbi

Supervised by
Dr. Ignacio Gil Galí
Dr. Raúl Fernández García

Barcelona, June 2023

Acknowledgement

I would like to express my deepest appreciation to my supervisor Prof. Ignacio Gil for providing me with the opportunity to begin the PhD degree. His knowledge, motivation and continuous help during these years have been vital in the completion of this thesis. I appreciate our meeting conversations from fundamental physics to more potential topics. I am really grateful for his guidance throughout this journey.

I am grateful to my co-supervisor Prof. Raúl Fernández García for his invaluable guidance, and expertise throughout the duration of this thesis. I appreciate his support in research knowledge and paper writing. For each of my published articles, he helped me review them very carefully.

In our lab, I would like to express my sincere gratitude and appreciation to my friend Marc. His dedication, expertise, and support are invaluable throughout our time working together. Additionally, I want to recognize his exceptional knowledge and expertise in textile field. His deep understanding of the subject matter and his innovative thinking have greatly enhanced my research and experiments.

Another very nice friend I need to keep in heat forever is Cheng yang Luo. I would like to extend my heartfelt appreciation for his friendship. His kindness, sense of humor, and approachable nature have made the lab feel like a welcoming and supportive community. It is a privilege to have such a wonderful colleague and friend.

I would like to take a moment to express my deepest appreciation and gratitude to my friends Soukaina, Sanae, Youness and Moustapha. Throughout the journey of life, they have been a constant source of support, encouragement, and inspiration. Their presence has enriched my life in countless ways, and I am truly blessed to have them by my side.

Finally, thanks must also go to all my family, especially to my parents, Mohammed and Rachida, and my sister Ahlam for the endless love and sup-

port they have given to me. Thank you for being so patient, understanding me always, and for the support you have given to me throughout my life.

Summary

Wearable antenna sensors are a promising technology for developing new applications in the healthcare field since textiles are widely used by everyone due to the maturity of textile manufacturing. According to the last decade's market behavior, it is expected that consumers will claim smaller and more intelligent communications systems which will improve their quality of life. In this respect, wearable antenna sensor technology is one of the key implementations of the future smart clothes field and they may find their place in our daily life. Currently, the researches on wearable antenna sensors are receiving increasing interest while wearable antenna sensors on textile have less research, thus it is a novelty and motivation of this thesis. This thesis deals with challenges regarding wearable antenna sensor design, characterization, and measurements on textile.

Based on the analysis of the current state of the art, there are several new research that merits to be explored, thus generating the specific objectives of this thesis. The first objective is to develop new textile antenna sensors with high performance including low profile, high sensitivity, low cost, and high durability; the second objective is to explore wearable antenna-based sensors that can be used for body signal/healthcare monitoring and communication purposes; the third objective is to test the performance of the antenna sensor in real-world scenarios, such as breathing monitoring, and the fourth objective is to develop antenna sensors that can be integrated into clothing for breathing monitoring combined with other commercial electronic components, such as Bluetooth/WIFI transmitter.

For achieving the first objective, an embroidered fully textile antenna-based sensor is proposed to detect various concentrations of salt and sugar using microwave signals. Different concentrations of salt and sugar are identified through variations in frequency shifts and magnitude levels observed in reflection coefficient measurements. In addition, the rinsing reliability valida-

tion measurements are performed. The proposed sensor offers high sensitivity and compact size. To achieve the second objective, a textile antenna sensor for in vitro diagnostics of diabetes for monitoring blood glucose levels is proposed. The experiments are performed to detect different diabetic conditions including hypoglycemia, normoglycemia, and hyperglycemia. To attain the third objective, a new embroidered meander dipole antenna-based sensor for real-time breath detection using the technique based on chest well movement analysis is proposed. For the fourth objective, an embroidered antenna-based sensor is integrated into the T-shirt to demonstrate the sensing mechanism based on the detection of different breathing patterns through the resonance shift frequency and the received signal strength indicator (RSSI) using a Bluetooth transmitter. The results show a good sensing performance and its ability to detect and monitor different breathing patterns.

This thesis has been developed at RFLEX (Radio Frequency Identification and Flexible Electronics) group, which is part of the Electronic Engineering Department at UPC partially supported by projects: TEC2016-79465-R, TED2021-131209B-I0, and PID2021-124288OB-I0. This Ph.D. thesis has been written as a Compendium of articles, five articles indexed in the Journal Citation Report are already published and one additional is under submission, which are included as an annex in this thesis.

Keywords – Antenna-based sensors, embroidered textile, frequency shift, microwave sensing, breathing patterns, wearable system, e-textile, breathing monitoring.

Resumen

Los sensores de antena portátiles son una tecnología prometedora para el desarrollo de nuevas aplicaciones en el campo de la salud, ya que los textiles son ampliamente utilizados por todos debido a la madurez de los métodos de fabricación textil. De acuerdo con el comportamiento del mercado de la última década, se espera que los consumidores reclamen sistemas de comunicaciones más pequeños e inteligentes que mejoren su calidad de vida. En este sentido, la tecnología de sensor de antena portátil es una de las implementaciones clave del futuro campo de la ropa inteligente y puede encontrar su lugar en nuestra vida diaria. Actualmente, las investigaciones sobre sensores de antena portátiles están recibiendo un interés creciente, mientras que los sensores de antena portátiles en textiles han sido sometidos a menor investigación, por lo que es una novedad y motivación de esta tesis. Esta tesis aborda los desafíos relacionados con el diseño, la caracterización y las mediciones de sensores antena portátiles.

En base al análisis del estado del arte actual, hay varias investigaciones nuevas que merecen ser exploradas y que constituyen los objetivos específicos de esta tesis. El primer objetivo es desarrollar nuevos sensores de antena textil con alto rendimiento que incluyan bajo perfil, alta sensibilidad, bajo costo y alta durabilidad; el segundo objetivo es explorar sensores portátiles basados en antenas que se puedan integrarse en la ropa para propósitos de comunicación y monitoreo de señales corporales/salud; el tercer objetivo es probar el rendimiento del sensor de antena en escenarios del mundo real, como el control de la respiración, y el cuarto objetivo es desarrollar sensores de antena que se puedan integrar en la ropa para para monitorear la respiración junto con otros componentes electrónicos comerciales, como el transmisor Bluetooth/WIFI.

Para lograr el primer objetivo, se propone un sensor basado en una antena totalmente textil bordado para detectar diferentes concentraciones de sal y

azúcar utilizando señales de microondas. Las diferentes concentraciones de sal y azúcar se identifican a través de variaciones en los cambios de frecuencia y los niveles de magnitud observados en las mediciones del coeficiente de reflexión. Además, se realizan las medidas de validación de la fiabilidad del enjuague. El sensor propuesto ofrece alta sensibilidad y tamaño compacto. Para lograr el segundo objetivo, se propone un sensor de antena textil para el diagnóstico in vitro de diabetes para monitorear los niveles de glucosa en sangre. Los experimentos se realizan para detectar diferentes condiciones diabéticas que incluyen hipoglucemia, normoglucemia e hiperglucemia. Para lograr el tercer objetivo, se propone un nuevo sensor basado en una antena dipolo de meandro bordado para la detección de la respiración en tiempo real utilizando la técnica basada en el análisis del movimiento del pecho. Para el cuarto objetivo, se integra un sensor basado en antena bordado en la camiseta para demostrar el mecanismo de detección basado en la detección de diferentes patrones de respiración a través de la frecuencia de cambio de resonancia y el indicador de intensidad de la señal recibida (RSSI) usando un transmisor Bluetooth. Los resultados muestran un buen rendimiento de detección y su capacidad para detectar y monitorear diferentes patrones de respiración.

Esta tesis ha sido desarrollada en el grupo RFLEX (Identificación por Radio Frecuencia y Electrónica Flexible), que forma parte del Departamento de Ingeniería Electrónica en la UPC apoyado parcialmente por los proyectos: TEC2016-79465-R, TED2021-131209B-I0, y PID2021-124288OB-I0. Esta tesis doctoral se ha escrito bajo la modalidad de compendio de artículos. Cinco artículos indexados en el Journal Citation Report ya están publicados y uno adicional está en proceso de presentación, los cuales se incluyen como anexo en esta tesis.

Palabras clave- sensores basados en antenas, tejido bordado, cambio de frecuencia, detección de microondas, patrones de respiración, sistema portátil, tejido electrónico, monitorización de la respiración.

Contents

List of Figures

List of Tables

Publications included in this thesis

This part shows the list of papers of international journals and conferences that are published in the scope of this thesis.

(Listed by the following order: Authors, "full title", Publication, JCR position, Impact factor, Number of citations, (Year))

Journal publications

- Mariam El Gharbi, Raúl Fernández-García, Saida Ahyoud and Ignacio Gil, "A Review of Flexible Wearable Antenna Sensors: Design, Fabrication Methods, and Applications", Materials, Q1,3.623, 68, (2020).

- Mariam El Gharbi, Raúl Fernández-García and Ignacio Gil, "Textile Antenna-Sensor for In Vitro Diagnostics of Diabetes", Electronics, Q2, 2.690, 2, (2021).

- Mariam El Gharbi, Raúl Fernández-García and Ignacio Gil, "Determination of Salinity and Sugar Concentration by Means of a Circular-Ring Monopole Textile Antenna-Based Sensor", IEEE Sensors Journal, Q1, 4.325, 8, (2021).

- Mariam El Gharbi, Raúl Fernández-García and Ignacio Gil," Embroidered wearable Antenna-based sensor for Real-Time breath monitoring", Measurement, Q1, 5.131,10, (2022).

- Mariam El Gharbi, Raúl Fernández-García and Ignacio Gil, "Wireless Communication Platform Based on an Embroidered Antenna-Sensor for Real-Time Breathing Detection", Sensors, Q2, 3.847, (2022).

- Mariam El Gharbi, Maurizo Bozzi, Raúl Fernández-García and Ignacio Gil, "Embroidered Circular Cavity Antenna Sensor in SIW Technology for Liquids' Characterization", Sensors, **To be submitted**

Conferences

- Mariam El Gharbi, Raúl Fernández-García, and Ignacio Gil. "Breathing pattern characterization based on wireless e-textile antenna-sensor for respiratory disease surveillance." In 2023 17th European Conference on Antennas and Propagation (EuCAP), pp. 1-4. IEEE, 2023

Other publications of the author related but not included in this thesis

- Yilmazer, Nuri, Mariam El Gharbi, Raul Fernandez-Garcia, and Ignacio Gil. "Mutual coupling reduction in a textile ultra-wide band MIMO antenna." The Journal of The Textile Institute (2023): 1-11.

- Mariam El Gharbi, Marc Martínez-Estrada, Raúl Fernández-García, Saida Ahyoud, and Ignacio Gil. "A novel ultra-wide band wearable antenna under different bending conditions for electronic-textile applications." The Journal of The Textile Institute 112, no. 3 (2021): 437-443.

- Mariam El Gharbi, Saida Ahyoud, Noura Aknin, Ignacio Gil and Raúl Fernández-García, "Analysis on the Effects of the Human Body on the Performance of Wearable Textile Antenna in Substrate Integrated Waveguide Technology," 2020 Global Congress on Electrical Engineering (GC-ElecEng), Valencia, Spain, 2020, pp. 51-55.

1

Introduction

The industrial and academic world have generated a lot of interest in the field of wearable and flexible electronics in recent years. Flexible electronics, whose mechanical properties include to be wrinkled, bent, and stressed/collapsed, would considerably extend the applications of modern electronic devices to multiple real non-flat scenarios, including the shape of the human body. As a consequence, flexible electronics combined with textile materials offer many advantages that make them an attractive technology for boosting the next generation of consumer electronics, among them are low-cost manufacturing, inexpensive flexible substrates, lightweight, and ease of fabrication. Recently, much interest has been focused on antenna sensors due to their simple configuration, multimodality sensing, passive operation, and low cost. Antenna sensors are electronic devices with dual functionality for communicating and sensing, and they can be implemented by minimizing the number of components. The operating principle of antenna sensors is demonstrated by their geometrical or intrinsic material change influence in terms of their antenna resonance frequency, which is evaluated by means of the impact on the return loss and the S-parameters (S_{11}). In addition, antenna sensors have evolved as another process to measure diverse physical parameters such as pressure, temperature, motion, humidity, strain, snow, and gas.

Wearable antenna sensors refer to integrating an antenna with a sensing function onto wearable textiles, such as clothing or accessories, to monitor various physiological and environmental parameters. These sensors are designed to be flexible, comfortable, and unobtrusive, making them ideal for various applications such as health monitoring, military, space, emergency, sports, and fitness. Figure 1.1 depicts the general concept of using antenna-based sensors to monitor parameters of interest for wearable applications [1]. In fact, the flexible electronics global market is expected to reach 56.27 $ billion in 2027 [2]. As a result, wearable antenna sensors open up a new horizon of bendable/flexible devices for new applications.

Textile wearable antenna sensors use a combination of conductive materials and textile fibers or flexible dielectric substrates to create the antenna structure. The conductive materials can be metallic, such as copper or silver, or non-metallic, such as conductive polymers or carbon nanotubes. These materials are then integrated onto the textile substrate using techniques such as embroidery, weaving, or printing.

Antenna sensors can be designed to detect a variety of signals, including electromagnetic radiation, temperature, pressure, and humidity. These signals can be transmitted wirelessly to a receiver for real-time monitoring and analysis. Textile wearable antenna sensors have the potential to revo-
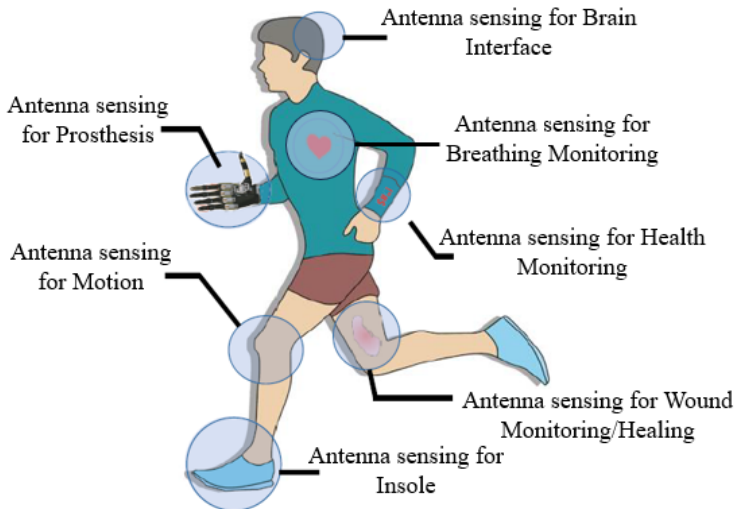
Figure 1.1: Illustration of using antenna sensors to monitor parameters of interest for wearable applications.

lutionize the way we monitor and manage our health and well-being. They can provide continuous, non-invasive monitoring of vital signs, such as heart rate and respiratory rate, and can be used to detect early warning signs of medical conditions. They can also be used to monitor environmental factors, such as air quality and temperature, to improve safety and comfort in various scenarios.

Overall, textile wearable antenna sensors represent a promising area of research and development, with the potential to create new opportunities for healthcare, leisure/sports, industry, and military applications.

1.1 Motivations and Objectives

Up to now, antenna sensors are used for many applications, such as agricultural activities and gardening, structural health, biomedical sensing, food quality monitoring, and so on, which are mostly designed on rigid materials. Several researches have already been reported in the literature using rigid materials for different types of antenna sensors, including temperature sensing [3], crack sensing [4], strain sensing [5], and dielectric sensing [6], but applications based on other features and materials are expected to be explored. In fact, one of the main objectives of the thesis is to explore useful textile antenna sensors with novel functions and wearable materials. Nowadays, the research on wearable antenna sensors are receiving increasing interest. Figure 1.2represents a comparison of the number of publications in the areas of wearable sensors, wearable antenna, and antenna sensors, including all the articles in different fields for JCR journals. From 2010 onwards, an exponential growth is observed concerning the demand for antenna-based sensors research. This trend is expected to continue or even increase in the coming years as an emerging solution for the challenges expected in multi-sensory wearable devices. In particular wearable antenna sensors on textile and flexible substrates have been barely researched in comparison with conventional materials. Thus, this is a novelty and motivation for this thesis. Wearable antenna sensors are a rapidly growing field with a wide range of potential applications, from healthcare and sports to military and industrial settings. However, developing such sensors presents several significant challenges. Some of the challenges and expected research outputs for developing textile wearable antenna sensors are summarized in Figure 1.3.

Overall, the objectives of developing textile wearable antenna sensors are to provide a comfortable and convenient way to monitor vital signs and track physical activity, improve biometric monitoring, increase mobility, and enable
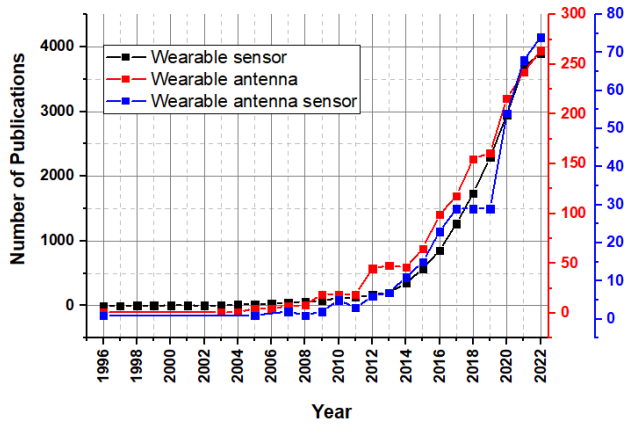
Figure 1.2: The total number of publications in the areas of wearable antenna, wearable sensor and antenna sensor in the last 27 years. Source: Web of Science.
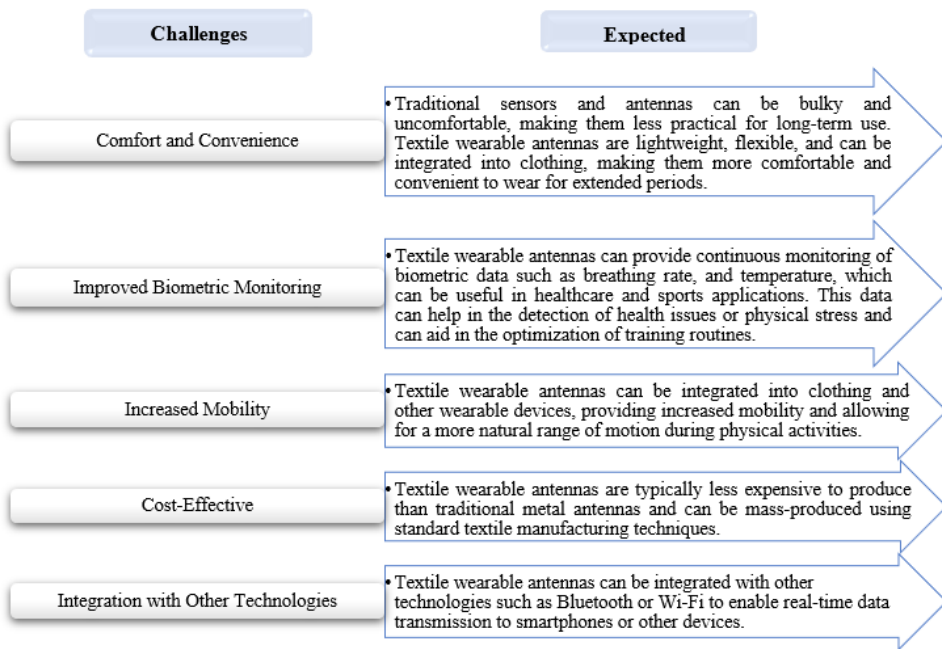
Figure 1.3: Challenges and expected research outputs for developing textile wearable antenna sensors.

integration with other technologies, while remaining cost-effective. Therefore, the objectives of this PhD thesis are listed as follows:

- Objective 1: Develop new textile antenna-based sensors with high performance: low profile and area, high sensitivity, low cost, and high durability.

- Objective 2: Explore wearable antenna-based sensors that can be integrated into clothing for body signal/healthcare monitoring and communication purposes.

- Objective 3: Test the performance of the antenna sensor in real-world scenarios, such as breathing monitoring and blood glucose level.

- Objective 4: Develop an antenna-based sensor to be integrated with other commercial electronic components, such as Bluetooth/WIFI transmitter.

1.2 Structure of the thesis

This thesis is focused on investigating novel wearable antenna-based sensor structures deployed on textiles substrates for healthcare monitoring. The aim of the research thesis is to facilitate and offer new possibilities in the development of smart textiles and their application in the field of wearable devices. The present thesis addresses the design, simulation and characterization of antenna-based sensors which serve the dual function of sensing and communicating using manufacturing textile techniques. It will be explained how one can use textiles to develop new antenna-based sensors using materials such as conductive threads, produced by available textile technology. Overall, this thesis can contribute to the growing field of wearable technology and provide new insights into how we can use wireless sensors to improve our lives and the world around us.

This Ph.D. thesis has been written as a Compendium of articles, which means that all the results presented over this report thesis have been already published in international JCR journals and conference proceedings. Furthermore, another research paper is under submission. The list of published Journal articles and conference proceedings are summarized in the Section Publications included in this thesis.

The organization and content of the thesis are as follows:

Chapter 1 is the present introduction to the thesis which is aimed at the motivations and objectives, including the addressed challenges and potential expected outputs. In addition, the structure and organization of the manuscript are detailed. Finally, the research group where the thesis has been developed as well as the projects and grants funding this thesis are described.

Chapter 2 presents an extensive review on wearable antenna-based sensors. The operating principle and the classification of antenna sensors are presented. Furthermore, the implementation of antenna-based sensors including rigid and textile antenna sensors are proposed. The influence of the body when the antenna is worn, the bending effects and Specific Absorption Rate (SAR) are covered. Besides, challenges and opportunities to improve the performance of wearable antenna sensor are addressed.

Chapter 3 introduces a survey and analysis of the textile materials and their EM characteristics (dielectric and conductive materials), different manufacturing techniques of wearable antenna sensors and also the numerical method to simulate various antenna sensor. In addition, the main antenna sensor characterization techniques and methods are discussed.

Chapter 4 is the most important part of this thesis, which describes the research and development of different proposed textile antenna sensors for healthcare applications as well as their applications in real scenarios. This chapter contains: a textile antenna sensor for in vitro diagnostics of diabetes for monitoring blood glucose levels. Furthermore, a novel antenna-based sensor is proposed to demonstrate for the first time the capability of a fully-textile antenna sensor to detect different amounts and concentrations of salt and sugar using microwave signals. Along this chapter, a novel kind of antenna-based sensors which combines the benefits of textile substrates with the advantages of SIW technology is presented for liquid characterization. Last but not least, a wearable stretching T-shirt is proposed in this chapter to explain the sensing mechanism based on the detection of different breathing patterns through the resonance shift frequency and the received signal strength indicator (RSSI). This research is supported by "TELEBREATH", a project which focuses on the application of electronic textile sensors for monitoring and control of respiratory diseases for elderly and vulnerable people.

Chapter 5 summarizes the main conclusion of the presented research work and provides future directions for taking the current work forward.

The work conducted during the realization of this thesis, from 2020 to 2023, is carried out within the group RFLEX (Radio Frequency Identification and Flexible Electronics), which is part of the Electronic Engineering

department at the Universitat Politècnica de Catalunya (Campus de Terrasa).

RFLEX is also associated with the INTEXTER (Institute of Textile Research and Industrial Cooperation of Terrassa). The aim of the RFLEX group is to research, study, design and test all kinds of electronic systems using flexible substrates, such as fabrics, paper and polymers.

2

State of the art

Ref A: El Gharbi, M., Fernández-García, R., Ahyoud, S., & Gil, I. (2020). A review of flexible wearable antenna sensors: design, fabrication methods, and applications. Materials, 13(17), 3781.

2.1   Introduction

This chapter presents an overview of wearable antenna sensors state of the art providing readers with a survey of different areas and applications of wearable antenna-based sensors. The operating principle and the classification of available antenna-based sensors in the literature will be discussed. The substrate implementation including rigid and textile antenna-based sensors are also presented. In addition, the influence of the body when the antenna is worn, the bending effects, and Specific Absorption Rate (SAR) are covered. Besides, discussion of research challenges of wearable antenna sensors will be presented.

2.2 Overview of wearable antenna sensors

Wearable antenna sensors have been in development since the 1990s. The first generation of these sensors are primarily used for military applications, such as tracking and communications for soldiers in the field. In the early 2000s, wearable antenna sensors began to be used in the medical field, particularly for remote monitoring of patients. These sensors are designed to be attached to the body and measure various physiological signals, such as heart rate and blood pressure. As technology advanced, wearable antenna sensors became more sophisticated, with the ability to transmit data wirelessly to a central monitoring station or to a smartphone app. They also became more widely available for consumer use, with applications in fitness tracking and sports performance monitoring.

In recent years, there has been a growing interest in the use of wearable antenna sensors for applications in the Internet of Things (IoT), where they can be used to collect data in real time from a range of sources and transmit it to other devices for analysis and processing. Furthermore, wearable antenna sensors are a type of electronic devices that combine the functionality of both antennas and sensors to enable wireless communication and sensing capabilities in a compact, wearable form factor. Wearable antenna sensors can be used in a wide range of applications, including healthcare, sports and fitness, safety and security, and industrial monitoring, among others. They offer several advantages, such as non-invasiveness, comfort, portability, and ease of integration into everyday life. The key components of wearable antenna sensors include the antenna itself, which is responsible for transmitting and receiving wireless signals, and the sensor, which collects data from the user/wearer or the environment. These sensors need to be flexible, lightweight, and comfortable to wear for extended periods without causing discomfort or hindering the wearer's movements.

Wearable antenna sensors can enable a wide range of sensing capabilities, such as physiological monitoring (e.g., heart rate, temperature, respiratory rate) [7], motion tracking (e.g., acceleration, rotation), environmental sensing [8] and location tracking (e.g., GPS, RFID) [9], among others. The data collected by wearable antenna sensors can be processed locally on the device itself or transmitted wirelessly to other devices or systems for further analysis, storage, or action. This data can be used for various purposes, such as health monitoring, sports performance tracking, safety and security applications, and industrial process optimization. Overall, wearable antenna sensors represent a growing area of research and development with immense potential
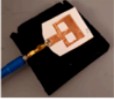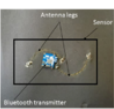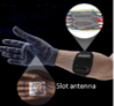
Applications	Examples	Ref
Sweat analysis	Wearable antenna sensors for biochemical sweat analysis	(a)
Breathing rate	Wearable antenna based sensor for real-time breath detection	(b)
Motion detection	Antenna based sensor for wireless human motion detection and structural health monitoring	(c)
Muscle electrical activity	Wearable comprehensive capture and analysis of muscle activity during human locomotion	(d)
Blood levels	Wearable antenna sensor for blood glucose monitoring	(e)

Figure 2.1: Areas and applications of wearable antenna sensors, (a) [10],(b) [11],(c) [12],(d) [13] and (e) [14].

for numerous applications. They offer unique advantages in terms of comfort, portability, and integration into everyday life, making them a promising technology for the future of wearable computing and the Internet of Things (IoT). Figure 2.1 shows some of the areas and applications of wearable antenna sensors. An antenna-based sensor for sweat monitoring is presented as shown in Figure 2.1 (a) [10], The patch antenna sensor used a cellulose filter paper substrate, which is capable of absorbing liquids, such as sweat on the skin. In this paper, the feasibility of sweat detection is validated by artificial sweat and salt solutions measurements, in which the frequency mainly shifted with changing NaCl (sodium chloride) concentration (8.5–200 mmol/L). The proposed system demonstrates for the first time the capability of microwave signals to detect sweat using a paper substrate, but certainly, some important validation measurements such as bending, environment impacts, and washing for performance and reliability need to be considered.

In the medical field, many common wearable antenna sensors on rigid and flexible substrates have been presented and applied for commercial healthcare monitoring applications. Furthermore, textile antenna sensors for healthcare

applications are still in the early stages and most investigations are at the stage of laboratory research. For instance, A T-shirt based on an antenna sensor is proposed for real-time breathing monitoring as shown in Figure 2.1(b) [11]. In this work, the sensor is a spiral antenna made by a multi-material metal glass–polymer fiber emitting and receiving at 2.4 GHz, which is integrated into a standard T-shirt. The paper demonstrates the capability of the proposed system to detect the breath of four volunteers in real time via RSSI measurements. These research achievements are helpful for future applications, but some safety and reliability validation measurements need to be considered.

In another example of a wearable application, a paper-based patch antenna sensor is proposed for strain detection as shown in Figure 2.1(c) [12]. The antenna sensor is fabricated by a radiation patch as the antenna and sensor, a layer of cellulose filter paper as the substrate, and an aluminum tape as the ground pane. In this work, after hundreds of bending cycles in the bending strain tests, the performance of the antenna sensor is still stable. In addition, through small cracks identification, bending angle analysis, and real human motion detection applied to gloves, the antenna sensor is fully evaluated and proved to be feasible to be used in medical, healthcare, and modern electronic device areas.

A wearable sensing system with wirelessly transmitted real-time ultrasound imaging for muscle electrical activity is shown in Figure 2.1(d) [13]. From the observed measurement results, the proposed system is capable to provide in real-time ultrasound image of muscles, and measuring the joint angle, muscle vibration and muscle activation, simultaneously. However, this work presents several limitations. The proposed system still needed wires to connect multiple sensors. This could be improved with flexible devices that are tailored to make such measurements in a way that is mechanically invisible in the future.

Monitoring blood glucose levels is an essential part of case management in patients with diabetes. Therefore, continuous glucose monitoring (CGM) sensors are needed to improve the quality of life of diabetic patients and manage the progression of diabetes. A non-invasive and portable system inspired by the anatomy of the vasculature, based on an electro-magnetism (EM) antenna sensor for continuous glucose monitoring is shown in Figure 2.1(e) [14]. The proposed antenna-based sensor is validated on animal models, serum, and animal tissues of diabetes and in a clinical setting. The aim of this work is to demonstrate the ability of the proposed antenna sensor to detect glucose variations over the diabetic range covering the hypo-to-hyperglycemic range.

This work indicates the high potential of sensing systems for continuous glucose monitoring, but other factors need to be addressed such as the comfort and electromagnetic safety for pregnant women and infants.

2.3 Principle of operation

In this section, a rectangular microstrip patch antenna is used to explain the principle of operation of an antenna sensor. A microstrip patch antenna contains four elements: a radiation patch, a dielectric substrate, a ground plane, and a transmission feed line as shown in Figure 2.2(a). The radiation patch and the conductive ground plane (which can take any possible shape) are detached by a dielectric substrate. As a consequence, an effective electromagnetic resonance cavity allows radiation at particular frequencies. The radiation patch is supplied by a microstrip feed line, and an incident signal is provided. This signal is transmitted or reflected by the radiation patch.

Consequently, the S_{11} parameter of the microstrip patch antenna can be determined by the ratio between the reflected power and the incident power. The radiation characteristics of the microstrip patch antenna can be characterized by the resonant bandwidth BW and the resonance frequency f_0. These two specifications can be extracted from the reflection coefficient S_{11} [15]. The operating frequency of the antenna is determined as the frequency at which the reflection coefficient is minimum, i.e., little energy is reflected by the antenna and most of the incident power is radiated. The resonant band-
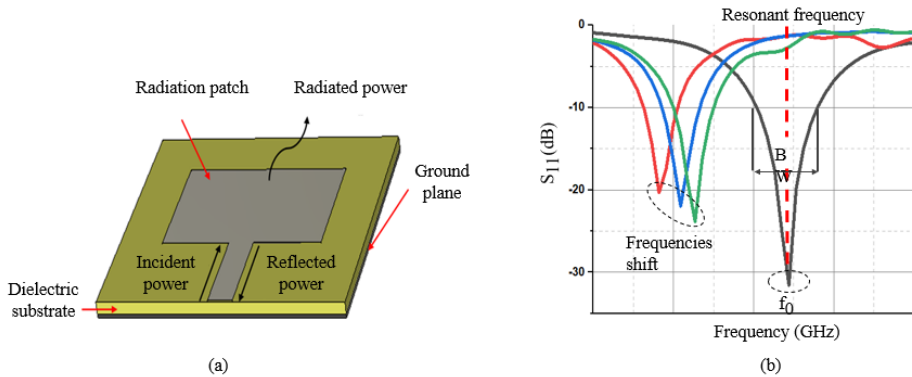
Figure 2.2: (a) Basic configuration of a microstrip antenna sensor and (b) illustration of frequencies shift of the antenna sensor.

width of the antenna can be defined as the range of resonance frequencies at a given S_{11} typically at $S_{11} = -10dB$. In theory, all of these radiation parameters can be used to convert a physical quantity (strain, temperature, pressure, pH level, concentration of aqueous solution, etc.) into a measurable radiation parameter. In fact, a physical variation leads to a resonance frequency shift (see Figure 2.2(b)).

The basic principle behind textile antenna sensors is that they utilize conductive threads or fibers embedded within the fabric to create an antenna structure that can transmit and receive electromagnetic waves. These conductive elements can be either metallic wires, conductive polymers, or conductive coatings applied to the textile surface. The conductive threads or fibers are woven or knitted into the fabric to create the antenna structure, which can be customized in terms of size, shape, and orientation depending on the specific application requirements.

2.4 Classification of antenna sensors

Antenna sensors can be classified into diverse categories as presented in the Figure 2.3. There are four main types of antenna sensors according to their measurement principle, namely, the temperature, dielectric, crack, and mechanical sensing. All these types of antenna sensors are able to detect changes using microwave signals or radio frequency (RF). The details of each type are described as follows:
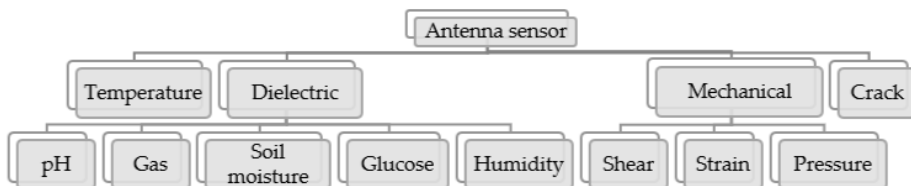
Figure 2.3: Different types of antenna sensors.

2.4.1 Dielectric Sensing

An antenna dielectric sensor can be represented by a patch antenna or by other standard planar antennas. Antenna-based sensor for dielectric sensing is based on the principle of measuring changes in the dielectric constant due to a measurand in the sensing area of the antenna. When the effec-

tive dielectric constant of the surrounding antenna including the measurand changes, it affects on the resonance frequency of the antenna sensor. Figure 2.4 presents a patch antenna where the radiation patch is covered with a dielectric material (superstrate). The choice of superstrate material depends on the selected measurand (humidity, salt and sugar, gas, etc.). The substrate can use different materials such as carbon nanotubes for gas sensing or polymer for humidity sensing or a textile material such as denim for blood glucose sensing [16]. However, the effective dielectric constant (relative permittivity) of the antenna sensor is provided by both the superstrate and the substrate [17]. Table 2.1 presents a summary of previously reported works on antenna dielectric sensors with different properties such as the measurand, the size, the operation frequency, material, and the sensing parameters.
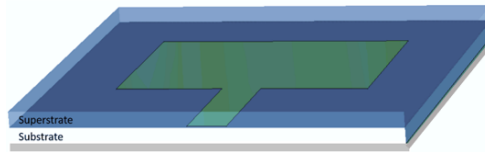
Figure 2.4: Configuration of an antenna dielectric sensor.

Table 2.1: Summary of previously reported works on antenna dielectric sensors.

Ref	Measurand	Type of Antenna	Size (mm^2)	Freq	Material	Type of Material	Sensing Parameters
[18]	PH	Hexagonal split-ring resonator	19×23.35	3–20 GHz	PCB	FR-4	Transmission coefficient
[19]	Salt and sugar	Crescent shaped patch	32×22	2.5–18 GHz	PCB	FR-4	Return loss
[20]	Humidity	H-shaped patch	90×85	880 MHz	Polymer	2 PEDOT: PSS	Threshold power
[21]	Gas	Patch antenna	41×41	2.4 GHz	PCB	Rogers	Frequency shift
[22]	Soil moisture	Spiral antenna	12×12	2.48 GHz	PCB	FR-4	Frequency shift
[23]	Moisture content	Patch antenna	48×48	2.26 GHz	Polymer	3 PDMS	Frequency shift
[24]	Humidity	Patch antenna	30×20	38 GHz	Textile	Cotton	Frequency shift
[25]	Relative humidity	Split ring resonator	35×35	0–1.5 GHz	Polyimide	Kapton	Frequency shift

2.4.2 strain Sensing

In order to check the structural integrity of the engineering components, strain is among the most important mechanical properties that must be used to

quantify the deformation of a material [26]. Regarding types of strains, there are two strains: shear strain and normal strain. The first type is determined from the change of angle from an original value of 90° and the second type is related to the change in the size of a design compared to its original size [27]. Figure 2.5(a) shows the operating principle of an antenna sensor for shear detection. An antenna patch with a slot in the ground plane is used to visualize the effect of the shear on the behavior of the antenna. The principle of a loop antenna sensor for pressure detection is presented in Figure 2.5(b). The variation of the parameter d in the geometry of the antenna structure detunes its operating frequency [28]. In order to provide accurate spatial resolution, it is recommended that the strain sensor presents a small size. Different types of antenna mechanical sensors are summarized in Table 2.2.
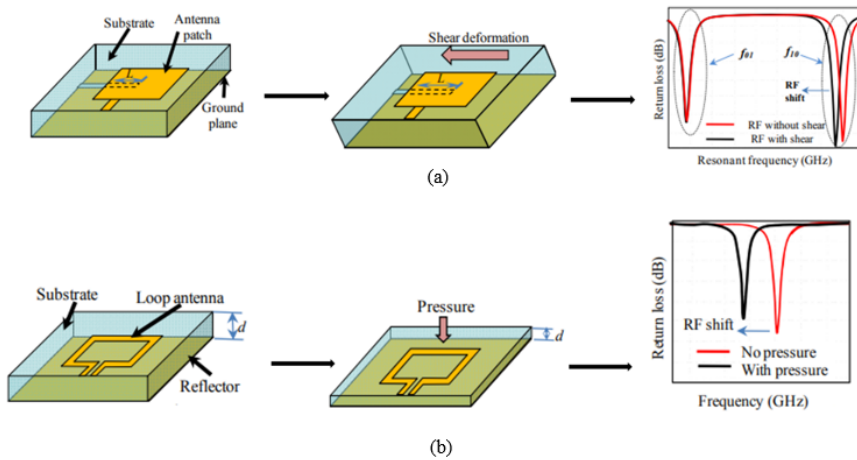
Figure 2.5: Antenna mechanical sensors for: (a) shear detection and (b) pressure detection.

Table 2.2: List of antenna mechanical sensors

Ref	Measurand	Type of Antenna	Size (mm²)	Freq (GHz)	Material	Type of Material	Sensing Parameters
[27]	Strain	Dipole antenna	17 × 16	8–12	Polymer	Polyimide	Frequency shift
[29]	Pressure	Slot antenna	17.55 × 13.5	5.5	PCB	Rogers laminate	Frequency shift
[30]	Strain	Patch antenna	94.58 × 52.36	1.8–2.4	Textile	Felt	Frequency shift
[31]	Shear and pressure	Patch antenna	12.1 × 66.9	6–7	Polyimide	Kapton	Frequency shift

2.4.3 Temperature Sensing

The temperature of an antenna sensor is an important parameter to know as it indicates whether or not the antenna sensor is in control. As the temperature changes, the temperature-sensitive material expands or contracts, causing a shift in the dimensions of the microstrip patch antenna. This change in dimensions alters the electrical characteristics of the antenna, particularly its resonant frequency. The antenna temperature sensor is useful for many applications, e.g., food production, manufacturing process control, human health monitoring, etc. There are many different types of antenna temperature sensors available and all have different characteristics depending upon their application [32]. Table 2.3 presents some research works reported in the literature for temperature sensing with several properties: the type of the antenna sensor, the size, the operation frequency, the used materials, and the sensing parameters.

Table 2.3: Summary of previously reported works on antenna temperature sensors.

Ref	Measurand	Type of Antenna	Size (mm²)	Freq	Material	Type of Material	Sensing Parameters
[33]	Body temperature	Patch antenna	10 × 6	38 GHz	Textile	Cotton	Frequency shift
[34]	Temperature	Slotted patch	38 × 38	900 MHz	PCB	FR-4	Frequency shift
[35]	Temperature	Rectangular patch	11.8 × 9.8	4.85 GHz 5.95 GHz	PCB	Rogers Laminate	Frequency shift
[36]	Temperature	Patch antenna	13.6 × 10.9	2.4–2.8 GHz	PCB	Rogers RO3210	Frequency shift
[37]	Temperature	Patch antenna	71 × 64	2.45 GHz 9.5 GHz 38 GHz	Textile	Cotton Jeans Viscose Lycra Cotton	Frequency shift

2.4.4 Crack Sensing

In order to reduce catastrophic structural breakdowns, cracks must be monitored because they are a direct indicator of structural damage monitoring. In fact, it is important to know the length, direction, and location of the crack to gather sufficient information to maintain structural integrity. Figure 2.6 presents a configuration of an antenna patch for crack detection. The direction and growth of the crack can be detected by observing the changes in the resonance frequency shifts. The resonance frequency shift of the crack antenna is generally much larger than the resonance frequency shift caused

9
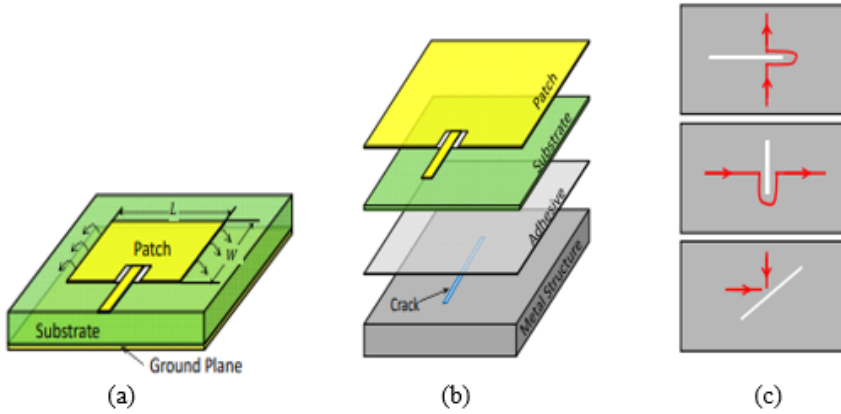
Figure 2.6: Antenna crack sensor: (a) schematic configuration of a patch antenna, (b) antenna sensor with crack, and (c) effect of cracks on the current model of the sensor.

Table 2.4: Summary of previously reported works on antenna crack sensors.

Ref	Measurand	Type of Antenna	Size (mm^2)	Freq (GHz)	Material	Type of Material	Sensing Parameters
[38]	Crack orientation	Rectangular patch	15 × 12.75	5.75 6	PCB	Rogers laminate RO4350B	Frequency shift
[39]	Crack opening and growth	Rectangular patch	15 × 12.5	6.1 8.6	Polyimide	Kapton	Frequency shift
[40]	Crack	Patch antenna	35 × 20.6	2.4	PCB	Rogers RT/duroid 5880	Frequency shift
[41]	Crack and monitoring	Patch antenna	50.8 × 25.4	6.1 7.6	Polyimide	Kapton	Frequency shift

by strain or temperature. Some examples of antenna crack sensors are given in Table 2.4.

2.5 Implementation of antenna sensors

2.5.1 Rigid wearable antenna sensors

Rigid wearable antenna sensors are designed to be attached or integrated into wearable devices, such as smartwatches, fitness trackers, or other wearable gadgets. Unlike flexible or conformal antenna sensors, which can bend or conform to the shape of the wearable device, rigid antennas are typically made of stiff materials, such as metal or printed circuit boards (PCBs), and maintain their shape without bending. Therefore, rigid wearable antenna sen-

sors present some limitations, including limited flexibility compared to soft or textile-based sensors, potential discomfort during prolonged wear, and sensitivity to body movements that may affect the performance of the antenna sensors. Additionally, the design and integration of rigid antennas into wearable devices can pose challenges in terms of size, shape, and aesthetics. Table 2.5 summarizes the limitations of rigid wearable antenna sensors.

Table 2.5: Limitations of rigid wearable antenna sensors.

Limitations	Description
Comfort and flexibility	Rigid wearable antenna sensors may not be comfortable to wear for long durations, especially on curved or irregular body surfaces.
Integration	Rigid wearable antenna sensors may face challenges in integrating with other wearable technologies or clothing, such as smart textiles or other sensors, due to their rigid nature.
User acceptance	Rigid wearable antenna sensors may face challenges in user acceptance, as some users may be reluctant to wear or use devices that are rigid or uncomfortable.
Manufacturing and cost	Rigid wearable antenna sensors may require complex manufacturing processes, including specialized materials and fabrication techniques, which can add to the cost of production.
Discreteness	Rigid wearable antenna sensors may not be aesthetically pleasing or discreet, which can be a concern for wearable applications where appearance matters, such as in fashion or lifestyle.

It's important to consider the aforementioned limitations when designing and implementing rigid wearable antenna sensors and explore potential solutions or alternatives, such as flexible or conformable antenna designs. The new generation wearable antenna sensor design ought to overcome these limitations and improve the overall performance and user experience.

Several researches have been reported in the literature using rigid materials for different types of antenna sensors, including temperature sensing, crack sensing, strain sensing, and dielectric sensing. For instance, a microstrip patch antenna-based sensor using flame retardant 4 (FR-4) substrate has been presented in [18]. The proposed antenna is employed as a sensor to detect different percentages of sugar and salt in terms of return loss based on the dielectric properties of the solution. In [7], a microstrip patch antenna sensor is printed on a Rogers (R03006) substrate. The presented antenna has been designed for temperature detection by subjecting a patch bonded to

various metal bases to thermal cycling. These types of substrates are not quite suitable for wearable antenna sensors as they cannot be stretched and bent. A wearable antenna sensor often should have additional characteristics such as robustness and flexibility, which claims the consideration of flexible non-conventional materials to exchange traditional printed circuit boards.

2.5.2 Textile wearable antenna sensors

Electro-textiles, also known as e-textiles, are fabrics or textiles that incorporate electronic components and systems. These textiles are designed to provide a range of functions, from sensing and actuating to communication and data collection. E-textiles are an emerging field that combines the traditionally separate domains of textiles and electronics, enabling the creation of interactive, smart fabrics that can be used in a variety of advanced applications. The integration of electronic components into textiles has opened up new possibilities for wearable technology, smart clothing, and other applications. Figure 2.7 represents different applications of the e-textiles. A wearable antenna integrated into a military beret to achieve an indoor/outdoor positioning system is presented in [42]. The proposed antenna is fabricated using a conductive textile, and a felt substrate. It is designed for the Global Positioning System (GPS). For healthcare applications, a wearable antenna-based sensor for the diagnosis of pulmonary edema is proposed in [43]. The results demonstrated the system feasibility and robust remote sensing capability. In addition, a textile antenna for spacesuit applications is presented in [44]. The results revealed that textile spacesuit performed in an excellent way and the achievements had the potential for future space applications. Furthermore, a dual-band textile antenna for electromagnetic energy harvesting, operating at global system for mobile communication is presented [45]. The proposed work presents an innovative solution that demonstrates the first antenna prototype fabricated directly into clothing since it is made of the same textile material as the cloth. This work indicates the high potential of textile antenna for communication applications. A high-gain textile antenna array system, fully integrated into a firefighters vest is proposed in [46], The results demonstrated that the textile antenna provides an excellent on-body performance. In addition to its low weight, compact dimensions which makes the antenna very well-suited for emergency applications.

The electro-textiles can be designed to be flexible, lightweight, and comfortable, making them ideal for use in clothing, accessories, and other textile-based products. The development of electro-textiles involves a range of tech-

Figure 2.7: Different applications of the E-textiles adapted from ref. (a) [42] ,(b) [43], (c) [44], (d) [45], (e) [46].

nologies, including conductive materials, sensors, microcontrollers, and power sources. These technologies are combined in various ways to create textiles that can sense, process, and transmit information, or control external devices.

Textile antenna sensors are a type of smart textile that integrate antenna functionality with sensing capabilities. These antenna sensors are designed to be woven, knitted, or embroidered into fabrics, allowing them to be integrated into garments, or other textile-based products. As their rigid counterparts, textile antenna sensors are capable to detect and measure various physical and environmental parameters, such as temperature, humidity, pressure, strain, and motion, among others. In addition, they offer several advantages over traditional sensors (rigid antenna-sensors). Firstly, they are flexible, lightweight, and conformable, making them ideal for wearable applications where comfort and flexibility are important. They can be easily integrated into textiles without adding bulk or weight, making them discreet and unobtrusive. Secondly, textile antenna sensors can be fabricated using standard textile manufacturing processes, such as weaving or knitting, allowing for scalable and cost-effective production. Figure 2.8 shows typical textile antenna-based sensors for different applications, the related achievement of each application presented is
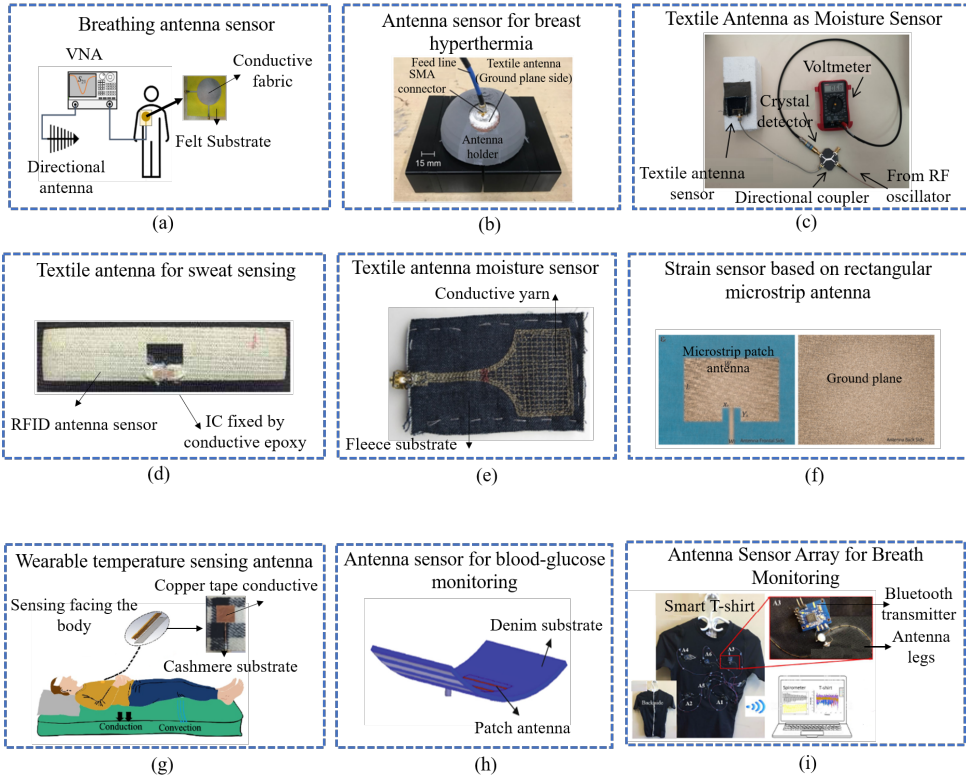
Figure 2.8: Typical textile antenna-based sensor applications adapted from ref. (a) [47]; (b) [48]; (c) [49]; (d) [50], (e) [51], (f) [52], (g) [53], (h)[16], (i) [54]

listed in Table 2.6. Thirdly, they can be easily washed, making them suitable for applications where regular cleaning is required, such as in sports or healthcare. Textile antenna sensors have a wide range of potential applications. They can be used in sports and fitness wearables for tracking body movements and vital signs [55], in healthcare for monitoring patients' health conditions [56], in automotive and aerospace industries for structural health monitoring [57], in smart homes for environmental sensing [58], and in military and defense for monitoring soldiers' physiological parameters [59], among others. They are also being explored for applications in Internet of Things (IoT), where they can be integrated into everyday textiles to enable smart functionalities.

Table 2.6: Achievements of the researchers as shown in Figure 2.8

Label	Achievements	Ref.
(a)	A wearable textile antenna-based sensor for respiration monitoring exhibits high accuracy in detecting the breathing rate and pattern of the user.	[47]
(b)	A wearable patch antenna-sensor fabricated with a textile material for a more comfortable breast hyperthermia therapy. The proposed system is flexible, breathable, and lightweight and therefore, can be inherently embedded into clothing.	[48]
(c)	A textile antenna for moisture sensing shows better sensitivity and accuracy for moisture measurement.	[49]
(d)	Health-care-based RFID antenna sweat sensor for sweat rate measurements in exercise, by comparing the graphene-printed pattern and the silver-plated pattern.	[50]
(e)	A textile monopole antenna-based sensor offered more reliable and accurate results for moisture content measurement.	[51]
(f)	Textile antenna strain sensor to explore the relationship between antenna elongation and resonant frequency, based on a stretchable antenna made of conductive fabrics.	[52]
(g)	A wearable temperature-sensing antenna indicated a frequency shift of about 60–80 MHz for each 2°C change in temperature, being suitable for measuring fever.	[53]
(h)	A non-invasive textile antenna-sensor for blood glucose monitoring offered an accurate correlation between the antenna reflection response and the blood glucose level.	[16]
(i)	A smart textile T-shirt based on antenna-sensor for real-time breathing monitoring, by obtaining the relationship between the RSSI and respiratory periods.	[54]

Textile antenna sensors can operate in different frequency ranges, such as ultra-high frequency (UHF), microwave, and radio frequency (RF) bands, depending on the desired sensing capabilities. They can be designed as passive antennas, which reflect or transmit signals from an external source, or as active antennas, which generate their own signals for sensing purposes.

One of the main advantages of textile antenna sensors is their flexibility and conformability to the shape of the body or other objects, allowing for comfortable and unobtrusive sensing without restricting movement. Additionally, textile antenna sensors can be washable and durable, allowing for long-term and practical use in real-world environments.

2.6 Human body impact

Antenna-sensors are an essential component of wireless communication systems, in order to transmit and receive electromagnetic waves. The performance of an antenna-sensor is influenced by several factors, including its geometrical design, orientation, and environment. One critical factor that can significantly impact the performance of an antenna-based sensor is the proximity of the human body to the antenna. When a human body comes in close proximity to an antenna, it can affect the antenna's radiation pattern, realized gain, efficiency, and resonance frequency, leading to changes in its performance. This is because the human body behaves as a lossy medium

and degrades the efficiency and the electromagnetic radiation pattern emitted by the antenna. In addition, the change in the effective permittivity detunes the operation frequency of the system.

Concerning the design of on-body antenna-sensors, there are two effects that need to be considered: First, the different electromechanical properties such as bending effects which refer to the change of the antenna sensor electrical properties when it is bent or deformed. Second, a significant amount of the power is usually radiated toward the body and absorbed. As a consequence, the specific absorption rate (SAR) must be considered. These effects can be particularly significant for antennas operating at high frequencies, such as those used for mobile communication systems. For this reason, antenna designers and engineers must consider the impact of the human body's proximity when designing and testing antennas for these applications. Overall, understanding the effects of the human body's proximity on the antenna performance is crucial for ensuring reliable and effective wireless communication systems.

2.6.1 Bending effects

The bending effect of a wearable antenna sensor refers to the phenomenon where the performance of the antenna changes as it bends. Wearable antenna sensors are designed to be integrated into clothing or other flexible materials, allowing for unobtrusive monitoring of vital signs or other physiological parameters. However, the flexibility of the material can cause the antenna to deform, leading to changes in its resonance frequency, radiation pattern, and other characteristics that can affect its ability to transmit or receive signals. Understanding and mitigating (re-tuning) the bending effect is crucial for the reliable operation of wearable antenna sensors in real-world applications. In this context, this effect is an important consideration for antenna design and optimization. When a textile antenna is bent, several effects may occur that can impact its performance. These effects include:

- Changes in the resonance frequency: The resonance frequency of an antenna is the frequency at which it operates most efficiently. When a textile antenna is bent, its resonance frequency may shift, which can cause it to operate less efficiently.

- Changes in radiation pattern: The radiation pattern of an antenna is the directional pattern of the emitted/received electromagnetic. When a textile antenna is bent, the radiation pattern may change, which can impact its ability to communicate effectively.

- Changes in impedance: The impedance of an antenna is the measure of its opposition to the flow of electrical current. When a textile antenna is bent, its impedance may change, which can affect its ability to match the impedance of the transmitting or receiving device.

The antenna-based sensor can be positioned on the typical arm or chest. To minimize the bending effects of a textile antenna, it is important to design the antenna with these effects in mind. This can include selecting the right materials, optimizing the antenna shape and size, and carefully positioning the antenna on the wearable device to minimize bending. The majority of prior studies found in the literature included an analysis of antenna performance under bending [60–63]. These antennas are designed with wide enough bandwidth, such that the return loss remains below $-10dB$ at the desired frequency. Table 2.7 summarizes research works that investigate the influence of bending on antenna performance.

Table 2.7: A summary of bending effects on the performances of wearable antennas.

Ref	Substrate	Radius (mm)	Bandwidth (GHz)	Applications
[64]	Silicon	30	3.88	Medical telemetry
[65]	Polyimide	20, 30, 40, 50, 60, 70, 180,360	0.36	WBAN
[66]	Denim	28.5, 42.5	0.14	ISM band
[67]	Jeans	33.5, 47.5, 58.5	3.84	WLAN
[68]	Shieldit conducting fabric	34,40,50,70	2.4	ISM band
[69]	Polyester textile	10,20,30,40,50,60,70,80,90	3.37	WiMAX
[70]	Thin planar textile	0°,45°,90°	2.45	ISM band
[71]	Polyamide	8, 15, 30, 80	11.5	UWB
[72]	Felt	10, 15, 20	4	Medical imaging
[73]	Polyimide	50, 100,150	2.45	ISM

There are several advantages of using a bent or flexible antenna, including:

- Improved performance: Bending or curving an antenna can help to improve its performance by increasing its gain and directivity. This can lead to better signal reception and transmission in certain situations.

- Reduced size: A bent or flexible antenna can be made smaller than a straight antenna of the same frequency and gain. This can be beneficial in applications where size is a critical factor, such as in portable devices or wearables.

- Increased durability: A bent or flexible antenna can be more durable than a straight antenna, as it is less likely to break or snap off if it is

bumped or bent. This can be important in applications where the antenna may be exposed to rough handling or harsh environments. Overall, the use of a bent or flexible antenna can provide several benefits depending on the specific application and requirements.

2.6.2 Specific Absorption Rate (SAR)

Specific absorption rate (SAR) is a measure of the amount of radio frequency (RF) energy absorbed by the human body when exposed to an electromagnetic field (EMF). SAR is expressed in units of watts per kilogram (W/kg) and is used to evaluate the potential health risks of exposure to RF radiation. When an electronic device, such as a cell phone, emits RF energy, it can be absorbed by the body tissues nearest to the device. SAR is the measure of how much energy is absorbed by the body tissue per unit of mass. SAR values can vary depending on the frequency of the EMF, the power of the RF energy, and the distance between the body and the source of the EMF. The SAR value is used as a standard for measuring the potential health risks associated with exposure to EMF radiation. Exposure to high levels of EMF radiation has been linked to various health risks, such as cancer, DNA damage, and other biological effects [74]. Therefore, SAR is an important parameter in evaluating the safety of wireless devices. Regulatory agencies, such as the Federal Communications Commission (FCC), require electronic devices to comply with SAR limits to ensure that the amount of RF energy absorbed by the body does not exceed safe levels. SAR limits vary by country and can differ depending on the type of device and the location of the exposure. These limits are designed to ensure that the level of exposure to EMF radiation does not exceed a safe threshold for human health. Mobile phone manufacturers are required to measure the SAR of their devices and to ensure that they comply with these regulatory limits before they are sold to consumers. Overall, SAR is an important metric for evaluating the potential health risks of exposure to RF radiation and ensuring that electronic devices are safe for use.

According to the Institute of Electrical and Electronics Engineers (IEEE) and the International Commission on Non Ionizing Radiation Protection (ICNIRP) organizations, the limit of SAR is set as: 1.6 W/Kg and 2 W/Kg averaged over 1 g and 10 g tissue, respectively [75, 76]. Table 2.8 represents a comparison of different kinds of wearable antennas of SAR over 1g and 10g.

Table 2.8: comparison of different kinds of wearable antennas SAR values in W/Kg.

Ref	Antenna design	Size (mm^2)	f_r (GHz)	SAR 1g (W/Kg)	SAR 10g (W/Kg)
[[77]]	Slotted rectangular patch	70 x 60	2.45	0.087	0.043
[[78]]	Meta surface antenna	50 x 50	5	0.291	0.0975
[[79]]	Patch antenna	90 x 90	2.45	0.09	0.04
[[80]]	Full ground UWB antenna	60 x 50	3.8-5.8	0.25/0.7	0.071/0.171
[[81]]	Folded-ring antenna	60 x 60	2.45	0.2	0.1
[[82]]	Handset antenna	40 x 80	1.8	0.87	0.58
[[83]]	Square patch antenna	29 x 29	2.4	0.302	0.176
[[84]]	Lotus-wearable antenna	54 x 54	5.8	0.175	0.549

2.7 Research challenges of wearable antenna sensors

Wearable antenna sensors are becoming increasingly popular as they offer the ability to monitor a person's vital signs and physical activity in real time. However, there are several research challenges that need to be addressed in order to improve the performance and reliability of these sensors. In this section, we will explore some of the key challenges associated with wearable antenna sensors, including miniaturization, robustness and durability, wireless connectivity, human body effects, signal interference, noise and security, and privacy. The details of these challenges are presented in figure 2.9:

In this thesis, several of the aforementioned challenges will be addressed, such as:

- Develop miniaturized antenna-based sensors with high performance: high sensitivity, low cost and high durability.

- Explore an antenna-based sensor platform to be integrated with other commercial electronic components, such as Bluetooth/WIFI transmitter, to be able to transmit data wirelessly.

Miniaturization
The system needs to be small and lightweight enough to be worn comfortably on the body

Robustness and durability
The system needs to be robust and durable, as they will be exposed to a wide range of environmental conditions and physical stress

Wireless connectivity
Wearable antenna sensors must be capable of wireless connectivity to transmit data to other devices

Human body effects
The human body can significantly affect the characteristics of the antenna sensor, and this needs to be taken into account during the design and testing phase

Signal interference and noise
Minimizing signal interference and noise, which can affect the accuracy and reliability of the data collected by the sensors

Security and privacy
Manufacturers must implement robust security measures to protect the data from unauthorized access and breaches

Challenges

Figure 2.9: Challenges of wearable antenna sensors.

- - Study the effects of the human body on the antenna sensor performance.

Addressing these challenges will contribute to the development of wearable antenna sensors, enabling their widespread adoption and unleashing their full potential in various applications.

3

Materials and methods

3.1 Introduction

The present chapter is devoted to describe the methodology for designing, manufacturing, and characterizing textile and flexible antenna-based sensors. The first step in designing an antenna sensor is to select a suitable textile fabric as a substrate for the antenna sensor, which is necessary to characterize the fabric by measuring the dielectric constant and loss tangent. These parameters play vital roles in antenna design. The dielectric constant affects parameters such as the resonance frequency, impedance, gain, and radiation pattern. The loss tangent defines the efficiency and power dissipation characteristics of the antenna. To achieve optimal antenna performance, a proper selection of materials with desirable dielectric properties needs to be considered. Therefore, advanced characterization and testing of textile fabrics are essential for ensuring their quality and suitability for various applications. Then, a survey of the textile materials and their EM characteristics (dielectric and conductive materials) will be discussed. The next step is to simulate the antenna-based sensor using an industrial 3D full electromagnetic software. A detailed description for the used simulator will be presented in this section. Finally, to fabricate the antenna-based sensor different manufacturing meth-

ods available in the literature will be presented in this chapter. In addition, the characterization methods for the different applications will be explained in this section.

3.2 Textile materials and their EM characterization

Textile materials are widely used in many different industries and applications. The electromagnetic (EM) characterization of textile materials is essential for the development of novel applications in the field of wearable technology, wireless communication, and electromagnetic shielding. The electrical properties of textile materials can be measured using a variety of techniques, including the parallel plate capacitor method [85], the coaxial line method [86], and the cavity resonator method [87]. These techniques are commonly used to determine the dielectric properties (dielectric constant and loss tangent) of textile materials.

The characterization of textile materials is important for several reasons. First, it helps manufacturers to ensure that their products meet quality standards and specifications. This includes testing for properties such as strength and durability, which are important for ensuring that textiles can withstand regular wear and tear. Second, the characterization of textile materials is critical for determining their performance in specific applications. For example, textiles used in outdoor clothing or technical fabrics must be able to withstand exposure to the elements and maintain their properties over time. Third, the characterization of textile materials is important for ensuring their safety. Certain textiles may be treated with chemicals or dyes that could be harmful to human health, and testing is necessary to ensure that these materials are safe for use. Overall, the characterization of textile materials is vital for ensuring that textiles are of high quality, perform as expected, and are safe for use. It plays a critical role in the textile industry and in the products that we use every day.

A wearable antenna-based sensor is composed of a minimum of two kind of materials: one is chosen for the dielectric part and the other for the conductive part (complex implementations can use n-dielectric and m-conductive layers). These materials must be carefully considered to design wearable antenna sensors. In this section, a detailed classification of these two groups is summarized in figure 3.1.
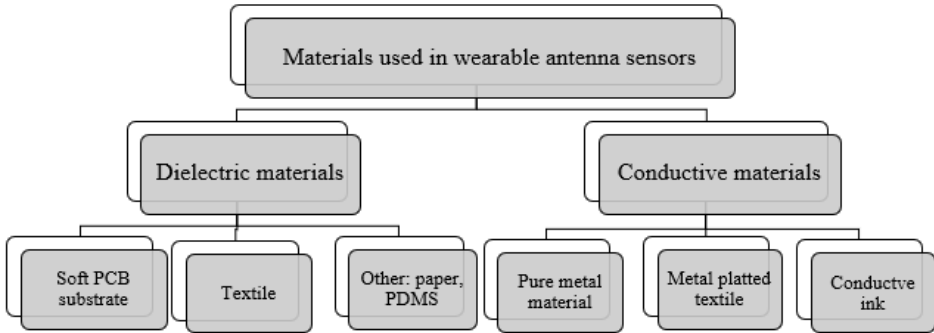
Figure 3.1: Classification of materials for wearable antenna sensors implementation.

3.2.1 Dielectric materials

Dielectric materials play an important role in the performance of wearable antenna-based sensors since they form the antenna substrate. In fact, wearable antenna sensors are designed to be integrated into clothing or other wearable devices, which often have a dielectric layer that surrounds the antenna. The dielectric material affects the electromagnetic field distribution around the antenna, which in turn affects the radiation pattern, impedance matching, and efficiency of the antenna. Table 3.1 presents the dielectric properties of common commercial materials used for designing wearable antenna-sensors.

Table 3.1: Dielectric properties of common materials.

Material	Dielectric constant (ε_r)	Loss tangent ($Tan\delta$)	Frequency (GHz)	Ref
Paper	1.4	0.01	2-4	[10]
PDMS	2.7	0.022	2.5-12.4	[88]
Cotton	1.3	0.0058	2.4	[89]
PET	3.4	0.01	Up to 60	[90]
Denim	1.8	0.07	3.3-5	[91]
Silk	1.75	0.012	2.45-5	[92]
Fleece	1.25	0.019	2.45	[93]
Velcro	1.34	0.006	2.4-5	[94]
Felt	1.2	0.0013	2.4	[95]

Figure 3.2 shows different dielectric materials used in wearable antenna sensors such as soft PCB substrate, textile, paper, and PDMS.

For soft PCB substrate, flexible films are the main base materials for supporting overlays, such as liquid crystal polymer films (LCP) [96], Polyethylene TerePhthalate (PET) films [97] and polyimide (PI) films [98]. Various soft PCB substrates have been used for flexible and transparent antennas because they offer high flexibility, low loss and thickness [99]. An example of an antenna-based sensor for microwave breast cancer detection using a polyimide substrate is presented in Figure 3.2 (a) [100]. This kind of dielectric is expensive due to the specialized materials and manufacturing processes required to produce them.

Textile substrate for antennas refers to the use of flexible and wearable textile materials as the base for antennas. The integration of antennas into textiles has gained significant attention in recent years due to the increasing demand for wearable electronic devices and the need for comfortable and convenient communication systems. Textile antennas offer several advantages over traditional antennas, including conformability, light weight, and flexibility. The use of textile substrates allows for the creation of conformal and wearable antennas that can be easily integrated into clothing, accessories, and other textile-based products. Numerous textile substrates have been investigated for wearable antennas sensors such as cotton [101], denim [102], jeans [103], cordura [104], fleece [105], and felt as presented in Figure 3.2 [106].
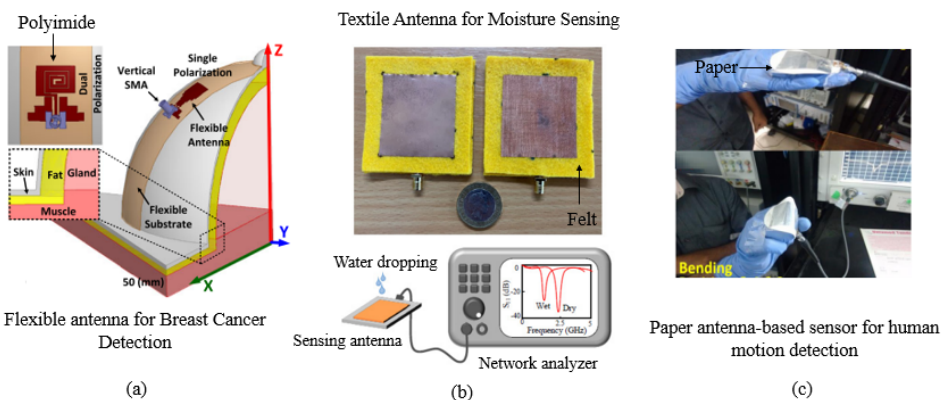
Figure 3.2: Various dielectric materials for different wearable antenna-sensors applications, (a) Polyimide, (b) Felt, and (c) Paper substrate.

Table 3.2: Comparison of different dielectric materials.

Properties	Polymer	Textile	Paper
Weight	Medium	Low	Low
Cost of fabrication	Medium	Low	Low
Robustness to Wetness	High	Medium	Low
Fabrication complexity	Simple/Printable	Simple	Simple/Printable
Deformability	Low	High	High
Tensile strength	High	Low	Low

Furthermore, paper materials are also used for the design of wearable antenna-based sensors using the screen-printing and inkjet methods. Paper substrates have been used in various applications such as healthcare [107] , agricultural [108], and military [109]. A paper antenna operating as electromechanical sensor for human motion detection is shown in Figure 3.2 [12]. Moreover, the paper material has some disadvantages, such as poor mechanical strength and sensitivity to moisture. A comparison of different dielectric materials is presented in Table 3.2.

Textile materials such as Felt and Cotton are chosen to be used in this thesis because of their many advantages including, flexibility, lightweight, low cost, textile material low losses, comfort, and washability.

3.2.2 Conductive materials

Conductive materials are a crucial component of wearable antenna-based sensor, they can be evaluated in terms of tensile strength, weather-proof, deformability, conductivity and their integration with flexible materials. Traditionally, conductive materials such as silver, copper, and gold have been used to manufacture wearable antenna sensors. However, these materials can be rigid, heavy, and uncomfortable to wear, which limits their practicality for everyday use. These materials have high low cost, conductivity, and can be incorporated with textile substrates using adhesive laminated materials without using sewing and embroidery and techniques; however, its rigid structure restricts their use for flexibility [110, 111]. Recently, there has been growing interest in the development of conductive materials that are lightweight, flexible, and comfortable to wear. Some of the promising materials being explored for wearable antennas such as Zelt [112], Shieldit Super [113], and Flectron [114] (Figure 3.3), and their electrical properties such as surface resistance and conductivity are presented in Table 3.3.

Furthermore, metal-plated textile is widely used as a conductive material
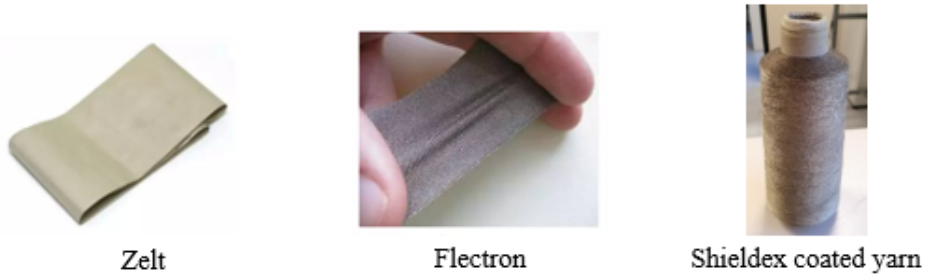
Figure 3.3: Different conductive textile materials.

Table 3.3: Conductive materials properties.

Properties	Conductivity (S/m)	Surface resistance (Ohm/sq)	Thickness (mm)	Ref
Pure Copper	$2.5.10^5$	0.05	0.08	[115]
Zelt	1.10^6	< 0.01	0.06	[92]
Shieldit Super	$6.67.10^5$	< 0.1	0.17	[116]
Flectron	3.10^5	< 0.07	0.04	[117]

for manufacturing wearable antenna-based sensors, it is often termed "electro-textile" and "E-textile". It offers the added benefit of being comfortable to wear and can be easily integrated into clothing. Several electro-textiles can be used for wearable antenna sensors, which provide high flexibility and can be sewn into clothing using fabric yarns. There are two common yarns used for manufacturing wearable antenna sensors. The first kind of yarn is commercial Bekaert yarns, which are produced by the ring yarn technique where conductive stainless-steel fibers are mixed with polyester or cotton fibers in different percentages. The second type of yarn is represented by a commercial Shieldex 117/17 dtex 2-ply, which is a polyamide multifilament yarn coated with pure silver 99. Table 3.4 describes these yarns properties.

Another kind of conductive materials is the conductive ink made of metal or carbon particles; these kinds of conductive material are promising for de-

Table 3.4: Yarns Properties[118].

Material	Density (tex)	Linear R (ohm/cm)	Type
Shieldex	11.7/2	≤30	Twisted multifil
Bekaert	20/2	≤50	Ring yarn

signing wearable antenna sensors. Conductive inks have the advantages of simplicity of manufacture and compatibility with standard inkjet printing and screen-printing process. In this thesis, a Less EMF Shieldit super fabric and Shieldex 117/17 dtex 2-ply yarn have been used as conductive materials for the metal layer radiation parts of the antenna sensors for different applications.

3.3 Fabrication methods for wearable antenna sensors

Fabrication methods play a vital role in creating reliable and efficient wearable antenna sensors that can seamlessly incorporate with the human body. Fabrication methods for wearable antenna sensors involve the process of designing and manufacturing antennas that are flexible, lightweight, compact, and capable of conforming to the contours of the human body. Different fabrication techniques are employed to manufacture wearable antenna sensors, each offering unique advantages and challenges. However, advances in materials science and manufacturing techniques have paved the way for innovative approaches such as screen printing, inkjet printing and embroidery techniques. An interesting review of these manufacturing methods is presented in [119],[120].

Screen printing is a simple and economical approach used by many electronics manufacturers. In addition, this method is an additive operation, which makes it environmentally friendly [121]. Instead of hiding the woven screen that has different thread densities and thicknesses, the mask with the required pattern is adjusted directly to the substrate where the conductive ink is handled and thermally annealed. Moreover, the screen-printing technique faces diverse limitations. It comprises its limited number of realizable layers, lack of thickness control for the conductive layer, and low printing resolution. These aspects lead to the limited implementation of this technology, because wearable printing requires better precision for the convenient operation of the communications for wearable devices.

Inkjet printing is one of the relatively low-cost printing technologies. This technology is capable of producing a very high precision pattern due to its use of ink droplets the size of up to a few picolitres' [122]. Additionally, this technique allows the design pattern to be transmitted directly to the substrate with no requirement for masks. In addition, inkjet printing projects the single ink droplet from the nozzle to the required position, from which no waste is founded, which makes it among the economical manufacturing methods. This

is a clear advantage in comparison with traditional etching technology, which has been generally used in industry [123]. The main drawbacks of inkjet printing technology are the incompatibility of certain types of conductive inks due to the larger particle size and clogging of the nozzles.

Embroidery method has gained attention in recent years due to their capability to incorporate antenna-based sensors into textile materials. Fibers or conductive threads are embroidered onto textile substrates, offering a combination of functionality and aesthetics. This technique is used to fabricate all the antenna-based sensors presented in this thesis; therefore, the details of the embroidery method are discussed below.

The embroidery manufacturing uses specialized conductive threads, from which the antenna sensor can be embroidered on the base substrate textile fabric. Before embroidering, it is very important to know the properties of the conductive threads that are going to be used (conductivity, DC resistance, and mechanical parameters), because when the conductive thread is characterized, it is then easier to find methods to improve the performance of the antenna sensor [124]. Therefore, the conductive threads must have adequate resistance and flexibility to avoid undesired breaks produced by high tensions in the embroidery machine [125]. This technique is evolved to allow a digital image or layout to be directly embroidered using a computer-assisted embroidery machine.Figure 3.4 depicts the embroidery technique, starting with the simulated model of the desired design (Figure 3.4 (a)). The 3D model is designed using the commercial CST studio 3D full electromagnetic simulator and exported to 2D model as a Gerber format (single layer) from CST, so once the geometry image is obtained, this image should be converted into the readable format of the manufacturing machine using the Digitizer EX software, as presented in Figure 3.4 (b). The software allows the user to carefully modify some textile properties for the embroidery structure such as the stitch pattern, the structural boundaries and yarn density. After importing the file which contained the identification of the desired layout geometry into the embroidery machine in digital format, the computerized embroidery process is implemented to embroider the conductive part of the design. A needle with the conductive yarn is threaded through the substrate material and interwoven with a bobbin assistant yarn to form the stitch as demonstrated in Figure 3.4 (c). The stitches appear the same on the top and bottom of the substrate. In this example, a satin fill stitch pattern is selected and implemented because it is well-suited to a narrow shape. Threads converge in the center of the seam. The number of points is fixed; therefore, the stitches are denser for narrower antenna sensor geometries.
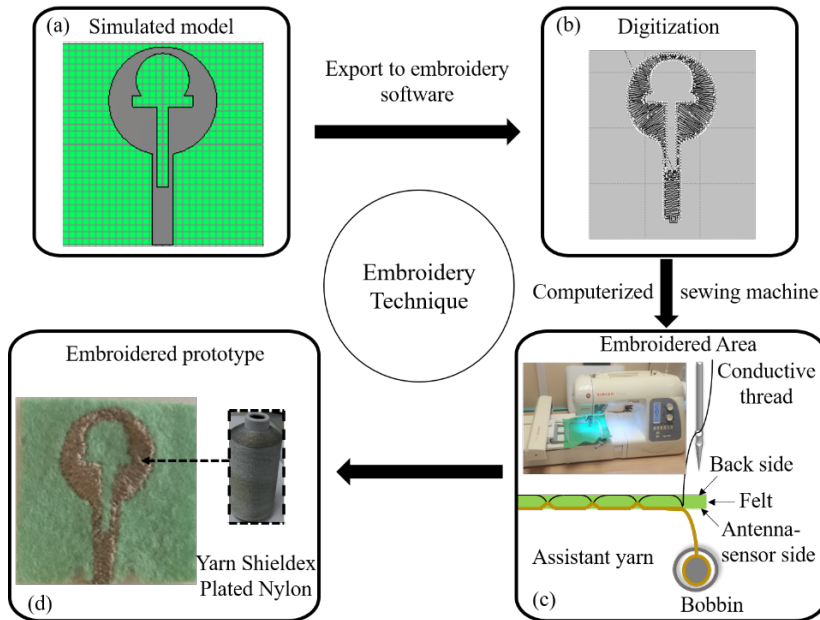
Figure 3.4: Embroidery process.

The conductive yarn is relatively thick compared to the conventional embroidery yarn, due to the mechanical constraints of the embroidery machine. In order to optimize the fabrication, a processed conductive yarn is employed in the bobbin of the embroidery machine. A certain degree of tension control is performed on the yarn in order to increase the precision of stitch geometry and patterns. The stitch spacing is a significant feature for good design, and it can be defined as the distance between two needle penetrations on the same side of the shape. In order to avoid damaging the tissue sample, less dense stitches should be used in areas with narrow columns. For fabrication, a popular fabrication machine (Singer Futura XL-550) is adopted, an example for an embroidered prototype is presented in Figure 3.4 (d). The embroidery process is advantageous over other techniques and embroidery machines are more recommended in the industry. This technique is easier to apply for mass production of clothing with integrated embroidered antenna sensors. With embroidery, the use of glue is not always a requirement to connect the textile layers together and also it allows to create reproducible geometries via computerized embroidery machines [126]. This can improve the washability of the clothing with the integrated antenna sensor. To conclude, a comparison of different textile fabrication techniques is presented in Table 3.5.

Table 3.5: Comparison of different textile manufacturing techniques.

Method	Embroidery	Inkjet Printing	Screen Printing
Process	Stitching designs using thread and needle	Spraying inkon the fabric using inkjet technology	Applying ink through a mesh screen onto fabric
Design options	Limited to stitching designs and patterns	Virtually unlimited	Can accommodate various designs
Complexity	Simple	Simple and versatile	Moderate complexity
Durability	Highly durable and long lasting	Less durable	Durable and long lasting
Cost	Medium	Lower	Moderate
Customization	Suited for intricate and personalized designs	Ideal for customization and on-demand printing	Well-suited for multicolor designs and large quantities

3.4 Simulation method

The initial design of the antenna-based sensor starts with the choice of the material for the substrate and the geometry of the antenna sensor. The choice of geometry needs to be guided from the design requirements such as low profile, small size, simple structure and light weight. The antenna-based sensor design procedure starts with the definition of the design goal and target antenna sensor specifications. In addition, the choice of materials for the antenna-based sensor and characterization of their electromagnetic properties needs to be defined. In this thesis, the design, optimization and numerical evaluation of the antenna sensors performance are carried out using CST Microwave Studio. This 3D full-wave electromagnetic commercial software is based on the Finite Integration Time Domain Method (FITD) which is used to compute the modelled antenna sensor structures and VOXEL human body models. Figure 3.5 presents a generic flowchart of the antenna-based sensor process. The steps taken to achieve the desired model in CST are:

- Determine the parameters and design the antenna sensor model.

- Calculate the antenna sensor model dimensions for the required antenna.

- Optimize the parameters of the antenna sensor to achieve a specific objective.

- Evaluate the behavior of the desired design (sensing performance, human body impact).
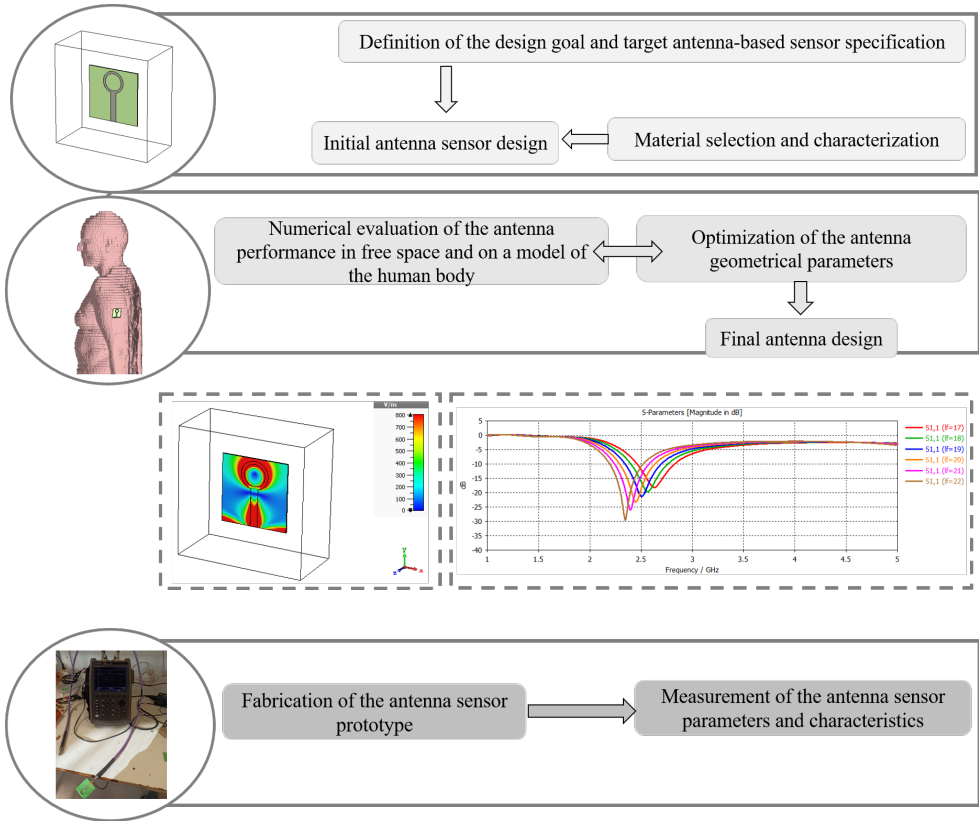
Figure 3.5: Flowchart of the design, optimization, fabrication and measurement process of an antenna-based sensor.

Most of the antenna sensors used in this thesis are based on resonance frequency shift, thus, S_{11} simulations are highly used to evaluate the behavior of the proposed design.

For evaluating the performance of the antenna sensor, there are some parameters need to be simulated:

- S_{11} parameter: helps to analyze the antenna's sensor performance across different operating frequencies and identify resonance points, bandwidth, and other frequency-dependent characteristics.

- Gain: to determine the directionality, beamwidth, and coverage area of the antenna sensor.
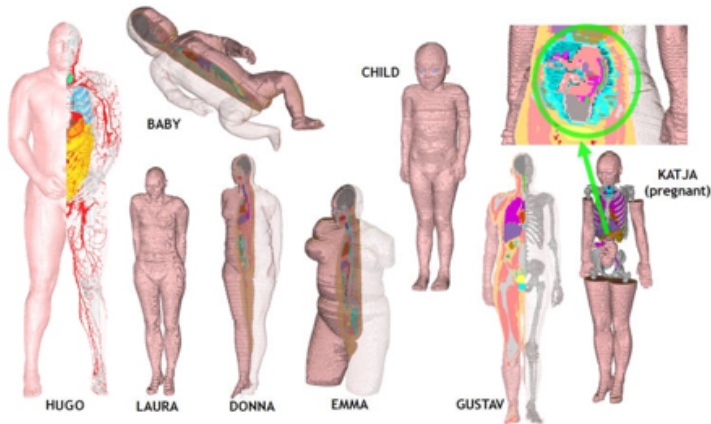
Figure 3.6: CST Voxel family.

Table 3.6: CST Voxel family details.

Voxel model	Age (Year)	Size (cm)	Mass (kg)	Sex	Resolution/mm
Baby	8-weeks	57	4.2	F	0.85 x 0.85 x 4
Child	7	115	21.7	F	1.54 x 1.54 x 8
Donna	40	176	79	F	1.875 x 1.875 x 10
Emma	26	170	81	F	0.98 x 0.98 10
Gustav	38	176	69	M	2.08 x 2.08 x 8
Laura	43	163	51	F	1.875 x 1.875 5
Katja	43	163	62	F-P	1.775 x 1.775 x 4.84

- E-field: helps to select the sensing region that provides the highest sensitivity, this region should have the maximum electric field distribution.

- Specific Absorption Rate (SAR): to ensure that the SAR levels are within acceptable limits to protect human health and safety. To simulate the SAR, CST Microwave Studio offers a variety of human body models for numerical analysis, which offers a vast collection of biological body models as shown in Figure 3.6.

These human body voxel models are made of different weight, height, ages and resolution. CST provides the option for the users to explore material properties for any desired frequencies. Table 3.6 presents details of all models available in the CST Voxel Family obtained from the CST website.

3.5   Characterization methods

This section is dedicated to describe the characterization methods used in this thesis. The first method is to characterize the substrate materials by measuring the dielectric constant and loss tangent. Subsequently, the resonance frequency shift measurement will be discussed. In addition, sample preparation of salinity, sugar, and glucose concentration will be determined. The different measurement methods adopted to monitor different breathing patterns will also be presented. Besides, to retrieve the electromagnetic properties of liquids, a method using a SIW antenna sensor will be explained as well.

3.5.1   Characterization of the substrate materials

Measuring the dielectric properties of the used substrate is required for simulation and design. In this thesis, considering that the addressed applications need different substrates, the textile materials are tested every time. The relative dielectric constant and loss tangent of the substrate can be measured by a Microwave Frequency Q-Meter as shown in Figure 3.1 (a). Also, an Electronic Outside Micrometer is utilized to determinate the thickness (h) of the substrate (Figure 3.1 (b)). In this thesis, felt is chosen as one of the substrates due to its better hygroscopicity and low losses compared with other fabrics. Its relative experimental dielectric constant and loss tangent are $\varepsilon_r = 1.2$ and $Tan\delta = 0.0013$, respectively. The textile substrate material corresponds to a non-woven structure with a 100 polyester (PES) composition and it has a weight of 211 g/m^2. Therefore, this textile substrate is resistant to tearing and humidity, whereas it has several advantages including heat stability,
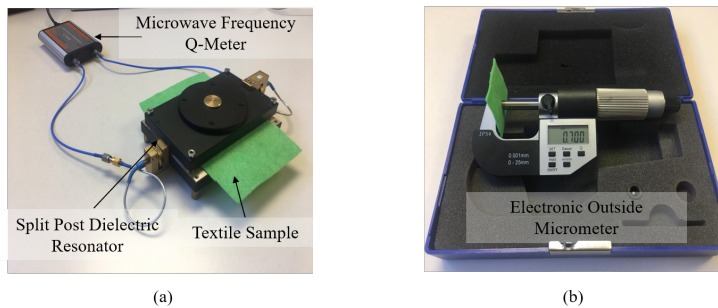
Figure 3.7: Substrate parameters measurements,(a) Permittivity and loss tangent measurements and (b) thickness measurement.

chemical moisture resistance, and durability. Furthermore, a cotton T-shirt is used to monitor breathing patterns. The dielectric properties of the T-shirt are accurately characterized by a dielectric constant and loss tangent corresponding to $\varepsilon_r = 1.3$ and $Tan\delta = 0.0058$, respectively.

3.5.2   Resonance frequency shift measurement

The principle of operation of an antenna-based sensor is explained in section 2.3, using the microstrip rectangular patch antenna as an example. As explained, a microstrip patch antenna radiates EM signals at its resonance frequencies. An incident signal is provided to feed the microstrip line. This incident signal is either transmitted by the radiation patch or reflected by it. The spectrum of the reflected signal, thus, shows significant losses at the antenna resonance frequencies. This phenomenon is represented by the S_{11} curve from which the resonance frequency can be extracted. The resonance frequency is determined as the frequency at which the S_{11} is a local minimum; at this frequency, most of the incident power is radiated by the antenna, and thus, little power is reflected back. However, the resonance frequency shift is the most commonly used sensing parameter. The resonance frequency shift technique for antenna-based sensor is based on the principle of monitoring the changes in resonance frequency of an antenna when its surroundings or properties are changed. This method is widely used in various sensing applications, including liquid characterization, healthcare monitoring, environmental monitoring, and wireless communication systems.

The resonance frequency of a rectangular patch antenna can be calculated as [127]:

$$f_{mn} = \frac{c}{2\pi\sqrt{\varepsilon_{reff}}}\sqrt{\left(\frac{m\pi}{L_e}\right)^2 + \left(\frac{n\pi}{W_e}\right)^2} \qquad (3.1)$$

Where c is the speed of light and ε_{reff} is the effective dielectric constant; m, n represents the resonant orders; for an antenna with rectangular radiation patch, the fundamental mode is TM_{10}. The electric length L_e and the electric width W_e can be calculated from the geometric dimensions of the radiation patch and the fringe extensions as:

$$L_e = L + \Delta L \qquad (3.2)$$

$$W_e = W + \Delta W \qquad (3.3)$$

Where, L, W are the width and length of the antenna patch, respectively.

Therefore, the resonant frequency of the TM_{10} mode can be simplified from equation 3.1 as:

$$f_{10} = \frac{c}{2\sqrt{\varepsilon_{reff}}} \frac{1}{L_e} \tag{3.4}$$

The line extension Δ_L can be neglected, when the substrate height h is much smaller than the dimensions of the radiation patch. Thus, equation 3.4 can be simplified to:

$$f_{10} = \frac{c}{2L\sqrt{\varepsilon_{reff}}} \tag{3.5}$$

The relationship between the antenna frequency shift ∂f_{10} and the changes in L and ε_{reff} can be derived by taking the full derivative of equation 3.5[128]:

$$\partial f_{10} = \frac{\partial f_{10}}{\partial \varepsilon_{reff}} \partial \varepsilon_{reff} + \frac{\partial f_{10}}{\partial L} \partial L \tag{3.6}$$

Thus,

$$\frac{\partial f_{10}}{\partial \varepsilon_{reff}} = \left(-\frac{1}{2\varepsilon_{reff}} \right) \frac{c}{2L\sqrt{\varepsilon_{reff}}} = \left(-\frac{1}{2\varepsilon_{reff}} \right) f_{10} \tag{3.7}$$

and

$$\frac{\partial f_{10}}{\partial L} = \left(-\frac{1}{L} \right) \frac{c}{2L\sqrt{\varepsilon_{reff}}} = \left(-\frac{1}{L} \right) f_{10} \tag{3.8}$$

Normalizing ∂f_{10} with respect to f_{10} results in:

$$\frac{\partial f_{10}}{f_{10}} = -\frac{1}{2} \frac{\partial \varepsilon_{reff}}{\varepsilon_{reff}} - \frac{\partial L}{L} \tag{3.9}$$

This equation serves as the theoretical basis for the antenna-based sensors:

- The first expression of the right-hand side represents the sensitivity of the antenna's resonant frequency to the changes of the effective dielectric constant of the sensing area of the antenna, which can be used for monitoring blood glucose levels and PH levels.

- The second term represents the resonant frequency sensitivity of the antenna with respect to changes in radiation patch dimensions, which can be used for strain sensing.

In this thesis, the resonance frequency shift technique is used for:

Liquid sensing: resonance frequency shift can be used in liquid concentration level sensing, such as blood glucose level for diabetes or salinity/sugar concentration. Liquid sensing is based on the principle of measuring changes in the dielectric constant due to a measurand in the sensing area of the antenna. When the effective dielectric constant of the surrounding antenna including the measurand changes, it affects on the resonance frequency of the antenna sensor. The resonance frequency can be defined by the antenna reflection coefficient (S_{11}) plot. In the S_{11} curve between frequency (x-axis) and S11 results (y-axis), the minimum point of the S_{11} curve is determined as the resonance frequency of the antenna-based sensor. Figure 3.8 presents the details for the resonant frequency shift measurement technique for liquid sensing.
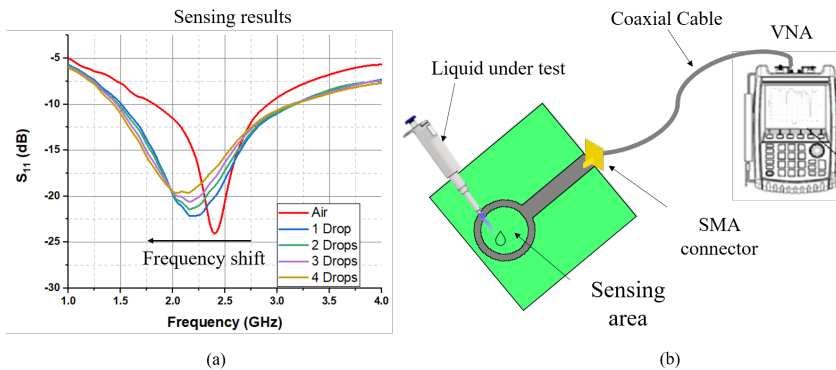
Figure 3.8: (a) Illustration of frequencies shift of the antenna sensor, (b) Measurement setup configuration.

Strain sensing: an antenna sensor for strain sensing is a device that utilizes changes in the mechanical strain applied to it to alter its electrical properties. When the strain is applied, the antenna effective length changes with structural deformation, which influences the resonance frequency of the antenna sensor. This sensing method is used for breathing monitoring. The sensing mechanism is based on the resonance frequency shift of the embroidered antenna-based sensor. When the textile antenna sensor is worn by a human body, its geometry is subjected to significant deformation due to the body's respiration process. As a result, the operation frequency of the antenna-based sensor shifts downward or upward because of the strain applied on the antenna by the chest movement as shown in Figure 3.9.
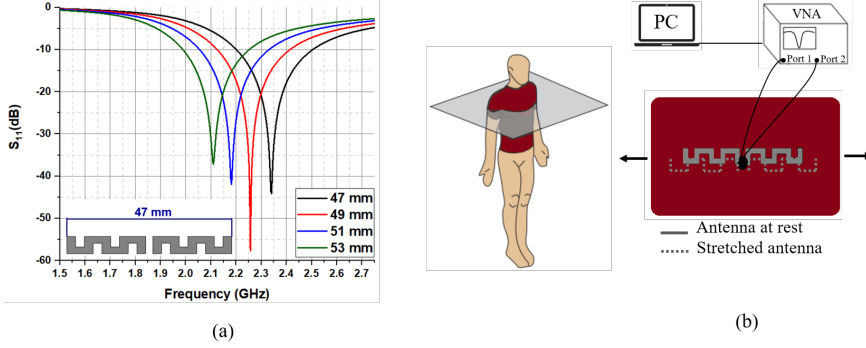
Figure 3.9: S_{11} Simulation results of the antenna-sensor under stretching, (b) Configuration of the proposed antenna-sensor under the stretching caused by the chest expansion during the breathing.

3.5.3 Samples preparation

3.5.3.1 Salinity and sugar concentration

Salt and sugar solutions are ionic compounds. These compounds appear in the ionic state when they are dissolved in water. The solubility of sugar and salt in water at room temperature are 2000 g/l and 360 g/l, respectively. Therefore, sugar is much more soluble in water than salt. Using the following equation, the percentage of salt and sugar concentration is calculated:

$$Mass_{percent} = \frac{M_{solute}}{M_{solution}} \cdot 100 \qquad (3.10)$$

where,
M_{solute}: Mass of solute(g)
$M_{solution}$: Mass of solution(g)
Density of water:

$$\rho = \frac{Mass_{water}}{volume_{water}} = 1 \text{ g/ml} \qquad (3.11)$$

Both compounds are added individually to distilled water to obtain different percentages of salt and sugar concentration using equation 3.10. The mass of the solution is equal to the mass of the solvent (distilled water) plus the mass of the solute (sugar or salt), the mass of water 1g = 1mL according to equation 3.11. Table 3.7 presents the mass of the solute and the distilled water to calculate the percentage of different concentrations of salt and sugar.

Table 3.7: Calculation of the percentage of varying concentrations

Concentration (%)	Mass of solute (g)	Mass of water (g)
5	2.5	47.5
10	5	45
20	10	40

In this thesis, the calculations are carried out to find the 5, 10, and 20 % of sugar and salt concentrated solutions.

3.5.3.2   Blood mimicking by means of aqueous solutions

The entire human blood consists of glucose, water, and other components. Furthermore, water makes up about 92% of an adult's total body weight (Figure 3.10 (a)). Therefore, it can be supposed that the dielectric properties of the blood are related to the properties of aqueous glucose solutions. To imitate the blood behavior for in vitro experiments, several aqueous glucose concentrations are prepared by mixing distilled water and D_Glucose powder for various diabetic conditions of type-2 diabetes. The glucose/water solutions are prepared to verify the functionality of the proposed antenna-based sensor. Figure 3.10 (b) presents the diabetes control chart for three diabetic conditions. The international unit for measuring the concentration of blood glucose is mmol/L.

Formula to calculate mg/dL from mmol/L:

$$mg/dL = 18 mmol/L \tag{3.12}$$

The glucose/water solutions are prepared to cover diabetes patients for three states concerning glucose concentration level (G_{con}):

- Hypoglycemia: $G_{con} \leq 70$ mg/dL.

- Normoglycemia: $80 \leq G_{con} \leq 110$ mg/dL.

- Hyperglycemia: $G_{con} > 120$ mg/dL.

3.5.4   Measurement of different breathing patterns

Monitoring breathing patterns can provide valuable insights into an individual's respiratory health and overall well-being. By analyzing diverse breathing
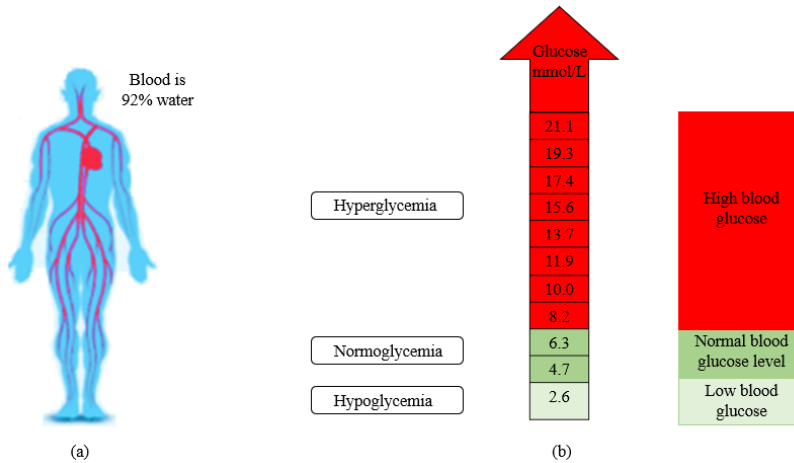
Figure 3.10: (a) Water proportion in the human body, (b) Diabetes control chart.

patterns, researchers and healthcare professionals can identify changes or abnormalities that may indicate underlying medical conditions. Two different methods are addressed in this section.

3.5.4.1 Breathing detection based on resonance frequency shift measurements

In this thesis, two different techniques are used to monitor different breathing patterns. The first one is based on the resonance frequency shift of the antenna-based sensor induced by the chest expansion and the displacement of the air volume in the lungs during breathing. The working principle is based on strain sensing as explained in the previous section.The resonance frequency shift is continuously measured using a VNA linked to a remote PC via LAN interface in real-time. A program via Matlab is developed to collect respiration data information using a PC host via LAN interface to be able to transfer over TCP/IP. The measurement setup configuration is presented in Figure 3.11 (a).

3.5.4.2 Breathing detection based on RSSI measurements

The breathing system is composed of four parts: an embroidered antenna-based sensor integrated into a cotton T-shirt and placed on the middle of the

39
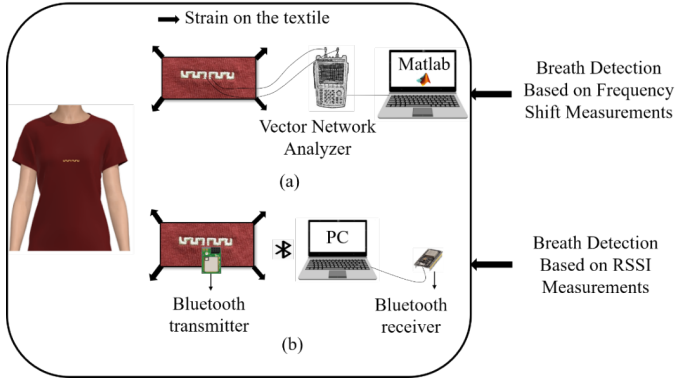
Figure 3.11: Breathing detection systems embedded into textile T-shirt: (a) based on the resonant frequency shift using VNA (b) based on RSSI detected wirelessly using a base station.

human chest, a transmission Bluetooth module, a receiver Bluetooth module, and a base station. The measurement setup configuration is presented in Figure 3.11 (b). The breathing antenna sensor is connected to a Bluetooth transmitter, and during breath, the transmitted signal from the antenna sensor is sensitive to strain caused by the movement of the abdomen and chest wall. The respiratory signal is extracted from the variation of the RSSI signal emitted from the detuned embroidered antenna sensor integrated into a T-shirt. A base station contains a laptop and a receiver Bluetooth which are used to receive the Bluetooth signal from the transmitter antenna sensor. MATLAB is used to collect and visualize the breathing data information in real-time. The block diagram for the breathing monitoring system is shown in Figure 3.12.

3.5.5 Liquid characterization

The determination of the dielectric properties for liquid under test by using an antenna sensor based on Substrate Integrated Waveguide (SIW) technology will be discussed in this section.

The principle of operation is based on the SIW cavity antenna sensor consisting of a circular resonant cavity with a hole in the center to introduce the pipe which contains the liquid under test (Figure 3.13). The cavity resonates on the fundamental mode, whose electric field amplitude is maximum at the center. Furthermore, when the pipe is inserted through the cavity hole, the presence of the liquid under test perturbs the EM field inside the cavity, by

(a)

(b)
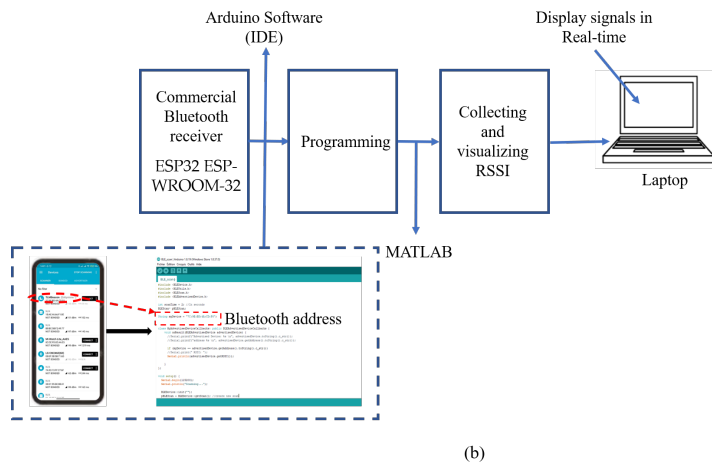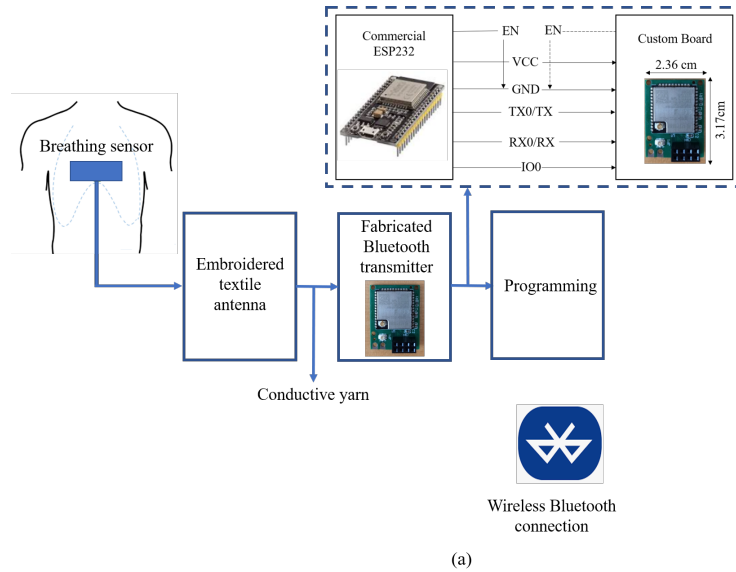
Figure 3.12: Block diagram of breathing monitoring: (a) Wearable unit, (b) Receiver

changing the quality factor and shifting the resonance frequency. To increase the sensitivity of the device, a metal sheath is covered on the wall of the pipe to enhance the penetration of the EM field into the pipe.

This phenomenon is present in Figure 3.14 which shows the amplitude

41
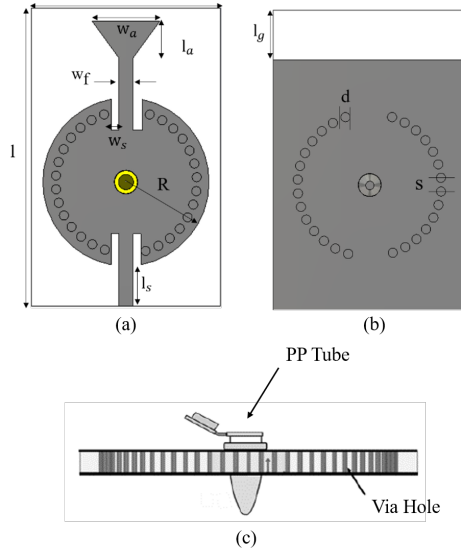
Figure 3.13: Design layout of the proposed sensor: (a) Front view, (b) Back view, and (c) Side view.

of the electric field inside the cavity with and without metal sheath. This permits the electromagnetic field to penetrate profoundly inside the liquid under test and has a better accuracy to retrieve the dielectric properties of Liquid Under Test (LUT).
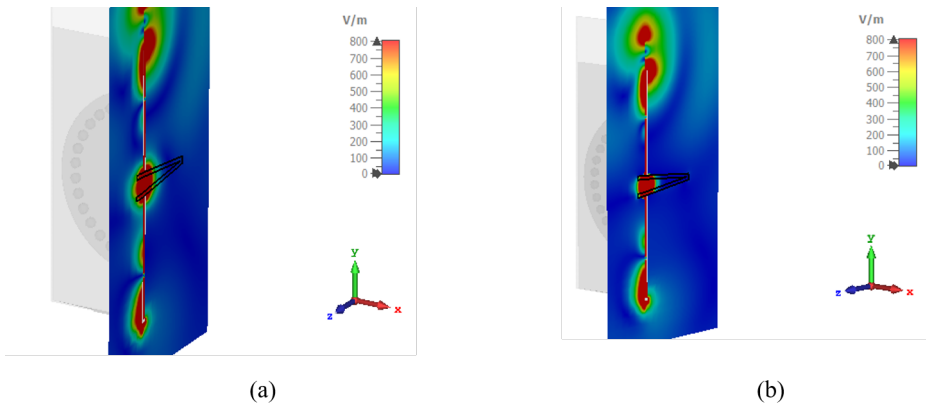
Figure 3.14: Amplitude of the electric field: (a) without metal sheath, (b) with metal sheath

42

The resonance frequency shift and quality factor are two important parameters used to extract the liquid properties. Therefore, the S-parameters allow for determining the resonance frequency and the unloaded quality factor of the cavity and, in turn the EM properties of the liquid under test.

The resonance frequency is calculated as the frequency corresponding to the minimum of S_{11}. Figure 3.15 explains the process calculation of the quality factor from S_{11}, where:
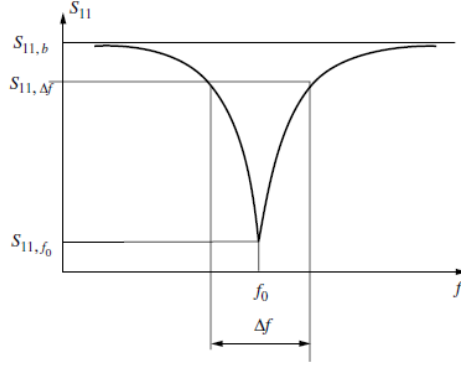
Figure 3.15: Measurement of quality factor from S_{11}.

$$S_{11,\Delta f} = 10 \cdot \log_{10} \left(\frac{10^{S_{11,b}/10} + 10^{S_{12,f0}/10}}{2} \right) (dB) \qquad (3.13)$$

Where, $10^{S_{11,b}/10}$ is the base line of S_{11} is the S_{11} value at the resonance frequency.

The loaded quality factor can be calculated from:

$$Q_L = \frac{f_0}{f_2 - f_1} \qquad (3.14)$$

To obtain the unloaded quality factor (Q_u), the coupling coefficient k has to be calculated from the linear value of S_{11}, f_0:

$$k = \frac{1 - S_{11,f_0}}{1 + S_{11,f_0}} \qquad (3.15)$$

Therefore, the unloaded quality factor can be calculated as:

$$Q_u = Q_L(1 + k) \qquad (3.16)$$

3.5.5.1 Retrieval of LUT dielectric constant

The following process is used to determine the real part of the complex permittivity (ε_r) in terms of the resonant frequency shift. CST simulations are performed, considering the pipe filled with liquids with different dielectric constant ε_r ranging from 1 to 90, to calculate the corresponding frequency shift. The simulated frequency shift $\Delta_f = f_0\text{-}f_{res}$, where:

f_0: represents the resonant frequency in the case of empty or air-filled.

f_{res}: represents the resonant frequency in filled pipe.

The simulation results (simulated resonant frequency shift versus the dielectric constant of LUT) are fit using a curve fitting technique to retrieve the real part of the complex permittivity of the liquid under test from the measured frequency shift.

3.5.5.2 Retrieval of LUT loss tangent

The variation of the unloaded quality factor Q_u is exploited to extract the loss tangent $Tan\delta$ of the liquid under test. The relationship between loss tangent and quality factor can be obtained by:

$$Q_u = \frac{1}{Tan\delta} \tag{3.17}$$

In the simulations, the unloaded quality factor obtained from the system (Q_u^{sim}) contains the losses from the substrate structure and the conductors (defined by Q_{S+c}^{sim} and also the losses from the liquid in the pipe (defined by Q_{liq}^{sim}), therefore:

$$\frac{1}{Q_u^{sim}} = \frac{1}{Q_{liq}^{sim}} + \frac{1}{Q_{S+c}^{sim}} \tag{3.18}$$

Based on 3.18, the value of the quality factor Q_{liq}^{sim}, due to losses in the liquid, can be expressed as:

$$\frac{1}{Q_{liq}^{sim}} = \frac{1}{Q_u^{sim}} - \frac{1}{Q_{S+c}^{sim}} \tag{3.19}$$

Where:

Q_u^{sim}: quality factor calculated from the simulation of the full system including the losses of the liquid pipe.

Q_{S+c}^{sim}: quality factor obtained from the simulation of the system including the losses of the substrate material and conductors and with lossless of the liquid pipe.

An estimation of the losses in the structure can be retrieved from the measurements. Therefore, the quality factor $Q_{S+c}^{m}eas$ can be estimated by the measured quality factor $Q_{U,air}^{m}eas$ of the system with an empty pipe (equation 3.19).

$$Q_{S+c}^{sim} \longrightarrow Q_{S+c}^{meas} = Q_{U,air}^{meas} \tag{3.20}$$

By substituting 3.19 and 3.20 in 3.18, the combination of the measured and simulated quality factor can be obtained from this expression:

$$\frac{1}{Q_u^{sim,ref}} = \frac{1}{Q_u^{sim}} - \frac{1}{Q_{S+c}^{sim}} + \frac{1}{Q_{u,air}^{meas}} \tag{3.21}$$

Where, the first term of the right-hand side contains the losses in the liquid under test, and the second and third terms demonstrate the refinement of the losses in the structure, obtained by replacing the simulated value with the measured one. Furthermore, this proposed technique is based on retrieving the dielectric properties of the liquid injected into the pipe. The dielectric constant (ε_r) of the liquid is retrieved from the shift of the resonance frequency relative to the case of an empty pipe. Particularly, the loss tangent ($Tan\delta$) of the liquid is extracted from the variation of the quality factor, after removing the actual losses of the structure.

4

Results

This section contains the main research findings obtained in this thesis. Over the course of our study, we conducted extensive investigation and analysis to address specific applications. The following subsections will provide different applications, and the corresponding publications from the author will be cited. In particular, we worked on the following cases: textile antenna sensors for in Vitro diagnostics of diabetes, determination of salinity and sugar concentration by means of textile antenna sensor, an embroidered wearable antenna-based sensor for real-time breath monitoring, a wireless communication platform based on an embroidered antenna sensor, and a textile antenna sensor in SIW technology for liquids characterization. By presenting these key findings, we aim to showcase the contributions to developing knowledge and understanding of the topics discussed in this thesis.

4.1 Textile antenna sensors for in Vitro diagnostics of diabetes

Ref B: Gharbi, Mariam El, Raúl Fernández-García, and Ignacio Gil. 2021. "Textile Antenna-Sensor for In Vitro Diagnostics of Diabetes" Electronics 10, no. 13: 1570.

4.1.1 Introduction

Nowadays, the healthcare field has seen great advances in developing wearable antenna sensors to monitor various vital signs and medical conditions. One such breakthrough innovation is the textile antenna sensor, which can be used for monitoring blood glucose levels. By integrating electronics with textiles, this technology provides a discreet, convenient, and real-time solution for individuals dealing with diabetes. Furthermore, electronic textiles could be developed on common garments which are lighter and more comfortable. They can also easily adapt to rapid changes in the computational and sensing conditions of any application.

This section proposes a textile antenna-based sensor for in vitro exper-iments to monitor blood glucose level. The proposed system uses a square ring incorporated within a textile monopole antenna to absorb and sense dif-ferent glucose concentrations through the sensing area. Hence, the substrate dielectric properties are changed according to the properties of the glucose concentration. The experiments are carried out with blood mimicking by us-ing D(+)-glucose with distilled water for various diabetic conditions including hypoglycemia, normoglycemia and hyperglycemia. These differences in glu-cose concentration are detected as different frequency shifts in reflection co-efficient measurements. Moreover, the proposed system demonstrates a proof of concept for monitoring blood glucose level and diagnostics of diabetes. The details of the full research are provided in Ref B.

4.1.2 Structure of the proposed antenna-based sensor design

The design of the proposed antenna sensor is based on a square ring that con-tains the sensing area and a partial ground plane. To design it and perform a realistic simulation, the dielectric properties of the textile substrate need to be defined. A split-post dielectric resonator (SPDR) is used to characterize the dielectric parameters of the substrate as explained in Chapter 3.2.1. Felt is chosen as a substrate due to its low loss tangent and low cost in comparison with other fabrics (see Table 3.1). This antenna-based sensor is designed to

operate at 2.4 GHz. The proposed textile antenna-sensor is embroidered using a professional embroidery machine (Singer Futura XL-550). Figure 4.1(a) illustrates the simulated model which is embroidered by the mentioned technique in the previous section as shown in Figure 4.1(b). A parametric study is carried out by means of a geometric tuning process on various parameters of the proposed antenna-sensor in order to obtain a better understanding of the physical behavior of the antenna sensor and optimize its behavior at 2.4 GHz. Table4.1 presents a list of the optimized geometrical parameters of the proposed antenna sensor.
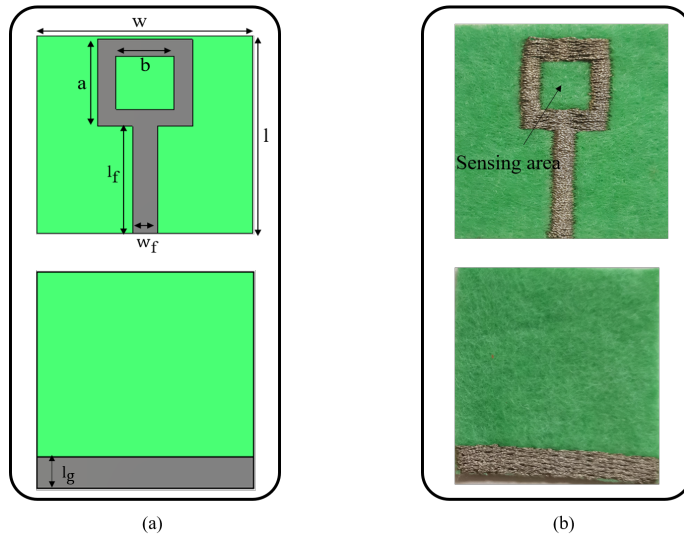
Figure 4.1: (a) Geometry of the proposed antenna sensor, (b) Embroidered prototype.

Table 4.1: Antenna-based sensor parameter dimensions.

Parameters	Dimensions (mm)
w	35
l	35
w_f	3.1
l_f	19
a	15.4
b	9.4
l_g	5

4.1.3 Preparation test

For the sake of simplicity, to mimic the blood behavior, various aqueous glucose concentrations are prepared by mixing distilled water and D (+)- glucose powder. In order to obtain the glucose solutions with different concentration levels, accurate weighing is realized by a precise balance (PCE-BS 300). The glucose/water solutions are prepared to cover various diabetic conditions of type-2 diabetes. Three sets of samples of the proposed antenna sensor are prepared to test different glucose concentration levels G_{con} for:

- Hypoglycemia: $G_{con} \leq 70$ mg/dL.

- Normoglycemia: $80 \leq G_{con} \leq 110$ mg/dL.

- Hyperglycemia: $G_{con} > 120$ mg/dL.

The measurement setup for the preparation test is presented in Figure 4.2. Each set is composed of four newly embroidered antenna sensors for a specific state of diabetes. The proposed antenna sensor is connected to an N9916A FieldFox microwave analyzer operating as a Vector Network Analyzer (VNA) for saving data of the reflection coefficient for the in vitro experiment. A digital micropipette device is used to drop a specific volume of each concentration on the sensing area. In order to reduce the measurement errors due to uncertainty in the solution volume (V), a V=2μL is chosen to test different glucose concentrations. The environmental conditions are maintained during the experiment.
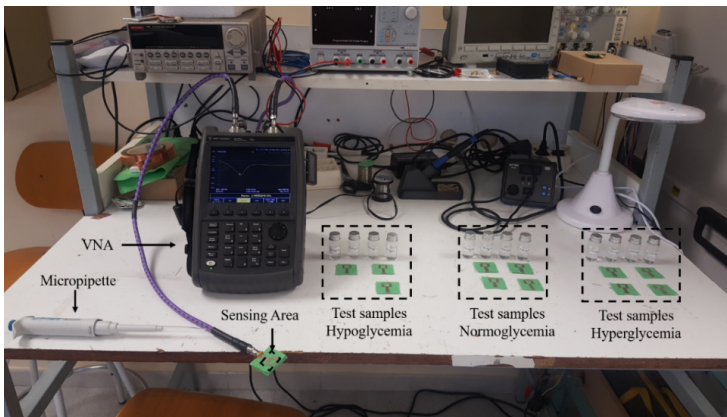
Figure 4.2: Photograph of measurement setup for the preparation test.

4.1.4 Simulation and measurement

The performance of the proposed antenna-sensor is simulated using the commercial CST Studio Suite 3D full electromagnetic simulator. Since, three sets of samples are prepared over three diabetic conditions (hypoglycemia, normoglycemia, and hyperglycemia), each set contains four new antenna-sensors. The initial testing is implemented for different glucose concentrations ranging from 10 to 70 mg/dL to cover diabetes patients with hypoglycemia. A second test is performed to cover patients with normoglycemia (80-110mg/dL). The last test is implemented to reach the indicated concentrations for hyperglycemia ranging from 130 to 190mg/dL. Therefore, 12 antenna sensors are fabricated and measured to verify the implementation of the proposed system. All the fabricated antenna sensors are tested in free space by measuring the S_{11}. The simulated and measured S_{11} for five samples of the fabricated antenna sensors are compared in Figure 4.3. The five samples are taken as an example to emphasize the consistency of our antenna sensor. The S_{11} simulated reaches -24 dB at resonance frequency 2.4 GHz. The measured results of the five antenna sensors have a resonance frequency of 2.4 GHz and exhibited a small declination of the S_{11} amplitude due to embroidery fabrication tolerance.
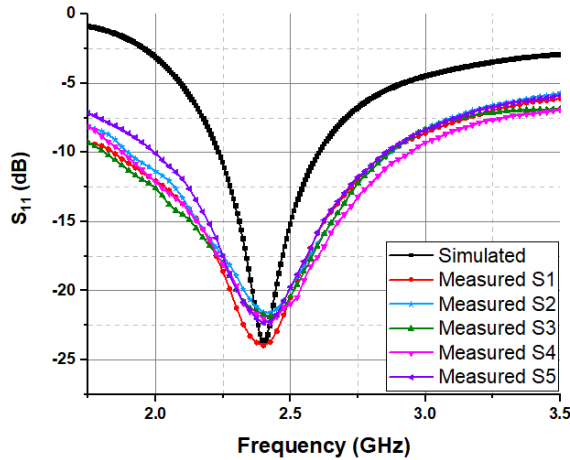
Figure 4.3: Simulated and measured S_{11} of the proposed antenna-sensors in free space.

4.1.5 Results and discussion

The radio frequency (RF) microwave sensing of the glucose level is based on the resonance concept of the antenna sensor. The glucose solutions have dielectric properties that alter the propagation of electromagnetic waves. As glucose interacts with the textile fabric, it causes changes in the dielectric properties of the surrounding medium, altering the resonance frequency of the antenna sensor. Therefore, the frequency shift is considered as the principal sensing parameter of the proposed antenna-sensor. The square ring is selected as the sensing area to apply a drop of $2\mu L$ by micropipette of different glucose concentration. The S_{11} response of each concentration for different diabetic conditions are recorded immediately ($<6s$) after the solution is dropped on the sensing area. Figure 4.4 presents the measured S_{11} of the proposed antenna sensor for the hypoglycemia state. We observed that the resonance frequency of the proposed antenna sensor shifts up when increasing the concentration of the glucose/water solutions. The electromagnetic interaction between the antenna-based sensor and glucose with a different dielectric constant is the main cause of the change in the resonance frequency. After recording the antenna-based sensor performance results, the resonance frequencies resulting from loading a specific glucose concentration can be estimated using linear regression analysis. Figure 4.5 presents the applied linear
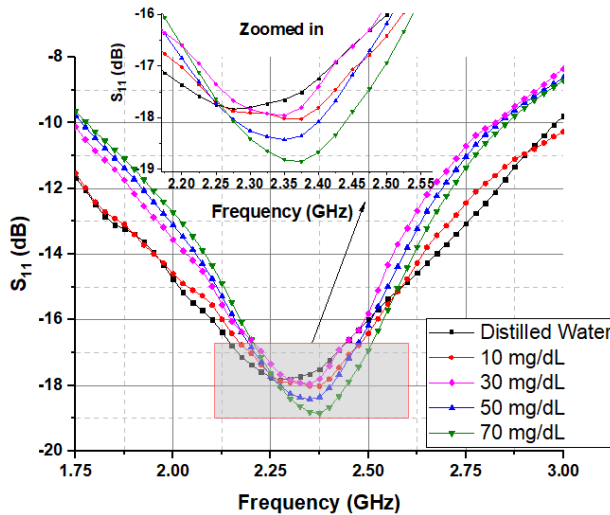
Figure 4.4: Measured S_{11} of the proposed antenna sensor for the hypoglycemia state.
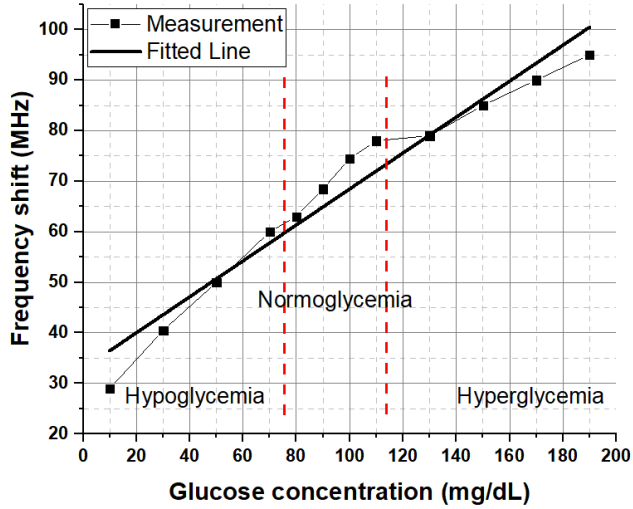
Figure 4.5: Linear correlation for the frequency shift as a function of glucose concentration in different diabetic conditions.

regression of the resonance frequency shift for the different diabetic conditions. It can be observed that the results show a good linear relationship between different glucose concentrations and the resonance frequency shift. The obtained results demonstrate a correlation coefficient (R^2) of 0.96 between the indicated concentrations and the resonance frequency shift.

The sensitivity (S) of the proposed sensor is calculated by:

$$S = \frac{\Delta f}{\Delta c} \text{MHz/mgdL}^{-1} \tag{4.1}$$

The measurement results of the proposed antenna-sensor succeed to differentiate different glucose concentrations for different diabetic conditions. In order to demonstrate the performance of our device, Table 4.2 presents a comparison of the proposed antenna-based sensor with previous works. It can be observed that the proposed sensor offers a higher sensitivity in comparison with other sensors reported in the literature which are based on diverse sensing mechanisms.

Furthermore, the proposed antenna sensor has a compact size comparing areas with other works. All of the antenna sensors reported in Table 4.2 used rigid substrates. Therefore, the proposed work is a novel approach for monitoring blood glucose levels based on a textile antenna.

Table 4.2: Comparisons of different methods for monitoring glucose concentration using microwave sensors.

Ref	Measurement technique	Concentration (mg/dL)	Area (mm^2)	f_r(GHz)	Substrate	Sensing parameters	S (kHz per mg/dL)
[[129]	Rectangular Waveguide Cavity	0-25000	110 x 54.5	1.9	Rigid	$f_r(S_{21})$	0.4
[[130]	Inverted F Antenna (PIFA)	0-530	38 x 38	0.53	Rigid	$f_r(S_{11})$	3.54
[[131]	CSRR resonator	70-150	59 x 20	1-6	Rigid (FR-4)	$f_r(S_{21})$	67-11
[[132]	Split ring resonator	0-5000	50 x 20	4.18	Rigid (Rogers)	$f_r(S_{21})$	26
[[133]	Microstrip Patch Antenna Sensor	0-400	42.97 x 34.60	2.4	Rigid	$f_r(S_{21})$	25
[[134]	Transmission lines	0-347.8	-	16	Rigid	$f_r(S_{11})$	16.4
[[135]	Single-port sensor	100-1000	55 x 30	4.8	Rigid (Rogers)	$f_r(S_{11})$	14
This work	Monopole Antenna Sensor	0-190	35 x 35	2.4	Textile	$f_r(S_{11})$	350

4.1.6 Conclusion

In this section, a textile monopole antenna sensor is proposed to monitor glycemia levels for diabetes. The proposed sensor is tested in vitro experiments to verify the functionality of the microwave glucose antenna sensor. The sensing method is based on the absorption of different glucose/water concentrations by the textile substrate in the sensing area. The sensing parameter is based on the resonance frequency of the reflection response. A linear regression is applied to the resonance frequency shift and it can be clearly seen a good correlation between glucose concentration and the frequency shift. Furthermore, the results demonstrated the ability of the proposed device to cover different glucose levels of diabetes, hypoglycemia, normoglycemia, and hyperglycemia with a sensitivity of 350 kHz/(mg/dL). The proposed antenna-based sensor, besides its capability to monitor glucose levels, presents various other features such as miniatured size, simple design, and low cost. Such attractive characteristics promote the proposed sensor to be used as a preliminary screening for monitoring blood glucose levels.

4.2 Determination of salinity and sugar concentration by means of textile antenna sensor.

Ref C: Mariam El Gharbi, Marc Martinez-Estrada, Raul Fernández-García and Ignacio Gil, "Determination of Salinity and Sugar Concentration by Means of a Circular-Ring Monopole Textile Antenna-Based Sensor," in IEEE Sensors Journal, vol. 21, no. 21, pp. 23751-23760, 1 Nov.1, 2021.

4.2.1 Introduction

The accurate and rapid assessment of salinity and sugar concentration in various liquids is of extreme importance in different areas. However, recent advancements in sensor technology, specifically textile antenna sensors, have opened up new approaches for efficient and cost-effective analysis. Moreover, the use of textile antenna sensors offers opportunities for cost-effective and scalable solutions. Textiles are affordable, readily available, and can be easily fabricated in huge quantities. By exploiting the electromagnetic properties of these textiles, it is possible to design antenna sensors capable of detecting and quantifying salinity and sugar concentration in liquids.

In this section, an innovative method used the microwave signals to monitor and measure different concentrations of salt and sugar. The measurements are provided by a fully textile circular-ring antenna sensor operating at 2.4GHz. The sensing approach is based on the absorption of salt and sugar concentration by the textile substrate. Different concentration of salt and sugar are identified through variations in frequency shifts and magnitude levels observed in reflection coefficient measurements. Moreover, to assess the rinsing reliability of the antenna sensor, we conducted reflection measurements by applying different amounts and concentrations of salt and sugar before and after the rinsing process. The details of the full research are provided in Ref C.

4.2.2 Antenna sensor design and analysis

The selection of appropriate materials for the conductive and non-conductive elements of an antenna sensor is critical, particularly when targeting properties such as lightweight, low-profile, compactness, and flexibility. It is necessary to choose cost-effective, flexible and thinner materials in order to create an antenna suitable for wear potential. In this work, we used a felt textile material as an appropriate substrate due to its dielectric constant (ε_r=1.2) and low tangent loss $Tan\delta$=0.0013. Figure 4.6 shows the antenna-based sensor configuration proposed in this study. It consists of a monopole antenna with a circular ring shape and a partial ground plane. Table 4.3 presents the optimal geometric parameters of the antenna sensor. The proposed textile antenna sensor is designed and simulated by means of the full 3D electromagnetic CST Microwave Studio software at a 2.4 GHz operation frequency. The antenna has a circular ring slot of length 7.7 mm as shown in Figure 4.6. The slot is incorporated to help absorb saline/sugar solutions. Absorbed solutions with different characteristics change the substrate dielectric properties and
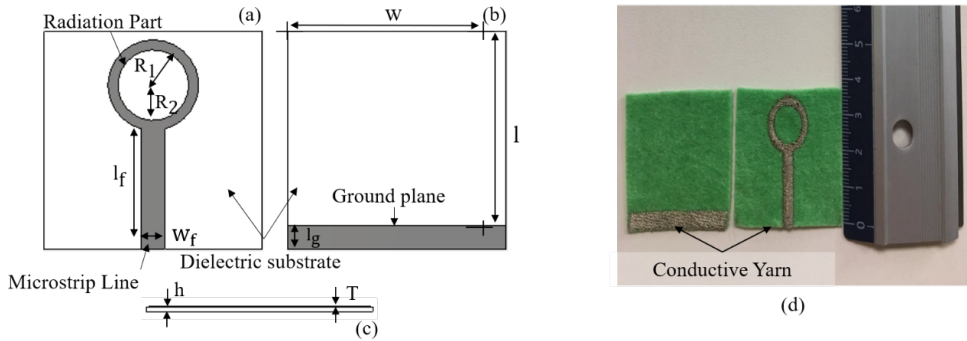
Figure 4.6: Geometry of the proposed antenna sensor, (a) Front view, (b) Back view, (c) Side view, and (d) Embroidered prototype.

Table 4.3: Size parameters of the design.

Parameters	Dimensions (mm)
w	37
l	37
w_f	3.1
l_f	21
R_1	7.7
R_2	6
h	0.7
l_g	4

thus reflection measurements will change accordingly.

4.2.3   Antenna sensing methodology and solution preparation

The key idea in this work is to use the textile material to absorb salt and sugar solutions, which then changes the dielectric constant of the textile. When different concentrations of salt and sugar are dropped on the sensing area, the dielectric constant is expected to change according to the concentration level because each concentration induces its own (and different) dielectric constant of the mixture medium of substrate material and solution. The frequency of minimum reflection and corresponding magnitude of the reflection coefficient (S_{11}) before and after applying different solutions are recorded and compared. The differences between these two recorded measurements for dry

and wet antenna sensor are related to changes in the dielectric properties
of the substrate. This process can be used to collect a sample during an
examination, so that both quantity and content are of interest.

To validate the operation of the proposed antenna sensor, different con-
centrations of salt and sugar solutions of 5%, 10%, and 20% are prepared.
Both compounds are added individually to distilled water to obtain different
percentages of salt and sugar concentration. Various concentration calcula-
tions of salt and sugar are shown in the previous section. Different solution
volumes are tested using a polyethylene graduated transfer Pasteur pipette
with salt or sugar solutions on the sensing area of the proposed antenna sen-
sor. Thereafter, the resonance frequency and the magnitude of the reflection
coefficient variations are detected and recorded. The S11 is measured by using
an N9916A FieldFox microwave analyzer operating as Vector Network Ana-
lyzer (VNA) in a laboratory environment. The configuration of the proposed
antenna sensor setup is shown in Figure 4.7.
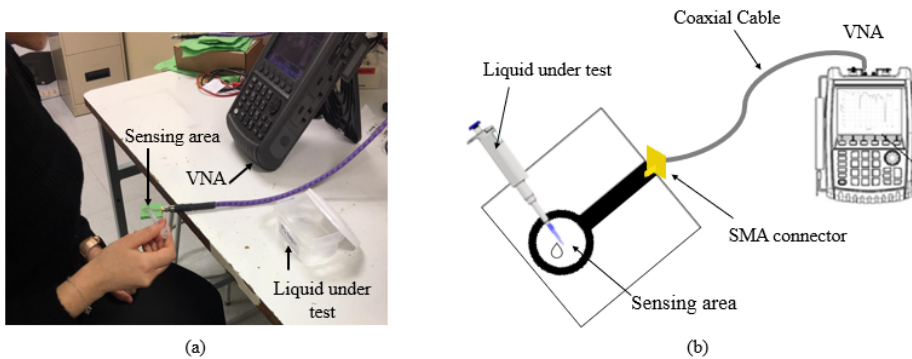
Figure 4.7: Measurement setup for the preparation test, (a) Photograph of
measurement setup, (b) configuration of measurement setup.

4.2.4 Experimental measurements and performance

The proposed antenna sensor is tested in terms of detecting the amount of
salt/sugar concentration solution. Six new fabricated antenna sensors are
prepared and different quantities and concentrations are applied to each sen-
sor. Three of the fabricated antenna-sensors are assigned to detect different
amounts and concentrations of salt solution and the last three are customized
to detect sugar concentration. To enhance measurement accuracy and re-
duce errors due to uncertainty in solution volume, a polyethylene graduated

transfer pipette is used in the experimental setup. This pipette allowed the precise dispensing of a predetermined volume of liquid samples into the sensing area. All the prepared solutions are performed at room temperature of $25\pm1°C$ to minimize the environmental effect on the collected measurements and preserve consistent operating conditions for all data. To generate high-accuracy measurement results, it is necessary to drop the liquid under test within an area of strong electric field intensity. The quantities varying from 1 to 4 drops, each drop equivalent to 0.08 mL. Different quantities are applied to each antenna sensor with different concentrations of salt/sugar.

The simulated and measured S_{11} in free space and with distilled water for three examples of antenna sensor samples (A1, A2, and A3) are presented in Figure 4.8 Note that A1, A2, and A3 are assigned for measuring different amounts of salt concentrations. Therefore, the proposed textile antenna sensors demonstrated good matching between the simulated and the measured results. By applying distilled water to the sensing area of the three antenna sensors, the resonance frequency in free space experienced a shift to 1.68 GHz. This shift can be attributed to the higher dielectric constant of the distilled water. All the antenna sensors are presented a good impedance matching with return loss below -10 dB. However, there are minor variations noticed, which could possibly be attributed to the tolerance levels in the embroidery
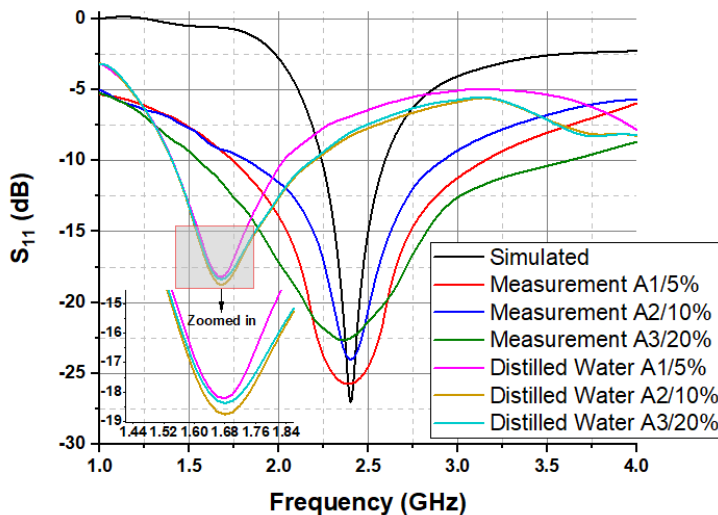
Figure 4.8: Simulated and measured S_{11} versus frequency for three antenna sensors samples in free space and with distilled water.

manufacturing process. In order to maintain result consistency, various concentrations, and quantities are used to test each antenna sensor. Sample testing is performed at room temperature. The salt/sugar solution is applied in 4 consecutive rounds of 1 drop (0.08 mL) each. The presented results are recorded instantly (< 10 s) after the test sample is dropped into the sensing area.

Results shown in Figure 4.9 represent the calculated resonance frequency shift for different salt concentrations and quantities. The resonance frequency shift increases as the quantity of salt increases at various concentrations. Based on the obtained results, it can be concluded that each salt concentration exhibits a distinct resonance frequency shift. This fact is key to achieve a good salinity detector. A linear regression is applied to analyze the resonance frequency shift with different salt concentrations and quantities as presented in Figure 4.9. The three antenna sensors demonstrate high sensitivities of 550, 475, and 325 MHz/mL for 5%, 10%, and 20% respectively. Each of the three solutions of different salt concentrations are applied to a textile antenna sensor in increments of drops, and the changes in the magnitude of S_{11} are recorded after the application of each drop. These results indicate that the presented textile antenna sensor is able to differentiate between different amounts of salt concentration. To detect different amounts of sugar concentration, three sample antennas A4, A5 and A6 of the same dimensions and materials as
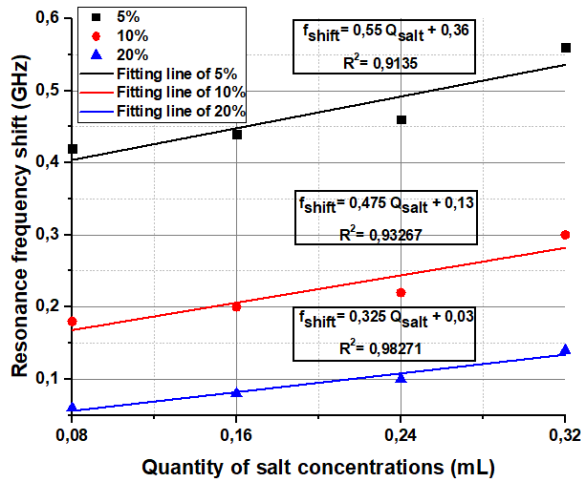
Figure 4.9: Linear regression of the calibration curve of the resonance frequency shift at different salt concentrations and quantities.

shown in Figure 4.6 are prepared. Each antenna sensors A4, A5, and A6 are assigned to measure three different amounts of sugar concentrations: 5%, 10%, and 20%, respectively. The amounts varying from 1 to 4 drops (1 drop = 0.08mL). The aim of this experiment is to monitor the effect of sugar solutions on the antenna sensor's performance. During testing, the first solution is carefully dropped into the sensor, drop by drop, while measuring changes in resonant frequency after each application. This process allowed us to monitor the immediate impact of each droplet on the behavior of the sensor. The results of applied linear regression analysis of the resonance frequency shift at different sugar concentrations and quantities are presented in Figure 4.10. Based on the obtained data, it can be concluded that each sugar concentration exhibits a resonance frequency shift, which is crucial for developing an efficient sugar detector. The applied linear regression analysis, as presented in Figure 4.10, shows a good linear fit of R2 = 0.9827 (R=correlation coefficient) of 10% of sugar. The three antenna sensors exhibit notable sensitivities of 550, 325, and 500 MHz/mL for sugar concentrations of 5%, 10%, and 20%, respectively. From the obtained results, we explore the ability of the textile antenna sensor to differentiate between different quantities of sugar concentrations.
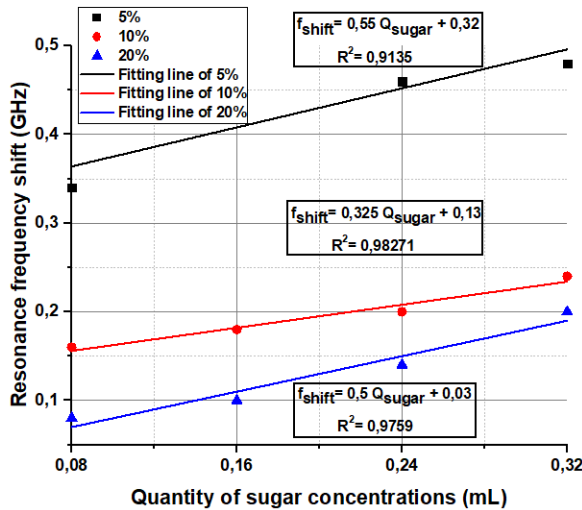
Figure 4.10: Linear regression of the calibration curve of the resonance frequency shift at different sugar concentrations and quantities.

4.2.5 Reliability of the textile antenna sensor

In order to evaluate the reliability of the proposed antenna sensors, two extra textile antenna sensors are fabricated to test diverse quantities and concentrations of salt and sugar solutions. The measurements are divided into two parts. The initial part comprised three salt solutions with concentrations of 5%, 10%, and 20%, which are applied to one of the fabricated antenna sensors. After testing the antenna sensor with different quantities of 5% salt concentration, we rinsed the antenna sensor and dried it for reuse for testing the two last concentrations. The embroidered antenna sensor underwent a manual rinsing process using tap water. Subsequently, the textile antenna sensors are subjected to multiple rinses, each lasting 10 minutes. The second part consists of three sugar solutions with identical concentration and procedure as the salt. After drying the proposed antenna sensor, the return loss is recorded to evaluate the performance degradation in terms of the resonance frequency. To assess the repeatability error of the antenna sensor, the measurements are conducted four times for each concentration. As mentioned, the first part is dedicated to evaluate the impact of rinsing in detecting salt concentration. Only a single antenna sensor is used, which is rinsed each time for detecting different salt concentrations and amounts ranging from 0.08 mL to 0.32 mL. Note that the resonance frequency of the textile antenna sensor remains unchanged even after rinsing, and its performance reverts back to its original state. This confirmed that the proposed antenna sensor is not damaged during wetting. The resonance frequency shift with different salt concentrations and quantities are analyzed using linear regression. The applied linear regression analysis for the rinsed antenna presented in Figure 4.11 reveals a good correlation with the linear fit between different quantities of salt concentrations and resonance frequency shift. The rinsed antenna sensor exhibits high sensitivities of 800, 350, and 337.5 MHz/mL for 5%, 10%, and 20% of salt, respectively. By comparing the previous results of Figure 4.9 and Figure 4.11, they reveal that the resonance frequency shifts in both cases (dry and wet) maintain the same behavior (the frequency of the resonant frequency increases with the increasing amount of salt in all concentrations). This is due to the fact that the textile antenna sensor is not damaged during wetting and therefore we obtain significant reliability. The second part is dedicated to evaluate the effect of rinsing in detecting sugar concentration. Only a single antenna sensor is rinsed each time for detecting different sugar concentrations and quantities varying from 0.08 mL to 0.32 mL. A linear regression of the calibration curve of the resonance frequency shift at different sugar concentrations and quantities is presented in Figure 4.12. Based on the
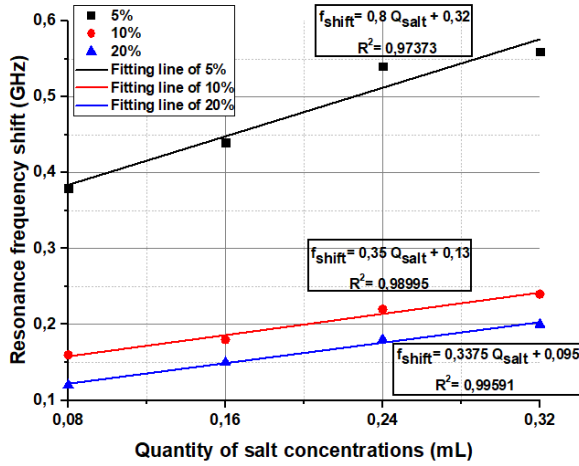
Figure 4.11: Linear regression of the calibration curve of the resonance frequency shift at different salt concentrations and quantities after rinsing.
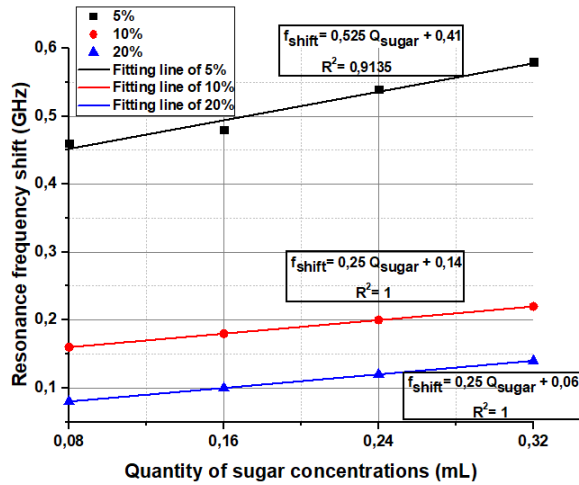
Figure 4.12: Linear regression of the calibration curve of the resonance frequency shift at different sugar concentrations and quantities after rinsing.

obtained results, we observed that the textile antenna sensor is not damaged during wetting, which indicates good reliability. The applied linear regression analysis demonstrates a good correlation with the linear fit between resonance frequency shift and different quantities of sugar concentrations. The rinsed antenna sensor exhibits high sensitivities of 525, 250, and 250 MHz/mL for

5%, 10%, and 20% of sugar, respectively. Based on the results presented in this section, it can be inferred that the proposed antenna sensor maintained its performance even after rinsing. This indicates that the rinsing process has no appreciable detrimental effect on the performance of the antenna sensor.

4.2.6 Conclusion

This work presents a proof of concept for a new approach using an embroidered fully textile antenna-based sensor to detect different concentrations of salt and sugar concentrations using microwave signals. The sensing mechanism relies on the absorption of salt and sugar solution into a felt textile substrate through a circular ring integrated into the radiating element. Changes in reflection-based measurements are used to detect salt and sugar concentrations. The proposed textile antenna sensor demonstrated its ability to distinguish between different amounts of salt and sugar concentrations, ranging from 1 to 4 droplets. The proposed antenna sensor demonstrates a high sensitivity of 800 MHz/mL and 550 MHz/mL for 5% salt and sugar concentration solutions, respectively. In addition, we assessed the rinsing reliability of the textile antenna sensor by measuring the S_{11} of varying amounts and concentrations of salt and sugar. This evaluation is used to ensure that the antenna sensor remains undamaged when exposed to wet conditions. The proposed antenna sensor offers several benefits, including high sensitivity, compact size, consistent performance, and no fabrication complexities.

4.3 Embroidered wearable antenna-based sensor for real-time breath monitoring

Ref D: El Gharbi, Mariam, Raúl Fernández-García, and Ignacio Gil. "Embroidered wearable Antenna-based sensor for Real-Time breath monitoring." Measurement 195 (2022): 111080.

4.3.1 Introduction

An embroidered wearable antenna-based sensor presents immense potential for real-time breath monitoring. The integration of the antenna into clothing, enables continuous monitoring of breathing patterns, offering a comfortable and convenient solution for individuals with breathing conditions. This approach enables healthcare professionals to collect timely and accurate data

on breathing patterns, facilitating early detection of breathing and health abnormalities.

This work introduces a new embroidered meander dipole antenna-based sensor for real-time breath detection using the technique based on chest well movement analysis. The proposed antenna-based sensor is placed on the middle of the human chest and takes into account the user's comfort with no movement constraints. The sensing mechanism is based on the resonance frequency shift of the antenna- based sensor, which is caused by the movement of the chest and the displacement of air volume in the lungs during breathing. Respiration data information is consistently monitored in real-time using a Vector Network Analyzer (VNA), and the data is transmitted to a remote PC through a LAN interface, using MATLAB. The measurements aimed to monitor the breathing patterns of volunteers under different scenarios (standing and sitting) at diverse breathing conditions: eupnea (normal respiration), apnea (no breathing), hyperpnea (deep breathing), and hypopnea (shallow breathing). The details of the full research are provided in Ref D.

4.3.2 Mechanism of breathing detection

A simplified illustration of the lungs during inspiration and expiration is shown in Figure 4.13(a). During respiration, the volume of the respiratory system alters due to the movement of the abdomen and chest wall caused by contractions of the intercostal muscles and the diaphragm. During inhalation

Figure 4.13: (a) Simplified illustration of the lings during inspiration and expiration, (b) Geometry of the proposed antenna sensor, (c) Embroidered prototype.

(inspiration), the diaphragm contracts, leading to the downward movement of the abdominal organs and a subsequent reduction in intrathoracic pressure. Conversely, during exhalation (expiration), the intercostal muscles and diaphragm relax, the abdomen and chest take back relax position and lung volumes decrease as shown in the lower portrait of Figure 4.13(a). A technique based on the analysis of chest wall movement is used to monitor breathing using a meander dipole embroidered antenna sensor integrated into a cotton T-Shirt. The proposed antenna sensor is positioned in the center of the human chest. Breath sensing is accomplished by detecting the mechanical thoracic chamber changes with the resonance frequency variation of the embroidered antenna sensor. These changes are caused by the movement of the abdomen and chest during respiration.

4.3.3 Antenna sensor design

The material used for the antenna conductive part is a commercial Shieldex 117/17 dtex 2-ply material. This specific conductive yarn available in the market is composed of 99% pure silver-plated nylon yarn 140/17 dtex, which ensures excellent conductivity. For the dielectric (nonconductive) part, a cotton substrate of a commercial T-shirt is used. The dielectric properties of the T-shirt are characterized using a Split Post-Dielectric Resonator (SPDR). The cotton relative dielectric constant and loss tangent are ε_r=1.3 and $Tan\delta = 0.0058$, respectively. On the other hand, the thickness of cotton substrate is of 0.464 mm, measured using an Electronic Outside Micrometer. To begin the design process, we started with a conventional dipole antenna, which is known for its large dimensions. Next, we performed a comprehensive analysis of several parameters, aiming to reduce its size and improve its performance specifically at 2.4 GHz. As a result, we successfully achieved a significant reduction of up to 54% in the overall size of the proposed folded meander dipole antenna when compared to the normal textile dipole reported in the literature [136]. The proposed antenna sensor is integrated into a commercially available T-shirt at the pectoral region of the chest. The optimized parameters of the antenna sensor are presented in Figure 4.13 (b), with: W =45 mm, L =4.8 mm, d =7.6 mm, g =2 mm.

4.3.4 Data collection and treatment

The textile dipole antenna-sensor is integrated into the T- Shirt to monitor respiration data with the help of a woman volunteer in a laboratory environment. The main feature of the proposed antenna sensor is the reso-

nance frequency shift exhibited due to the change of lung volume and textile stretching under the chest movement. In order to evaluate this concept, a Vector Network Analyzer (VNA) is connected to a PC host for data processing through a LAN interface. Respiration data is recorded and processed in a MATLAB environment. Figure 4.14 illustrates the configuration of the measurement setup for real-time respiration detection using the antenna sensor integrated into a T-Shirt. The volunteer is asked to proceed two different positions (standing and sitting) for monitoring different breathing patterns, including eupnea, apnea, hypopnea (shallow breathing) and hyperpnea (deep breathing). A MATLAB program is developed to gather breathing data information from VNA. The most important step is to configure the VNA with the same IP address used in the PC host via LAN interface to be able to transfer data with instrumentation over TCP/IP. The program is able to detect continuously respiration data information and measure the resonant frequency shift. The obtained breathing signals are compared with the standard respiration signal for different breathing patterns, as explained in Figure 4.15. Respiratory signals manifest in different ways that are determined by breathing patterns. These breathing patterns can be categorized into four common types of respiration, as illustrated in Figure 4.15. The eupnea represents the natural respiration of an individual during relaxed conditions. Apnea refers to stopping breathing. Hypopnea refers to decreased signal amplitude due to shallow breathing. The hyperpnea is a deep breathing, the amplitude of the signal breathing is higher than the eupnea. Table 4.4 provides an overview of typical breathing patterns along with their descriptions and possible causes. Therefore, continuous monitoring of breathing is critical to evaluate the subject's health status, as it helps in the identification, diagnosis, and treatment of various pathological conditions.
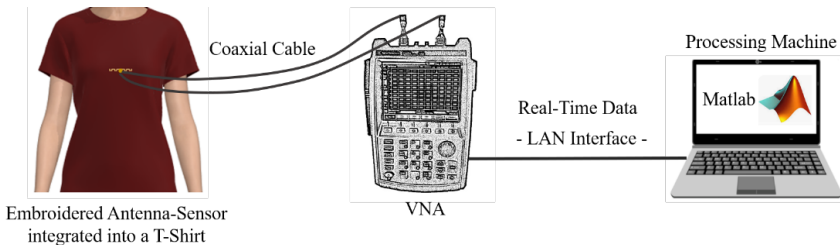
Figure 4.14: Measurement setup configuration.
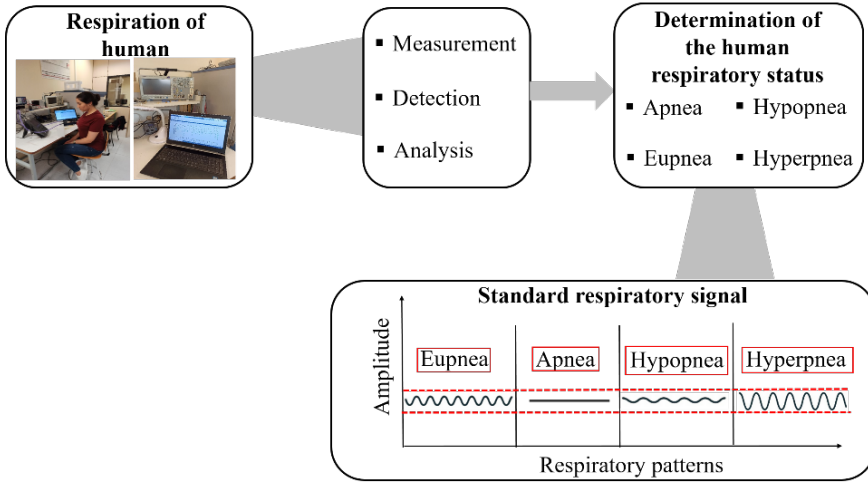
Figure 4.15: Process to detect human respirtory status.

Table 4.4: Different breathing patterns and their causes.

Breathing Patterns	Description	Causes
Eupnea	Quiet breathing or resting respiratory rate	Normal breathing
Apnea	Absence of breathing	Diabetes, Heart failure, cardiomyopathy
Hypopnea	Shallow breathing or an abnormally low respiratory rate	Anxiety, Asthma, Pneumonia, Shock, Pulmonary Edema
Hyperpnea	Increased rate and depth of breathing	Emotional stress, Diabetic ketoacidosis

4.3.5   Results and analysis

The antenna resonant frequency is mainly determined by the parameters S, more especially S_{11}. The proposed antenna sensor prototype is characterized in terms of S11 and Specific Absorption Rate (SAR) to evaluate its performance for wireless communication. The antenna-sensor integrated into the T-shirt is tested by measuring S_{11} using the Vector Network Analyzer in order to verify the accuracy of the embroidery technique. The simulated and measured S_{11} for the proposed antenna-sensor is presented in Figure 4.16. Based on this figure, we can observe that the experimental measurement of the S_{11} has a good agreement with the numerical simulation result. Both the experimental and simulated results are obtained at an operating frequency of
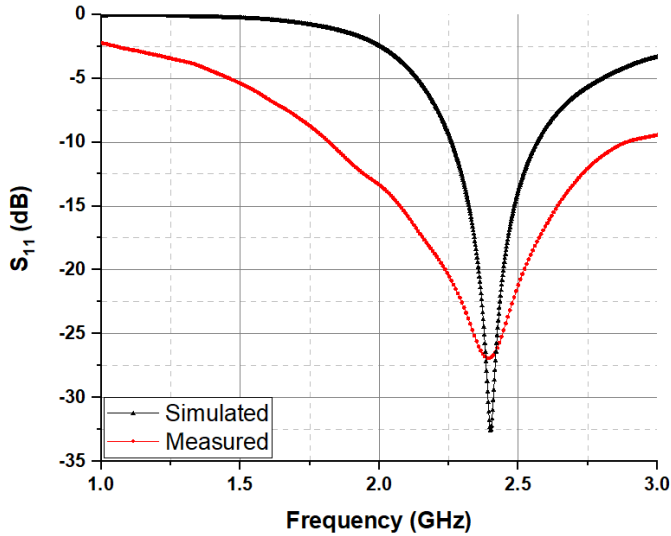
Figure 4.16: Simulated and measured S_{11} of the textile meander dipole antenna-based sensor.

2.4 GHz. However, slight variations in the S_{11} amplitude are noticed due to manufacturing tolerance process. The operating frequency of 2.4 GHz belongs to the ISM (Industrial, Scientific, and Medical) band and is chosen according to the requirements of medical monitoring applications.

Since the proposed antenna-sensor operates close to the human body, it becomes crucial to take into account the absorption rate of radio frequency (RF) energy in the surrounding tissues. The Specific Absorption Rate (SAR) serves as a measure of the power absorbed by biological tissue when exposed to an RF electromagnetic field. Specific Absorption Rate (SAR) plays an important role in ensuring the safety of individuals exposed to Radio Frequency (RF) energy. The Institute of Electrical and Electronics Engineers (IEEE) and the International Commission on Non-Ionizing Radiation Protection (ICNIRP) have set recommended SAR limits, which are referenced in the section 3.4 (chapter 3). Since the proposed breathing sensor can be used by people of different ages and gender such as monitoring the respiration status of a newborn infant, different voxel models are used for simulation the SAR under two standards. Table 4.5 presents the results of a comprehensive SAR analysis conducted by performing simulations on various voxel models of different ages, sizes, and weights. The table includes the absolute SAR values and the corresponding safety percentage (%) in relation to the standard

Table 4.5: Specific absorption rate values at different voxel model and standards.

Voxel model	Age (Year)	Size (cm)	Mass (kg)	Sex	Resolution/mm	SAR (1g) W/kg	SAR (10g) W/kg
Baby	8-weeks	57	4.2	F	0.85 x 0.85 x 4	1.53 (4%)	0.86 (57%)
Child	7	115	21.7	F	1.54 x 1.54 x 8	1.54 (4%)	0.064 (96%)
Donna	40	176	79	F	1.875 x 1.875 x 10	0.295 (81%)	0.141 (92%)
Emma	26	170	81	F	0.98 x 0.98 10	0.878 (45%)	0.414 (79%)
Gustav	38	176	69	M	2.08 x 2.08 x 8	1.57 (2%)	0.786 (60%)
Laura	43	163	51	F	1.875 x 1.875 5	0.489 (69%)	0.247 (87%)
Katja	43	163	62	F-P	1.775 x 1.775 x 4.84	0.456 (71%)	0.226 (88%)
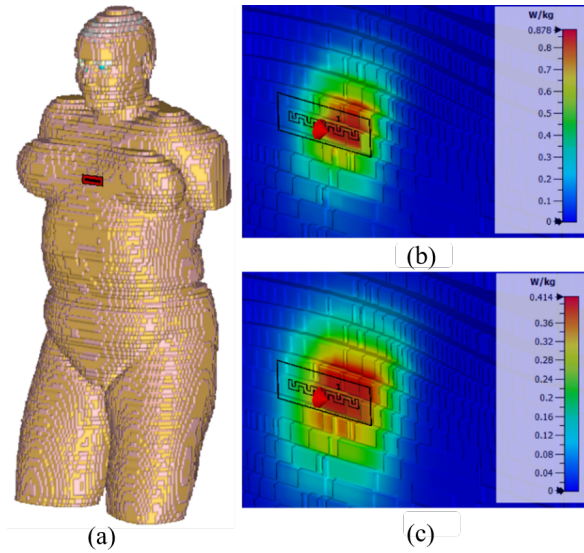
Figure 4.17: (a) Antenna-sensor on human Emma voxel model, SAR at 2.4GHz: (b) 1g, (c) 2g.

SAR limits. This table shows that the proposed breathing sensor offers an acceptable SARs at different voxel model for both standards. As an example, the proposed antenna-sensor is placed on the chest of a realistic Emma voxel human model with a SAR distribution at 2.4 GHz for two standards (1 g and 10 g) as shown in Figure 4.17.

The main concept of this study is to validate the integration of an antenna-sensor into a commercially available T-Shirt for real-time breathing monitoring. A female volunteer (28 years old, 1.67 cm tall, weighing 70 kg) with

similar characteristics to the human Emma voxel model participated in the breathing tests. Real-time simulations of various respiratory patterns, as described in Table 4.4, are performed by the volunteer. Figure 4.18 depicts a photograph of the volunteer wearing the T-shirt during laboratory testing while sitting and standing. To assess the feasibility and consistency of the proposed antenna-based sensor, several experimental tests are conducted to monitor different breathing patterns, including eupnea, apnea, hypopnea, and hyperpnea. During the test, the volunteer is asked to:

- Normal breath.

- Deep breaths (hyperpnea) followed by shallow breaths (hypopnea).

- Deep breaths (hypernea) followed by apnea (absence breathing).

For the normal respiration (eupnea), the female volunteer is asked to breathe normally and at ease in different positions (standing and sitting on a chair). During the apnea test, there is no air exchange either through the mouth or the nose means that no diaphragmatic and intercostal muscle activity. The resonant frequency shift is continuously measured using an N9916A FieldFox microwave analyzer operating as Vector Network Analyzer (VNA) to a remote PC via LAN interface in real-time. The volunteer is then instructed to engage in deep breathing (hyperpnea), causing the resonance frequency to shift to 3.2GHz. Next, the volunteer switched to shallow breathing (hypopnea), which shifted the resonant frequency to 2 GHz (Figure 4.19(b)). The

(a)   (b)
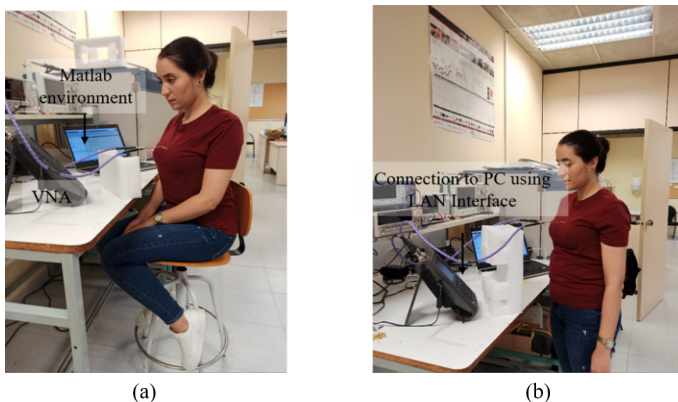
Figure 4.18: Photograph of the embroidered antenna-based sensor into a cotton T-shirt under laboratory testing for different scenarios, (a) sitting, (b) standing.

hypopnea has a low breathing signal according to a low respiratory taking by the volunteer. During apnea, the volunteer begins a deep inhalation, followed by a pause in breathing for several seconds (Figure 4.19(c)), without exchanging air through the mouth or nose. It can be seen that the signal becomes saturated across different breathing patterns, as the female volunteer maintains a constant breathing cycle during inhalation, which displays the accuracy of the proposed system for different breathing patterns. The peak saturation of the curve for apnea is due to the absence of respiration, and this corresponds to the standard breathing signal. The obtained results demonstrate that our antenna is able to monitor different breathing patterns. The measurements are repeated in sitting position for different breathing patterns as shown in Figure 4.20. In the case of normal breathing (eupnea), a resonant frequency shift of 2.84 GHz is observed (Figure 4.20(a)). The measured resonant frequency shift for hypopnea and hyperpnea are 2.15 GHz and 2.95 GHz, respectively (Figure 4.20(b)). Therefore, all obtained results showed similar characteristics to the standard breathing signal shown in Figure 4.15. This
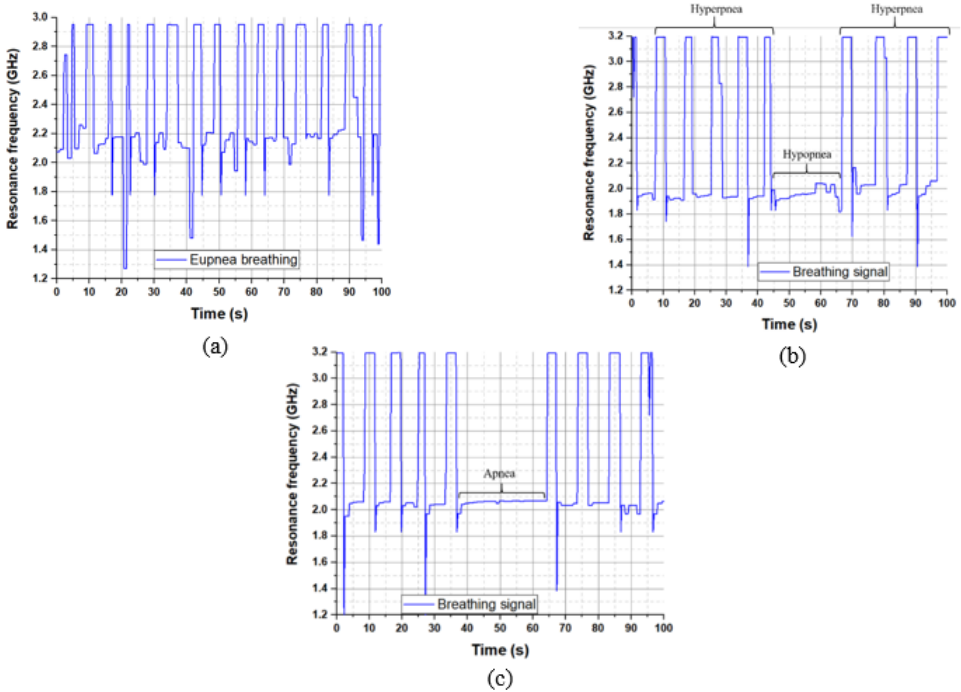
Figure 4.19: Measured respiratory patterns of an adult female volunteer in standing position, (a) Eupnea, (b) hypopnea and hyperpnea, and (c) Apnea.
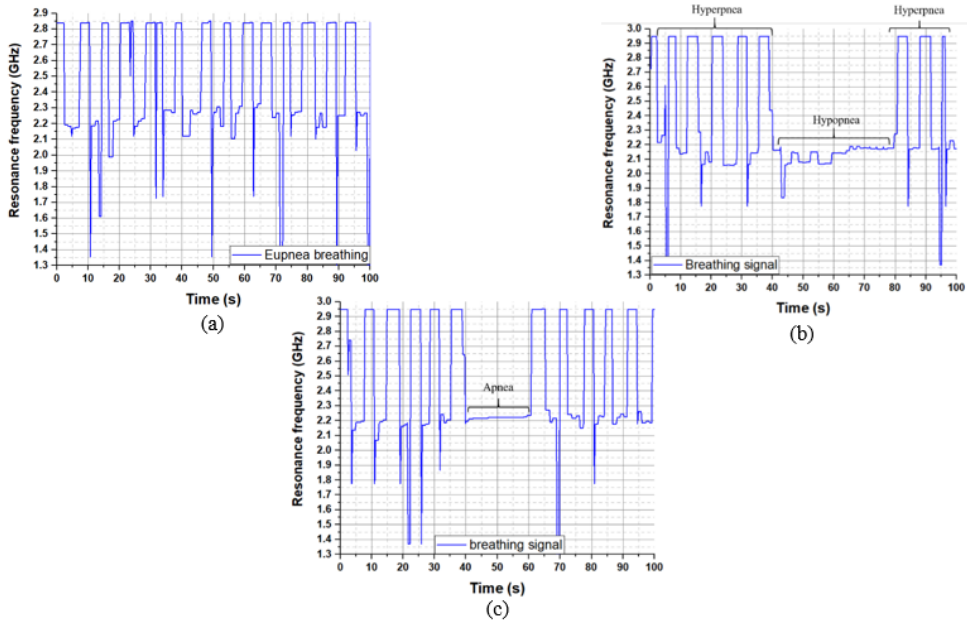
Figure 4.20: Measured respiratory patterns of an adult female volunteer sitting position, (a) Eupnea, (b) Hypopnea and hyperpnea, and (c) Apnea.

consistency enhances the potential of the embroidered antenna-based sensor for monitoring human breathing. The proposed approach succeeded to monitor different breathing patterns, which could prove valuable in assessing the health status of an individual.

4.3.6 Conclusion

This study presents a new antenna sensor integrated into a commercially available T-shirt to monitor respiration in real time. The sensor uses a meander dipole antenna and operates at a frequency of 2.4GHz. The working principle is based on detecting the change in the resonance frequency of the antenna caused by expansion of the chest and displacement of the air during breathing. Sensor efficacy is verified across different breathing patterns (apnea, apnea, hypopnea, and hyperpnea) and two different body positions (standing and sitting). Real-time detection of a female volunteer's breathing patterns has been successfully demonstrated using an antenna-based sensor. The system holds potential for healthcare applications, including diagnosing respiratory diseases and monitoring individuals with conditions such as

pulmonary edema and asthma. The proposed antenna-based sensor has the advantages of combining wearability, compact size, consistent performance and no fabrication complexities.

4.4 Wireless communication platform based on an embroidered antenna sensor

Ref E: El Gharbi, Mariam, Raúl Fernández-García, and Ignacio Gil. "Wireless Communication Platform Based on an Embroidered Antenna-Sensor for Real-Time Breathing Detection." Sensors 22, no. 22 (2022): 8667.

4.4.1 Introduction

Breathing is a critical vital sign that holds immense significance in assessing the physiological and physical condition of human health. It serves as a critical indicator for evaluating various medical conditions, including sleep apnea, asthma, and heart and lung diseases. Thus, continuous monitoring of breathing plays an important role in determining the general health status of a patient. The growing demand for improved medical breathing monitoring systems, extensive research has been undertaken to develop simple, convenient, and accurate measurement solutions. Recently, the need for wireless respiratory monitoring technologies has increased because of their convenience and ability to continuously monitor the physiological status of patients over long periods. These wireless methods provide a great user experience through the use of a remote sensing system. This enables patients to engage in their daily activities while remaining under surveillance.

This study investigates and evaluates a wireless textile sensor platform for monitoring breathing in real-time. Specifically, we propose to integrate a sensor based on a meander dipole antenna into an e-textile T-shirt connected to a Bluetooth transmitter for real-time breathing monitoring. The sensor, based on the antenna design, enables data to be transmitted wirelessly through communication networks operating at 2.4GHz frequency. Respiration is detected through the use of Received Signal Strength Index (RSSI) measurements. The respiratory system is placed centrally on the human chest. The respiratory signal is extracted from the variation of the RSSI signal emitted at 2.4 GHz from the embroidered antenna-based sensor embedded into a commercially made T-shirt and detected using a base station (laptop). The details of the full research are provided in Ref E.

4.4.2   Design and characteristics of the antenna sensor

The textile antenna sensor plays a vital role in wearable technologies, particularly within an e-textile system that incorporates wireless communication, localization, and sensing capabilities seamlessly and comfortably into garments. Before integrating the antenna sensor into textile materials, it is necessary to conduct a dielectric material characterization. The details of the proposed antenna design and its parameter are presented in the previous section.

The breathing sensing mechanism of the proposed system is based on the operation frequency shift of the embroidered antenna sensor. When the textile antenna-based sensor is worn by a human body, its geometry is subject to significant deformation caused by respiratory movements (expansion/contraction). Thus, the operating frequency of the antenna either increases or decreases in response to the stress applied on the antenna by the chest movement. The breathing antenna sensor is connected to a Bluetooth transmitter positioned at the center of the chest. The frequency detuning of the antenna leads to a mismatch in the transmitter, which affects the received RSSI (Received Signal Strength Indication). A base station, equipped with a laptop and a Bluetooth receiver, is used to continuously record the changes of the RSSI signal emitted from the beaded antenna sensor.

4.4.3   Experimental measurement and performance analysis

A novel detection system based on the measurement of the power transmitted by an embroidered meander dipole antenna-based sensor through a Bluetooth protocol is presented. The innovative breathing system consists of four main components: an antenna sensor integrated into a cotton T-shirt, positioned at the center of the human chest, a transmission Bluetooth module, a receiver Bluetooth module, and a base station. The base station, which can be a laptop or tablet equipped with a receiver Bluetooth module, is responsible for detecting the signals. The Bluetooth transmitter module is fabricated by means of a commercial ESP32-WROOM-32UE [137], which contains a U. FL connector that needs to be connected to an external antenna. For our specific implementation, the external antenna is a fully embroidered meander dipole antenna-based sensor. The manufactured transmission module includes a ESP32, which is a cost-effective and energy-efficient system on a chip (SoC) that integrates Bluetooth and Wi-Fi capabilities. This ESP32-based transmission module functions as an advertising beacon following the Bluetooth Low Energy (BLE) protocol at a frequency of 2.4 GHz. The transmitter Bluetooth module is fabricated and sewn into the T-shirt. A commercial

74

ESP32-WROOM-32U is used to program our fabricated transmitter module. Figure 4.21 illustrates the block diagram of the proposed breathing monitoring system. The custom board, depicted in Figure 4.21 has a compact size of 2.36×3.17 cm$\hat{2}$. This compact design ensures a high level of comfort for users when wearing the T-shirt.

The proposed breathing wireless system is sewn into the T-shirt. To extract the RSSI over the Bluetooth protocol, a code is created using Arduino Software (IDE). This code enabled to display of RSSI signal variations resulting from the physical detuning of the antenna sensor integrated into the T-shirt during the process of respiration. Bluetooth provides the RSSI as an integer value in dBm, serving as a measure of the received power of a Bluetooth Low Energy (BLE) signal. The breathing signal is obtained by analyzing the changes in the received signal strength indicator (RSSI) from the antenna sensor embedded in the T-shirt. The RSSI measurement is detected using a laptop connected to a receiver Bluetooth module (ESP32 ESP-WROOM-32). The respiratory signal is acquired from the RSSI signal emitted by the sensor based on the antenna. This sensor is able to detect strain caused by movement of the abdomen and chest wall. After programming the receiver Bluetooth module, the receiver module receives the Bluetooth signal from the transmitter antenna sensor. By using the RSSI data, the receiver unit estimates the received power of the BLE signal. Then it transfers all the collected values to a laptop computer via a serial connection. To collect and visualize breathing data in real-time, MATLAB is used. Figure 4.22 summarizes the proposed approach to detect and classify human breathing status.
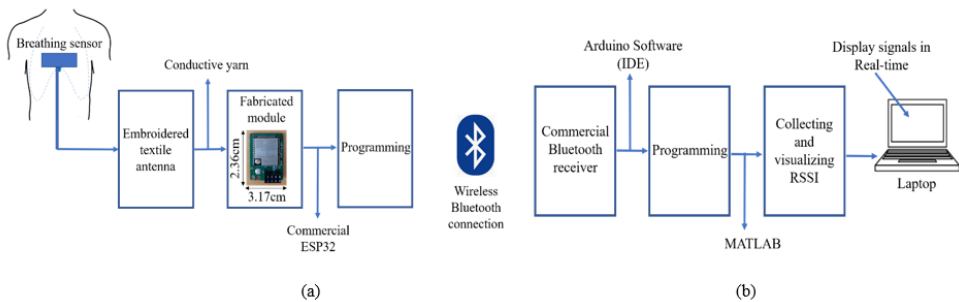
Figure 4.21: Block diagram of breathing monitoring: (a) Wearable unit, (b) Receiver.
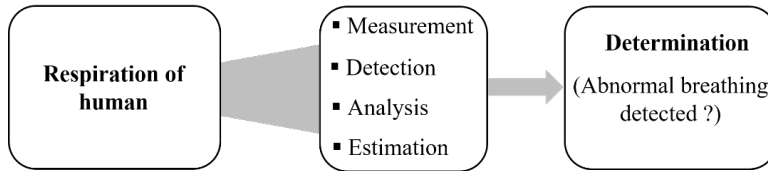
Figure 4.22: Procedure to detect human breathing status.

4.4.4 Detection of different breathing patterns

The transmitted signal from the embroidered antenna-based sensor is obtained and recorded by the movements of the chest and the abdominal wall. It should be noted that the transmitted signal is sensitive to stretching caused by mechanical changes during breathing, as explained in detail in [89]. Breathing patterns are typically classified into two categories: normal (eupnea) and abnormal (apnea). Abnormal respiration serves as a crucial indicator for chronic diseases such as chronic obstructive lung disease, pneumonia, or physiological instability. Hence, there is a significant practical need for a continuous real-time respiratory system that is cost-effective. The proposed system's signal acquisition is performed in a real environment by an adult female. Various precautions are taken to ensure accurate measurements, including the avoidance of any human movements or actions. To assess normal breathing, the participant is instructed to adhere to the following conditions:

- Respiration with small movement (walking);

- Respiration with speaking activities (reading a book);

- Stable pause without any other activities.

To acquire abnormal breathing, the signal is produced by pausing respiration for a few seconds to imitate apnea. During the experiment, the transmitter module is stitched into a T-shirt and worn by the participant, as depicted in Figure4.23. A base station is set up, and the receiver Bluetooth module is connected to the laptop. The base station consistently records the transmitted received signal strength indicator (RSSI) emitted by the embroidered antenna sensor. The participant followed the prescribed breathing patterns. The IDE software displayed the RSSI values, which are read by MATLAB through the serial port and plotted in real-time. Figure 4.24 displays the recorded raw RSSI data and the corresponding smoothed RSSI curves representing eupnea breathing signals under different conditions. The smoothed

(a)   (b)

Figure 4.23: Person under test wearing the e-textile for breathing monitoring:
(a) experimental setup configuration and (b) photograph of the experimental
setup.
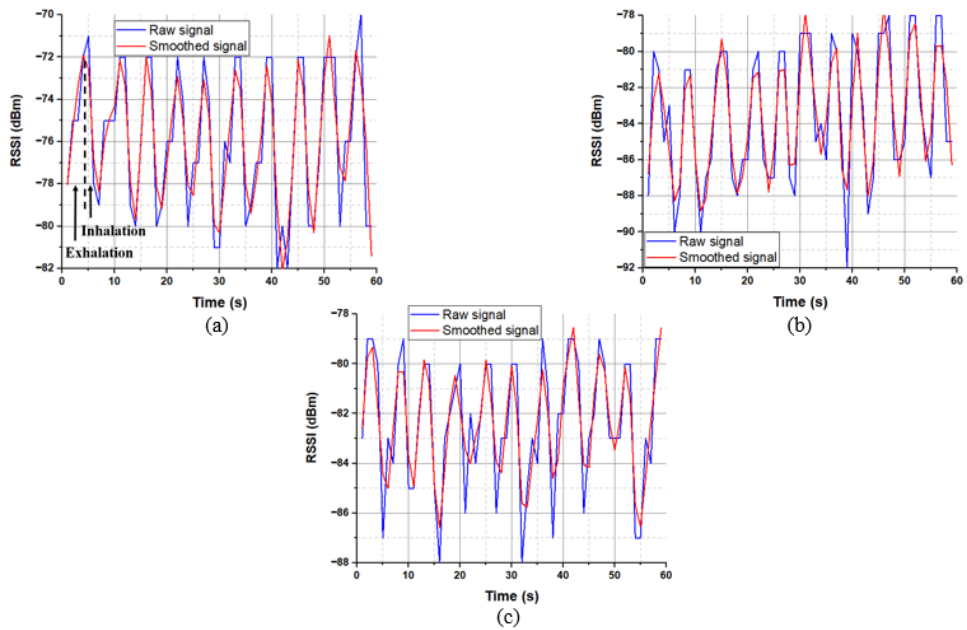
Figure 4.24: Examples of eupnea breathing signals: (a) normal breathing in
stable position, (b) normal breathing while speaking and (c) normal breathing
while moving.

RSSI signal is obtained by the Loess fitting method using data analysis and graphic software. The signal of eupnea is generated, a signal that is similar to sinusoidal breathing, and the breathing period is clear and could be distinguished. Therefore, expiration and inspiration phases in each respiration period are clearly extracted for different examples of the normal respiration status. The obtained results demonstrated that breathing signals can be acquired wirelessly by the RSSI via Bluetooth. The RSSI range varied from -80 dBm to -72 dBm, -88 dBm to -79 dBm, and -85 dBm to -80 dBm, for expiration and inspiration during normal breathing, speaking, and movement, respectively.The RSSI measurements are collected at a distance of 1 meter from the base station. It's important to note that during the movement, the participant maintained the physical separation between the receiver and transmitter. We can observe that the transmitted received signal strength oscillates as the participant breathes. By analyzing the data, we obtained the respiration signal which consisted of 11 breathing cycles within a 60-second timeframe. Note that normal breathing rates for an adult person range from 11 to 16 breaths per minute according to the respiratory rate chart [138]. The estimated period for expiration and inspiration is 5 seconds, which is in good agreement with the typical breathing cycle of 3 to 6 seconds. Figure 4.25 demonstrates an example of abnormal breathing (apnea) where there is an absence of breathing due to a very brief expiration and inspiration period.
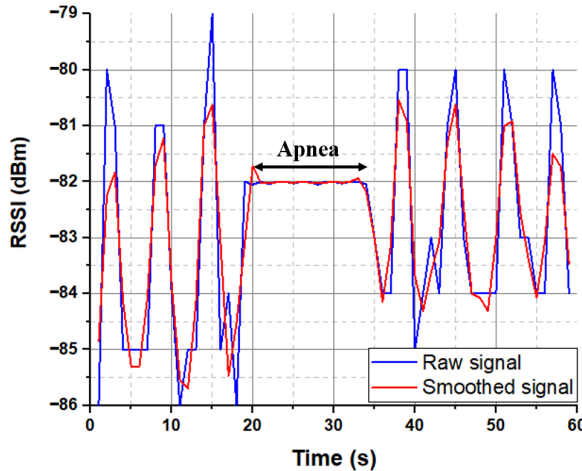
Figure 4.25: Example of abnormal breathing status.

4.4.5   Conclusion

A fully embroidered antenna-based sensor integrated into a commercial T-shirt is developed and tested for breathing monitoring. We have demonstrated the ability of the wireless communicating portable system to monitor breathing in real time. The system successfully transmitted the collected data to a base station using a Bluetooth protocol operating at a frequency of 2.4 GHz. Experimental tests are shown that the proposed wireless system can effectively detect the breathing signal using the received signal strength indicator (RSSI) through the standard Bluetooth protocol. The wearable device demonstrated its ability to accurately detect and monitor the breathing signal of a female volunteer in real-time. These promising results indicate that our e-textile T-shirt holds potential for various healthcare applications such as in chronic obstructive pulmonary illness or sleep apnea and various respiration disorders in neonates, children and adults.

4.5   Textile antenna sensor in SIW Technology for liquids Characterization

4.5.1   Introduction

In recent years, there has been significant interest in the development of new sensors for characterizing the electromagnetic properties of liquids. Various methods are currently employed for liquid characterization, such as transmission line techniques, free space methods, coaxial probes, and cavity resonator methods. Cavity resonators, in particular, are well-suited for precise and narrowband characterization, offering a high level of accuracy. Cavity resonators find great benefits in substrate-integrated waveguide (SIW) technology, offering cost-effective solutions and a relatively high-quality factor. In the present era, textiles are becoming the first choice for developing and fabricating wearable antenna sensors due to their ability to offer wearer comfort and flexibility. Therefore, the convergence of textile and SIW technology has resulted in a remarkable fusion of wireless communications and liquid sensing capabilities. SIW, an innovative transmission line technology, enables the design and integration of various electromagnetic structures on low-cost substrates. By integrating this technology with textile antenna sensors, we can now create smart fabrics that are able to distinguish and monitor liquids in real time. The textile antenna-based sensor represents a significant advancement in healthcare applications. This novel approach provides a non-destructive, and versatile

solution for liquid characterization, overcoming many limitations of conventional techniques.

This work presents the implementation of a novel textile antenna sensor based on a resonant cavity for liquid characterization. The cavity is based on circular substrate integrated waveguide (SIW) technology with a hole in the middle and a pipe passing through, which contains the liquid under test. the pipe is covered by means of a metal sheath to enhance the electromagnetic field to penetrate into the tube, thus increasing the device's sensitivity. The S_{11} measurement enables the extraction of electromagnetic properties of the liquid injected into the pipe. Specifically, the dielectric constant of the liquid is determined by observing the resonance frequency shift relative to the case of an air-filled pipe. The loss tangent of the liquid is extracted by comparing the variation in the quality factor with that of an air-filled pipe, after eliminating the inherent losses of the structure.

4.5.2 Antenna sensor SIW design and working principle

In this work, the SIW antenna-based sensor structure is implemented by a circular waveguide constructed using two circular conductor planes, which are separated by a dielectric material. The substrate adopted for the realization of the SIW antenna-based sensor is a felt material. furthermore, the top and bottom metal layers of the SIW structure are implemented using Less EMF Shieldit Super Fabric. The resonant frequency (f_{cnm}) of TM_{0N} mode for designing the circular SIW cavity is defined by the following equations:

$$f_{cnm} = \frac{k_c}{2\pi\sqrt{\mu\varepsilon}} = \frac{\rho_{nm}}{2\pi a_{\mu\varepsilon}} \tag{4.2}$$

where,

k_c : wavenumber $k_c = \frac{\rho_{nm}}{a}$

ρ_{nm} : root of Bessel's function

Based on this formula, the value of ρ_{nm} derived from Bessel's function of TM_{01}, is determined as 2.045. The a parameter represents an indicator of the radius of the circular cavity, while μ and ε express the permeability and permittivity, respectively. The simulation specifications are implemented using a commercial CST Studio Suite 3D full electromagnetic simulator. The dimensions of the proposed system are shown in figure 4.26(a) and (b). The dimensions of the antenna sensor SIW are depicted in Table4.6. This SIW cavity is designed to operate at 5.8GHz. A photograph of the textile antenna SIW sensor is presented in Figure 4.26(c) and (d). Subsequently, the spacing
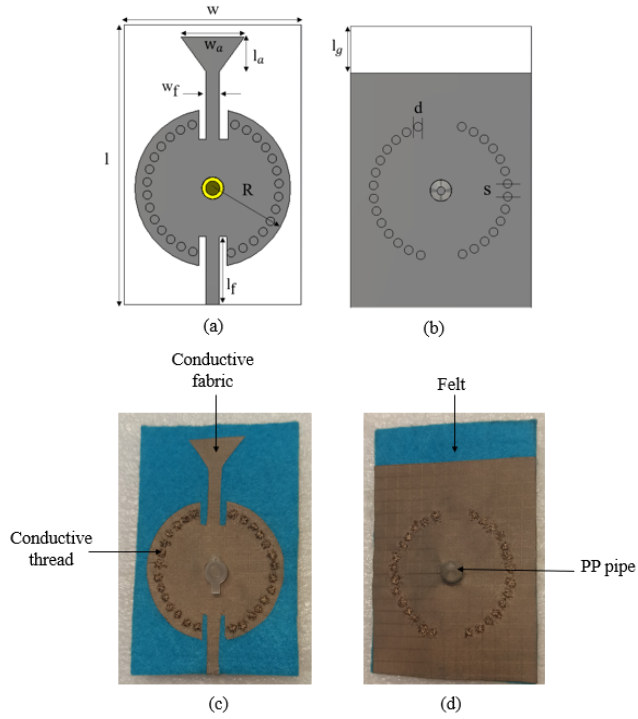
Figure 4.26: Geometry of the proposed SIW antenna-based sensor, (a) Front view, (b) Back view, Prototype of the proposed SIW antenna-based sensor, (c) Front view, (d) Back view.

Table 4.6: Dimensions of the proposed SIW antenna-based sensor.

Parameters	Dimensions (mm)
w	50
l	78
w_f	3.84
w_a	22
l_a	11.84
w_s	2
R	22
l_s	8.1
l_g	13

between the hole diameter, $d = 1.5$ mm, and the vias, $p = 2.8mm$ of SIW structure, indicates that the wave is propagating through to the waveguide structure of electric fields spreading meets the condition $d/p \leq 0.5$ and $d > 0.2\lambda_g$. However, if the position between vias is too far, there is a potential risk of field leakage that could impact the performance of the SIW structure [139]. The structure is based on a SIW cavity with a pipe in the middle which contains the liquid under test. The pipe used to characterize the liquid is a polypropylene (PP) tube. The advantages of this tube are its ability to reduce sample effluent and measure time compared to other liquid handling processes [140],[141]. This pipe is covered by means of a metal sheath to enhance the electromagnetic field to penetrate into the tube, thus increasing the device's sensitivity. The structure of the proposed sensor consists of a circular SIW cavity that contains an embedded pipe for liquid injection and extraction. By introducing liquid into the pipe, the effective permittivity inside the cavity changes, thus causing a variation in the resonance frequency and the quality factor of the cavity. Furthermore, the working principle of the proposed system is based on measuring changes in the properties of the liquid surrounding the sensor. It used the interaction between the electromagnetic fields radiated by the sensor and the liquid medium to extract the dielectric properties of the liquid under test.

4.5.3   Measurements and results

The S_{11} of the SIW antenna-based sensor is measured when filling the pipe with different liquids. It is measured by using an N9916A FieldFox microwave analyzer operating as Vector Network Analyzer (VNA) in a laboratory environment. Figure 4.27 shows the measured S_{11} for four different cases (air, distilled water, pure Isopropanol, and a mixture of 90% Isopropanol and 10% water). From the obtained results, the resonance frequency of the SIW sensor decreases when different liquids are injected into the pipe, i.e., when increasing the dielectric constant of the liquid under test. To be precise, the resonance frequencies shift from 5.8 GHz for the empty pipe to 5.32 GHz for the water-filled pipe. In addition to the frequency shift, the quality factor of the SIW sensor also alters when changing the liquid in the pipe. The resonance frequency shift can be used to retrieve the dielectric constant of the liquid under test. In order to achieve this, CST simulations are performed, considering the tube filled with liquid with different dielectric constants ranging from 10 to 80. The purpose is to calculate the corresponding frequency shift Δ_f. The results of these analyses are presented in Figure 4.28. The example of the
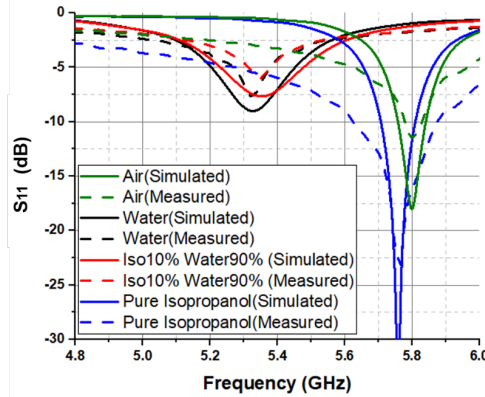
Figure 4.27: Simulated and measured S_{11} for air, distilled water, pure Isopropanol and a mixture of 90% Isopropanol and 10% water.

mixture of 10% iso 90% water is presented in Figure4.28. When the mixture is injected into the pipe, the measured frequency shift (with respect to the case with empty pipe) is $\Delta_f = 0.44 GHz$. According to the plot in Figure 4.28, the corresponding dielectric constant of the mixture is 61.24 (indicated in the plot). This process is employed for all liquids under test examined within this article. The dielectric properties of different liquids are measured using a commercial open-ended coaxial probe Keysight N1501A Dielectric Probe Kit, which is used as the reference technique. The dielectric constant and the loss
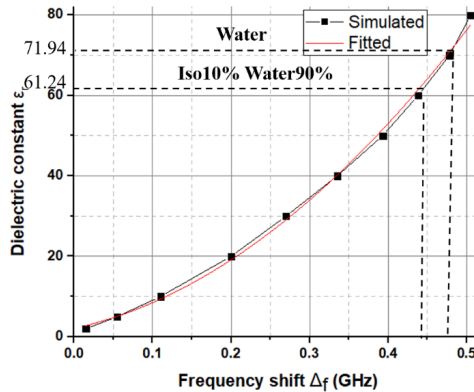
Figure 4.28: Simulated values of the dielectric constant versus the resonance frequency shift, and experimental validation example for water and pure Isopropanol.

Table 4.7: Dielectric constant retrieved with the proposed technique and reference values measured with the coaxial probe.

Mixture under test	Antenna SIW sensor	Coaxial probe	Relative error %
Pure Water	71.94	72.44	0.69
10% Iso 90% Water	61.24	61.37	0.21
30% Iso 70% Water	38.84	37.92	2.42
50% Iso 50% Water	23.72	22.52	5.32
70% Iso 30% Water	14.23	12.10	17.60
90% Iso 10% Water	6.37	5.70	11.75
Pure Isopropanol	4.36	3.89	19.79

tangent of all liquids under test are compared with the values of the dielectric properties measured by the coaxial probe. Table 4.7 represents the values of the dielectric constant obtained from the presented method compared with the measured values obtained by the coaxial probe characterization technique.In order to retrieve the loss tangent of the liquid under test, the variation of the unloaded quality factor is used. The methodology used to retrieve the loss tangent is explained in the previous chapter. Figure 4.29 presents the simulated values of the loss tangent versus the unloaded quality factor. By calculating the unloaded quality factor obtained from the measured S_{11} for LUT, the loss tangent of the liquid under test can be retrieved by using Figure 4.29. Since the unloaded quality factor of the mixture of 10% Iso 90% Water
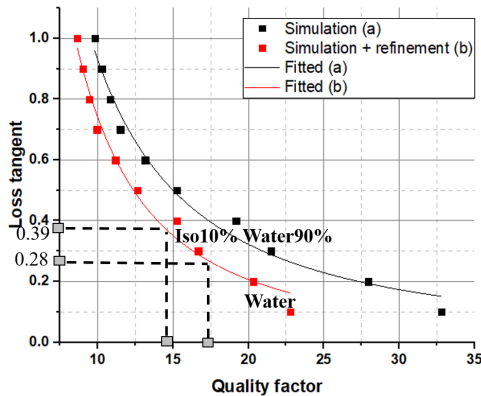
Figure 4.29: Simulated values of the loss tangent versus the unloaded quality factor with the experimental validation example for water and 90% Isopropanol and 10% water.

Table 4.8: Loss tangent retrieved with the proposed technique and reference values measured with the coaxial probe

Mixture under test	Antenna SIW sensor	Coaxial probe	Relative error %
Pure Water	0.28	0.29	3.44
10% Iso 90% Water	0.39	0.41	4.87
30% Iso 70% Water	0.69	0.67	2.98
50% Iso 50% Water	0.84	0.79	6.32
70% Iso 30% Water	0.82	0.81	1.23
90% Iso 10% Water	0.72	0.64	12.50
Pure Isopropanol	0.37	0.35	5.71

is 14.9, the resulting loss tangent is 0.39 (indicated in the plot). The value obtained is quite close to the reference value obtained with the coaxial probe, which is 0.40. Table 4.8 represents the values of the loss tangent obtained from the presented method compared with the measured values obtained by the coaxial probe characterization technique.

4.5.4 Conclusion

A textile circular cavity of the SIW antenna-based sensor is developed to characterize the dielectric properties of liquid samples. The proposed system is designed, simulated, fabricated, and measured at a resonance frequency of 5.8 GHz. A pipe is inserted at the center of the cavity SIW, where the LUT can be injected and extracted, to define its electromagnetic properties. This proposed SIW antenna-based sensor is used to retrieve the dielectric constant and loss tangent of different liquid mixtures, and the values obtained are compared with the result measured by the coaxial probe. To the best of our knowledge, this work demonstrates for the first time the capability of a fully-textile SIW antenna-based sensor to retrieve dielectric properties of liquid under test using microwave signals.

5

Conclusions and Future Work

5.1 Conclusions

This thesis presents the analysis, design, and testing of several wearable antenna-based sensors for healthcare monitoring. The antenna sensor structures are implemented using embroidery on different textile substrates. The thesis covers five JCR articles that document various applications of textile antenna sensors. In the first chapter, the research objectives are presented from a comprehensive analysis of the current advancements through a systematic review. By conducting a comprehensive analysis of the state, the four main objectives are suggested including (1) Developing new textile antenna-based sensors with high performance: low profile and area, high sensitivity, low cost, and high durability; (2) Exploring wearable antenna-based sensors that can be used for body signal/healthcare monitoring and communication purposes; (3) Test the performance of the antenna sensor in real-world scenarios, such as breathing monitoring and blood glucose level; and (4) Develop an antenna-based sensor to be integrated with other commercial electronic components, such as Bluetooth/WIFI transmitter.

An overview of the actual state of the art of wearable antenna sensors is presented in Chapter 2, including the working principle, classification, and

implementation of antenna sensors. In this section, the operating principle of antenna-based sensor is explained. The main types of antenna sensors including dielectric, strain, temperature, and crack sensing are described in detail. Furthermore, the substrate implementation including rigid and textile antenna sensors is discussed. The chapter finishes with several challenges and opportunities to improve the performance of wearable antenna sensors.

The materials and methods for designing, manufacturing, and characterizing textile and flexible antenna-based sensors are presented in Chapter 3. The textile materials and their EM characteristics (dielectric and conductive materials) and different manufacturing methods of wearable antenna sensors are explained. This survey of textile materials reveals the extensive range of design possibilities currently offered by textile antenna sensors. In this section, several characterization methods are used for wearable antenna sensors, and they present valuable insights into their functionality.

Chapter 4 presents the main research results carried out in the thesis. A textile antenna-based sensor for in vitro experiments to monitor blood glucose levels is presented. The proposed textile device demonstrates a proof of concept for efficient in vitro blood glucose level measurements and diagnostics of diabetes. The performance of the antenna sensor is practically validated. The sensor demonstrates its functionality and the ability to detect different concentrations to cover diabetes patients with hypoglycemia, normoglycemia, and hyperglycemia relevant to type-2 diabetes. In addition to its ability to monitor glucose levels, the proposed antenna-based sensor offers a range of other features. These include its compact size, simple design, and low cost. Furthermore, a novel antenna-based sensor is proposed to demonstrate for the first time the capability of a fully-textile antenna sensor to detect different amounts and concentrations of salt and sugar using microwave signals. Moreover, the accuracy in detection is guaranteed, since small amounts of volume change can be detected by means of resonance frequency shift. Some additional tests are considered, such as rinsing reliability and repeatability results. This evaluation is used to ensure that the antenna sensor remains undamaged when exposed to wet conditions. Besides, the experimental results showed that the rinsing process has no appreciable detrimental effect on the performance of the antenna sensor.

A novel fully embroidered meander dipole antenna-based sensor integrated into a cotton T-shirt for real-time breathing monitoring using the technique based on chest well movement analysis is presented. The antenna sensor has proven its effectiveness in detecting various breathing patterns. However, this method is inconvenient due to the use of a connecting cable for the Vector

Network Analyzer (VNA), which limits the usability of the proposed system. In order to improve user comfort, we proposed an e-textile T-shirt based on the received signal strength indicator (RSSI) detected wirelessly using a base station that presents a high level of comfort for the user. The innovative system consists of a contactless antenna-based sensor embedded in a cotton T-shirt and a laptop with a receiver Bluetooth module. The main novelty of our research is the development of a new wireless communications platform for breathing monitoring using a fully embroidered antenna sensor embedded into a commercial T-shirt and connected to a transmission Bluetooth module that provides high comfort for the user and is comfortable for long-term use.

Overall, the thesis provides novel sensing applications using a fully textile antenna sensor. The outcome of the research activities presented in this thesis is expected to serve as a baseline for the development of new approaches and antenna-based sensor systems as well as lead to new research ideas.

5.2   Future works

Wearable antenna sensors are a topic of increasing interest in the industry and the scientific community. Some further work may be carried out in the research lines that emerged from this thesis. Among them, we would like to highlight:

- Develop new antenna-based sensor to be integrated with other commercial electronic components, such as WIFI transmitter for breathing monitoring (Project TED2021-131209B-I00).

- Investigate new designs and sensing functions of textile antenna sensors with common or novel textile materials using printing technology, which could provide high accuracy.

- Studying the reliability of textile antenna sensors such as humidity and temperature and human activity factors such as washing and sweat corrosion that can imply certain effects on performance.

Bibliography

[1]   Ravinder Dahiya. "E-skin: From humanoids to humans [point of view]".
        In: *Proceedings of the IEEE* 107.2 (2019), pp. 247–252. ISSN: 0018-9219.

[2]   Author. *Global flexible electronics Market*. 2022. URL: `https://www.
        thebusinessresearchcompany.com/report`.

[3]   Dario B Rodrigues et al. "Design and optimization of an ultra wide-
        band and compact microwave antenna for radiometric monitoring of
        brain temperature". In: *IEEE transactions on biomedical engineering*
        61.7 (2014), pp. 2154–2160. ISSN: 0018-9294.

[4]   T V Padmavathy et al. "Design and development of microstrip patch
        antenna with circular and rectangular slot for structural health moni-
        toring". In: *Personal and Ubiquitous Computing* 22.5-6 (2018), pp. 883–
        893. ISSN: 1617-4909.

[5]   F Mbanya Tchafa and H Huang. "Microstrip patch antenna for si-
        multaneous strain and temperature sensing". In: *Smart Materials and
        Structures* 27.6 (2018), p. 65019. ISSN: 0964-1726.

[6]   E M Cheng et al. "Development of microstrip patch antenna sensing
        system for salinity and sugar detection in water". In: *Int. J. Mech.
        Mechatronics Eng* 15.5 (2014), pp. 31–36.

[7]   Jeremiah W Sanders, Jun Yao, and Haiying Huang. "Microstrip patch
        antenna temperature sensor". In: *IEEE sensors journal* 15.9 (2015),
        pp. 5312–5319. ISSN: 1530-437X.

[8]   Kasra Khorsand Kazemi et al. "Low-profile planar antenna sensor
        based on Ti3C2Tx MXene membrane for VOC and humidity mon-
        itoring". In: *Advanced Materials Interfaces* 9.13 (2022), p. 2102411.
        ISSN: 2196-7350.

[9]   Chin-Lung Yang, Saurabh Bagchi, and William J Chappell. "Location tracking with directional antennas in wireless sensor networks". In: *IEEE MTT-S International Microwave Symposium Digest, 2005.* IEEE, 2005, pp. 131–134. ISBN: 0780388453.

[10]   Angie R Eldamak and Elise C Fear. "Conformal and disposable antenna-based sensor for non-invasive sweat monitoring". In: *Sensors* 18.12 (2018), p. 4088.

[11]   Mourad Roudjane et al. "A portable wireless communication platform based on a multi-material fiber sensor for real-time breath detection". In: *Sensors* 18.4 (2018), p. 973.

[12]   Srinivasulu Kanaparthi, Veerla Raja Sekhar, and Sushmee Badhulika. "Flexible, eco-friendly and highly sensitive paper antenna based electromechanical sensor for wireless human motion detection and structural health monitoring". In: *Extreme Mechanics Letters* 9 (2016), pp. 324–330. ISSN: 2352-4316.

[13]   Christina Zong-Hao Ma et al. "Towards wearable comprehensive capture and analysis of skeletal muscle activity during human locomotion". In: *Sensors* 19.1 (2019), p. 195. ISSN: 1424-8220.

[14]   Jessica Hanna et al. "Noninvasive, wearable, and tunable electromagnetic multisensing system for continuous glucose monitoring, mimicking vasculature anatomy". In: *Science Advances* 6.24 (2020), eaba5320. ISSN: 2375-2548.

[15]   Constantine A Balanis. "Microstrip antennas". In: *Antenna theory: analysis and design* 3 (2005), pp. 811–882.

[16]   Vincenzo Cioffi and Sandra Costanzo. "Wearable Approach for Contactless Blood-Glucose Monitoring by Textile Antenna Sensor". In: *World Conference on Information Systems and Technologies.* Springer, 2019, pp. 287–291.

[17]   Mohammad Tariqul Islam et al. "A new metasurface superstrate structure for antenna performance enhancement". In: *Materials* 6.8 (2013), pp. 3226–3240.

[18]   Mohammad Tariqul Islam et al. "Detection of salt and sugar contents in water on the basis of dielectric properties using microstrip antenna-based sensor". In: *IEEE Access* 6 (2018), pp. 4118–4126. ISSN: 2169-3536.

[19] Mohammad Tariqul Islam et al. "A compact ultrawideband antenna based on hexagonal split-ring resonator for pH sensor application". In: *Sensors* 18.9 (2018), p. 2959.

[20] Sabina Manzari et al. "Humidity sensing by polymer-loaded UHF RFID antennas". In: *IEEE Sensors Journal* 12.9 (2012), pp. 2851–2858. ISSN: 1530-437X.

[21] Rajesh Verma et al. "Carbon nanotube-based microstrip antenna gas sensor". In: *2013 IEEE 56th International Midwest Symposium on Circuits and Systems (MWSCAS)*. IEEE, 2013, pp. 724–727. ISBN: 1479900664.

[22] A S Pathma Priyaa et al. "Microwave Sensor Antenna for Soil Moisture Measurement". In: *2015 Fifth International Conference on Advances in Computing and Communications (ICACC)*. IEEE, 2015, pp. 258–262. ISBN: 1467369942.

[23] Lin Zhu et al. "Microfluidic Flexible Substrate Integrated Microstrip Antenna Sensor for Sensing of Moisture Content in Lubricating Oil". In: *International Journal of Antennas and Propagation* 2020 (2020). ISSN: 1687-5869.

[24] Xiaoyou Lin, Boon-Chong Seet, and Frances Joseph. "Wearable humidity sensing antenna for BAN applications over 5G networks". In: *2018 IEEE 19th Wireless and Microwave Technology Conference (WAMICON)*. IEEE, 2018, pp. 1–4. ISBN: 1538612674.

[25] Siti Aminah Md Akhir et al. "Antenna for humidity sensor using split ring resonator". In: *Indonesian Journal of Electrical Engineering and Computer Science* 13.2 (2019), pp. 584–592.

[26] Marie-Aline Mattelin et al. "Imprinted Polymer-Based Guided Mode Resonance Grating Strain Sensors". In: *Sensors* 20.11 (2020), p. 3221.

[27] Sang-Dong Jang and Jaehwan Kim. "Passive wireless structural health monitoring sensor made with a flexible planar dipole antenna". In: *Smart materials and structures* 21.2 (2012), p. 27001. ISSN: 0964-1726.

[28] Przemyslaw Lopato and Michal Herbko. "A circular microstrip antenna sensor for direction sensitive strain evaluation". In: *Sensors* 18.1 (2018), p. 310.

[29] J Yao et al. "Pressure sensing using low-cost microstrip antenna sensor". In: *Sensors and Smart Structures Technologies for Civil, Mechanical, and Aerospace Systems 2015*. Vol. 9435. International Society for Optics and Photonics, 2015, p. 943537.

[30] Hamse Abdillahi Haji Omer et al. "Structural health monitoring sensor based on a flexible microstrip patch antenna". In: *Indonesian J. Electr. Eng. Comp. Sci* 10 (2018), pp. 917–924.

[31] Haiying Huang, Farnaz Farahanipad, and Abhay Kumar Singh. "A stacked dual-frequency microstrip patch antenna for simultaneous shear and pressure displacement sensing". In: *IEEE Sensors Journal* 17.24 (2017), pp. 8314–8323. ISSN: 1530-437X.

[32] Christos Goumopoulos. "A high precision, wireless temperature measurement system for pervasive computing applications". In: *Sensors* 18.10 (2018), p. 3445.

[33] Xiaoyou Lin, Boon-Chong Seet, and Frances Joseph. "Fabric antenna with body temperature sensing for BAN applications over 5G wireless systems". In: *2015 9th International Conference on Sensing Technology (ICST)*. IEEE, 2015, pp. 591–595. ISBN: 1479963143.

[34] Fan Yang et al. "Reconfigurable sensing antenna: A slotted patch design with temperature sensation". In: *IEEE Antennas and Wireless Propagation Letters* 11 (2012), pp. 632–635. ISSN: 1536-1225.

[35] Hao Jiang et al. "Patch antenna based temperature sensor". In: *Nondestructive Characterization for Composite Materials, Aerospace Engineering, Civil Infrastructure, and Homeland Security 2014*. Vol. 9063. International Society for Optics and Photonics, 2014, 90631P.

[36] F Mbanya Tchafa and H Huang. "Microstrip patch antenna for simultaneous temperature sensing and superstrate characterization". In: *Smart Materials and Structures* 28.10 (2019), p. 105009. ISSN: 0964-1726.

[37] Isidoro Ibanez-Labiano and Akram Alomainy. "Dielectric Characterization of Non-Conductive Fabrics for Temperature Sensing through Resonating Antenna Structures". In: *Materials* 13.6 (2020), p. 1271.

[38] I Mohammad et al. "Detecting crack orientation using patch antenna sensors". In: *Measurement Science and Technology* 23.1 (2011), p. 15102. ISSN: 0957-0233.

[39] I Mohammad and H Huang. "Monitoring fatigue crack growth and opening using antenna sensors". In: *Smart Materials and Structures* 19.5 (2010), p. 55023. ISSN: 0964-1726.

[40] Songtao Xue et al. "A Passive Wireless Crack Sensor Based on Patch Antenna with Overlapping Sub-Patch". In: *Sensors* 19.19 (2019), p. 4327.

[41] Irshad Mohammad and Haiying Huang. "An antenna sensor for crack detection and monitoring". In: *Advances in Structural Engineering* 14.1 (2011), pp. 47–53. ISSN: 1369-4332.

[42] Hojoo Lee and Jaehoon Choi. "A compact all-textile on-body SIW antenna for IoT applications". In: *2017 IEEE International Symposium on Antennas and Propagation USNC/URSI National Radio Science Meeting.* IEEE, 2017, pp. 825–826. ISBN: 1538632845.

[43] Safa Salman et al. "Pulmonary edema monitoring sensor with integrated body-area network for remote medical sensing". In: *IEEE transactions on Antennas and Propagation* 62.5 (2014), pp. 2787–2794. ISSN: 0018-926X.

[44] Tessa Haagenson et al. "Textile Antennas for Spacesuit Applications: Design, simulation, manufacturing, and testing of textile patch antennas for spacesuit applications." In: *IEEE Antennas and Propagation Magazine* 57.4 (2015), pp. 64–73. ISSN: 1045-9243.

[45] Caroline Loss et al. "Smart coat with a fully-embedded textile antenna for IoT applications". In: *Sensors* 16.6 (2016), p. 938. ISSN: 1424-8220.

[46] Maria Lucia Scarpello et al. "Stability and efficiency of screen-printed wearable and washable antennas". In: *IEEE antennas and wireless propagation letters* 11 (2012), pp. 838–841. ISSN: 1536-1225.

[47] Mahmoud Wagih et al. "E-textile breathing sensor using fully textile wearable antennas". In: *Engineering Proceedings* 15.1 (2022), p. 9. ISSN: 2673-4591.

[48] Yusuke Mukai and Minyoung Suh. "Development of a conformal woven fabric antenna for wearable breast hyperthermia". In: *Fashion and Textiles* 8 (2021), pp. 1–12.

[49] Davor Bonefacic. "Textile antenna as moisture sensor". In: *2020 14th European Conference on Antennas and Propagation (EuCAP).* IEEE, 2020, pp. 1–3. ISBN: 883129900X.

[50] Sari Merilampi et al. "The possibilities of passive UHF RFID textile tags as comfortable wearable sweat rate sensors". In: *2016 Progress in Electromagnetic Research Symposium (PIERS)*. IEEE, 2016, pp. 3984–3987. ISBN: 1509060936.

[51] Davor Bonefačić and Juraj Bartolić. "Embroidered textile antennas: Influence of moisture in communication and sensor applications". In: *Sensors* 21.12 (2021), p. 3988. ISSN: 1424-8220.

[52] Julian Arango Toro, Willer Ferney Montes Granada, and Sara Maria Yepes Zuluaga. "Design and implementation of a wearable patch antenna that serves as a longitudinal strain sensor". In: *Textile Research Journal* 91.23-24 (2021), pp. 2795–2812. ISSN: 0040-5175.

[53] Sina Rahmani Charvadeh and Javad Ghalibafan. "Investigation of textile permittivity under the influence of fever for designing a wearable temperature sensing antenna". In: *Biosensors and Bioelectronics: X* 12 (2022), p. 100264. ISSN: 2590-1370.

[54] Mourad Roudjane et al. "Smart T-shirt based on wireless communication spiral fiber sensor array for real-time breath monitoring: validation of the technology". In: *IEEE Sensors Journal* 20.18 (2020), pp. 10841–10850. ISSN: 1530-437X.

[55] Yulong Liu et al. "E-textile battery-less displacement and strain sensor for human activities tracking". In: *IEEE Internet of Things Journal* 8.22 (2021), pp. 16486–16497. ISSN: 2327-4662.

[56] Quoc Hung Dang et al. "Modular integration of a passive RFID sensor with wearable textile antennas for patient monitoring". In: *IEEE Transactions on Components, Packaging and Manufacturing Technology* 10.12 (2020), pp. 1979–1988. ISSN: 2156-3950.

[57] A Oral Salman, Emrullah Bicak, and Mehmet Sezgin. "Textile antenna for the multi-sensor (impulse GPREMI) subsurface detection system". In: *Proceedings of the XIII Internarional Conference on Ground Penetrating Radar*. IEEE, 2010, pp. 1–5. ISBN: 142444604X.

[58] Kasra Khorsand Kazemi et al. "Smart superhydrophobic textiles utilizing a long-range antenna sensor for hazardous aqueous droplet detection plus prevention". In: *ACS Applied Materials Interfaces* 13.29 (2021), pp. 34877–34888. ISSN: 1944-8244.

[59] Esra Çelenk and Nurhan Türker Tokan. "All-textile on-body antenna for military applications". In: *IEEE Antennas and Wireless Propagation Letters* 21.5 (2022), pp. 1065–1069. ISSN: 1536-1225.

[60] Xiaoyou Lin et al. "Ultrawideband textile antenna for wearable microwave medical imaging applications". In: *IEEE Transactions on Antennas and Propagation* 68.6 (2020), pp. 4238–4249. ISSN: 0018-926X.

[61] Abirami Anbalagan et al. "Realization and analysis of a novel low-profile embroidered textile antenna for real-time pulse monitoring". In: *IETE Journal of Research* 68.6 (2022), pp. 4142–4149. ISSN: 0377-2063.

[62] Hongcai Yang et al. "Dual-band textile antenna with dual circular polarizations using polarization rotation AMC for off-body communications". In: *IEEE Transactions on Antennas and Propagation* 70.6 (2022), pp. 4189–4199. ISSN: 0018-926X.

[63] N I Zaidi et al. "Analysis on different shape of textile antenna under bending condition for GPS application". In: *Bulletin of Electrical Engineering and Informatics* 9.5 (2020), pp. 1964–1970. ISSN: 2302-9285.

[64] Rajni Bala et al. "Wearable Graphene Based Curved Patch Antenna for Medical Telemetry Applications." In: *Applied Computational Electromagnetics Society Journal* 31.5 (2016). ISSN: 1054-4887.

[65] Liu Jianying et al. "Bending effects on a flexible Yagi-Uda antenna for wireless body area network". In: *2016 Asia-Pacific International Symposium on Electromagnetic Compatibility (APEMC)*. Vol. 1. IEEE, 2016, pp. 1001–1003. ISBN: 1467394947.

[66] David Ferreira et al. "Wearable Textile Antennas: Examining the effect of bending on their performance." In: *IEEE Antennas and Propagation Magazine* 59.3 (2017), pp. 54–59. ISSN: 1045-9243.

[67] M S M Isa et al. "Textile dual band circular ring patch antenna under bending condition". In: *Journal of Telecommunication, Electronic and Computer Engineering (JTEC)* 9.3 (2017), pp. 37–43. ISSN: 2289-8131.

[68] Adel Y I Ashyap et al. "Inverted E-shaped wearable textile antenna for medical applications". In: *IEEE Access* 6 (2018), pp. 35214–35222. ISSN: 2169-3536.

[69] Satheesh Babu Roshni et al. "Design and fabrication of an E-shaped wearable textile antenna on PVB-coated hydrophobic polyester fabric". In: *Smart Materials and Structures* 26.10 (2017), p. 105011. ISSN: 0964-1726.

[70]   Chun Xu Mao et al. "Low-profile strip-loaded textile antenna with en-
       hanced bandwidth and isolation for full-duplex wearable applications".
       In: *IEEE Transactions on Antennas and Propagation* 68.9 (2020),
       pp. 6527–6537. ISSN: 0018-926X.

[71]   Susila Mohandoss et al. "On the bending and time domain analysis of
       compact wideband flexible monopole antennas". In: *AEU-International
       Journal of Electronics and Communications* 101 (2019), pp. 168–181.
       ISSN: 1434-8411.

[72]   Ameni Mersani, Lotfi Osman, and Jean-Marc Ribero. "Flexible UWB
       AMC antenna for early stage skin cancer identification". In: *Progress
       in Electromagnetics Research* 80 (2019), pp. 71–81. ISSN: 1937-8726.

[73]   Bo Yin et al. "A low SAR value wearable antenna for wireless body
       area network based on AMC structure". In: *Progress In Electromag-
       netics Research* 95 (2019), pp. 119–129. ISSN: 1937-8718.

[74]   Ricardo Gómez-Villanueva, Hildeberto Jardón-Aguilar, and Roberto
       Linares y Miranda. "State of the art methods for low SAR antenna
       implementation". In: *Proceedings of the Fourth European Conference
       on Antennas and Propagation*. IEEE, 2010, pp. 1–4. ISBN: 1424464315.

[75]   American National Standards Institute (ANSI). "Safety levels with
       respect to human exposure to radio frequency electromagnetic fields,
       3 kHz to 300 GHz, ANSI/IEEE standard C95. 1". In: (1999).

[76]   Icnirp. "International Commission on Non-Ionizing Radiation Protec-
       tion. Guidelines for limiting exposure to time-varying electric, mag-
       netic, and electromagnetic fields (up to 300 GHz)". In: *Health Physics*
       74.4 (1998), pp. 494–522.

[77]   Arpan Shah and Piyush Patel. "E-textile slot antenna with spurious
       mode suppression and low SAR for medical wearable applications".
       In: *Journal of Electromagnetic Waves and Applications* 35.16 (2021),
       pp. 2224–2238. ISSN: 0920-5071.

[78]   Guoping Gao et al. "Design of a wide bandwidth and high gain wear-
       able antenna based on nonuniform metasurface". In: *Microwave and
       Optical Technology Letters* 63.10 (2021), pp. 2606–2613. ISSN: 0895-
       2477.

[79]   I Gil and R Fernandez-Garcia. "Wearable embroidered GPS textile
       antenna". In: *2017 Progress In Electromagnetics Research Symposium-
       Spring (PIERS)*. IEEE, 2017, pp. 655–659. ISBN: 1509062696.

[80] Sarmad Nozad Mahmood et al. "Full ground ultra-wideband wearable textile antenna for breast cancer and wireless body area network applications". In: *Micromachines* 12.3 (2021), p. 322. ISSN: 2072-666X.

[81] Tu Tuan Le and Tae-Yeoul Yun. "Wearable dual-band high-gain low-SAR antenna for off-body communication". In: *IEEE Antennas and Wireless Propagation Letters* 20.7 (2021), pp. 1175–1179. ISSN: 1536-1225.

[82] Andi Hakim Kusuma et al. "A new low SAR antenna structure for wireless handset applications". In: *Progress In Electromagnetics Research* 112 (2011), pp. 23–40. ISSN: 1070-4698.

[83] Israa H Ali, Huda I Hamd, and Ali I Abdalla. "Design and comparison of two types of antennas for SAR calculation in wireless applications". In: *2018 Advances in Science and Engineering Technology International Conferences (ASET)*. IEEE, 2018, pp. 1–5. ISBN: 1538623994.

[84] Mohamed Ismail Ahmed, Mai Fouad Ahmed, and Abdel Hamied Abdel Shaalan. "SAR calculations of novel textile dual-layer UWB lotus antenna for astronauts spacesuit". In: *Progress In Electromagnetics Research C* 82 (2018), pp. 135–144. ISSN: 1937-8718.

[85] Jacek Lesnikowski. "Dielectric permittivity measurement methods of textile substrate of textile transmission lines". In: *Przeglad Elektrotechniczny* 88.3A (2012), pp. 148–151.

[86] Kausik Bal and V K Kothari. "Measurement of dielectric properties of textile materials and their applications". In: (2009). ISSN: 0971-0426.

[87] Muhammad Talha Khan and Syed Muzamil Ali. "A brief review of measuring techniques for characterization of dielectric materials". In: *International Journal of Information Technology and Electrical Engineering* 1.1 (2012).

[88] Abdulrahman Shueai Mohsen Alqadami and M F Jamlos. "Design and development of a flexible and elastic UWB wearable antenna on PDMS substrate". In: *2014 IEEE Asia-Pacific Conference on Applied Electromagnetics (APACE)*. IEEE, 2014, pp. 27–30. ISBN: 1479966037.

[89] Mariam El Gharbi, Raúl Fernández-García, and Ignacio Gil. "Embroidered Wearable Antenna-based Sensor for Real-Time Breath Monitoring". In: *Measurement* (2022), p. 111080. ISSN: 0263-2241.

[90] K Hettak et al. "Flexible polyethylene terephthalate-based inkjet printed CPW-fed monopole antenna for 60 GHz ISM applications". In: *2013 European Microwave Conference*. IEEE, 2013, pp. 1447–1450. ISBN: 2874870315.

[91] Benito Sanz-Izquierdo, John C Batchelor, and M I Sobhy. "Button antenna on textiles for wireless local area network on body applications". In: *IET microwaves, antennas propagation* 4.11 (2010), pp. 1980–1987. ISSN: 1751-8733.

[92] Shaozhen Zhu and Richard Langley. "Dual-band wearable textile antenna on an EBG substrate". In: *IEEE transactions on Antennas and Propagation* 57.4 (2009), pp. 926–935. ISSN: 0018-926X.

[93] Carla Hertleer et al. "Aperture-coupled patch antenna for integration into wearable textile systems". In: *IEEE antennas and wireless propagation letters* 6 (2007), pp. 392–395. ISSN: 1536-1225.

[94] Benito Sanz-Izquierdo et al. "Textile integrated waveguide slot antenna". In: *2010 IEEE Antennas and Propagation Society International Symposium*. IEEE, 2010, pp. 1–4. ISBN: 1424449677.

[95] Mariam El Gharbi et al. "Determination of Salinity and Sugar Concentration by means of a Circular-Ring Monopole Textile Antenna-based Sensor". In: *IEEE Sensors Journal* (2021). ISSN: 1530-437X.

[96] Symeon Nikolaou et al. "Conformal double exponentially tapered slot antenna (DETSA) on LCP for UWB applications". In: *IEEE Transactions on Antennas and Propagation* 54.6 (2006), pp. 1663–1669. ISSN: 0018-926X.

[97] Giovanni Andrea Casula, Giorgio Montisci, and Giuseppe Mazzarella. "A wideband PET inkjet-printed antenna for UHF RFID". In: *IEEE Antennas and Wireless Propagation Letters* 12 (2013), pp. 1400–1403. ISSN: 1536-1225.

[98] Haider R Khaleel et al. "A compact polyimide-based UWB antenna for flexible electronics". In: *IEEE Antennas and Wireless Propagation Letters* 11 (2012), pp. 564–567. ISSN: 1536-1225.

[99] G DeJean et al. "Liquid crystal polymer (LCP): A new organic material for the development of multilayer dual-frequency/dual-polarization flexible antenna arrays". In: *IEEE Antennas and Wireless Propagation Letters* 4 (2005), pp. 22–26. ISSN: 1536-1225.

[100] Hadi Bahramiabarghouei et al. "Flexible 16 antenna array for microwave breast cancer detection". In: *IEEE Transactions on Biomedical Engineering* 62.10 (2015), pp. 2516–2525. ISSN: 0018-9294.

[101] Gabriela Atanasova and Nikolay Atanasov. "Small antennas for wearable sensor networks: impact of the electromagnetic properties of the textiles on antenna performance". In: *Sensors* 20.18 (2020), p. 5157. ISSN: 1424-8220.

[102] Hong-Kuai Nie et al. "Wearable antenna sensor based on EBG structure for cervical curvature monitoring". In: *IEEE Sensors Journal* 22.1 (2021), pp. 315–323. ISSN: 1530-437X.

[103] Mohammad Monirujjaman Khan and Arifa Sultana. "Novel and compact ultra-wideband wearable band-notch antenna design for body sensor networks and mobile healthcare system". In: *Engineering Proceedings* 3.1 (2020), p. 1. ISSN: 2673-4591.

[104] Arpan H Shah and Piyush N Patel. "Embroidered Annular Elliptical E-Textile Antenna Sensor for Knee Effusion Diagnosis". In: *IEEE Sensors Journal* 23.5 (2023), pp. 4809–4818. ISSN: 1530-437X.

[105] Saumya Lal, Kavya Subramanya, and Ramesh Abhari. "Miniaturized EBG-backed textile microstrip patch antenna for Bluetooth wearable sensor applications". In: *2016 IEEE International Symposium on Antennas and Propagation (APSURSI)*. IEEE, 2016, pp. 285–286. ISBN: 1509028862.

[106] Irfan Ullah, Mahmoud Wagih, and Steve P Beeby. "Design of textile antenna for moisture sensing". In: *Engineering Proceedings* 15.1 (2022), p. 11. ISSN: 2673-4591.

[107] Abubakar Sharif et al. "Low-cost inkjet-printed RFID tag antenna design for remote healthcare applications". In: *IEEE Journal of Electromagnetics, RF and Microwaves in Medicine and Biology* 3.4 (2019), pp. 261–268. ISSN: 2469-7249.

[108] Sangkil Kim et al. "Inkjet-printed sensors on paper substrate for agricultural applications". In: *2013 European Microwave Conference*. IEEE, 2013, pp. 866–869. ISBN: 2874870315.

[109] Janice Booth et al. "Military comparison of 3D printed vs commercial components". In: *Nano-, Bio-, Info-Tech Sensors, and 3D Systems II*. Vol. 10597. SPIE, 2018, pp. 52–66.

[110] Sang-Jun Ha and Chang Won Jung. "Reconfigurable beam steering using a microstrip patch antenna with a U-slot for wearable fabric applications". In: *IEEE Antennas and Wireless Propagation Letters* 10 (2011), pp. 1228–1231. ISSN: 1536-1225.

[111] Nacer Chahat et al. "60-GHz textile antenna array for body-centric communications". In: *IEEE Transactions on Antennas and Propagation* 61.4 (2012), pp. 1816–1824. ISSN: 0018-926X.

[112] Praveen Kumar Rao, Anamika Mani Tripathi, and Rajan Mishra. "Circular Shaped Flexible Antenna with Artificial Magnetic Conductor for Skin and Breast Cancer Detection". In: *Sensor Letters* 18.7 (2020), pp. 550–555. ISSN: 1546-198X.

[113] M Abdulmalek et al. "Design of a 5.2 GHz circularly polarized textile patch antenna for on/off body radio propagation channel evaluation". In: *2016 5th International Conference on Electronic Devices, Systems and Applications (ICEDSA)*. IEEE, 2016, pp. 1–4. ISBN: 1509053069.

[114] Hendrik Rogier et al. "Active textile antennas in professional garments for sensing, localisation and communication". In: *2013 European Microwave Conference*. IEEE, 2013, pp. 850–853. ISBN: 2874870315.

[115] Pei Cheng Ooi et al. "Performance Characteristics of 'Triangle-Like'Shape Textile Antennas". In: *Columbia International Publishing Journal of Modeling, Simulation, Identification, and Control* 1.1 (2013), pp. 44–51.

[116] Mohamad Mantash et al. "Zip based monopole antenna for wearable communication systems". In: *2012 6th European Conference on Antennas and Propagation (EUCAP)*. IEEE, 2012, pp. 762–764. ISBN: 1457709201.

[117] Marco Virili et al. "Wearable textile antenna magnetically coupled to flexible active electronic circuits". In: *IEEE Antennas and Wireless Propagation Letters* 13 (2014), pp. 209–212. ISSN: 1536-1225.

[118] Marc Martínez-Estrada et al. "Impact of conductive yarns on an embroidery textile moisture sensor". In: *Sensors* 19.5 (2019), p. 1004. ISSN: 1424-8220.

[119] Rob Seager et al. "Effect of the fabrication parameters on the performance of embroidered antennas". In: *IET Microwaves, Antennas Propagation* 7.14 (2013), pp. 1174–1181. ISSN: 1751-8733.

[120] Hendrik Rogier. "Textile antenna systems: design, fabrication, and characterization". In: *Handbook of Smart Textiles* (2015), pp. 433–458.

[121] Isidoro Ibanez Labiano et al. "Screen printing carbon nanotubes textiles antennas for smart wearables". In: *Sensors* 21.14 (2021), p. 4934. ISSN: 1424-8220.

[122] Vasileios Lakafosis et al. "Progress towards the first wireless sensor networks consisting of inkjet-printed, paper-based RFID-enabled sensor tags". In: *Proceedings of the IEEE* 98.9 (2010), pp. 1601–1609. ISSN: 0018-9219.

[123] Li Yang et al. "RFID tag and RF structures on a paper substrate using inkjet-printing technology". In: *IEEE transactions on microwave theory and techniques* 55.12 (2007), pp. 2894–2901. ISSN: 0018-9480.

[124] Tessa Acti et al. "High performance flexible fabric electronics for megahertz frequency communications". In: *2011 Loughborough Antennas Propagation Conference.* IEEE, 2011, pp. 1–4. ISBN: 1457710161.

[125] Zheyu Wang et al. "Embroidered multiband body-worn antenna for GSM/PCS/WLAN communications". In: *IEEE Transactions on Antennas and Propagation* 62.6 (2014), pp. 3321–3329. ISSN: 0018-926X.

[126] Thomas Kaufmann, Ilse-Marie Fumeaux, and Christophe Fumeaux. "Comparison of fabric and embroidered dipole antennas". In: *2013 7th European Conference on Antennas and Propagation (EuCAP).* IEEE, 2013, pp. 3252–3255. ISBN: 8890701838.

[127] Constantine A Balanis. *Antenna theory: analysis and design.* John wiley sons, 2016. ISBN: 1118642066.

[128] H Huang and Z N Chen. "Antenna sensors in passive wireless sensing systems". In: *Handbook of Antenna Technologies.* Springer Singapore, 2015, pp. 1–34.

[129] Gianluca Gennarelli et al. "A microwave resonant sensor for concentration measurements of liquid solutions". In: *IEEE Sensors Journal* 13.5 (2013), pp. 1857–1864. ISSN: 1530-437X.

[130] R Khadase and A Nandgaonkar. "Design of Implantable MSA for Glucose Monitoring". In: *International Conference on Communication and Signal Processing 2016 (ICCASP 2016).* Atlantis Press, 2016. ISBN: 9462523053.

[131] Ala Eldin Omer et al. "Multiple-cell microfluidic dielectric resonator for liquid sensing applications". In: *IEEE Sensors Journal* 21.5 (2020), pp. 6094–6104. ISSN: 1530-437X.

[132] Greeshmaja Govind and M Jaleel Akhtar. "Metamaterial-inspired microwave microfluidic sensor for glucose monitoring in aqueous solutions". In: *IEEE Sensors Journal* 19.24 (2019), pp. 11900–11907. ISSN: 1530-437X.

[133] Kushal Sen and Sneh Anand. "Demonstration of Microstrip Sensor for the Feasibility Study of Non-invasive Blood-Glucose Sensing". In: *Mapan* (2020), pp. 1–7. ISSN: 0974-9853.

[134] Lijie Li and Deepak Uttamchandani. "A microwave dielectric biosensor based on suspended distributed MEMS transmission lines". In: *IEEE Sensors Journal* 9.12 (2009), pp. 1825–1830. ISSN: 1530-437X.

[135] Volkan Turgul and Izzet Kale. "Simulating the effects of skin thickness and fingerprints to highlight problems with non-invasive RF blood glucose sensing from fingertips". In: *IEEE sensors journal* 17.22 (2017), pp. 7553–7560. ISSN: 1530-437X.

[136] N A Elias et al. "The effects of human body and bending on dipole textile antenna performance and SAR". In: *2012 Asia Pacific Microwave Conference Proceedings*. IEEE, 2012, pp. 34–36. ISBN: 1457713322.

[137] Abbas K Abbas et al. "Neonatal non-contact respiratory monitoring based on real-time infrared thermography". In: *Biomedical engineering online* 10.1 (2011), pp. 1–17. ISSN: 1475-925X.

[138] Susannah Fleming et al. "Normal ranges of heart rate and respiratory rate in children from birth to 18 years of age: a systematic review of observational studies". In: *The Lancet* 377.9770 (2011), pp. 1011–1018. ISSN: 0140-6736.

[139] Abhishek Sahu et al. "Recent advances in theory and applications of substrate-integrated waveguides: a review". In: *International Journal of RF and Microwave Computer-Aided Engineering* 26.2 (2016), pp. 129–145. ISSN: 1096-4290.

[140] Kunyi Zhang et al. "Microwave sensing of water quality". In: *IEEE Access* 7 (2019), pp. 69481–69493. ISSN: 2169-3536.

[141]   Euclides Lourenço Chuma et al. "Microwave sensor for liquid dielectric characterization based on metamaterial complementary split ring resonator". In: *IEEE Sensors Journal* 18.24 (2018), pp. 9978–9983. ISSN: 1530-437X.

Appendix

Ref A

Mariam El Gharbi, Raúl Fernández-García, Saida Ahyoud, and Ignacio Gil. 2020. "A Review of Flexible Wearable Antenna Sensors: Design, Fabrication Methods, and Applications" Materials 13, no. 17: 3781. Under a CC BY 4.0 license. https://doi.org/10.3390/ma13173781.

A Review of Flexible Wearable Antenna Sensors: Design, Fabrication Methods, and Applications

Mariam El Gharbi [1], **Raúl Fernández-García [1]**, **Saida Ahyoud [2]** and **Ignacio Gil [1,*]**

[1] Department of Electronic Engineering, Universitat Politècnica de Catalunya, 08222 Terrassa, Spain; mariam.el.gharbi2@upc.edu (M.E.G.); raul.fernandez-garcia@upc.edu (R.F.-G.)
[2] Information Technology & Systems Modeling Team, Faculty of Sciences, Abdelmalek Essaadi University, 93002 Tetouan, Morocco; sahyoud@uae.ac.ma
* Correspondence: ignasi.gil@upc.edu

Abstract: This review paper summarizes various approaches developed in the literature for antenna sensors with an emphasis on flexible solutions. The survey helps to recognize the limitations and advantages of this technology. Furthermore, it offers an overview of the main points for the development and design of flexible antenna sensors from the selection of the materials to the framing of the antenna including the different scenario applications. With regard to wearable antenna sensors deployment, a review of the textile materials that have been employed is also presented. Several examples related to human body applications of flexible antenna sensors such as the detection of NaCl and sugar solutions, blood and bodily variables such as temperature, strain, and finger postures are also presented. Future investigation directions and research challenges are proposed.

Keywords: antenna sensor; textile materials; wearable antenna sensor; flexible

1. Introduction

The industrial and academic world have generated a lot of interest in the field of wearable and flexible electronics in recent years [1]. Flexible electronics, whose mechanical properties include to be wrinkled, bent, and stressed/collapsed, would considerably extend the applications of modern electronic devices to multiple real nonflat scenarios [2], including the shape of the human body [3]. As a consequence, flexible electronics combined with textile materials offer many advantages that make them an attractive technology for boosting the next generation of consumer electronics, among them are low-cost manufacturing, inexpensive flexible substrates, light weight, and ease of fabrication [4].

Recently, there has been a lot of interest focused on antenna sensors due to their simple configuration, multimodality sensing, passive operation, and low cost [5]. Antenna sensors are electronic devices with dual functionality for communicating and sensing, and they can be implemented by minimizing the number of components. The function principle of antenna sensors is demonstrated by their geometrical or intrinsic material change influence in terms of their antenna resonance frequency, which is evaluated by means of the impact on the reflection coefficient. In addition, antenna sensors have been evolved as another process to measure diverse physical parameters. To provide the wireless communication required by today's information-oriented community, it is necessary to integrate flexible antenna sensors into flexible electronic systems [6].

In the literature, the first antenna sensor is published in [7]. A circular antenna is proposed to measure the humidity content of sludge samples. Above the antenna sensor, the sludge sample was placed inside a plastic beaker. The Bottcher model was used to calculate the humidity content of a sample from measurements of the dielectric effective permittivity of the antenna sensor. Several antenna sensors have been reported in the literature for measuring the relative permittivity of soils

and snow [8], gas [9], relative humidity [10], pH [11], soil moisture [12], and glucose [13]. All of these antenna sensors can be categorized as antenna dielectric sensors. The relation between the physical measurement and the radiation parameters of the antenna is determined by the properties of the material. This issue cannot be modeled analytically in the majority of the cases [14], and it is one of the challenges of the development of antenna dielectric sensor. Therefore, almost all the reported works of antenna dielectric sensors are mainly based on direct characterization and experimental tests. With regard to antenna temperature sensors, the first one found in the literature is devoted to temperature threshold detection [15]. The antenna sensor was fabricated from a shape memory polymer (SMP) paper sandwiched between a radio frequency identification (RFID) tag and a metallic sheet. The shape memory polymer changed its relative permittivity as the temperature crossed a doorstep, which in turn could be recognized from the turn-on power of the RFID tag.

Up to now, antenna sensors are applied for many applications, such as agricultural activities and gardening, structural health, biomedical sensing, food quality monitoring, and so on, which are mostly designed on rigid materials. Several researches have already been reported in the literature using rigid materials for different types of antenna sensors, including temperature sensing [16], crack sensing [17], strain sensing [18], and dielectric sensing [19]. Microstrip patch antennas are usually employed in sensing applications because they are characterized by several advantages: low manufacturing cost, low weight, durability and reliability, and small size. Patch antennas act as sensors through the interaction between dielectric properties and electromagnetic waves. For instance, a microstrip patch antenna-based sensor using flame retardant 4 (FR-4) substrate has been presented in [20]. The proposed antenna is employed as a sensor to detect different percentage of sugar and salt in terms of return loss based on the dielectric properties of the solution. In [21], a microstrip patch antenna sensor was printed on a Rogers (R03006) substrate. The presented antenna has been designed for temperature detection by subjecting a patch antenna bonded to various metal bases to thermal cycling. These types of substrates are not quite suitable for wearable antenna sensors as they cannot be stretched and bent. A wearable antenna sensor often should have additional characteristics such as robustness and flexibility, which claims the consideration of flexible nonconventional materials to exchange traditional printed circuit boards [22].

Wearable textile antenna sensors are becoming more and more essential in on-body applications in the last decade [23], due to their ability to detect microstructure deformations and human motions and to monitor and supervise the human health [24,25]. Compared with conventional antenna sensors, textile antenna sensors are able to be integrated on the outfits and they offer key features such as comfort, light weight, and washability. Various wearable flexible antenna sensors have been proposed in the literature. An example of a finger motion antenna sensor based on a dipole antenna proposed to realize dual function of sensing and communicating in the wireless sensor system was presented in [26]. Moreover, this dipole antenna sensor was attached on a glove to assess the human bending impact in the actual wearable device scenario. Taking into account the previous examples and as a future trend, the antenna sensor technology could be used in human machine interfacing, healthcare, robotics, and virtual reality.

Conference proceedings and full-text articles were chosen from a comprehensive search including diverse sources and databases such as ScienceDirect, Springer, Web of Science, and IEEE Xplore. Keywords were selected in each source as follows: (wearable OR flexible) AND (textile OR electro-textile) AND antenna sensor. The initial search returned 180 results. All results were screened and analyzed to eliminate duplicates and the final total was 83 studies, of which 33.4% were focused on the classification of antenna sensors, 52.3% were associated researches on technological feasibility and reliability, and the remaining 14.3% were investigative researches on scenario-based applications.

The Section 2 details the operating principle and the types of available antenna sensors in the literature. Section 3 presents a survey of the impact of certain characteristics of textile materials, different manufacturing techniques and particular examples and applications of flexible textile antenna

sensors. Finally, Section 4 exhibits the main conclusions and future research directions and challenges related with antenna sensors.

2. Principle of Operation and Classification of Antenna Sensors

2.1. Principle of Operation

In this section, a rectangular microstrip patch antenna is used to explain the principle of operation of an antenna sensor. A microstrip patch antenna contains four elements: a radiation patch, a dielectric substrate, a ground plane, and a transmission feed line as shown in Figure 1a. The radiation patch and the conductive ground plane (which can take any possible shape) are detached by a dielectric substrate. As a consequence, an effective electromagnetic resonance cavity allows radiation at particular frequencies [27]. The radiation patch is supplied by a microstrip feed line (Figure 1a), and an incident signal is provided. This signal is transmitted or reflected by the radiation patch. Consequently, the return loss of the microstrip patch antenna can be determined by the ratio between the reflected power and the incident power, also named "reflection coefficient" [21]. The radiation characteristics of the microstrip patch antenna can be characterized by the resonant bandwidth BW and the resonant frequency f_0. These two specifications can be extracted from the reflection coefficient (S11) [28]. The operating frequency of the antenna is determined as the frequency at which the reflection coefficient is minimum, i.e., little energy is reflected by the antenna and most of the incident power is radiated [29]. The resonant bandwidth of the antenna can be defined as the range of resonant frequencies at a given return loss, e.g., at −10 dB. In theory, all of these radiation parameters can be used to convert a physical quantity (strain, temperature, pressure, pH level, concentration of aqueous solution, etc.) into a measurable radiation parameter which leads to a resonance frequency shift (see Figure 1b).
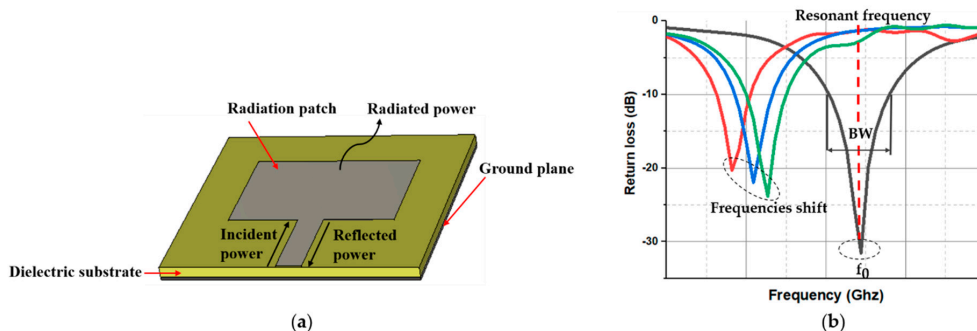
Figure 1. (**a**) Basic configuration of a microstrip antenna sensor and (**b**) illustration of frequencies shift of the antenna sensor.

2.2. Classification of Antenna Sensors

Antenna sensors can be classified into diverse categories as presented in the Figure 2. There are four main types of antenna sensors, namely, the temperature, dielectric, crack, and mechanical sensing. All these types of antenna sensors are able to detect changes using microwave signals or radio frequency (RF). Details of each types are described as follows.

2.2.1. Dielectric Sensing

An antenna dielectric sensor can be represented by a patch antenna or by other standard planar antennas. Figure 3 presents a patch antenna where the radiation patch is covered with a dielectric material (superstrate). The choice of superstrate material depends on the selected measurand (humidity, salt and sugar, gas, etc.). The substrate can use different materials such as carbon nanotubes for

gas sensing or polymer for humidity sensing or a textile material such as denim for blood glucose sensing [30]. However, the effective dielectric constant (relative permittivity) of the antenna sensor is provided by both the superstrate and the substrate [31]. Table 1 presents a summary of previously reported works on antenna dielectric sensors with different properties such as the measurand, the size, the operation frequency, material, and the sensing parameters.
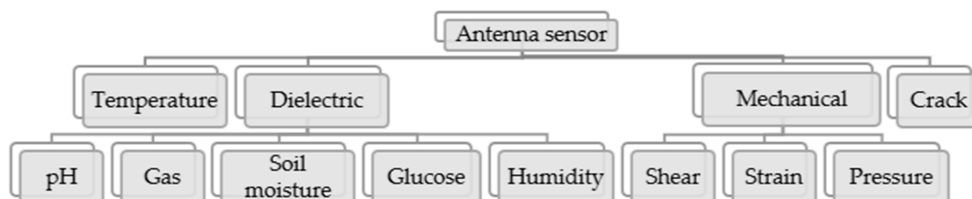
Figure 2. Different types of antenna sensors.
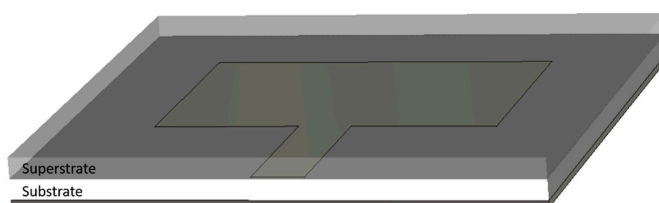
Figure 3. Configuration of an antenna dielectric sensor.

Table 1. Summary of previously reported works on antenna dielectric sensors.

Ref	Measurand	Type of Antenna	Size (mm²)	Freq	Material	Type of Material	Sensing Parameters
[11]	PH	Hexagonal split-ring resonator	19 × 23.35	3–20 GHz	[1] PCB	FR-4	Transmission coefficient
[20]	Salt and sugar	Crescent-shaped patch	32 × 22	2.5–18 GHz	[1] PCB	FR-4	Return loss
[32]	Humidity	H-shaped patch	90 × 85	880 MHz	Polymer	[2] PEDOT: PSS/	Threshold power
[33]	Gas	Patch antenna	41 × 41	2.4 Ghz	[1] PCB	Rogers RT/duroid 5880	Frequency shift
[34]	Soil moisture	Spiral antenna	12 × 12	2.48 GHz	[1] PCB	FR-4	Frequency shift
[35]	Moisture content	Patch antenna	48 × 48	2.26 GHz	Polymer	[3] PDMS	Frequency shift
[36]	Humidity	Patch antenna	30 × 20	38 GHz	Textile	Cotton	Frequency shift
[37]	Relative humidity	Split ring resonator	35 × 35	0–1.5 GHz	Polyimide	Kapton	Frequency shift

[1] Printed circuit board. [2] Poly (3,4-ethylenedioxythiophene) polystyrene sulfonate. [3] Polydimethylsiloxane.

2.2.2. Strain Sensing

In order to check the structural integrity of the engineering components, strain is among the most important mechanical properties that must be used to quantify the deformation of a material [38]. Regarding types of strains, there are two strains: shear strain and normal strain. The first type is determined from the change of angle from an original value of 90° and the second type is related to the change in the size of a design compared to its original size [39]. Figure 4a shows the operating principle of an antenna sensor for shear detection. An antenna patch with a slot in the ground plane is used to visualize the effect of the shear on the behavior of the antenna. The principle of a loop antenna sensor for pressure detection is presented in Figure 4b. The variation of the parameter d in the geometry of the antenna structure detunes its operating frequency [40].

In order to provide accurate spatial resolution, it is recommended that the strain sensor presents a small size [41]. Different types of antenna mechanical sensors are summarized in Table 2.

(a)

(b)
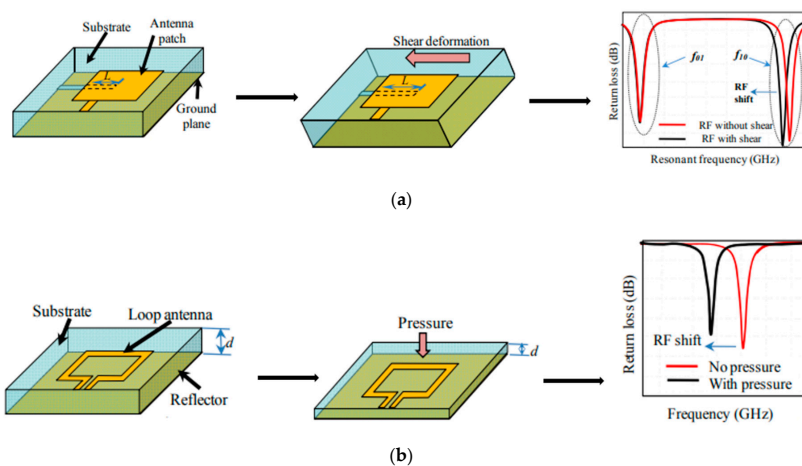
Figure 4. Antenna mechanical sensors for: (**a**) shear detection and (**b**) pressure detection, reproduced with permission from [45].

Table 2. List of antenna mechanical sensors.

Ref	Measurand	Type of Antenna	Size (mm²)	Freq	Material	Type of Material	Sensing Parameters
[39]	Strain	Dipole antenna	17 × 16	8–12 GHz	Polymer	Polyimide	Frequency shift
[42]	Pressure	Slot antenna	17.55 × 13.5	5.5 GHz	[1] PCB	Rogers laminate RO4350b	Frequency shift
[43]	Strain	Patch antenna	94.58 × 52.36	1.8–2.4 GHz	Textile	Felt	Frequency shift
[44]	Shear and pressure	Patch antenna	12.1 × 66.9	6–7 Ghz	Polyimide	Kapton	Frequency shift

[1] Printed circuit board.

2.2.3. Temperature Sensing

The temperature of an antenna sensor is an important parameter to know as it indicates whether or not the antenna sensor is in control. This parameter is useful for many applications, e.g., food production, manufacturing process control, human health monitoring, etc. There are many different types of antenna temperature sensors available and all have different characteristics depending upon their application [46]. Table 3 presents some research works reported in the literature for temperature sensing with several properties: the type of the antenna sensor, the size, the operation frequency, the used materials, and the sensing parameters.

Table 3. Summary of previously reported works on antenna temperature sensors.

Ref	Measurand	Type of Antenna	Size (mm²)	Freq	Material	Type of Material	Sensing Parameters
[47]	Body temperature	Patch antenna	10 × 6	38 GHz	Textile	Cotton	Frequency shift
[48]	Temperature	Slotted patch	38 × 38	900 MHz	[1] PCB	FR-4	Frequency shift
[49]	Temperature	Rectangular patch	11.8 × 9.8	4.85 GHz 5.95 GHz	[1] PCB	Rogers laminate RO3006	Frequency shift
[50]	Temperature	Patch antenna	13.6 × 10.9	2.4–2.8 GHz	[1] PCB	Rogers RO3210	Frequency shift
[51]	Temperature	Patch antenna	71 × 64	2.45 GHz 9.5 GHz 38 GHz	Textile	Cotton Jeans Viscose Lycra Cotton	Frequency shift

[1] Printed circuit board.

2.2.4. Crack Sensing

In order to reduce catastrophic structural breakdowns, cracks must be monitored because they are a direct indicator of structural damage monitoring. In fact, it is important to know the length, direction, and location of the crack to gather sufficient information to maintain structural integrity [52]. Figure 5 presents a configuration of an antenna patch for crack detection. The direction and growth of the crack can be detected by observing the changes in the resonance frequency shifts. The resonance frequency shift of the crack antenna is generally much larger than the resonance frequency shift caused by strain or temperature [53]. Some examples for antenna crack sensors are given in Table 4.

(**a**)　　　　　　　　　　　　　(**b**)　　　　　　　　　　　　　(**c**)
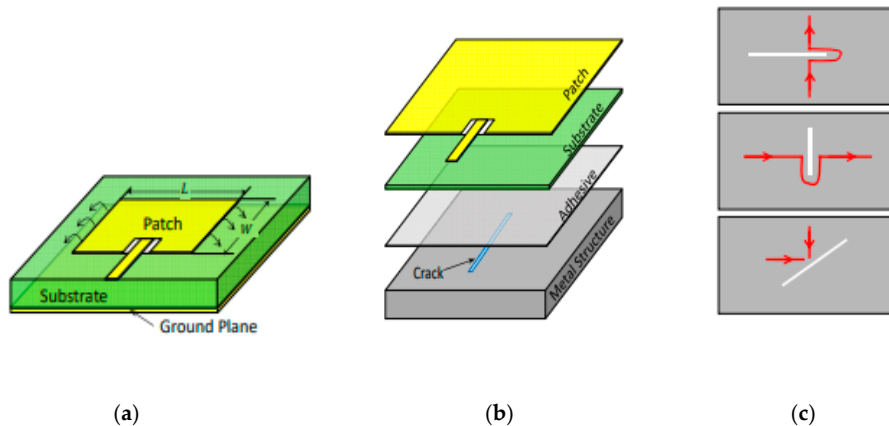
Figure 5. Antenna crack sensor: (**a**) schematic configuration of a patch antenna, (**b**) antenna sensor with crack, and (**c**) effect of cracks on the current model of the sensor [54].

Table 4. Summary of previously reported works on antenna crack sensors.

Ref	Measurand	Type of Antenna	Size (mm²)	Freq	Material	Type of Material	Sensing Parameters
[53]	Crack orientation	Rectangular patch	15 × 12.75	5.75 GHz 6 GHz	[1] PCB	Rogers laminate RO4350B	Frequency shift
[55]	Crack opening and growth	Rectangular patch	15 × 12.5	6.1 GHz 8.6 GHz	Polyimide	Kapton	Frequency shift
[56]	Crack	Patch antenna	35 × 20.6	2.4 GHz	[1] PCB	Rogers RT/duroid 5880	Frequency shift
[57]	Crack and monitoring	Patch antenna	50.8 × 25.4	6.1 GHz 7.6 GHz	Polyimide	Kapton	Frequency shift

[1] Printed circuit board.

3. Flexible Wearable Antenna Sensor

In order to provide good electrical performance as well as stability for the flexible devices, it is necessary to choose quality materials during manufacturing. The substrate selection for antenna sensor requires a low loss material so as to have better chances of increased antenna sensor efficiency when placed on the body. In fact, this is one of the important considerations for wearable electronics design [58]. Several flexible wearable antenna sensors are implemented on different types of materials such as papers [59], fabrics [60], and plastics [61]. Plastic substrates are neither recyclable nor biodegradable, as they affect environmental pollution and involve many health problems. Alternatively, textile materials are among the most internationally used and easily available materials for the design of flexible wearable antenna sensors with regard to body area networks (BANs).

3.1. Key Characteristics of Textile Materials in the Design of Antenna Sensors

The properties of the fabrics are determined from the properties of their constituent fibers and the structure of the fabric and/or the yarns. They are fibrous and porous materials, in which the pore size, fiber density, and air volume determine the general behavior, e.g., thermal insulation and air permeability [62]. Consistently, the density and thickness of fabrics can change with pressure as they are flexible, compressible, and stretchable materials. In addition, the fibers are constantly exchanging water molecules with the surrounding environment, which can sometimes affect their shape and properties [63]. It would be difficult to control these features in textile applications and, thus, it is necessary to know the influence of these factors on the behavior of the antenna sensor to reduce the undesirable and parasitic effects. Furthermore, the impact of the properties of textile materials on the performance of the antenna sensor is presented in this section.

3.1.1. Relative Permittivity (Dielectric Constant) of the Fabrics

The dielectric permittivity of the substrate or material is one of the most important parameters affecting on the ability to transmit rapidly changing signals through the textile transmission line. The operation frequency and reflection coefficient in the transmission line can be affected by this phenomenon. The dielectric permittivity is defined as Equation (1):

$$\varepsilon = \varepsilon_0 \varepsilon_r = \varepsilon_0 (\varepsilon_r' - j\varepsilon_r'') \tag{1}$$

where $\varepsilon_0 = 8.854 \times 10{-}12$ F/m is the permittivity of vacuum [64]. Generally, the moisture content, the temperature, the frequency, and also the surface roughness depend on the dielectric properties of the material under test [65]. The real part of the dielectric constant, ε_r', is also named "the relative permittivity". It should be noted that this parameter is not constant in frequency. In addition, the material losses are typically given by the loss tangent, defined as $\tan \delta = \varepsilon_r'' / \varepsilon_r'$.

The dielectric properties of textiles are reviewed and studied in [66,67]. The textile materials dielectric behavior depends on the characteristics of the constituent polymers and fibers. Various experimental methods have been used to determine an accurate measurement of the dielectric characteristics of textiles. Among these techniques, there are the cavity perturbation method [68], the MoM-segment method [69], the free-space method [70], and the transmission line method [71]. Generally, textiles offer a very low relative permittivity (in comparison with typical rigid substrate materials for electronic applications) as they are very porous fabrics. Table 5 presents the dielectric properties of common commercial textile fabrics.

Table 5. Dielectric properties of normal fabrics. Data from reference [72].

Nonconductive Fabric	ε_r	$\tan \delta$
Cordura$^{(r)}$	1.90	0.0098
Cotton	1.6	0.0400
100% polyester	1.90	0.0045
Quartzel$^{(r)}$ fabric	1.95	0.0004
Felt	1.215–1.225	0.016
Silk	1.75	0.012
Jeans	1.7	0.025
Fleece	1.17	0.0035
Denim	1.6–1.65	0.05

3.1.2. Surface Resistivity of Fabrics

The electronic performance of fabrics can be determined by the surface resistance. Hence, the surface resistance is the ratio of a direct voltage applied to the current obtained from two electrodes placed on the surface of a material [73], and it also can be defined by the ratio between the DC voltage drop

per unit length and the surface current per unit width. Surface resistivity is thus a property of the fabric considering a constant thickness, not depending on the design of the electrodes used for the measurement [62]. It is usually indicated by Ohm/square (Ω/sq).

3.1.3. Regain of the Fabrics

Relative humidity (RH) of the fabrics is determined as the amount of water in a sample of air compared to the maximum amount of water the air can hold at a given temperature. It is expressed in a form of 0% to 100% [74]. In [65], some studies are presented on various textile fibers which indicate the relationship between relative humidity of the air and regain (amount of humidity present in a fabric calculated as a percentage of its oven-dry weight). Note that for the same relative humidity conditions, there are textile fibers with different humidity contents. For example, at 65% RH, cotton fiber could offer a regain of 7.5%, polyester fiber might offer a regain of 0.2%, and wool fiber might offer a regain of 14.5% [65]. Generally, the humidity absorption changes the properties of fibers, such as the effective permittivity or the mechanical rigidity. For this reason, fabric metrology is carried out at a specified temperature of 20 °C and relative humidity of 65% [62].

3.1.4. Mechanical Deformations of the Fabrics

Textile fabrics are characterized by their good elasticity and flexibility, which makes them adaptive to curvature of the human body. However, after adapting to the topology of the surface, the structure is usually deformed and bent. These geometrical modifications influence the performance of the antenna sensor and they also lead to changes in the electromagnetic properties of textile fabrics [75]. In fact, the elongation and the bending of the dielectric fabric affect their thickness and their effective permittivity, which influences the resonance frequency of the antenna sensor. Furthermore, when the antenna sensor is compressed or elongated, the geometric accuracy decreases, affecting the behavior of the antenna sensor and, as a result, a resonant frequency shift can be produced.

3.2. Fabrication Methods for Wearable Antenna Sensor

Fabrication techniques are the determinants of the accuracy and manufacturing speed of low-cost wearable antenna sensor designs. The most popular wearable fabrication techniques are listed as follows: wet-etching [75], screen printing [76], inkjet printing [77], and embroidery methods [78]. To ensure durability, low cost, and high comfort to users in their daily wear, these techniques can be used for antenna sensors fabrication. An interesting review of these manufacturing methods is presented in [79–81]. Several of the aforementioned manufacturing techniques are discussed below.

3.2.1. Screen Printing

To produce a lightweight and flexible antenna sensor, screen printing is a simple and economical approach used by many electronics manufacturers. In addition, the screen printing is an additive operation, which makes it environmentally friendly [82]. Instead of hiding the woven screen that has different thread densities and thicknesses, the mask with the required pattern is adjusted directly to the substrate where the conductive ink is handled and thermally annealed.

Moreover, the screen-printing technique faces diverse limitations. It comprises its limited number of realizable layers, lack of thickness control for the conductive layer, and low printing resolution. These aspects lead to the limited implementation of this technology, because wearable printing requires better precision for the convenient operation of the communications for wearable devices.

3.2.2. Inkjet Printing

Inkjet printing is one of the relatively low-cost printing technologies [83]. This technology is capable of producing a very high precision pattern due to its use of ink droplets of the size of up to a few picoliters [84]. Additionally, this technique allows the design pattern to be transmitted directly to

the substrate with no requirement for masks. In addition, inkjet printing projects the single ink droplet from the nozzle to the required position, from which no waste is founded, which makes it among the economical manufacturing methods. This is a clear advantage in comparison with traditional etching technology, which has been generally used in industry [85]. The main drawbacks of inkjet printing technology are the incompatibility of certain types of conductive inks due to the larger particle size and clogging of the nozzles. Figure 6 presents an example of the inkjet-printing method using electroconductive layers on the surface of textile.
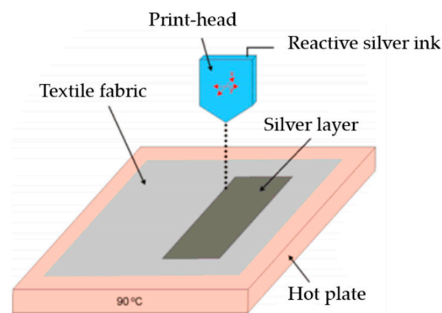

Figure 6. Silver deposition on textile surface using inkjet printing, reproduced with permission from [86].

3.2.3. Embroidery

This technique has been evolved to allow a digital image or layout to be directly embroidered using a computer-assisted embroidery machine. The embroidery manufacturing uses specialized conductive threads, from which the antenna sensor can be embroidered on the base substrate textile fabric. Before embroidering, it is very important to know the properties of the conductive threads that are going to be used (conductivity, DC resistance, and mechanical parameters), because when the conductive thread is characterized, it is then easier to find methods to improve the performance of the antenna sensor [87]. Therefore, the conductive threads must have adequate resistance and flexibility to avoid undesired breaks produced by high tensions in the embroidery machine [88]. Figure 7 depicts the embroidery technique, starting with the simulated design model to embroider the antenna integrated with the textile substrate.

Although embroidered antenna sensors are greatly considered as an ideal solution to replace traditional antennas in flexible electronics, compared with antenna sensors fabricate of metallic materials, they present some limitations, e.g., the embroidered geometry is much stretchable than metallic antenna sensors on inlays. This stretching impact, combined with the low resolution of the yarn stitches, makes fine geometries impractical [89]. The resistance of conductive yarn is much higher than metallic materials. They are either made of nylon cores coated with silver plating or carbon. The resistivity of the antenna sensors made from these yarns is order-of-magnitude higher than metallic ones even printed ones (made of silver paste or made of aluminum or copper).

3.2.4. Comparison of Embroidery with Other Techniques

The embroidery process is advantageous over other techniques and embroidery machines are more recommended in the industry. This technique is easier to apply for mass production of clothing with integrated embroidered antenna sensors. In embroidery, the currents in the fabric flow along the yarns, making linear antenna sensors such as spirals or dipoles suitable for this fabrication technique, because it is very difficult to manufacture this type of structure using a Nora dell cloths or copper tape. With embroidery, the use of glue is not always a requirement to connect the textile layers together and also it allows to create reproducible geometries via computerized embroidery machines [91]. This can improve the washability of the clothing with the integrated antenna sensor.
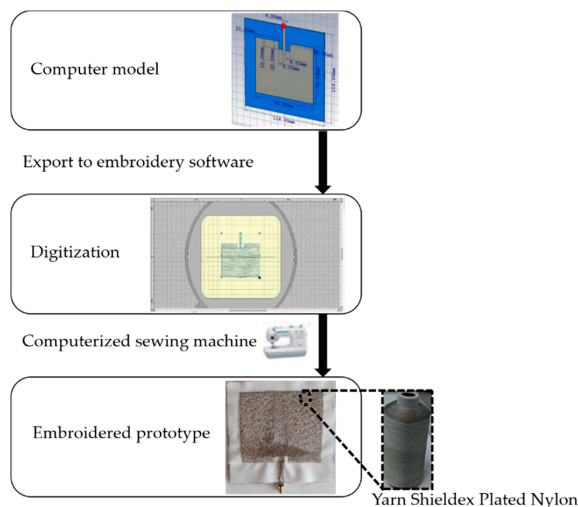
Figure 7. Embroidery process, reproduced with permission from [90].

3.3. Alternative Materials for the Deployment of Flexible Antenna Sensors

Various flexible wearable antenna sensors are implemented on different types of materials such as Kapton polyimide [92], cellulose filter paper [93], polydimethylsiloxane (PDMS) film [94], and graphene film (FGF) [95]. These materials are being applied as promising candidates for innovative flexible antenna sensors. All of these antenna sensors are discussed in the next section. Furthermore, the graphene has attracted tremendous interest in wearable communication devices due to its outstanding electronic properties and performance. However, the applications of graphene in antenna sensors are limited because the use of single or few layer graphene films exhibit insufficient electrical conductivity and high sheet resistance. Figure 8 represents the manufacturing process of an antenna sensor. This antenna is fabricated on a cellulose paper substrate with a radiating patch of aluminum tape and a ground plane.
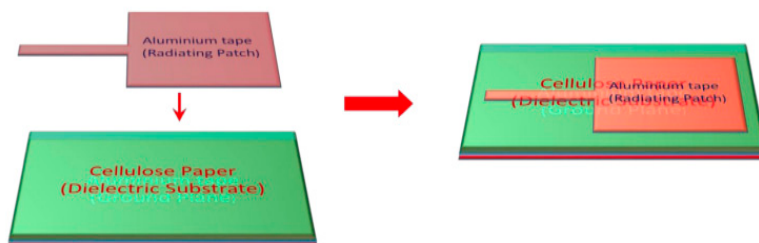
Figure 8. Manufacturing process of rectangular patch antenna sensor, reproduced with permission from [96].

3.4. Applications and Specific Examples of Flexible Textile Antenna Sensor Designs

In current society, sensing applications are always based on some specific scenarios, which require different functions for the antenna sensors. Flexible antenna sensors are an attracted research orientation in the field, and there are some typical samples as listed in Table 6, including dipole antenna sensors [26], patch antenna sensors [93,95–98], and RFID tag sensors [99,100].

A cellulose filter paper substrate for liquids detection was presented as shown in Figure 9b [93]. The patch antenna sensor utilized the special feature of the paper substrate, which is capable of absorbing liquids, such as sweat on the skin. The dielectric constant of the paper substrate is sensitive

to the properties of the absorbed liquid through the 2 slots in the structure. In this paper, the feasibility of the sweat detection is validated by artificial sweat and salt solutions measurements, in which the frequency mainly shifted with changing NaCl (sodium chloride) concentration (8.5–200 mmol/L).

(**a**)

(**b**)

(**c**)

(**d**)
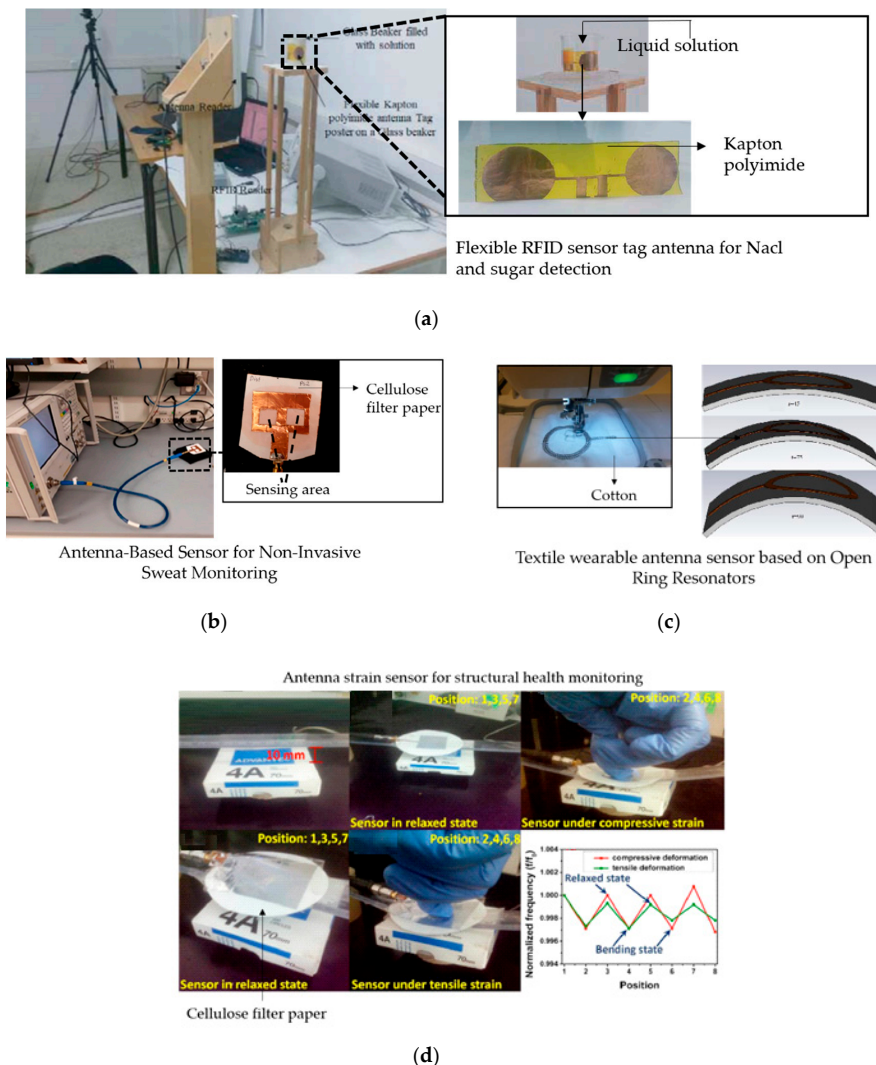
Figure 9. (**a**) Experimental setup for the measurements of the concentration of aqueous solutions, reproduced by courtesy of The Electromagnetics Academy [99]; (**b**) antenna sensor photo after absorbing saline solution [93]; (**c**) antenna sensor under bending stress, reproduced with permission from [101]; and (**d**) photographs of an antenna sensor in state tensile strain and compressive, reproduced with permission from [96].

Compared with the mentioned flexible based antenna sensor for solution detection, another antenna sensor with RFID techniques [99] was designed to detect the concentration of NaCl (sodium chloride) solutions and sucrose solutions, which was printed on a polyimide substrate as shown in Figure 9a. The proposed RFID tag antenna was used to detect the solutions based on sensitivity to different levels of concentration. From tests with concentration levels from 0% to 80% at the different

frequency points (864, 868, 915, and 926 MHz), the results revealed that sensitivity increases with the rise of concentration levels of NaCl and sucrose solutions.

Table 6. List of some previously reported work of flexible textile antenna sensor.

Ref	Measurand	Type of Antenna	Size (mm²)	Freq	Material	Type of Material	Sensing Parameters
[26]	Finger postures	Dipole antenna	100×20	426 MHz	Filter paper	Cellulose filter paper	Frequency shift
[93]	Noninvasive Sweat	Patch antenna	50×60	2–4 GHz	Filter paper	Cellulose filter paper	Frequency shift
[95]	Strain	Patch antenna	35×27.4	1.63 GHz	Carbon	Graphene Film (FGF)	Frequency shift
[96]	Strain	Patch antenna	29.5×37.7	2.4 GHz	Filter paper	Cellulose filter paper	Frequency shift
[97]	Blood glucose	Patch antenna	40×40	2.4 GHz	Textile	Denim	Specific Absorption Rate
[98]	Temperature	Patch antenna	71×64	2.45 GHz	Textile	Cotton	Frequency shift
[99]	NaCl and sugar	RFID tag	100×32	860–960 MHz	Polyimide	Kapton	Frequency shift
[100]	Strain	RFID tag	100×20	866.6 MHz	Textile	Polyester	Frequency shift

For the body fluids detection field, another typical textile-based antenna sensor was proposed for the blood glucose monitoring as shown in Table 6 [97]. This proposed antenna sensor was designed to operate at 2.4 GHz in a noninvasive manner. In this work, the SAR analysis was taken into account since the antenna sensor would radiate towards the body when operating on the arm. In addition, the work revealed the SAR was also sensitive to the substrate thickness. For instance, when the thickness value was 4 mm, the SAR value would be 3.86 W/kg, which was lower than the safety limit value of 4 W/kg.

A microstrip patch antenna sensor was designed to detect temperature as detailed in Table 6 [98]. The proposed antenna sensor was embroidered on a cotton substrate and developed to operate at ISM band around 2.45 GHz. In this work, the relative permittivity of the substrate sensitive to the temperature was utilized to affect the resonant frequency points. Through this way, the low-cost solution for heat monitoring could be used for body temperature detection.

A textile-based antenna sensor was proposed for the research on bending impact as shown in Figure 9c [101]. This proposed antenna sensor was designed with an open ring resonator structure, which was sensitive to the bending levels of the structure. In this work, the antenna sensor was tested under different bending radius (45 and 90 mm) and results showed an output sensitivity from 0.4 to 2.2 MHz/mm. The feasibility and usefulness could be validated for developments of the antenna sensor based on textile materials with an open ring resonator structure.

A paper-based patch antenna sensor was proposed for strain detection as shown in Figure 9d [96]. The antenna sensor was fabricated by a radiation patch as the antenna and sensor, a layer of cellulose filter paper as the substrate, and an aluminum tape as the ground pane. In this work, after hundreds of bending cycles in the bending strain tests, the performance of the antenna sensor was still stable. In addition, through small cracks identification, bending angle analysis, and real human motion detection applied to gloves, the antenna sensor was fully evaluated and proved to be feasible to be used in medical, healthcare, and modern electronic device areas.

A graphene-based antenna sensor was proposed for high strain detection as listed in Table 6 [95]. This antenna sensor was designed to operate at 1.63 GHz with the flexible multilayer graphene film (FGF) whose conductivity reaches 106 S/m. In this work, the performance of the proposed antenna sensor with the special material was tested under tensile and compressive bending situations, respectively. In addition, compared with the antenna sensor with similar copper material, the strain sensitivity of the graphene-based antenna sensor was higher. The kind of antenna sensor had some good features in reversible deformability, mechanical flexibility, and structure stability, which made it suitable for some applications such as wireless strain sensing and wearable devices.

4. Conclusions and Future Research Directions

In the realization and implementation of wearable devices, flexible antenna sensors are getting more attention due to their conformal characteristics, lightweight, and low cost, being ideal for wireless communication and sensing applications. This review starts with the principle of operation and the types of antenna sensors used and their state-of-the-art including technologies to realize these devices. For any presented type, divers reference examples are provided. Next, a survey of the effect of some features of the wearable materials, including dielectrics and conductors, in the behavior of the antenna sensors is reported. The work also details some guidelines for the choice of materials for designing textile antenna sensors. The current advanced manufacturing techniques for flexible wearable antenna sensors are discussed. Finally, several applications and specific examples of flexible wearable antenna sensor designs are reviewed. Flexible antenna sensors are promising devices to enhance and boost the development of wireless communication technology and contribute to the miniaturization and improvement of performance of the future communication systems, especially with regard to wearable applications and human body area network scenarios.

Flexible wearable antenna sensors are a topic of increasing interest for industry and the scientific community. For this reason, some research key issues and challenges foreseen for future research in this area are presented as follows:

- Improving the precision and efficiency of the current manufacturing and measuring methods.
- Introducing new yarns and conductive fabrics in the market with less resistivity or higher conductivity.
- Introducing new flexible wearable materials for embroidery technique or new proposed manufacturing techniques.
- Introducing new antenna sensors based on textile substrates to operate on body.

Textile antenna sensors are expected to be used in various fields such as industry, healthcare, security, and so on. In addition, it is still a long way for wearable antenna sensors to improve their performance and increase their reliability in future applications. Further research is still needed to explore novel designs with new manufacturing processes and textile materials. New materials such as graphene and conductive ink on textile substrates have been employed in order to improve the performance of textile sensors and are promising candidates for next-generation antenna sensors.

Textile antenna sensors present great potential applications in many areas of life and production. In fact, the reported research in the scientific literature is mainly focused on the basic functions of textile antenna sensors such as humidity sensing, temperature sensing, and strain sensing. Nowadays, there are some uses for the textile antenna sensors that do not cover advanced functions and significant research is in progress. For example, there are wearable textile antenna sensors that can only detect the temperature without analyzing any other element such as bending and reliability, which requires more research. In addition, textile antenna sensors are more suitable for different applications such as for medical applications due to the various medical textiles employed for elderly or patients. Many types of parameters including moisture, strain, blood-glucose, and pH could be detected by means of textile antenna sensor systems. As a consequence, numerous scenarios could create many opportunities for new designs and applications of textile antenna sensors in the future.

References

1. Venkatesan, M.; Veeramuthu, L.; Liang, F.-C.; Chen, W.-C.; Cho, C.-J.; Chen, C.-W.; Chen, J.-Y.; Yan, Y.; Chang, S.-H.; Kuo, C.-C. Evolution of electrospun nanofibers fluorescent and colorimetric sensors for environmental toxicants, pH, temperature, and cancer cells—A review with insights on applications. *Chem. Eng. J.* **2020**, *397*, 125413. [CrossRef]
2. Lim, C.; Shin, Y.; Jung, J.; Kim, J.H.; Lee, S.; Kim, D.-H. Stretchable conductive nanocomposite based on alginate hydrogel and silver nanowires for wearable electronics. *APL Mater.* **2019**, *7*, 31502. [CrossRef]
3. Wang, G.; Hou, C.; Wang, H. *Flexible and Wearable Electronics for Smart Clothing*; John Wiley & Sons: Hoboken, NJ, USA, 2020.
4. Nathan, A.; Chalamala, B.R. Special issue on flexible electronics technology, Part 1: Systems and applications. *Proc. IEEE* **2005**, *93*, 1235–1238. [CrossRef]
5. Huang, H. Flexible wireless antenna sensor: A review. *IEEE Sens. J.* **2013**, *13*, 3865–3872. [CrossRef]
6. Feliu-Batlle, V.; Feliu-Talegon, D.; Castillo-Berrio, C.F. Improved object detection using a robotic sensing antenna with vibration damping control. *Sensors* **2017**, *17*, 852. [CrossRef]
7. Gagnadre, I.; Gagnadre, C.; Fenelon, J.P. Circular patch antenna sensor for moisture content measurement on dielectric material. *Electron. Lett.* **1995**, *31*, 1167–1168. [CrossRef]
8. Denoth, A. The monopole-antenna: A practical snow and soil wetness sensor. *IEEE Trans. Geosci. Remote Sens.* **1997**, *35*, 1371–1375. [CrossRef]
9. McGrath, M.P.; Sabouni, R.N.; Pham, A.-V.H. Development of nanobased resonator gas sensors for wireless sensing systems. *Nano Sens. Mater. Devices* **2004**, *5593*, 62–72.
10. Chang, K.; Kim, Y.-H.; Kim, Y.-J.; Yoon, Y.J. Patch antenna using synthesized polyimide for RFID sensing. In Proceedings of the 2006 European Conference on Wireless Technology, Manchester, UK, 10–12 September 2006; pp. 83–86.
11. Islam, M.T.; Ashraf, F.B.; Alam, T.; Misran, N.; Mat, K.B. A compact ultrawideband antenna based on hexagonal split-ring resonator for pH sensor application. *Sensors* **2018**, *18*, 2959. [CrossRef]
12. You, K.Y.; Salleh, J.; Abbas, Z.; You, L.L. A rectangular patch antenna technique for the determination of moisture content in soil. *Prog. Electromagn. Res. C* **2010**, 850–854. Available online: https://www.researchgate.net/publication/236615978_A_Rectangular_Patch_Antenna_Technique_for_the_Determination_of_Moisture_Content_in_Soil (accessed on 2 June 2020).
13. Wiwatwithaya, S.; Phasukkit, P.; Tungjitkusolmun, S.; Wongtrairat, W. Real-time monitoring glucose by used microwave antenna apply to biosensor. In Proceedings of the 4th 2011 Biomedical Engineering International Conference, Shanghai, China, 15–17 October 2011; pp. 135–137.
14. Huang, H.; Chen, Z.N. Antenna sensors in passive wireless sensing systems. In *Handbook of Antenna Technologies*; Springer: Singapore, 2015; pp. 1–34.
15. Bhattacharyya, R.; Floerkemeier, C.; Sarma, S.; Deavours, D. RFID tag antenna based temperature sensing in the frequency domain. In Proceedings of the 2011 IEEE International Conference on RFID, Orlando, FL, USA, 12–14 April 2011; pp. 70–77.
16. Rodrigues, D.B.; Maccarini, P.F.; Salachi, S.; Oliveira, T.R.; Pereira, P.J.S.; Limão-Vieira, P.; Snow, B.W.; Reudink, D.; Stauffer, P.R. Design and optimization of an ultra wideband and compact microwave antenna for radiometric monitoring of brain temperature. *IEEE Trans. Biomed. Eng.* **2014**, *61*, 2154–2160. [CrossRef]
17. Padmavathy, T.V.; Bhargava, D.S.; Venkatesh, P.; Sivakumar, N. Design and development of microstrip patch antenna with circular and rectangular slot for structural health monitoring. *Pers. Ubiquitous Comput.* **2018**, *22*, 5–6. [CrossRef]
18. Tchafa, F.M.; Huang, H. Microstrip patch antenna for simultaneous strain and temperature sensing. *Smart Mater. Struct.* **2018**, *27*, 65019. [CrossRef]
19. Cheng, E.M.; Fareq, M.; Shahriman, A.B.; Mohd Afendi, R.; Lee, Y.S.; Khor, S.F.; Tan, W.H.; Nashrul Fazli, M.N.; Abdullah, A.Z.; Jusoh, M.A. Development of microstrip patch antenna sensing system for salinity and sugar detection in water. *Int. J. Mech. Mechatron. Eng.* **2014**, *15*, 31–36.
20. Islam, M.T.; Rahman, M.N.; Singh, M.S.J.; Samsuzzaman, M. Detection of salt and sugar contents in water on the basis of dielectric properties using microstrip antenna-based sensor. *IEEE Access* **2018**, *6*, 4118–4126. [CrossRef]

21. Sanders, J.W.; Yao, J.; Huang, H. Microstrip patch antenna temperature sensor. *IEEE Sens. J.* **2015**, *15*, 5312–5319. [CrossRef]

22. Luo, C.; Gil, I.; Fernández-García, R. Wearable textile UHF-RFID sensors: A systematic review. *Materials* **2020**, *13*, 3292. [CrossRef]

23. Paracha, K.N.; Rahim, S.K.A.; Soh, P.J.; Khalily, M. Wearable antennas: A review of materials, structures, and innovative features for autonomous communication and sensing. *IEEE Access* **2019**, *7*, 56694–56712. [CrossRef]

24. Liu, Y.; Wang, H.; Zhao, W.; Zhang, M.; Qin, H.; Xie, Y. Flexible, stretchable sensors for wearable health monitoring: Sensing mechanisms, materials, fabrication strategies and features. *Sensors* **2018**, *18*, 645. [CrossRef]

25. Azeez, H.I.; Yang, H.-C.; Chen, W.-S. Wearable triband E-shaped dipole antenna with low SAR for IoT applications. *Electronics* **2019**, *8*, 665. [CrossRef]

26. Su, C.; Wu, H. An Antenna Sensor to Identify Finger Postures. In Proceedings of the 2019 IEEE Eurasia Conference on IOT, Communication and Engineering (ECICE), Yunlin, Taiwan, 3–6 October 2019; pp. 571–574.

27. Yang, J.; Wang, H.; Lv, Z.; Wang, H. Design of miniaturized dual-band microstrip antenna for WLAN application. *Sensors* **2016**, *16*, 983. [CrossRef]

28. Balanis, C.A. Microstrip antennas. *Antenna Theory Anal. Des.* **2005**, *3*, 811–882.

29. Howell, J.Q. Microstrip antennas. *ITAP* **1975**, *23*, 90–93. [CrossRef]

30. Cioffi, V.; Costanzo, S. Wearable approach for contactless blood-glucose monitoring by textile antenna sensor. In Proceedings of the World Conference on Information Systems and Technologies, La Toja Island, Spain, 16–19 April 2019; pp. 287–291.

31. Islam, M.T.; Ullah, M.H.; Singh, M.J.; Faruque, M.R.I. A new metasurface superstrate structure for antenna performance enhancement. *Materials* **2013**, *6*, 3226–3240. [CrossRef]

32. Manzari, S.; Occhiuzzi, C.; Nawale, S.; Catini, A.; di Natale, C.; Marrocco, G. Humidity sensing by polymer-loaded UHF RFID antennas. *IEEE Sens. J.* **2012**, *12*, 2851–2858. [CrossRef]

33. Verma, R.; Said, K.; Salim, J.; Kimathi, E.; Rizkalla, M.; Shrestha, S.; Agarwal, M.; Varahramyan, K. Carbon nanotube-based microstrip antenna gas sensor. In Proceedings of the 2013 IEEE 56th International Midwest Symposium on Circuits and Systems (MWSCAS), Columbus, OH, USA, 4–7 August 2013; pp. 724–727.

34. Priyaa, A.S.P.; Mohammed, A.; Ambili, C.; Anusree, N.S.; Thekekara, A.V.; Rajesh Mohan, R.; Mridula, S. Microwave Sensor Antenna for Soil Moisture Measurement. In Proceedings of the 2015 Fifth International Conference on Advances in Computing and Communications (ICACC), Kochi, India, 3–5 September 2015; pp. 258–262.

35. Zhu, L.; Li, W.; Han, X.; Peng, Y. Microfluidic flexible substrate integrated microstrip antenna sensor for sensing of moisture content in lubricating oil. *Int. J. Antennas Propag.* **2020**, *2020*. [CrossRef]

36. Lin, X.; Seet, B.-C.; Joseph, F. Wearable humidity sensing antenna for BAN applications over 5G networks. In Proceedings of the 2018 IEEE 19th Wireless and Microwave Technology Conference (WAMICON), Sand Key, FL, USA, 9–10 April 2018; pp. 1–4.

37. Akhir, S.A.M.; Ibrahim, S.Z.; Rosli, N.; Zain, A.S.M.; Khalid, N. Antenna for humidity sensor using split ring resonator. *Indones. J. Electr. Eng. Comput. Sci.* **2019**, *13*, 584–592. [CrossRef]

38. Mattelin, M.-A.; Missinne, J.; de Coensel, B.; van Steenberge, G. Imprinted polymer-based guided mode resonance grating strain sensors. *Sensors* **2020**, *20*, 3221. [CrossRef]

39. Jang, S.-D.; Kim, J. Passive wireless structural health monitoring sensor made with a flexible planar dipole antenna. *Smart Mater. Struct.* **2012**, *21*, 27001. [CrossRef]

40. Lopato, P.; Herbko, M. A circular microstrip antenna sensor for direction sensitive strain evaluation. *Sensors* **2018**, *18*, 310. [CrossRef]

41. Zhang, J.; Tian, G.Y.; Marindra, A.M.J.; Sunny, A.I.; Zhao, A.B. A review of passive RFID tag antenna-based sensors and systems for structural health monitoring applications. *Sensors* **2017**, *17*, 265. [CrossRef]

42. Yao, J.; Xu, C.C.; Mears, A.; Jaguan, M.; Tjuatja, S.; Huang, H. Pressure sensing using low-cost microstrip antenna sensor. *Sens. Smart Struct. Technol. Civ. Mech. Aerosp. Syst.* **2015**, *9435*, 943537.

43. Omer, H.A.H.; Azemi, S.N.; Al-Hadi, A.A.; Soh, P.J.; Jamlos, M.F. Structural health monitoring sensor based on a flexible microstrip patch antenna. *Indones. J. Electr. Eng. Comp. Sci.* **2018**, *10*, 917–924. [CrossRef]

44. Huang, H.; Farahanipad, F.; Singh, A.K. A stacked dual-frequency microstrip patch antenna for simultaneous shear and pressure displacement sensing. *IEEE Sens. J.* **2017**, *7*, 8314–8323. [CrossRef]

45. Mohammad, I.; Huang, H. Pressure and shear sensing based on microstrip antennas. In *Sensors and Smart Structures Technologies for Civil, Mechanical, and Aerospace Systems 2012*; Society of Photo-Optical Instrumentation Engineers (SPIE): Bellingham, WA, USA, 2012; p. 83451D.

46. Goumopoulos, C. A high precision, wireless temperature measurement system for pervasive computing applications. *Sensors* **2018**, *18*, 3445. [CrossRef] [PubMed]

47. Lin, X.; Seet, B.-C.; Joseph, F. Fabric antenna with body temperature sensing for BAN applications over 5G wireless systems. In Proceedings of the 2015 9th International Conference on Sensing Technology (ICST), Auckland, New Zealand, 8–10 December 2015; pp. 591–595.

48. Yang, F.; Qiao, Q.; Virtanen, J.; Elsherbeni, A.Z.; Ukkonen, L.; Sydanheimo, L. Reconfigurable sensing antenna: A slotted patch design with temperature sensation. *IEEE Antennas Wirel. Propag. Lett.* **2012**, *11*, 632–635. [CrossRef]

49. Jiang, H.; Sanders, J.; Yao, J.; Huang, H. *Patch antenna based temperature sensor. Nondestructive Characterization for Composite Materials, Aerospace Engineering, Civil Infrastructure, and Homeland Security 2014*; The International Society for Optical Engineering: Bellingham, WA, USA, 2014; p. 90631P.

50. Tchafa, F.M.; Huang, H. Microstrip patch antenna for simultaneous temperature sensing and superstrate characterization. *Smart Mater. Struct.* **2019**, *28*, 105009. [CrossRef]

51. Ibanez-Labiano, I.; Alomainy, A. Dielectric characterization of non-conductive fabrics for temperature sensing through resonating antenna structures. *Materials* **2020**, *13*, 1271. [CrossRef]

52. Zhang, J.; Huang, B.; Zhang, G.; Tian, G.Y. Wireless passive ultra high frequency RFID antenna sensor for surface crack monitoring and quantitative analysis. *Sensors* **2018**, *18*, 2130. [CrossRef]

53. Mohammad, I.; Gowda, V.; Zhai, H.; Huang, H. Detecting crack orientation using patch antenna sensors. *Meas. Sci. Technol.* **2011**, *23*, 15102. [CrossRef]

54. Ke, L.; Liu, Z.; Yu, H. Characterization of a patch antenna sensor's resonant frequency response in identifying the notch-shaped cracks on metal structure. *Sensors* **2019**, *19*, 110. [CrossRef]

55. Mohammad, I.; Huang, H. Monitoring fatigue crack growth and opening using antenna sensors. *Smart Mater. Struct.* **2010**, *19*, 55023.

56. Xue, S.; Yi, Z.; Xie, L.; Wan, G.; Ding, T. A passive wireless crack sensor based on patch antenna with overlapping sub-patch. *Sensors* **2019**, *19*, 4327. [CrossRef] [PubMed]

57. Mohammad, I.; Huang, H. An antenna sensor for crack detection and monitoring. *Adv. Struct. Eng.* **2011**, *14*, 47–53. [CrossRef]

58. Hatamie, A.; Angizi, S.; Kumar, S.; Pandey, C.M.; Simchi, A.; Willander, M.; Malhotra, B.D. Textile based chemical and physical sensors for healthcare monitoring. *J. Electrochem. Soc.* **2020**, *167*, 37546. [CrossRef]

59. Marasco, I.; Niro, G.; Lamanna, L.; Piro, L.; Guido, F.; Algieri, L.; Mastronardi, V.M.; Qualtieri, A.; Scarpa, E.; Desmaele, D.; et al. Compact and flexible meander antenna for Surface Acoustic Wave sensors. *Microelectron. Eng.* **2020**, *227*, 111322. [CrossRef]

60. Wagih, M.; Wei, Y.; Komolafe, A.; Torah, R.; Beeby, S. Reliable UHF long-range textile-integrated RFID tag based on a compact flexible antenna filament. *Sensors* **2020**, *20*, 3435. [CrossRef]

61. Ossa, O.D.; Lopez, F.E. Rectangular patch antenna strain sensor with plastic substrate for curvature measurements. *IEEE Lat. Am. Trans.* **2018**, *16*, 1358–1363. [CrossRef]

62. Salvado, R.; Loss, C.; Gonçalves, R.; Pinho, P. Textile materials for the design of wearable antennas: A survey. *Sensors* **2012**, *12*, 15841–15857. [CrossRef]

63. Liu, N.; Lu, Y.; Qiu, S.; Li, P. Electromagnetic properties of electro-textiles for wearable antennas applications. *Front. Electr. Electron. Eng. China* **2011**, *6*, 563–566. [CrossRef]

64. Baker-Jarvis, J.; Janezic, M.D.; DeGroot, D.C. High-frequency dielectric measurements. *IEEE Instrum. Meas. Mag.* **2010**, *13*, 24–31. [CrossRef]

65. Hearle, J.W.S.; Morton, W.E. *Physical Properties of Textile Fibres*; Elsevier: Amsterdam, The Netherlands, 2008.

66. Bal, K.; Kothari, V.K. Measurement of dielectric properties of textile materials and their applications. *NOPR* **2009**, *34*, 191–199.

67. Sankaralingam, S.; Gupta, B. Determination of dielectric constant of fabric materials and their use as substrates for design and development of antennas for wearable applications. *IEEE Trans. Instrum. Meas.* **2010**, *59*, 3122–3130. [CrossRef]

68. Ouyang, Y.; Chappell, W.J. High frequency properties of electro-textiles for wearable antenna applications. *IEEE Trans. Antennas Propag.* **2008**, *56*, 381–389. [CrossRef]

69. Shawl, R.K.; Longj, B.R.; Werner, D.H.; Gavrin, A. The characterization of conductive textile materials intended for radio frequency applications. *IEEE Antennas Propag. Mag.* **2007**, *49*, 28–40. [CrossRef]

70. Harmer, S.W.; Rezgui, N.; Bowring, N.; Luklinska, Z.; Ren, G. Determination of the complex permittivity of textiles and leather in the 14–40 GHz millimetre-wave band using a free-wave transmittance only method. *IET Microw. Antennas Propag.* **2008**, *2*, 606–614. [CrossRef]

71. Declercq, F.; Rogier, H.; Hertleer, C. Permittivity and loss tangent characterization for garment antennas based on a new matrix-pencil two-line method. *IEEE Trans. Antennas Propag.* **2008**, *6*, 2548–2554. [CrossRef]

72. Cicchetti, R.; Miozzi, E.; Testa, O. Wideband and UWB antennas for wireless applications: A comprehensive review. *Int. J. Antennas Propag.* **2017**, *2017*, 1–45. [CrossRef]

73. Petersen, P.; Helmer, R.; Pate, M.; Eichhoff, J. Electronic textile resistor design and fabric resistivity characterization. *Text. Res. J.* **2011**, *81*, 1395–1404. [CrossRef]

74. Dhupkariya, S.; Singh, V.K.; Shukla, A. A review of textile materials for wearable antenna. *J. Microw. Eng. Technol.* **2015**, *1*, 975–8887.

75. Locher, I.; Klemm, M.; Kirstein, T.; Troster, G. Design and characterization of purely textile patch antennas. *IEEE Trans. Adv. Packag.* **2006**, *29*, 777–788. [CrossRef]

76. Roshni, S.B.; Jayakrishnan, M.P.; Mohanan, P.; Surendran, K.P. Design and fabrication of an E-shaped wearable textile antenna on PVB-coated hydrophobic polyester fabric. *Smart Mater. Struct.* **2017**, *26*, 105011. [CrossRef]

77. Abutarboush, H.F.; Farooqui, M.F.; Shamim, A. Inkjet-printed wideband antenna on resin-coated paper substrate for curved wireless devices. *IEEE Antennas Wirel. Propag. Lett.* **2015**, *15*, 20–23. [CrossRef]

78. Tsolis, A.; Whittow, W.G.; Alexandridis, A.A.; Vardaxoglou, J.C. Embroidery and related manufacturing techniques for wearable antennas: Challenges and opportunities. *Electronics* **2014**, *3*, 314–338. [CrossRef]

79. Seager, R.; Zhang, S.; Chauraya, A.; Whittow, W.; Vardaxoglou, Y.; Acti, T.; Dias, T. Effect of the fabrication parameters on the performance of embroidered antennas. *IET Microw. Antennas Propag.* **2013**, *7*, 1174–1181. [CrossRef]

80. Rogier, H. Textile antenna systems: Design, fabrication, and characterization. In *Handbook of Smart Textiles*; Springer: Singapore, 2015; pp. 433–458.

81. Aun, N.F.M.; Soh, P.J.; Al-Hadi, A.A.; Jamlos, M.F.; Vandenbosch, G.A.E.; Schreurs, D. Revolutionizing wearables for 5G: 5G technologies: Recent developments and future perspectives for wearable devices and antennas. *IEEE Microw. Mag.* **2017**, *18*, 108–124. [CrossRef]

82. Khaleel, H.R. Design and fabrication of compact inkjet printed antennas for integration within flexible and wearable electronics. *IEEE Trans. Compon. Packag. Manuf. Technol.* **2014**, *4*, 1722–1728. [CrossRef]

83. Wang, Y.; Yan, C.; Cheng, S.-Y.; Xu, Z.-Q.; Sun, X.; Xu, Y.-H.; Chen, J.-J.; Jiang, Z.; Liang, K.; Feng, Z.-S. Flexible RFID Tag Metal Antenna on Paper-Based Substrate by Inkjet Printing Technology. *Adv. Funct. Mater.* **2019**, *29*, 1902579. [CrossRef]

84. Lakafosis, V.; Rida, A.; Vyas, R.; Yang, L.; Nikolaou, S.; Tentzeris, M.M. Progress towards the first wireless sensor networks consisting of inkjet-printed, paper-based RFID-enabled sensor tags. *Proc. IEEE* **2010**, *98*, 1601–1609. [CrossRef]

85. Yang, L.; Rida, A.; Vyas, R.; Tentzeris, M.M. RFID tag and RF structures on a paper substrate using inkjet-printing technology. *IEEE Trans. Microw. Theory Tech.* **2007**, *55*, 2894–2901. [CrossRef]

86. Stempien, Z.; Rybicki, E.; Rybicki, T.; Lesnikowski, J. Inkjet-printing deposition of silver electro-conductive layers on textile substrates at low sintering temperature by using an aqueous silver ions-containing ink for textronic applications. *Sens. Actuators B Chem.* **2016**, *224*, 714–725. [CrossRef]

87. Acti, T.; Zhang, S.; Chauraya, A.; Whittow, W.; Seager, R.; Dias, T. High performance flexible fabric electronics for megahertz frequency communications. In Proceedings of the 2011 Loughborough Antennas & Propagation Conference, Laughborough, UK, 14–25 November 2011; pp. 1–4.

88. Wang, Z.; Lee, L.Z.; Psychoudakis, D.; Volakis, J.L. Embroidered multiband body-worn antenna for GSM/PCS/WLAN communications. *IEEE Trans. Antennas Propag.* **2014**, *62*, 3321–3329. [CrossRef]

89. Liu, Y.; Xu, L.; Li, Y.; Ye, T.T. Textile based embroidery-friendly RFID antenna design techniques. In Proceedings of the 2019 IEEE International Conference on RFID (RFID), Pisa, Italy, 25–27 September 2019; pp. 1–6.

90. Gil, I.; Fernandez-Garcia, R. Wearable embroidered GPS textile antenna. In Proceedings of the 2017 Progress in Electromagnetics Research Symposium-Spring (PIERS), St. Petersburg, Russia, 22–25 May 2017; pp. 655–659.

91. Kaufmann, T.; Fumeaux, I.-M.; Fumeau, C.X. Comparison of fabric and embroidered dipole antennas. In Proceedings of the 2013 7th European Conference on Antennas and Propagation (EuCAP), Gorhenburg, Swiden, 8–12 April 2013; pp. 3252–3255.

92. el Khamlichi, M.; Melcon, A.A.; el Mrabet, O.; Ennasar, M.A.; Hinojosa, J. Flexible UHF RFID tag for blood tubes monitoring. *Sensors* **2019**, *19*, 4903. [CrossRef] [PubMed]

93. Eldamak, A.R.; Fear, E.C. Conformal and disposable antenna-based sensor for non-invasive sweat monitoring. *Sensors* **2018**, *18*, 4088. [CrossRef]

94. Xu, F.; Zhang, D.; Liao, Y.; Xie, F.; Zhang, H. Dispersion of LiZnTiBi ferrite particles into PMDS film for miniaturized flexible antenna application. *Ceram. Int.* **2019**, *45*, 8914–8918. [CrossRef]

95. Tang, D.; Xu, L.; Li, Y.; Ye, T.T. Highly sensitive wearable sensor based on a flexible multi-layer graphene film antenna. *Sci. Bull.* **2018**, *63*, 574–579. [CrossRef]

96. Kanaparthi, S.; Sekhar, V.R.; Badhulika, S. Flexible, eco-friendly and highly sensitive paper antenna based electromechanical sensor for wireless human motion detection and structural health monitoring. *Extrem. Mech. Lett.* **2016**, *9*, 324–330. [CrossRef]

97. Costanzo, S.; Cioffi, V. Preliminary SAR Analysis of Textile Antenna Sensor for Non-invasive Blood-Glucose Monitoring. In Proceedings of the International Conference on Information Technology & Systems, Bogotá, Colombia, 5–7 February 2020; pp. 607–612.

98. Labiano, I.I.; Alomainy, A. Fabric Antenna for Temperature Sensing over ISM Frequency Band. In Proceedings of the 2019 IEEE International Symposium on Antennas and Propagation and USNC-URSI Radio Science Meeting, Atlanta, GA, USA, 7–12 July 2019; pp. 1567–1568.

99. Ennasar, M.A.; el Mrabet, O.; Mohamed, K.; Essaaidi, M. Design and characterization of a broadband flexible polyimide RFID tag sensor for NaCl and sugar detection. *Prog. Electromagn. Res.* **2019**, *94*, 273–283. [CrossRef]

100. Chen, X.; Ukkonen, L.; Björninen, T. Passive E-textile UHF RFID-based wireless strain sensors with integrated references. *IEEE Sens. J.* **2016**, *16*, 7835–7836. [CrossRef]

101. Moradi, B.; Fernández-García, R.; Gil, I. Textile wearable antenna sensors based on open ring resonators. In Proceedings of the 12th European Conference on Antennas and Propagation (EuCAP), London, UK, 9–13 April 2018.

Ref B

Mariam El Gharbi, Raúl Fernández-García, and Ignacio Gil. 2021. "Textile Antenna-Sensor for In Vitro Diagnostics of Diabetes" Electronics 10, no. 13: 1570. Under a CC BY 4.0 license.
https://doi.org/10.3390/electronics10131570

Article

Textile Antenna-Sensor for In Vitro Diagnostics of Diabetes

Mariam El Gharbi * , **Raúl Fernández-García** and **Ignacio Gil**

Department of Electronic Engineering, Universitat Politècnica de Catalunya, 08222 Terrassa, Spain;
raul.fernandez-garcia@upc.edu (R.F.-G.); ignasi.gil@upc.edu (I.G.)
* Correspondence: mariam.el.gharbi2@upc.edu

Abstract: In this paper, a feasibility study of a microwave antenna-based sensor is proposed for in vitro experiments for monitoring blood glucose levels. The proposed device consists of a square-ring incorporated within a fully textile monopole antenna to absorb and sense different glucose concentrations, covering patients with different diabetic conditions. The designed antenna-sensor is optimized to operate at 2.4 GHz. The sensing principle is based on the resonance frequency shift of the reflection response of the antenna-based sensor under different glucose levels. The experiments were carried out with blood mimicking by means of aqueous solutions, using D(+)- glucose/water in different concentrations for various diabetic conditions of type-2 diabetes. The performance of the em-broidered antenna-based sensor is characterized and validated using a convenient setup for in vitro measurements. The results demonstrated the ability of the proposed antenna-based sensor to cover all the glucose levels of the diabetes range, including hypoglycemia (10–70 mg/dL), normoglycemia (80–110 mg/dL) and hyperglycemia (130–190 mg/dL) with a sensitivity of 350 kHz/(mg/dL). Besides its ability to detect different glucose concentrations of various diabetic conditions, the proposed antenna-sensor presents diverse features such as a simplistic design, compact size, wearability and low cost. The proposed textile device demonstrates a proof of concept for efficient in vitro blood glucose level measurements and diagnostics of diabetes.

Keywords: antenna-sensor; frequency shift; glucose detection; microwave sensing; sensitivity; textile monopole antenna

1. Introduction

Human beings suffer from several diseases related to genetic or lifestyle factors. Diabetes mellitus (DM) is one of the most common illnesses increasingly expanding among humankind, and it is a critical worldwide health problem due to the increase of diabetes patients and the lack of treatment [1]. Diabetes is caused by the malfunction of the insulin-producing cells of the pancreas. Insulin is a hormone that helps regulate the level of blood glucose, and it also helps introduce glucose molecules into cells for storage or energy production [2]. This illness can cause many complications in the human body including stroke, kidney failure, heart attacks and peripheral arterial disease. According to the World Health Organization (WHO), 422 million people worldwide have diabetes, particularly in low-and middle-income countries, and the number will increase to 592 million in 2035 [3]. According to the International Diabetes Federation (IDF), the diabetes is categorized into three main categories as Type-1 diabetes, Type-2 diabetes and gestational diabetes (GDM). The Type-2 is the most common among diabetics and accounts for around 90% of all diabetes cases [4,5]. The blood glucose level is classified into three categories: Hypoglycemia, Normoglycemia and Hyperglycemia [6]. The first one is typically defined as a blood glucose level less than 70 mg/dL. The primary signs and symptoms of hypoglycemia include shivering, accelerated heartbeat, dizziness and others [7]. When the patients feel any of these symptoms, they should consume food or drinks high in sugar until their blood glucose levels reach the normal range. The second one is the state of having a normal level of blood glucose and it encompasses the range of 80 to 110 mg/dL. The last category, called

hyperglycemia, was defined by WHO as a blood glucose level greater than 120 mg/dL and it is considered one of the most dangerous conditions for diabetic patients because it causes more complications such as nerve damage, cardiovascular disease, feet problems and eye diseases [8]. Therefore, diabetics have to check their blood glucose levels regularly to reduce the danger of additional illness.

In the literature, there are various techniques developed for glucose monitoring levels including Raman spectroscopy [9,10], electrochemistry [11], reverse iontophoresis (RI) [12] and optical [13], on which the researchers have been working to measure blood glucose levels. Microwave sensing is considered as a promising technique for monitoring blood glucose levels due to the miniaturization of the involved electronic systems, ease of handing, cost-effectiveness and quick response time [14]. The operation principle in most of the microwave sensors is based on detecting the variations in the dielectric properties of different concentrations of blood glucose on the sensing area. The changes in dielectric properties of the liquid under test in the sensing area are perceived and explained by the sensing parameters (resonance frequency and/or amplitude) of a readout device. To enhance the sensitivity and generate high-accuracy measurement results, the liquid under test should be placed in the zone of a high intensity electric field.

Recently, antennas operating as sensors established a growing demand for monitoring blood glucose levels [15]. Several studies have been reported in the literature using antenna-based sensors to detect blood glucose levels [16–18]. In [16], a microstrip patch antenna-sensor was developed to monitor blood glucose levels in an in vitro experiment. The glucose concentration ranged from 0 to 400 mg/dL, and the antenna-based sensor demonstrated a sensitivity of 25 kHz/(mg/dL). A planar inverted-F antenna (PIFA) was used as a sensor to test three diabetic conditions [17]. The antenna-sensor was optimized to operate at 530 MHz. A resonance frequency shift of 3.54 kHz/(mg/dL) was observed according to the change of glucose concentration. All the devices mentioned above used conventional electronic rigid substrates. Printed circuit boards (PCBs) are implemented by means of commercial substrates that are not suitable for electronic textile applications.

Wearable electronic textiles have grown rapidly in recent years for various research fields such as communication, sensing, information and medical [19]. Electronic textiles (e-textiles) could be developed on common clothes which are lighter and more comfortable than those implemented on PCBs, and they can also easily adapt to rapid changes in the computational and sensing conditions of any application. Recently, textile materials have been getting more attention due to their special characteristics including low weight, integration level, softness and flexibility [20].

In the current study, a textile embroidered monopole antenna-based sensor is proposed for monitoring blood glucose levels for in vitro experiment. The designed antenna-sensor was optimized to operate at 2.4 GHz. Different glucose concentrations were prepared to cover diabetes patients with Hypoglycemia, Normoglycemia and Hyperglycemia. The remainder of the paper is organized as follows. Section 2 details the methodology of the antenna-sensor design as well as the preparation of the blood mimicking aqueous solutions. Section 3 presents the results of the proposed antenna-based sensor for three diabetic conditions. A comparison of different techniques for detecting glucose concentration using microwave sensors is presented in Section 4. Finally, Section 5 exhibits the main conclusions.

2. Materials and Methods

2.1. Antenna-Sensor Design

To design an antenna-sensor and perform a realistic simulation, the substrate-related parameters have to be defined. For textile materials, it is essential to determine the permittivity and the losses of the substrates. A split-post dielectric resonator (SPDR) was used to characterize the dielectric parameters of the textile substrate by means of the resonance method. Felt was chosen as a substrate due to its low loss tangent and low cost in comparison with other fabrics. The experimental dielectric constant and loss tangent of the felt fabric were $\varepsilon_r = 1.2$ and $\tan \delta = 0.0013$. Furthermore, an electronic outside

micrometer was used to measure the thickness (h = 0.7 mm) of the felt substrate. The fabric material corresponds to a non-woven structure with a 100% polyester (PES) composition. The conductive antenna-sensor layer is embroidered by means of a commercial conductive yarn (Shieldex 117/17 dtex 2-ply) made of 99% pure silver-plated nylon yarn 140/17 dtex with a linear resistance < 30 Ω/cm.

The design of the proposed antenna-based sensor mainly consisted of a square ring (radiation part) and a partial ground plane. This antenna-sensor is designed to operate at 2.4 GHz. The embroidered textile monopole antenna-sensor was fabricated using a Singer Futura XL embroidery machine. The manufacturing embroidery process is depicted in Figure 1. Starting with the simulated design of the antenna-sensor using the commercial CST Studio Suite 3D full electromagnetic simulator 2019, the geometry of the proposed antenna-sensor as well as the sensing area are presented in Figure 1a. A parametric study was performed by means of a geometric tuning process on various parameters such as length and width of the substrate and square-ring of the proposed antenna-sensor in order to obtain better insight into the physical behavior of the antenna and to optimize its behavior at 2.4 GHz. The list of the optimized geometrical parameters are detailed in Table 1. The desired design layout was digitized, converting the antenna-sensor shape into the path that the needle was going to follow in the embroidery machine. After importing the file which contained the identification of the desired geometry into the embroidery machine in digital format, the computerized embroidery process was implemented to embroider the conductive part of the design. A needle with the conductive yarn was threaded through the substrate material and interwoven with a bobbin assistant yarn to form the stitch (Figure 1b). The stitches appeared the same on the top and bottom of the felt substrate. A satin fill stitch pattern was selected and implemented because it was well-suited to a narrow shape. This fact ensures the required resolution for the antenna dimensions. The final embroidered prototype of the textile antenna-sensor is shown in Figure 1c.
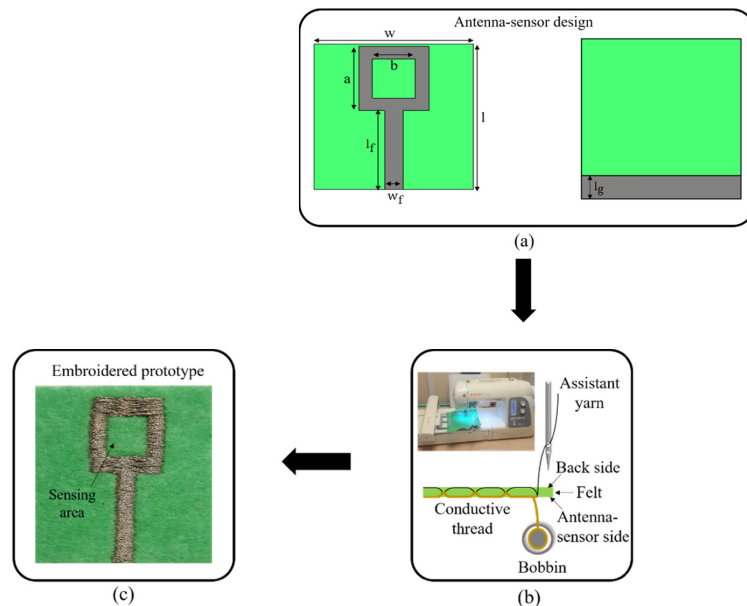

Figure 1. Embroidery process of the proposed antenna-sensor: (**a**) Antenna-sensor design; (**b**) Pattern embroidery; (**c**) Embroidered prototype.

Table 1. Geometrical parameters of the proposed antenna-sensor.

| Parameters	Dimensions (mm)
w	35
l	35
w_f	3.1
l_f	19
a	15.4
b	9.4
l_g	5

2.2. Samples Preparation and Test Setup

The entire human blood consists of glucose and other components, as well as water which accounts for a major proportion of its volume. Therefore, it can be predicted that the dielectric properties of the blood are related to the properties of aqueous glucose solutions. To imitate the blood behavior for in vitro experiments, several aqueous glucose concentrations were prepared by mixing distilled water and D(+)- glucose powder for various diabetic conditions of type-2 diabetes.. The glucose/water solutions were prepared to verify the functionality of the proposed antenna-based sensor.

The glucose/water solutions were prepared to cover diabetes patients for three states concerning glucose concentration level (G_{con}):

- Hypoglycemia: $G_{con} \leq 70$ mg/dL.
- Normoglycemia: $80 \leq G_{con} \leq 110$ mg/dL.
- Hyperglycemia: $G_{con} > 120$ mg/dL.

To test the antenna-sensor response for different concentration at each diabetic condition, three sets of samples were prepared. Each set consisted of four newly embroidered antenna-sensors for a specific state of the diabetes patients. A photograph of the measurement setup is shown in Figure 2. A digital micropipette device was used to drop a specific volume of each concentration on the sensing area. To reduce the measurement errors due to uncertainty in the solution volume, a minimum volume considered of V = 2 µL was selected for testing different glucose concentrations. The antenna-sensor was connected to an N9916A FieldFox microwave analyzer operating as a vector network analyzer (VNA) for recording data of the return loss for the in vitro experiment. Throughout the experiment, the controlled environmental conditions were maintained. Absorbed solutions in the sensing area (square ring) with various concentrations of glucose alter the dielectric properties of the substrate and therefore reflection measurements are expected to change accordingly.
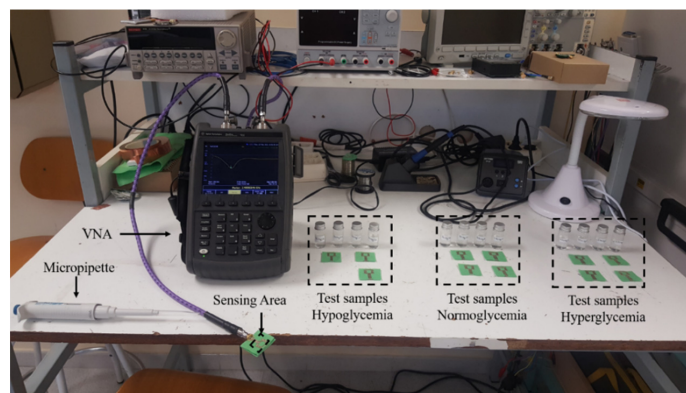
Figure 2. Test setup for verification of the antenna-sensor performance.

3. Results

In order to verify the accuracy of the fabrication technique of the antenna-sensor design, 12 antenna-sensors (same as presented in Figure 1a) were fabricated for testing and validation. All the fabricated antenna-sensors were tested in free space by measuring the return loss. The return loss of the simulated and measured device are compared in Figure 3. We presented five samples (S1, S2, S3, S4 and S5) as an example to emphasize consistency of our antenna-sensor output. The measured return loss of five fabricated antenna-sensors presented a slight deflection between measured and simulated results due to manufacturing tolerance. The simulated return loss reaches -24 dB at resonance frequency 2.4 GHz.
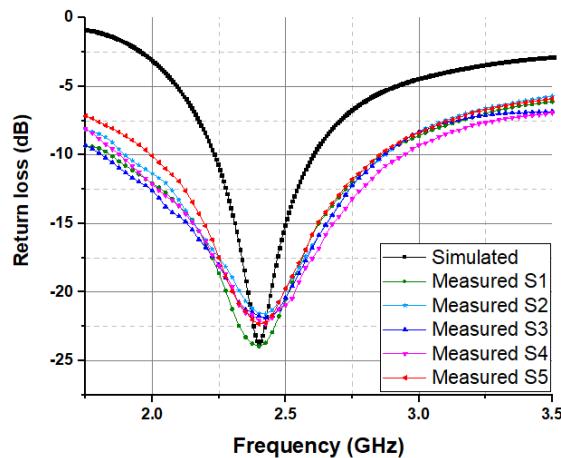

Figure 3. Return loss of simulated and measured for the proposed antenna-sensor.

All the measured results of the embroidered antenna-sensor have a resonant frequency of 2.4 GHz and exhibited a small declination in the amplitude of the return loss due to embroidery fabrication tolerance.

RF Response of the Glucose Level

The radio frequency (RF) microwave sensing of the glucose level relies on the resonance concept of the antenna-sensor. The main principle is based on the detection of the change in the RF signal induced by different concentrations of the glucose/water solutions, which present different dielectric properties. 12 measurements are performed to verify the functionality of the proposed antenna-sensor for several diabetic conditions. The measurement setup of the antenna-sensors is shown in Figure 2. Three sets of samples are prepared, with each set dedicated to one of the diabetic conditions. The initial testing was performed for four antenna-sensors to cover diabetes patients with hypoglycemia (10–70 mg/dL) within in vitro experiments. A second test was implemented for the glucose-based aqueous solution range from 80 to 110 mg/dL of four new fabricated antenna-sensors to cover diabetes patients with normoglycemia. Finally, the last four new microwave antenna-sensors were tested to reach the indicated concentrations for hyperglycemia (130–190 mg/dL) diabetic condition. All samples were tested with a fixed-volume micropipette and the return loss was immediately recorded (<6 s) after the solution was dropped on the sensing area.

When the textile antenna-sensor absorbs certain solutions, the electrical properties such as the resonance frequency are expected to change, since the overall permittivity of the textile substrate was modified. Therefore, the frequency shift was considered as the principal sensing parameter of the proposed antenna-sensor. The square ring was selected as the sensing area to apply a drop of 2 μL by micropipette of different concentrations, which can generate a detectable shift in the resonance frequency. Different

glucose/water solutions correspond to different dielectric properties. Therefore, this alteration in dielectric properties produced a shift in the resonance frequency. The return loss response of the antenna-sensor was recorded for each of the indicated concentrations for different diabetic conditions. Figure 4 illustrates the measured return loss of the proposed antenna-sensor for three diabetic conditions with a zoom-in zone of the main resonance points. The distilled water was considered as a reference sample. Due to the higher constant dielectric of the distilled water, the resonance frequency in the air shifted by 100 MHz. We observed that the resonance frequency of the antenna-based sensor for each diabetic condition shifts up when increasing the concentration of the glucose/water solutions. The electromagnetic interaction between the antenna-based sensor and glucose with a different dielectric constant was the main cause of the change in resonance frequency.
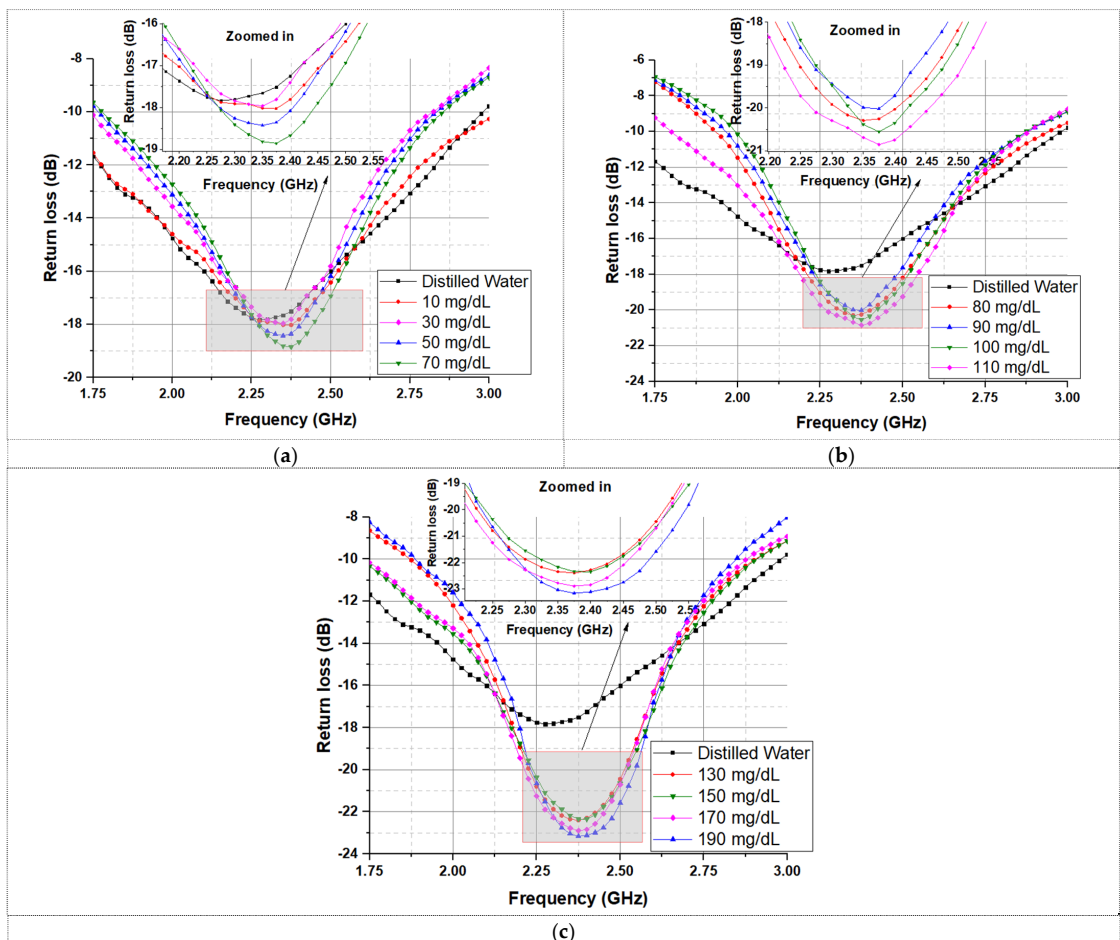

Figure 4. The measured return loss of the proposed antenna-based sensor of three diabetic conditions: (**a**) Hypoglycemia; (**b**) Normoglycemia; and (**c**) Hyperglycemia.

The behavior of the proposed device can be understood as an antenna-based sensor whose resonance frequency was altered by absorbing different glucose/water concentrations for each diabetic condition. This device can help to distinguish the glucose levels in diabetes patients. After recording the antenna-sensor performance results, a linear regression analysis was applied to evaluate the resonance frequency with various con-

centrations of glucose/water solutions for each diabetic condition. Figure 5 presents the applied linear regression of the resonance frequency shift for the three diabetic conditions. It can be observed that the results show a good linear relationship between different glucose concentrations and the resonance frequency shift. The obtained results reveal a correlation coefficient (R^2) of 0.96 between the indicated concentrations and the resonance frequency shift.
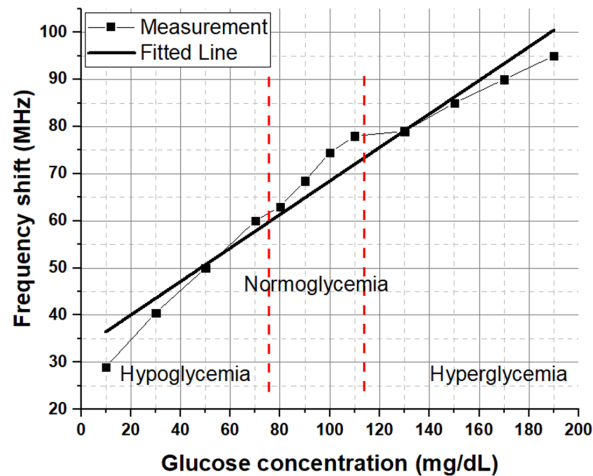

Figure 5. Linear correlation for the frequency shift as a function of glucose concentration in different diabetic conditions.

4. Discussion

This paper exhibits proof of how RF signals may be used to differentiate various glucose concentrations, covering diabetic patients with hypoglycemia, normoglycemia and hyperglycemia within in vitro experiments. The main concept is based on the absorption of different glucose/water solutions by the textile substrate on the sensing area. Therefore, the resonance frequency of the antenna-based sensor changes due to the variation in dielectric properties of different glucose concentrations inside the sensing area. Furthermore, the microwave measurements of the proposed antenna-sensor succeed to distinguish different glucose concentrations for the three diabetic conditions. In order to demonstrate the performance of our device, a comparison of the proposed antenna-sensor with previous works is listed in Table 2. It can be observed to have excellent sensor sensitivity and a reasonable measurement range of glucose concentrations. The sensing parameter is based on the resonance frequency of reflection response in some of the microwave sensors, while others used the resonance frequency of the transmission response variations for sensing. The sensitivity (S) was defined by the resonant frequency shift that the sensor can achieve for a unit change in glucose concentration. The proposed antenna-sensor offers higher sensitivity in comparison with microwave sensors reported in the literature which are based on various sensing mechanisms. Moreover, the area of the proposed antenna-sensor is competitive in comparison with the reported works. All of the techniques reported in Table 2 used rigid substrates. Therefore, the proposed work is a novel approach for monitoring blood glucose levels based on a textile antenna.

Table 2. Comparisons of different techniques for detecting glucose concentration using microwave sensors.

Ref	Measurement Technique	Concentration (mg/dL)	Area (mm²)	Resonant Frequency (GHz)	Substrate	Sensing Parameters	S (kHz per mg/dL)
[21]	Rectangular Waveguide Cavity	0–25,000	110 × 54.5	1.9	Rigid	$f_r(S_{21})$	0.4
[17]	Inverted-F Antenna (PIFA)	0–530	38 × 38	0.53	Rigid	$f_r(S_{11})$	3.54
[22]	CSRR resonator	70–150	59 × 20	1–6	Rigid (FR-4)	$f_r(S_{21})$	67–11
[23]	Split ring resonator	0–5000	50 × 20	4.18	Rigid (Rogers RT6006)	$f_r(S_{21})$	26
[16]	Microstrip Patch Antenna-Sensor	0–400	42.97 × 34.60	2.4	Rigid	$f_r(S_{11})$	25
[24]	Distributed MEMS transmission lines (DMTL)	0–347.8	-	16	Rigid	$f_r(S_{11})$	16.4
[25]	Single-port sensor	100–1000	55 × 30	4.8	Rigid (Rogers RO3006)	$f_r(S_{11})$	14
This work	**Monopole Antenna-Sensor**	**0–190**	**35 × 35**	**2.4**	**Textile**	$f_r(S_{11})$	**350**

5. Conclusions

In this article, a textile monopole antenna-based sensor was presented for the monitoring of glycemia level for diabetes. The performance of the antenna-sensor was practically validated. The measured results of the return loss in free space presented a good agreement with the simulation at 2.4 GHz. The proposed antenna-sensor was tested on in vitro experiments to verify the functionality of the microwave glucose antenna-sensor. A blood mimicking aqueous solution was prepared for different concentrations to cover diabetes patients with hypoglycemia, normoglycemia and hyperglycemia relevant to type-2 diabetes. The sensing method is based on the absorption of different glucose concentrations by textiles on the sensing area. The textile antenna-based sensor uses reflection measurement to monitor the glucose level change in the resonant frequency. The detection of different glucose/water solutions is based on the variation of the dielectric properties of the sensing area which produce a significant shift in the resonant frequency. A linear regression was applied to the resonant frequency shift and a good correlation can be clearly seen between glucose concentration and the frequency shift. The results demonstrate the capability of the proposed device to cover all the glucose levels of diabetes, hypoglycemia, normoglycemia and hyperglycemia, with a sensitivity of 350 kHz/(mg/dL). The proposed antenna-sensor presents a higher sensitivity compared to existing microwave sensors reported in the literature; together with other features such as simple design, low cost and miniature size, it can therefore be used as a preliminary screening for monitoring blood glucose levels.

Author Contributions: M.E.G. conducted the research and writing; I.G. and R.F.-G. supervised and reviewed the work. All authors have read and agreed to the published version of the manuscript.

Conflicts of Interest: The authors declare no conflict of interest.

References

1. Whiting, D.R.; Guariguata, L.; Weil, C.; Shaw, J. IDF diabetes atlas: Global estimates of the prevalence of diabetes for 2011 and 2030. *Diabetes Res. Clin. Pract.* **2011**, *94*, 311–321. [CrossRef] [PubMed]
2. International Diabetes Federation. Available online: https://www.idf.org/aboutdiabetes/what-is-diabetes.html (accessed on 21 May 2021).
3. World Health Organization. Available online: https://www.who.int/health-topics/diabetes#tab=tab_3 (accessed on 21 May 2021).
4. Nathan, D.M.; DCCT/Edic Research Group. The diabetes control and complications trial/epidemiology of diabetes interventions and complications study at 30 years: Overview. *Diabetes Care* **2014**, *37*, 9–16. [CrossRef]
5. Tang, L.; Chang, S.J.; Chen, C.-J.; Liu, J.-T. Non-Invasive Blood Glucose Monitoring Technology: A Review. *Sensors* **2020**, *20*, 6925. [CrossRef] [PubMed]
6. International Diabetes Federation Guideline Development Group. Global guideline for type 2 diabetes. *Diabetes Res. Clin. Pract.* **2014**, *104*, 1–52. [CrossRef] [PubMed]
7. Yi, S.-W.; Park, S.; Lee, Y.-H.; Balkau, B.; Yi, J.-J. Fasting Glucose and All-Cause Mortality by Age in Diabetes: A Prospective Cohort Study. *Diabetes Care* **2018**, *41*, 623–626. [CrossRef] [PubMed]
8. Wei, C.H.; Litwin, S.E. Hyperglycemia and adverse outcomes in acute coronary syndromes: Is serum glucose the provocateur or innocent bystander? *Diabetes* **2014**, *63*, 2209–2212. [CrossRef]
9. Stuart, D.A.; Yuen, J.M.; Shah, N.; Lyandres, O.; Yonzon, C.R.; Glucksberg, M.R.; Walsh, J.T.; Van Duyne, R.P. In Vivo Glucose Measurement by Surface-Enhanced Raman Spectroscopy. *Anal. Chem.* **2006**, *78*, 7211–7215. [CrossRef]
10. Li, N.; Zang, H.; Sun, H.; Jiao, X.; Wang, K.; Liu, T.C.-Y.; Meng, Y. A Noninvasive Accurate Measurement of Blood Glucose Levels with Raman Spectroscopy of Blood in Microvessels. *Molecules* **2019**, *24*, 1500. [CrossRef]
11. Wei, C.; Liu, Y.; Li, X.; Zhao, J.; Ren, Z.; Pang, H. Nitrogen-Doped Carbon–Copper Nanohybrids as Electrocatalysts in H_2O_2 and Glucose Sensing. *ChemElectroChem* **2014**, *1*, 799–807. [CrossRef]
12. Potts, R.O.; Tamada, J.A.; Tierney, M.J. Glucose monitoring by reverse iontophoresis. *Diabetes Metab. Res. Rev.* **2002**, *18*, S49–S53. [CrossRef]
13. Steiner, M.-S.; Duerkop, A.; Wolfbeis, O.S. Optical methods for sensing glucose. *Chem. Soc. Rev.* **2011**, *40*, 4805–4839. [CrossRef]
14. Qiang, T.; Wang, C.; Kim, N.-Y. Quantitative detection of glucose level based on radiofrequency patch biosensor combined with volume-fixed structures. *Biosens. Bioelectron.* **2017**, *98*, 357–363. [CrossRef]
15. El Gharbi, M.; Fernández-García, R.; Ahyoud, S.; Gil, I. A Review of Flexible Wearable Antenna Sensors: Design, Fabrication Methods, and Applications. *Materials* **2020**, *13*, 3781. [CrossRef]
16. Sen, K.; Anand, S. Demonstration of Microstrip Sensor for the Feasibility Study of Non-invasive Blood-Glucose Sensing. *MAPAN* **2020**, *36*, 193–199.
17. Khadase, R.; Nandgaonkar, A. Design of Implantable MSA for Glucose Monitoring. In Proceedings of the International Conference on Communication and Signal Processing 2016 (ICCASP 2016), Lonere, India, 26–27 December 2016.
18. Saha, S.; Cano-Garcia, H.; Sotiriou, I.; Lipscombe, O.; Gouzouasis, I.; Koutsoupidou, M.; Palikaras, G.; Mackenzie, R.; Reeve, T.; Kosmas, P.; et al. A Glucose Sensing System Based on Transmission Measurements at Millimetre Waves using Micro strip Patch Antennas. *Sci. Rep.* **2017**, *7*, 1–11. [CrossRef] [PubMed]
19. Gonçalves, C.; Ferreira da Silva, A.; Gomes, J.; Simoes, R. Wearable e-textile technologies: A review on sensors, actuators and control elements. *Inventions* **2018**, *3*, 14. [CrossRef]
20. Salvado, R.; Loss, C.; Gonçalves, R.; Pinho, P. Textile Materials for the Design of Wearable Antennas: A Survey. *Sensors* **2012**, *12*, 15841–15857. [CrossRef]
21. Gennarelli, G.; Romeo, S.; Scarfi, M.R.; Soldovieri, F. A Microwave Resonant Sensor for Concentration Measurements of Liquid Solutions. *IEEE Sens. J.* **2013**, *13*, 1857–1864. [CrossRef]
22. Omer, A.E.; Shaker, G.; Safavi-Naeini, S.; Ngo, K.; Shubair, R.M.; Alquie, G.; Deshours, F.; Kokabi, H. Multiple-Cell Microfluidic Dielectric Resonator for Liquid Sensing Applications. *IEEE Sens. J.* **2020**, *21*, 6094–6104. [CrossRef]
23. Govind, G.; Akhtar, M.J. Metamaterial-inspired microwave microfluidic sensor for glucose monitoring in aqueous solutions. *IEEE Sens. J.* **2019**, *19*, 11900–11907. [CrossRef]
24. Li, L.; Uttamchandani, D. A Microwave Dielectric Biosensor Based on Suspended Distributed MEMS Transmission Lines. *IEEE Sens. J.* **2009**, *9*, 1825–1830. [CrossRef]
25. Turgul, V.; Kale, I. Simulating the Effects of Skin Thickness and Fingerprints to Highlight Problems with Non-Invasive RF Blood Glucose Sensing from Fingertips. *IEEE Sens. J.* **2017**, *17*, 7553–7560. [CrossRef]

Ref C

Mariam El Gharbi, Raúl Fernández-García, and Ignacio Gil, "Determination of Salinity and Sugar Concentration by Means of a Circular-Ring Monopole Textile Antenna-Based Sensor," in IEEE Sensors Journal, vol. 21, no. 21, pp. 23751-23760, 1 Nov.1, 2021. doi: 10.1109/JSEN.2021.3112777.

Pages 143 to 152 of the thesis contain this article, which shoud be consulted on the publisher's website:

- Mariam El Gharbi, Raúl Fernández-García, and Ignacio Gil, "Determination of Salinity and Sugar Concentration by Means of a Circular-Ring Monopole Textile Antenna-Based Sensor," in *IEEE Sensors Journal*, vol. 21, no. 21, pp. 23751-23760, 1 Nov.1, 2021.
doi: 10.1109/JSEN.2021.3112777.

Ref D

Mariam El Gharbi, Raúl Fernández-García, Ignacio Gil, Embroidered wearable Antenna-based sensor for Real-Time breath monitoring, Measurement, Volume 195, 2022, 111080, ISSN 0263-2241. Under a CC BY 4.0 license. https://doi.org/10.1016/j.measurement.2022.111080.
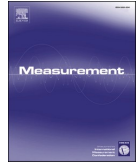
Embroidered wearable Antenna-based sensor for Real-Time breath monitoring

Mariam El Gharbi [*], Raúl Fernández-García , Ignacio Gil

Department of Electronic Engineering, Universitat Politècnica de Catalunya, 08222 Terrassa, Spain

ABSTRACT

In this paper we present the design and the validation of a novel fully embroidered meander dipole antenna-based sensor integrated into a commercially available T-shirt for real-time breathing monitoring using the technique based on chest well movement analysis. The embroidered antenna-based sensor is made of a silver-coated nylon thread. The proposed antenna-sensor is integrated into a cotton T-shirt and placed on the middle of the human chest. The breathing antenna-based sensor was designed to operate at 2.4 GHz. The sensing mechanism of the system is based on the resonant frequency shift of the meander dipole antenna-sensor induced by the chest expansion and the displacement of the air volume in the lungs during breathing. The resonant frequency shift was continuously measured using a Vector Network Analyzer (VNA) to a remote PC via LAN interface in real-time. A program was developed via Matlab to collect respiration data information using a PC host via LAN interface to be able to transfer data with instrumentation over TCP/IP. The measurements were carried out to monitor the breathing of a female volunteer for various positions (standing and sitting) with different breathing patterns: eupnea (normal respiration), apnea (absence of breathing), hypopnea (shallow breathing) and hyperpnea (deep breathing). The measured resonance frequency shift to 2.98 GHz, 3.2 GHz and 2 GHz for standing position and 2.84 GHz, 2.95 GHz and 2.15 GHz for sitting position, for eupnea, hyperpnea and hypopnea, respectively. The area of the textile sensor is 45×4.87 mm2, reducing the surface consumption significantly with regard to other reported breath wearable sensors for health monitoring.

1. Introduction

Health care expenditures are constantly increasing and take up a large part of the states national budget [1]. One of the current challenges in the state of the art is to investigate new strategies for the implementation of sensors fully integrated into fabrics (clothing, sheets, etc.) that allow monitoring and control in real time the state of health of people with maximum comfort. The benefits of this type of devices would generate an overall improvement of the healthcare system in terms of assistance efficiency and overall cost. During medical care, a vital sign such as breathing is an essential factor that must be continuously monitored [2]. Breathing is a principal physiological task in living organisms and is considered as an indicator of pathological instability such as sleep apnea, asthma, lung disease and cardiopulmonary arrest. Breathing monitoring may be used during the surveillance of patients or for treatment, it also plays an important role in the monitoring of newborns, some of whom are born in sensitive conditions, and this monitoring may avoid any injury due to sleep apnea in infants [3].

Hence, continuous monitoring of respiration is critical to evaluate the subject's health status.

Continuous monitoring of patients using wearable technologies is an important diagnostic technology as it opens a new era for medical assistance in advancing healthcare outside the hospital [4]. Various techniques were proposed in the literature to perform breathing monitoring [5]. To measure breathing parameters a sensor could be an alternative diagnostic device to monitor an important physiological sign for the human being in real-time. There are large differences among techniques determined by sensors and breathing parameters, sensing techniques, sensor locations, processing sensor data, software of analysis, and performance evaluation. In the literature, several non-invasive methods were proposed to monitor breathing [6] such as passive radars, camera-based system [7], optics infrared thermography, Ultra-Wide-Band (UWB) radar, and thermal imaging [8]. The main disadvantage of these techniques is that they require a complex measurement equipment and data analysis and they suffer from the implementation complexity for patients daily use. The most popular contact-based

---

* Corresponding author.
E-mail address: mariam.el.gharbi2@upc.edu (M. El Gharbi).

techniques for respiration monitoring are summarized as follows [9]:

- Technique based on air humidity: possible sensors are fiber optic sensors, resistive or capacitive sensors, impedance sensors, nanoparticles and nanocrystal sensors.
- Technique based on respiratory airflow that uses photoelectric sensors, hot wire anemometers, turbine flowmeters and differential flowmeters.
- Technique based on the modulation of cardiac activity: can used radar sensors, PPG (photoplethysmography) and ECG (electrocardiography) sensors.
- Technique based on chest well movement analysis, this technique contains three different measurement approaches: Firstly, the impedance analysis used transthoracic impedance sensors and secondly strain measurement that uses triboelectric nanogenator, pyroelectric and piezoelectric sensors, fiber optic sensors, resistive and inductive sensors. Thirdly, the movement measurement is based on ultrasonic proximity sensors, magnetometers and gyroscopes sensors, Kinect sensors, accelerometers and frequency shift sensors.

Recent technological advances in wireless communications and microelectronics ushered textiles into a novel era of smart wearable systems. The use of clothing is a major part of people's daily life, and is the most natural form of integrating electronic devices. These garments are often called smart textiles [10]. The latter can be defined as textiles that are able to sense and respond to changes in their environment. Smart textiles present a challenge in various areas such as military [11], fashion [12], sport [13] and medicine [14]. Thanks to new developments in textile research, smart textile clothing can now perform continuous monitoring of respiration. The sensing area is either incorporated into textile such as microbend multimode fiber technology [15], sensors based on fiber Bragg grating (FBG) [16,17], piezoelectric sensor [18], or integrated into fibers and threads composing the textiles such as conductive polymers [19] and conductive yarn [20].

For respiration monitoring, wearable devices such as smart T-shirt provides more comfort and user-friendly approaches using embedded sensors. Smart textile sensors have received a lot of research interest for the breath monitoring. A twelve Fibre Bragg Grating (FBG) sensors glued on the elastic T-shirt was validated to monitor breath and heart rates in two different positions standing and sitting [21]. This detection-based technology is complicated and expensive to manufacture the sensors as well as the use of FBG into the T-shirt causes a discomfort to the user when used for a long time. In [22], a spiral antenna-based sensor using multi-material metal-glass-polymer fibers was integrated into standard t-shirt to monitor the respiration rate of an adult. The breathing antenna-based sensor was incorporated into a T-Shirt using cyanoacrylate glue. For breathing monitoring using a T-shirt, most researchers have embedded the sensor into the T-shirt with a specific glue.

Nowadays, we are seeing an increasing demand for smart textiles as they can be applied directly to the body for sensing/communicating such as antenna sensors. Wearable antenna sensors have demonstrated a significant impact on the future of healthcare applications [23]. Despite their development, these devices face several challenges related to lack of reliability, rigid form, user convenience and challenges in data analysis that have limited their wide application. In order to address these problems, it is necessary to develop a new reliable and user-friendly approach that allows incorporating antenna-sensors into garments without restricting movement or compromising the comfort of the user. In this work, we have developed a new embroidered meander dipole antenna-based sensor for real-time breath detection of an adult using the technique based on chest well movement analysis. The proposed antenna-based sensor is placed on the middle of the human chest and takes into account the user's comfort with no movement constraints. The sensing method relies on the resosant frequency shift of the antenna-based sensor induced by the chest movement and the displacement of the air volume in the lungs during breathing. The respiration data

information was continuously measured using a Vector Network Analyzer (VNA) to a remote PC via LAN interface in real-time using Matlab. The measurements were carried out to monitor the breathing of a female volunteer for various scenarios (standing and sitting) with different breathing patterns: eupnea (normal respiration), apnea (absence of breathing), hyperpnea (deep breathing) and hypopnea (shaloow breathing). The paper is organized as follows: Section 2 describes the mechanism of breathing detection, the design of the proposed antenna-sensor and data collection and treatment. Section 3 shows the results obtained from the controlled experiments and analysis, Section 4 provides the discussion and finally the conclusions are drawn in Section 5.

2. Textile Antenna-Sensor for real time breath monitoring

2.1. Mechanism of breathing detection

A simplified illustration of the lungs during inspiration and expiration is shown in Fig. 1(a). During breathing, the volume of the respiratory system changes due to the movement of the abdomen and chest wall caused by contractions of the intercostal muscles and the diaphragm. The contraction of the diaphragm causes the abdominal organs to be pushed down, causing a decrease in intrathoracic pressure. The diaphragm contracts during inhalation (inspiration) and relaxes during exhalation (expiration). During inhalation, the external intercostal muscles and the diaphragm contract and this causes the rib cage to expand and move outward as well as the expansion of the lung volume and thoracic cavity. For the expiration, the intercostal muscles and diaphragm relax, the abdomen and chest take back relax position and lung volumes decrease as shown in the lower portrait of Fig. 1(a). A technique based on the analysis of chest wall movement was used to monitor breathing using a meander dipole embroidered antenna-sensor integrated into a cotton T-Shirt. The antenna-based sensor is located on the middle of the human chest whereas the breath sensing depends on the resonant frequency shift of the embroidered antenna-sensor induced by the abdominal and thoracic movement during respiration. The respiratory signal was continuously measured using a N9916A FieldFox microwave analyzer operating as Vector Network Analyzer (VNA) to a remote PC via LAN interface in real-time.

2.2. Antenna-Sensor design

Similar to conventional antennas, a wearable textile meander dipole antenna-sensor contain two elements: conductive and non-conductive parts. The material used for the conductive part is a commercial Shieldex 117/17 dtex 2-ply. This commercial conductive yarn is made of 99% pure silver-plated nylon yarn 140/17 dtex which furnishes a good conductivity. The non conductive part is a cotton substrate of a

Fig. 1. (a) Simplified illustration of the lungs during inspiration and expiration, **(b)** Fabrication process of the embroidered antenna-sensor integrated into a cotton T-Shirt.

commercially available T-Shirt. The dielectric properties of the T-shirt have been accurately characterized using a Split Post-Dielectric Resonator (SPDR). The cotton relative dielectric constant and loss tangent are $\varepsilon_r = 1.3$ and $\tan\delta = 0.0058$, respectively.

On the other hand, an Electronic Outside Micrometer was used to measure its thickness (0.464 mm). A meander dipole antenna-sensor was integrated into a commercially available T-shirt at the pectoral region of the chest. The dimensions of the proposed antenna sensor are depicted in Fig. 2. The breathing antenna-sensor was designed to operate at 2.4 GHz. The manufacturing embroidery process of the proposed antenna-sensor is represented in Fig. 1(b) and can be summarized in three steps:

- Step 1 (Antenna Design): The design of the proposed antena-sensor is simulated using the commercial CST Studio Suite 3D full electromagnetic simulator 2019. The design was developed to specify preset performance criteria (operating frequency and size).
- Step 2 (Digitization): The conductive part is converted to a stitch pattern using a Digitizer Ex Software. This software is used to produce a digital stitch format file to be readable by embroidery machine Singer Futura XL550.
- Step 3 (Embroiderd Protoype): The design was modified by the functions of the embroidery machine by means of the desired embroidery pattern, desired stitch density and thread tension.

2.3. Data collection and treatment

The meander dipole antenna-sensor is integrated into the cotton T-Shirt to monitor respiration data of a healthy woman volunteer in a lababoratory environment. The main figure of merit of the proposed antenna-sensor is the shift of the resonant frequency that appears due to the change in lung volume under the movement of the chest. To test this concept, a Vector Network Analyzer (VNA) was connected to PC host for data processing via a LAN interface. Data was analyzed in Matlab environment. The measurement setup configuration for the respiration detection in real time of the meander dipole antenna-sensor integrated into a T-Shirt is presented in Fig. 3. The volunteer was asked to perform two positions (standing and sitting) with different breathing patterns eupnea, apnea, hyperpnea (deep breathing) and hypopnea (shaloow breathing). The data process model is presented in Fig. 4. We developed a program via Matlab to collect respiration data information from VNA. The most important step is to configure the VNA with the same IP address used in the PC host via LAN interface to be able to transfer data with instrumentation over TCP/IP. The program was able to detect repetitive respiration and measure the resonant frequency shift continously. Table 1 outlines common breathing patterns with a description and possible causes. Therefore, continuous monitoring of respiration is critical to evaluate the subject's health status, as it helps in the diagnosis and management of a variety of pathological conditions.

The aim of this work was to provide a technique to detect human breathing status using a wearable meander dipole antenna-sensor embroidered into a cotton T-Shirt. The human respiratory status was compared with the standard respiration signal for different breathing patterns presented in the Fig. 5. The respiratory signals come in various forms depending on the breathing patterns, and are generally defined in four types of breathing, as presented in Fig. 5. For the eupnea, is a normal respiration of an individual under resting conditions. Apnea
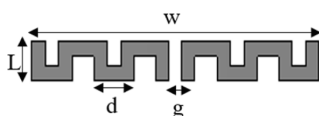

Fig. 2. Meander dipole antenna-based sensor. Dimensions are: W = 45 mm, L = 4.8 mm, d = 7.6 mm, g = 2 mm.

present a stop breathing. For the hypopnea describe a low signal amplitude due to the shallow breathing. The hyperpnea is a deep breathing, the amplitude of the signal breathing is higher than the eupnea.

3. Results and analysis

3.1. S-parameter

The main parameters characterizing the antenna resonant frequency are the parameters S, more specifically S_{11}. The prototype of the proposed antenna-sensor was characterized in terms of S_{11} and the Specific Absorption Rate (SAR) to evaluate its performance for the wireless communications. In order to verify the accuracy of the embroidery technique, the meander dipole antenna-sensor was tested by measuring S_{11} using the Vector Network Analyzer. The simulated and measured S_{11} for the proposed antenna-sensor is presented in Fig. 6. From this figure, we can observe that the experimental measurement of the S_{11} has a good agreement with the numerical 3D electromagnetic simulation. The operating frequency of the experimental and simulation results is 2.4 GHz. Due to manufacturing errors, a small deviation in the S_{11} amplitude is observed. It is noted that this proposed antenna-sensor has achieved a realized gain of 1.86 dB.

3.2. Antenna under stretching

When textile antenna-based sensor is worn by a human body, its geometry is subject to significant deformations caused by the body shape. The antenna-sensor deformation causes alterations to the radio frequency (RF) signal. Therefore, the impact of mechanical deformations needs to be quantified for the proposed antenna-sensor. The main feature of the proposed textile antenna is the resonance frequency shift caused by the change in lung volume and the stretching of the textile under the movement of the chest. The proposed antenna-based sensor is located on the middle of the human chest, allowing the chest expansion to slightly stretch the antenna-sensor as presented in Fig. 7. The resonance frequency shift as a function of stretching deformation have been performed for the proposed antenna-sensor. In order to evaluate the performance of the meander dipole antenna-sensor under stretching, the proposed antenna was simulated by different width (w) ranging from 47 mm to 53 mm to mimic the stretching of the antenna (Fig. 8). It is important to note that the stretching does not cause any deformation to the antenna, only the width changes. Note that the antenna at rest had w = 45 mm (Fig. 2). The simulated and measured results of the resonance frequency of the textile antenna-sensor as a function of the induced stretch are shown in the Fig. 9. From this figure, a linear function is used to fit the data and the coefficient of determination (R^2) shows the curves fitting well. From the obtained results, the feasibility of the textile antenna-sensor under stretching is confirmed and the proposed antenna-sensor can work to measure the resonant frequency with different values of w in a linear way at a determined frequency.

3.3. Specific absorption rate (SAR) analysis

Since the proposed antenna-sensor operates close to the human body, it is important to consider the rate of absorption of radio frequency (RF) energy in the involved tissues. Specific Absorption Rate (SAR) is defined as the power absorbed by the biological tissue when exposed to a RF electromagnetic field. Specifically, it is defined as:

$$SAR = \sigma |E|^2 / (\rho)$$

Where, E: Electric filed (V/m).

σ: Electrical conductivity (S/m).
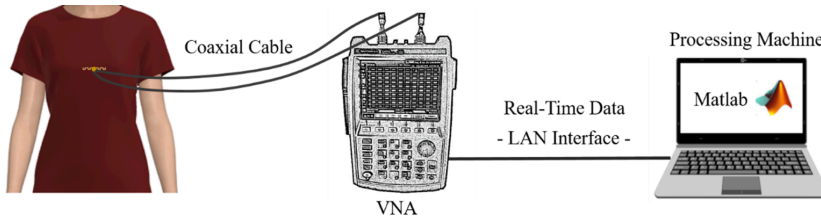
ρ: Tissue density (kg/m^3).

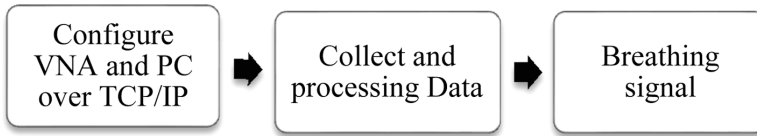**Fig. 3.** Measurement setup configuration.

Fig. 4. Data process model to monitor breathing.

Table 1
Different breathing patterns and their causes.

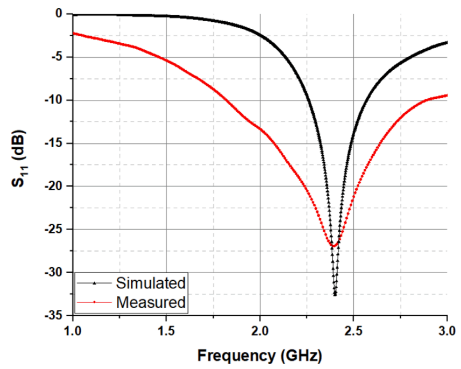| Breathing Patterns	Description	Causes
Eupnea	Quiet breathing or resting respiratory rate	Normal breathing
Apnea	Absence of breathing	Diabetes, Heart failure, cardiomyopathy
Hypopnea	Shallow breathing or an abnormally low respiratory rate	Anxiety, Asthma, Pneumonia, Shock, Pulmonary Edema
Hyperpnea	Increased rate and depth of breathing	Emotional stress, Diabetic ketoacidosis

Fig. 5. Process to detect human respiratory status.

Fig. 6. Simulated and measured S_{11} of the textile meander dipole antenna-based sensor.

Fig. 7. Configuration of the proposed antenna-sensor under the stretching caused by the chest expansion during the breathing.

SAR is a very important parameter used to help ensure safety aspects of exposure to RF energy. Institute of Electrical and Electronics Engineers (IEEE) and the International Commission on NonIonizing Radiation Protection (ICNIRP) have provided recommended SAR limits in order to protect users from the hazards of exposure to electromagnetic fields. According to the both organizations, the limit of SAR was set as: 1.6 W/Kg and 2 W/Kg averaged over 1 g and 10 g tissue, respectively [24,25]. Since the proposed respiration antenna-sensor can be used by people of different ages and gender such as monitoring the breathing status of a newborn infant, a voxel model was used for simulation. This voxel family is a group of seven realistic human model data sets created from seven persons of different stature, age and gender including their corresponding tissues. The complete SAR analysis is done by importing
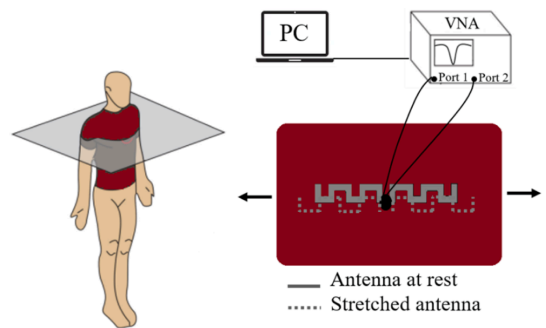
the proposed antenna into CST Studio Suite 3D full electromagnetic simulator 2019. The SAR simulations are carried out using different voxel models under two standard as presented in Table 2, which shows that the proposed antenna-sensor offers an acceptable SARs at different voxel model for both standards. The power used for the simulations is 50 mW. The SAR simulations were carried out considering the IEEE/IEC
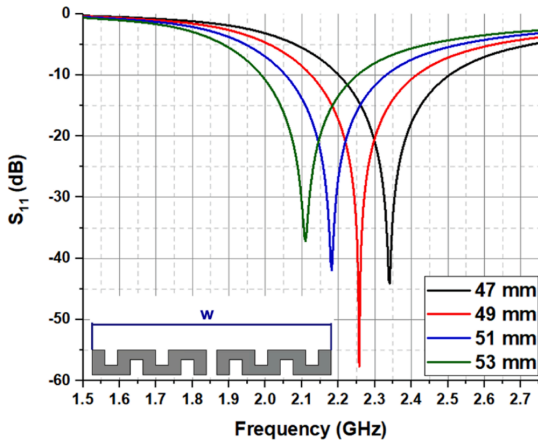
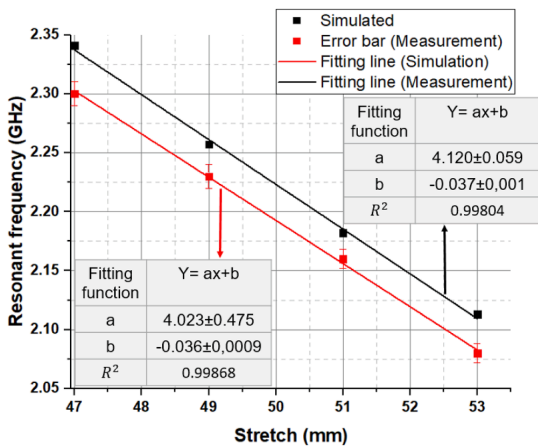**Fig. 8.** S_{11} Simulation results of the antenna-sensor under stretching.

Fig. 9. Simulated and measured results of the resonant frequency of the textile antenna-sensor as a function of the induced stretch.

Table 2
Specific absorption rate values at different voxel model and standards.

Voxel model	Age (Year)	Size (cm)	Mass (kg)	Sex	Resolution/ mm	SAR (1 g) W/kg	SAR (10 g) W/kg
Baby	8-weeks	57	4.2	F	0.85 × 0.85 × 4	1.53 (4%)	0.86 (57%)
Child	7	115	21.7	F	1.54 × 1.54 × 8	1.54 (4%)	0.064 (96%)
Donna	40	176	79	F	1.875 × 1.875 × 10	0.295 (81%)	0.141 (92%)
Emma	26	170	81	F	0.98 × 0.98 10	0.878 (45%)	0.414 (79%)
Gustav	38	176	69	M	2.08 × 2.08 × 8	1.57 (2%)	0.786 (60%)
Laura	43	163	51	F	1.875 × 1.875 5	0.489 (69%)	0.247 (87%)
Katja	43	163	62	F-P	1.775 × 1.775 × 4.84	0.456 (71%)	0.226 (88%)

62704–1 standard, according to the regulators. All models take into account up to 80 human tissues and organs. As an example, the proposed antenna-sensor is placed on the chest of a realistic Emma voxel human model with a SAR distribution at 2.4 GHz for two standard (1 g and 10 g) as shown in Fig. 10.

For SAR simulation, the proposed antenna-based sensor is placed at distance d = 10 mm from the voxel model to imitate realistic worn plac ements.In order to address a complete SAR analysis, the simulations over different voxel models with different age, size and weight have been performed.The absolute SAR value as well as the percentage of safety (%) with regard to the standard SAR limits are reported in Table 2.

3.4. On-body measurements

The main concept of this work is to validate the embroidered meander dipole antenna-sensor integrated into a commercially available T-Shirt for the breathing monitoring in real time. The breathing tests were attended with the help of a female volunteer (28 years, 1.67 cm, 70 kg) having approximately the same characteristics with human Emma voxel model. Various respiratory patterns were professionally role played in real time based on the description of the breathing patterns reported in Table 1. Fig. 11 shows a photograph of the volunteer wearing the T-shirt under laboratory testing for sitting and standing positions. To investigate the feasibility and consistency of the proposed antenna-based sensor, various experimental tests were performed to study different breathing patterns (eupnea, apnea, hypopnea and hyperpnea).

When the antenna-based sensor is placed on the human chest, the participant was asked to:

1- Normal breath.
2- Deep breaths (hyperpnea) followed by shallow breaths (hypopnea).
3- Deep breaths (hyerpnea) followed by apnea (absence breathing).

The normal respiration (eupnea), the female volunteer was asked to breath normally and at ease for different positions (standing and sitting on a chair). During the apnea test, there is no air exchange either through the mouth or the nose means that no diaphragmatic and intercostal muscle activity. The measured S_{11} for eupnea, hyperpnea and hypopnea patterns are presented in Fig. 12. The obtained results are taking during inhalation of the female volunteer for sitting position. This change in resonance frequency is caused by the change in lung volume
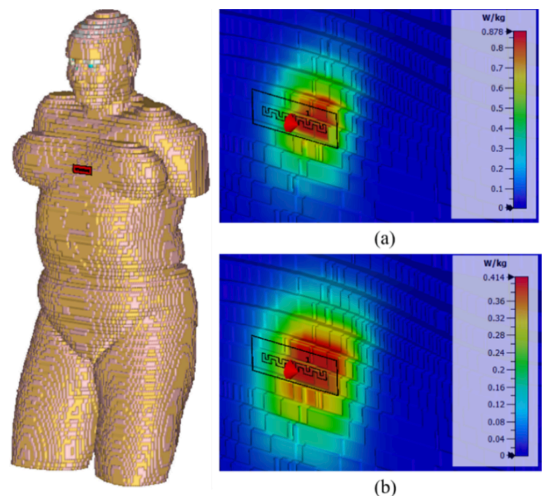

Fig. 10. Antenna-sensor on human Emma voxel model, SAR at 2.4 GHz (a) 1 g, (b) 10.
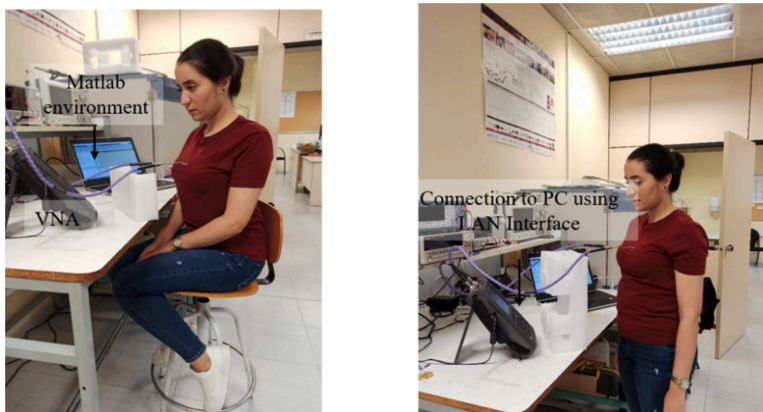
Fig. 11. Photograph of the embroidered antenna-based sensor into a cotton T-shirt under laboratory testing for different scenarios, (a) sitting, (b) standing.
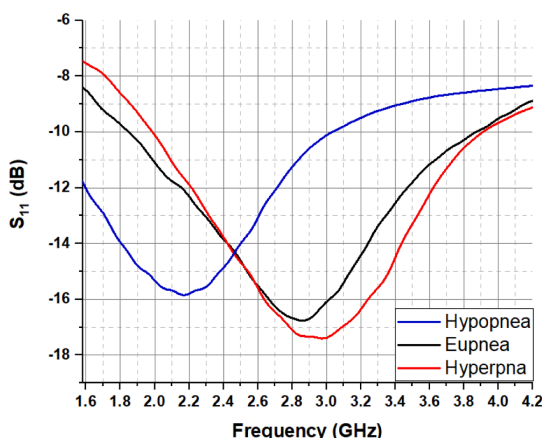

Fig. 12. Measured S_{11} for different breathing patterns in sitting position.

volunteer keeps her breathing cycle constant during inhalation to show the accuracy for the proposed system for different breathing patterns. The curve peak saturation for apnea is due to the absence of breathing, and this corresponds to the standard breathing signal. They are presented to demonstrate that our antenna is able to monitor different breathing patterns. The measurements was repeated in sitting position for different breathing patterns as presented in Fig. 14. For the eupnea, a resonant frequency shifted to 2.84 GHz (Fig. 14(a)). The measured resonant frequency shift for hypopnea and hyperpnea are 2.15 GHz and 2.95 GHz, respectively (Fig. 14(b)). All the results have the same behavior as the standard respiration signal presented in Fig. 5, this fact confirms that the obtained results from these measurements seem to be very promising for an embroidered antenna-based sensor to monitor human breathing, as the proposed approach is able to detect different breating patterns for several postions and this could be useful to evaluate the subject's health status.

4. Discussion

The objective of this study is to verify the proposed breathing antenna-sensor embroidered into a commercial cotton T-shirt for real time monitoring of a human being breath. The breathing antenna-sensor was designed to operate at 2.4 GHz. The proposed antenna sensor is placed on the middle of the human chest and takes into account the user's comfort with no movement constraints. The breathing sensing mechanism is based on the resonant frequency shifts of the embroidered antenna-sensor due to textile stretching induced by chest wall movements. The obtained results could make our embroidered antenna-sensor as a potential system for medical application such as: breathing troubles in neonates, children and adults, evaluating sleep apnea and monitor people suffering from asthma. The principal advantage of the proposed process consists of high user comfort associated with conventional clothing, as it does not require a connection of electrodes of any form. Table 3 presents a comparison of different techniques, sensor type, location, measuring parameter and size for previously reported works of the wearable category for respiration monitoring.

A breathing parameter (BP) was calculated from breath to-breath interval. BP is the time that elapses between two consecutive peaks of the respiratory signal during normal breathing. This parameter shows the accuracy of the system during the breathing cycle. Most of the reported works were fabricated using conventional printed circuit board substrates. There are two sensors made from textile substrates, one is a piezoresistive sensor stitched into a T-shirt and the other one is a spiral antenna based on multi-material fibers integrated into a T-shirt. As shown in the Table 3, both T-shirts have a large sensor size. The main

and the stretching of the textile under the movement of the chest. It can be clearly seen a consistent frequency shift of the main resonance frequency of the embroidered antenna-sensor.

The resonant frequency shift was continuously measured using a N9916A FieldFox microwave analyzer operating as Vector Network Analyzer (VNA) to a remote PC via LAN interface in real-time. Matlab environment was used to test our methodology for different breathing signals (Fig. 4). The acquisition rate was adjusted to provide the measurement per second. Real-world breathing tests were attended with help of a female volunteer. The different breathing patterns of the female volunteer for standing position were presented in Fig. 13. From this figure, a noticeable resonant frequency shift can be seen that allowed the correct detection of different breathing patterns (eupnea, apnea, hypopnea and hyperpnea) of the volunteer. For the eupnea, a stable rhythm breathing was observed with a large shift frequency up to 2.98 GHz (Fig. 13(a)). The participant was asked to take a deep breathing (hyperpnea) following by a shallow breathing (hypopnea), the resonant frequency shifted to 3.2 GHz and 2 GHz, respectively (Fig. 13(b)), the hypopnea has a low breathing signal according to a low respiratory taking by the volunteer. For the apnea, the volunteer take a deep breathing followed by a stop breathing for several seconds (no air exchange either through the mouth or the nose). We can observe that the signal is saturated for different breathing patterns, because the female

Fig. 13. Measured respiratory patterns of an adult female volunteer in standing position, (a) Eupnea, (b) hypopnea and hyperponea, and (c) Apnea.

Fig. 14. Measured respiratory patterns of an adult female volunteer sitting position, (a) Eupnea, (b) Hypopnea and hyperponea, and (c) Apnea.
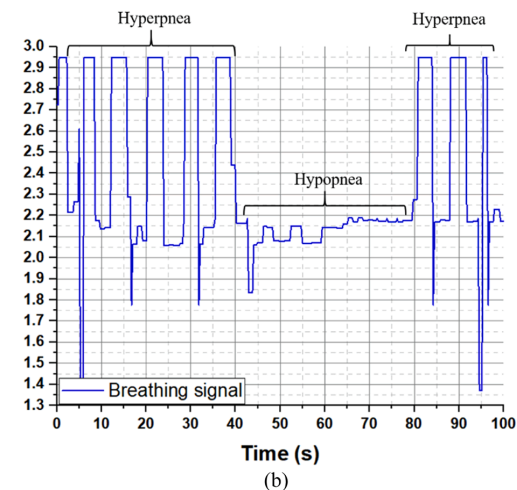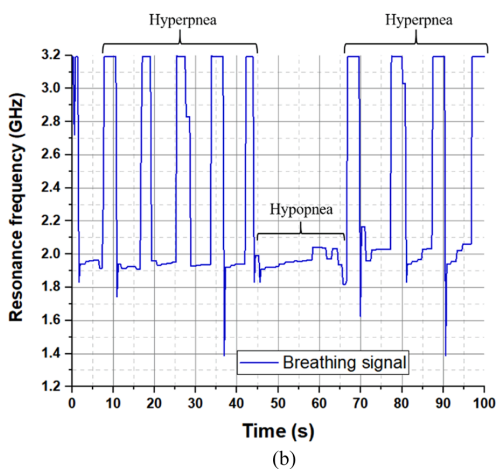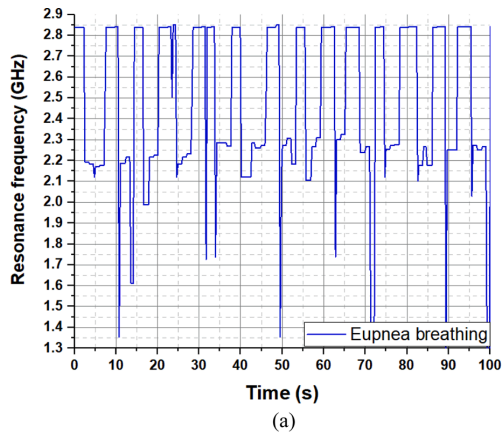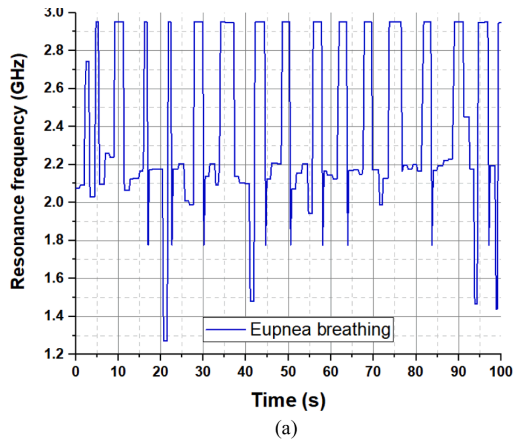
novelties of our research are to consider a new approach to monitor breathing using a a fully textile wearable meander dipole antenna-sensor embroidered into a cotton T-shirt with a compact size presenting a high comfort for the user. Moreover, the overall size of the

Table 3
Comparison of the respiratory monitoring systems.

Ref	Technique	Sensor Type	Location	Measuring parameter	Size (mm^2)	BP (s)	Textile
[26]	Abdomen movements/ Chest wall	Multimodal Patch	Abdomen Chest	Signal Amplitude	65.53 × 26.67	1.91 ± 0.12	✗
[27]	Respiratory air flow	Fiber optic	Cervical spine	FBG[1] signal	90 × 24	4.52 ± 0.35	✗
[28]	Chest wall movements	Piezoelectric	Mat	Raw signal	70 × 60	2.78 ± 0.27	✗
[29]	Air humidity	Nanoparticles	Mouth mask	Respiratory rate	–	4.50 ± 0.35	✗
[30]	Chest wall movements	Resistive	Chest (T-Shirt)	RIP[2] signal	310 × 40	5.34 ± 0.84	✓
[31]	Air temperature	Camera	–	Raw signal	72 × 26	–	✗
[22]	Chest wall movements	Spiral Antenna	Chest (T-Shirt)	Frequency shift	200 × 100	9.50 ± 0.74	✓
[32]	Modulation of Cardiac	Radar	Distance from subject (200 cm away)	Amplitude and phase shift	150 × 100	5.20 ± 0.14	✗
[33]	Chest wall movements	Capacitive	Chest	Amplitude and phase shift	478 × 478	5.10 ± 0.15	✗
[34]	Chest wall movements	Photoplethy-smographic	Shirt pocket	Cardia× signal	100 × 80	7.76 ± 0.21	✗
[35]	Respiratory sounds	Microphone	Ear	Digital audio signal	–	–	✗
This work	**Chest wall movements**	**Meander dipole antenna**	**Chest (T-Shirt)**	**Frequency shift**	**45 × 4.87**	**5.22 ± 0.33**	✓

[1] FBG: Fiber Bragg Grating.
[2] RIP: Respiratory Inductive Plethysmograph.

breathing antenna-based sensor is reduced by up to 90% compared to the reported works.

5. Conclusion

In this work, a new embroidered meander dipole antenna-based sensor integrated into a commercially available T-Shirt for real-time breathing monitoring using the technique based on chest well movement analysis is presented. The breathing antenna-sensor was designed to operate at 2.4 GHz. The working principle is based mainly on the resonant frequency shift of the meander dipole antenna-sensor induced by the chest expansion and the displacement of the air volume in the lungs during breathing. We have demonstrated the feasibility and consistency of the proposed antenna-based sensor in various breathing patterns (eupnea, apnea, hypopnea and hyperpnea) for two different postions (standing and sitting). The ability and accuracy of the embroidered antenna-based sensor to detect in real time the breathing patterns of a female volunteer has been demonstrated. Our system may be used for healthcare applications, such as in situ diagnose of breathing diseases and monitor people suffering from Pulmonary Edema, Asthma and so on. The proposed antenna-based sensor has the advantages of combining wearability, compact size, consistent performance and no fabrication complexities.

CRediT authorship contribution statement

Mariam El Gharbi: Conceptualization, Methodology, Investigation, Software, Data curation, Formal analysis, Writing – original draft. **Raúl Fernández-García:** Writing – review & editing, Supervision, Visualization, Project administration. **Ignacio Gil:** Writing – review & editing, Supervision, Validation, Visualization, Project administration.

Declaration of Competing Interest

The authors declare that they have no known competing financial interests or personal relationships that could have appeared to influence the work reported in this paper.

References

[1] M. Ridao-López, M. Comendeiro-Maaløe, N. Martínez-Lizaga, E. Bernal-Delgado, Evolution of public hospitals expenditure by healthcare area in the Spanish National Health System: the determinants to pay attention to, BMC Health Serv. Res. 18 (2018) 1–9.

[2] H. Fouad, A.S. Hassanein, A.M. Soliman, H. Al-Feel, Analyzing patient health information based on IoT sensor with AI for improving patient assistance in the future direction, Measurement 159 (2020), 107757.

[3] L. Maurya, P. Kaur, D. Chawla, P. Mahapatra, Non-contact breathing rate monitoring in newborns: A Review, Comput. Biol. Med. 104321 (2021).

[4] L. Gao, G. Zhang, B. Yu, Z. Qiao, J. Wang, Wearable human motion posture capture and medical health monitoring based on wireless sensor networks, Measurement 166 (2020), 108252.

[5] E. Vanegas, R. Igual, I. Plaza, Sensing systems for respiration monitoring: A technical systematic review, Sensors 20 (2020) 5446.

[6] M. Folke, L. Cernerud, M. Ekström, B. Hök, Critical review of non-invasive respiratory monitoring in medical care, Med. Biol. Eng. Comput. 41 (2003) 377–383.

[7] M. Bartula, T. Tigges, J. Muehlsteff, Camera-based system for contactless monitoring of respiration, in: 2013 35th Annu. Int. Conf. IEEE Eng. Med. Biol. Soc., IEEE, 2013: pp. 2672–2675.

[8] Z. Zhu, J. Fei, I. Pavlidis, Tracking human breath in infrared imaging, in: Fifth IEEE Symp. Bioinforma. Bioeng., IEEE, 2005: pp. 227–231.

[9] C. Massaroni, A. Nicolò, D. Lo Presti, M. Sacchetti, S. Silvestri, E. Schena, Contact-based methods for measuring respiratory rate, Sensors 19 (2019) 908.

[10] P. Veske, E. Ilén, Review of the end-of-life solutions in electronics-based smart textiles, J. Text. Inst. 112 (2021) 1500–1513.

[11] R. Nayak, L. Wang, R. Padhye, Electronic textiles for military personnel, in, Electron. Text., Elsevier (2015) 239–256.

[12] J. Berzowska, Very slowly animating textiles: shimmering flower, in: ACM SIGGRAPH 2004 Sketches, 2004: p. 34.

[13] D. Morris, B. Schazmann, Y. Wu, S. Coyle, S. Brady, J. Hayes, C. Slater, C. Fay, K.T. Lau, G. Wallace, Wearable sensors for monitoring sports performance and training, in: 2008 5th Int. Summer Sch. Symp. Med. Devices Biosens., IEEE, 2008: pp. 121–124.

[14] V. Koncar, Introduction to smart textiles and their applications, in: Smart Text. Their Appl., Elsevier, 2016: pp. 1–8.

[15] Z. Chen, D. Lau, J.T. Teo, S.H. Ng, X. Yang, P.L. Kei, Simultaneous measurement of breathing rate and heart rate using a microbend multimode fiber optic sensor, J. Biomed. Opt. 19 (2014) 57001.

[16] L. Dziuda, F.W. Skibniewski, M. Krej, J. Lewandowski, Monitoring respiration and cardiac activity using fiber Bragg grating-based sensor, IEEE Trans. Biomed. Eng. 59 (2012) 1934–1942.

[17] J.P. Carmo, A.M.F. da Silva, R.P. Rocha, J.H. Correia, Application of fiber Bragg gratings to wearable garments, IEEE Sens. J. 12 (2011) 261–266.

[18] I. Mahbub, S.A. Pullano, H. Wang, S.K. Islam, A.S. Fiorillo, G. To, M.R. Mahfouz, A low-power wireless piezoelectric sensor-based respiration monitoring system realized in CMOS process, IEEE Sens. J. 17 (2017) 1858–1864.

[19] Z. Zhao, C. Yan, Z. Liu, X. Fu, L. Peng, Y. Hu, Z. Zheng, Machine-washable textile triboelectric nanogenerators for effective human respiratory monitoring through loom weaving of metallic yarns, Adv. Mater. 28 (2016) 10267–10274.

[20] O. Atalay, W.R. Kennon, E. Demirok, Weft-knitted strain sensor for monitoring respiratory rate and its electro-mechanical modeling, IEEE Sens. J. 15 (2014) 110–122.

[21] D. Lo Presti, C. Massaroni, D. Formica, P. Saccomandi, F. Giurazza, M.A. Caponero, E. Schena, Smart textile based on 12 fiber Bragg gratings array for vital signs monitoring, IEEE Sens. J. 17 (2017) 6037–6043.

[22] P. Guay, S. Gorgutsa, S. LaRochelle, Y. Messaddeq, Wearable contactless respiration sensor based on multi-material fibers integrated into textile, Sensors. 17 (2017) 1050.

[23] M. El Gharbi, R. Fernández-García, S. Ahyoud, I. Gil, A Review of Flexible Wearable Antenna Sensors: Design, Fabrication Methods, and Applications, Materials (Basel). 13 (2020) 3781.

[24] A.N.S.I. (ANSI), Safety levels with respect to human exposure to radio frequency electromagnetic fields, 3 kHz to 300 GHz, ANSI/IEEE standard C95. 1, (1999).

[25] Icnirp, International Commission on Non-Ionizing Radiation Protection. Guidelines for limiting exposure to time-varying electric, magnetic, and electromagnetic fields (up to 300 GHz), Health Phys. 74 (1998) 494–522.

[26] T. Elfaramawy, C.L. Fall, S. Arab, M. Morissette, F. Lellouche, B. Gosselin, A wireless respiratory monitoring system using a wearable patch sensor network, IEEE Sens. J. 19 (2018) 650–657.

[27] D. Lo Presti, C. Massaroni, J. Di Tocco, E. Schena, A. Carnevale, U.G. Longo, J. D'Abbraccio, L. Massari, C.M. Oddo, M.A. Caponero, Single-plane neck movements

and respiratory frequency monitoring: A smart system for computer workers, in: 2019 II Work. Metrol. Ind. 4.0 IoT (MetroInd4. 0&IoT), IEEE, 2019: pp. 167–170.

[28] P. Gunaratne, H. Tamura, C. Yoshida, K. Sakurai, K. Tanno, N. Takahashi, J. Nagata, A Study on breathing and heartbeat monitoring system during sleeping using multi-piezoelectric elements, in: 2019 Moratuwa Eng. Res. Conf., IEEE, 2019: pp. 382–387.

[29] S. Kano, A. Yamamoto, A. Ishikawa, M. Fujii, Respiratory rate on exercise measured by nanoparticle-based humidity sensor, in: 2019 41st Annu. Int. Conf. IEEE Eng. Med. Biol. Soc., IEEE, 2019: pp. 3567–3570.

[30] R.I. Ramos-Garcia, F. Da Silva, Y. Kondi, E. Sazonov, L.E. Dunne, Analysis of a coverstitched stretch sensor for monitoring of breathing, in: 2016 10th Int. Conf. Sens. Technol., IEEE, 2016: pp. 1–6.

[31] Y. Cho, N. Bianchi-Berthouze, S.J. Julier, N. Marquardt, ThermSense: Smartphone-based breathing sensing platform using noncontact low-cost thermal camera, in: 2017 Seventh Int. Conf. Affect. Comput. Intell. Interact. Work. Demos, IEEE, 2017: pp. 83–84.

[32] K. Mostov, E. Liptsen, R. Boutchko, Medical applications of shortwave FM radar: Remote monitoring of cardiac and respiratory motion, Med. Phys. 37 (2010) 1332–1338.

[33] T. Mukai, K. Matsuo, Y. Kato, A. Shimizu, S. Guo, Determination of locations on a tactile sensor suitable for respiration and heartbeat measurement of a person on a bed, in: 2014 36th Annu. Int. Conf. IEEE Eng. Med. Biol. Soc., IEEE, 2014: pp. 66–69.

[34] D. Teichmann, D. De Matteis, T. Bartelt, M. Walter, S. Leonhardt, A bendable and wearable cardiorespiratory monitoring device fusing two noncontact sensor principles, IEEE J. Biomed. Heal. Informatics. 19 (2015) 784–793.

[35] A. Martin, J. Voix, In-ear audio wearable: Measurement of heart and breathing rates for health and safety monitoring, IEEE Trans. Biomed. Eng. 65 (2017) 1256–1263.

Ref E

Mariam El Gharbi, Raúl Fernández-García, and Ignacio Gil. 2022. "Wireless Communication Platform Based on an Embroidered Antenna-Sensor for Real-Time Breathing Detection" Sensors 22, no. 22: 8667. Under a CC BY 4.0 license. https://doi.org/10.3390/s22228667

MDPI

Article

Wireless Communication Platform Based on an Embroidered Antenna-Sensor for Real-Time Breathing Detection

Mariam El Gharbi * , **Raúl Fernández-García** and **Ignacio Gil**

Department of Electronic Engineering, Universitat Politècnica de Catalunya, 08222 Terrassa, Spain
* Correspondence: mariam.el.gharbi2@upc.edu

Abstract: Wearable technology has been getting more attention for monitoring vital signs in various medical fields, particularly in breathing monitoring. To monitor respiratory patterns, there is a current set of challenges related to the lack of user comfort, reliability, and rigidity of the systems, as well as challenges related to processing data. Therefore, the need to develop user-friendly and reliable wireless approaches to address these problems is required. In this paper, a novel, full, compact textile breathing sensor is investigated. Specifically, an embroidered meander dipole antenna sensor integrated into an e-textile T-shirt with a Bluetooth transmitter for real-time breathing monitoring was developed and tested. The proposed antenna-based sensor is designed to transmit data over wireless communication networks at 2.4 GHz and is made of a silver-coated nylon thread. The sensing mechanism of the proposed system is based on the detection of a received signal strength indicator (RSSI) transmitted wirelessly by the antenna-based sensor, which is found to be sensitive to stretch. The respiratory system is placed on the middle of the human chest; the area of the proposed system is 4.5×0.48 cm^2, with 2.36×3.17 cm^2 covered by the transmitter module. The respiratory signal is extracted from the variation of the RSSI signal emitted at 2.4 GHz from the detuned embroidered antenna-based sensor embedded into a commercial T-shirt and detected using a laptop. The experimental results demonstrated that breathing signals can be acquired wirelessly by the RSSI via Bluetooth. The RSSI range change was from -80 dBm to -72 dBm, -88 dBm to -79 dBm and -85 dBm to -80 dBm during inspiration and expiration for normal breathing, speaking and movement, respectively. We tested the feasibility assessment for breathing monitoring and we demonstrated experimentally that the standard wireless networks, which measure the RSSI signal via standard Bluetooth protocol, can be used to detect human respiratory status and patterns in real time.

Keywords: antenna sensor; breathing status; embroidered textile; e-textile; wearable system

1. Introduction

In recent years, the market for wearable technologies involving advanced electronic technologies, computer sciences and fashion has experienced significant growth. Among diverse wearable technologies, e-textiles are one of the most popular categories, with great influence in our daily lives and prevalence in many applications, including military, aerospace, automotive, and medical fields [1]. The e-textiles are based on adding sensing electronic components to clothes or creating fabrics based on conductive fibers/yarns/printing inks in order to sense and respond to various external and environmental effects: mechanical, electrical, chemical, etc. [2,3]. In the medical field in particular, e-textiles have been widely used for continuous monitoring of vital signs [4]. To acquire vital signs from a person, there are different types of devices, but in general, the measurement technique is divided into two categories: wired and wireless. Wired systems are generally attached to the human body to collect a vital sign using cables. These kinds of systems are often used in hospitals and medical centers to measure vital signs on a daily basis, although several patients face difficulties or discomfort during the measurement, particularly burn victims or child patients [5]. As a consequence, these techniques have restrictions for continuous monitoring,

because any activity or movement is not accepted, and this limitation can bother the patient. In contrast, wireless systems are gaining more popularity because they allow long-term usability and provide convenient continuous monitoring of vital signs that could provide additional understanding about disease progression, allowing prompt clinical intervention because the data is sent and received wirelessly in real time [6,7].

Breath is one of the most important vital signs, and it is considered as a crucial indicator to evaluate the physiological, physical state of human health, including diseases such as sleep apnea, asthma and cardiopulmonary diseases [8,9]. Therefore, continuous monitoring of breathing plays an important role in assessing a person's health status. The growth of demand for optimized medical breathing monitoring systems has led intensive research to obtain simple, comfortable and accurate measurement solutions [10]. In the literature, different methods were proposed for breathing monitoring. Breathing status assessment is usually evaluated through human body temperature, movements or sounds. Specifically, several techniques were proposed, such as the technique based on the modulation of cardiac activity, the technique based on air temperature and the technique based on chest wall movement analysis [11]. One of the techniques based on the modulation of cardiac activity is an electrocardiogram (ECG), which requires the distribution of electrodes on the patient's body [12]. The main drawback of this technique is the complexity of the equipment and difficulty of implementation. Another technique widely used for breathing monitoring is the Respiratory Inductive Plethysmography (RIP) method [13]. This technique was developed to evaluate respiratory status by measuring the abdominal wall and movement of the chest. The disadvantage of this method is that the equipment is expensive and cumbersome. The drawback of these methods is the complexity of their implementation for daily use by the patient due to the wired connection. In addition, they require complex techniques for processing data [14].

Recently, there has been an increasing demand for wireless respiratory monitoring methods, as they are practical to use for convenient and long-term continuous monitoring of patients' physiological status. These wireless techniques provide an excellent user experience because they usually involve a sensing system located at a remote location so that a person can perform their usual activities while they are continuously monitored. Various contactless methods were proposed to monitor breathing, such as ultra-wideband (UWB) radars [15], camera-based systems [16], thermal imaging [17] and infrared thermography based on wavelet decomposition [18]. Although these techniques are contactless, their main drawback is that they suffer from difficulty of usage and inaccuracy.

Recently, new noninvasive and contactless alternatives have emerged that rely on integrating sensors into clothing, which provides more comfortable and user-friendly approaches for breathing monitoring. Many studies have proposed sensing systems integrated into textiles for breathing monitoring, including fiber Bragg grating-based sensors [19], magnetometers [20], inertial measurement unit sensors [21] and multimaterial fiber antenna sensors [22]. Although the proposed sensor systems embedded in textiles were able to detect vital signs, methods for data processing and analysis must be developed, and user comfort is still a requirement.

In this work we investigate, design and test a textile sensor for real-time breathing detection. In particular, an embroidered meander dipole antenna-based sensor integrated into an e-textile T-shirt with a Bluetooth transmitter for real-time breathing monitoring is proposed in this work. The antenna-based sensor is designed to transmit data over wireless communication networks at 2.4 GHz. The breathing detection is based on the received signal strength indicator (RSSI) measurements. The respiratory system is placed on the middle of the human chest. During breathing, the transmitted signal from the antenna-based sensor is sensitive to the stretching caused by the expansion/contraction of the chest, so it can be used for monitoring the respiratory signal. The respiratory signal is extracted from the variation of the RSSI signal emitted at 2.4 GHz from the embroidered antenna-based sensor integrated into a commercially made T-shirt and detected using a base station (laptop). The paper is organized as follows: Section 2 presents the design of

the proposed system and the approach for the sensing and data collection. Section 3 shows the test results of breathing status. The discussion based on the results can be found in Section 4. Finally, conclusions are drawn in Section 5.

2. Design and Fabrication of E-Textile T-Shirt for Breathing Monitoring

2.1. Mechanism of Breath Detection

During respiration, the volume of the breathing system changes due to the movement of the chest wall and abdomen caused by contractions of the diaphragm and the intercostal muscles. Figure 1 presents a schematic representation of the ventral body cavity. The contraction of the diaphragm leads the abdominal organs down, causing a decrease in intrathoracic pressure. There are two various sorts of physical movements during a respiratory period: breathing in, or inhalation (draws air into the lungs), and breathing out, or exhalation (pushes air out of the lungs). During inhalation, the intercostal muscles contract and the size of the thoracic cavity increases, and this is related to the lowering of the diaphragm. Thus, this reduces the pressure within the alveolus so that air flows into the lungs, as shown in Figure 1a. During exhalation, the intercostal muscles and diaphragm relax, the abdomen and chest return to a resting position and lung volumes decrease, as shown in Figure 1b.
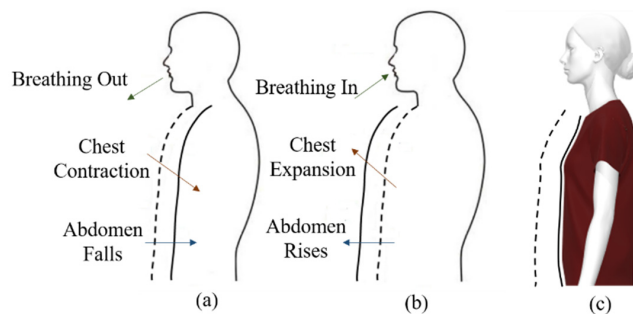

Figure 1. Schematic representation of the ventral body cavity: (**a**) expiration, (**b**) inspiration and (**c**) chest movement during inhalation and exhalation.

The breathing sensing mechanism of the proposed system is based on the operation frequency shift of the embroidered antenna sensor. When the textile antenna-based sensor is worn by a human body, its geometry is subject to significant deformation due to the body's respiration (expansion/contraction). As a result, the operation frequency of the embroidered antenna shifts downward or upward because of the strain applied on the antenna by the chest movement. The breathing antenna sensor is connected to a Bluetooth transmitter, which is placed on the middle of the chest position. The detuning of the antenna frequency generates a mismatching in the transmitter, which affects the received RSSI. A base station contains a laptop with a receiver Bluetooth module prepared to continuously record the variation of the RSSI signal emitted by the embroidered antenna sensor.

2.2. Embroidered Antenna-Based Sensor Design

The textile antenna-based sensor is a critical component of wearable technologies, especially in an e-textile system that implements wireless communication, localization and sensing functions while it is integrated unobtrusively and comfortably into the clothes. The implementation of the antenna-based sensor in textile materials first requires a dielectric material characterization, as shown in Figure 2a. In this particular case, a split-post dielectric resonator (SPDR) was used to determine the dielectric properties of the T-shirt by means of the resonance method. The substrate is the cotton of a commercially available T-shirt. The experimental dielectric constant and loss tangent of the cotton substrate were ε_r = 1.3 and $\tan \delta$ = 0.0058, respectively. Also, an Electronic Outside Micrometer was used

to measure the thickness (h) of the T-shirt, obtaining h = 0.464 mm. After measuring all the necessary parameters of the substrate, the proposed antenna-based sensor was designed using the commercial CST Studio Suite 3D full electromagnetic simulator 2021. For the design process, we started with a conventional dipole antenna, which has a large size, and we carried out a parametric study of different parameters in order to minimize the size and to optimize its behavior at 2.4 GHz. Moreover, the overall size of the proposed meander dipole antenna was reduced by up to 54% compared to the normal textile dipole reported in the literature [23]. A meander dipole antenna-based sensor was designed for compactness. Its dimensions are presented in Figure 2b: w = 45 mm, L = 4.8 mm, d = 7.6 mm and g = 2 mm. The layout of the proposed model is converted to a stitch pattern by using Digitizer Ex software (Figure 2c). This software is used in order to obtain a digital stitch format file that can be read by the Singer Futura XL550 embroidery machine. The final prototype of the proposed antenna-based sensor is depicted in Figure 2d. A commercial Shiel-dex 117/17 dtex 2-ply was used for the conductive layer. This commercial yarn is made of 99% pure silver-plated nylon yarn 140/17 dtex, which provides excellent conductivity. In addition, this conductive yarn allows the antenna-based sensor to be integrated into the cotton T-shirt without mobility restriction or compromising the comfort of the person under test, due to its high flexibility. Figure 2 summarizes all the fabrication steps of the proposed embroidered antenna-based sensor.
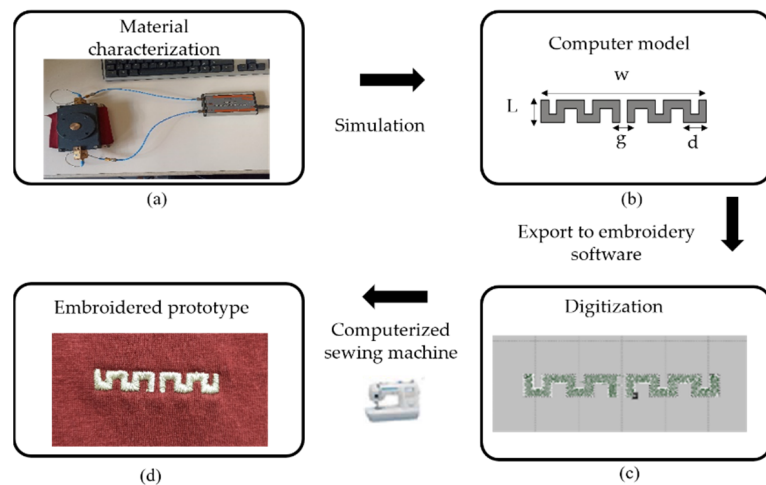

Figure 2. Main steps for the fabrication of the embroidered antenna-based sensor. (**a**) Measurement setup of the dielectric properties of material, (**b**) Antenna design model, (**c**) Digitization and (**d**) Embroidered prototype.

2.3. Respiratory Antenna-Sensor Based on RSSI Measurement

A novel detection system based on the measurement of the power transmitted by an embroidered meander dipole antenna-based sensor through a Bluetooth protocol was presented. The proposed breathing system is composed of four parts: an embroidered meander dipole antenna-based sensor integrated into a cotton T-shirt and placed on the middle of the human chest, a transmission Bluetooth module, a receiver Bluetooth module and a base station. The detection base station could be a laptop or tablet with a receiver Bluetooth module. The breathing antenna sensor is connected to a Bluetooth transmitter, which is placed on the middle of the chest position, maximizing the user's comfort with no restrictions of movement. The Bluetooth transmitter module is fabricated by means of a commercial ESP32-WROOM-32UE [18], which contains a U. FL connector that needs to be connected to an external antenna. In our case, the external antenna was a fully embroidered meander dipole antenna-based sensor integrated into a T-shirt, as described

in the previous section. The fabricated module was stitched by conductive yarn into the T-shirt by means of two metallic pads to insure a good connection with the embroidered antenna sensor. The ESP32 used in the fabricated transmitter module is a low-cost, low-power system on a chip (SoC) series with Bluetooth and Wi-Fi capabilities. It is often used for wearable electronics, mobile devices, and IoT applications. This transmission module acts as an advertising beacon that follows the Bluetooth Low Energy (BLE) protocol, with an operating frequency of 2.4 GHz. The transmitter Bluetooth module was fabricated and sewn into the T-shirt. A commercial ESP32-WROOM-32U was used for programming our fabricated transmitter module. The block diagram for the proposed breathing monitoring system is presented in Figure 3. The custom board has a compact size 2.36 × 3.17 cm^2, as shown in Figure 3, which provides a high comfort level for the user wearing the T-shirt. The proposed breathing wireless system was sewn into the T-shirt. To extract the received signal strength indicator through Bluetooth protocol, a code was developed using Arduino Software (IDE) to display the variation of the RSSI signal from the physical detuning of the antenna sensor embedded into the T-shirt during the respiration process. The received power of a BLE signal is disposable in the form of a received signal strength indicator (RSSI), which is given by Bluetooth. It is an integer value representing the received power in dBm. The breathing signal is extracted from the variation of the received signal strength indicator (RSSI) from the antenna sensor embedded into the T-shirt. The RSSI measurement was detected using a laptop connected to a receiver Bluetooth module (ESP32 ESP-WROOM-32). This receiver module is a low-cost and low-power system on a chip microcontroller with integrated dual-mode Bluetooth and Wi-Fi. It is well suited to a number of different IoT (Internet of Things) devices, such as smart security devices (smart locks and surveillance cameras), smart industrial devices and smart medical devices (wearable health monitors). The respiration signal is obtained from the RSSI signal transmitted by the antenna-based sensor, which is sensitive to the strain caused by the movement of the abdomen and chest wall. After programming the receiver Bluetooth module, the receiver module receives the Bluetooth signal from the transmitter antenna sensor, and it estimates the received power of a BLE signal through RSSI data and sends all the obtained values via a serial connection to the laptop. MATLAB was used to collect and visualize the breathing data information in real time.
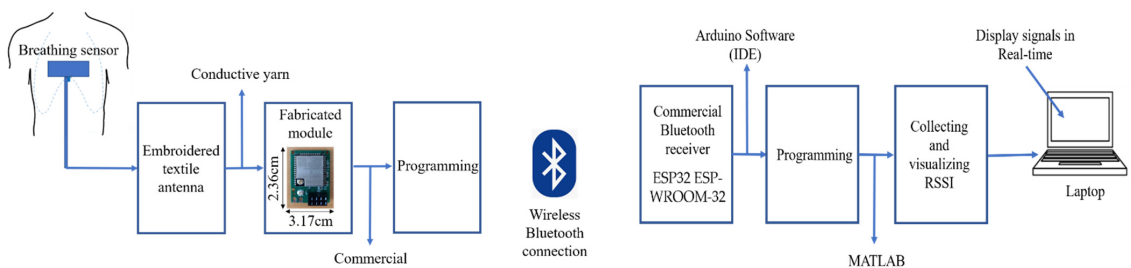

Figure 3. Block diagram of breathing monitoring.

3. Experimental Measurement and Performance Analysis

Breathing pattern monitoring is a mandatory and crucial task in healthcare fields. Indeed, the respiratory signal plays a key role in the estimation and prediction of the physiological status of patients. To acquire a breathing signal from a person, diverse systems and techniques are developed, but most of these techniques are generally attached to the human body using wires. This leads to difficulties and discomfort for the patients during the measurement, especially in burn victims or child patients. To improve user comfort, we proposed an e-textile T-shirt by means of a wireless system that was stitched to an embroidered antenna sensor for real-time breathing detection. During expiration (exhalation) and inspiration (inhalation), shape variation of the chest provides quantitative information about human breathing status. The transmitted signal from the embroidered

antenna-based sensor is obtained and recorded by the movements of the chest and the abdominal wall. Note that the transmitted signal from the antenna sensor is sensitive to stretch caused by the mechanical deformation during breathing. This behavior was described in detail in [24]. The breathing status is usually categorized into two types: normal (eupnea) and abnormal (apnea) breathing. Abnormal respiration is a very important indicator of chronic diseases such as chronic obstructive lung disease, pneumonia or physiological instability, so the demand for a continuous respiratory system in real time with a relatively low cost is very important in practice.

The signal acquisition of the proposed system was done by a female adult in a real environment. Several precautions are considered during measurements, avoiding any movements or action by other humans. For normal breathing, the participant was asked to follow several conditions:

1. Respiration with small movement (walking);
2. Respiration with speaking activities (reading a book);
3. Stable pause without any other activities.

To acquire abnormal breathing, the signal was produced by pausing respiration for a few seconds to imitate apnea, because real abnormal respiration is difficult to obtain.

Figure 4 summarizes the proposed approach to detect and classify human breathing status. In the experiment, the transmitter module was stitched into a T-shirt and was worn by the participant, as shown in Figure 5. The base station was prepared, and the receiver Bluetooth module was connected to a laptop. The base station records continuously the transmitted received signal strength indicator emitted by the embroidered antenna sensor. The participant was breathing according to the above conditions. The RSSI values were displayed in IDE software, and MATLAB read the data and plotted it in real time through the serial port. The measured raw RSSI data and related smoothed RSSI curves of eupnea breathing signals for different conditions are presented in Figure 6. The smoothed RSSI signal can be obtained by the Loess fitting method using data analysis and graphic software. The signal of normal breathing (eupnea) was generated, a signal that is similar to sinusoidal breathing, and the breathing period was clear and could be distinguished. Therefore, expiration (exhalation) and inspiration (inhalation) phases in each respiration period were clearly extracted for different examples of the normal respiration status. The experimental results demonstrated that breathing signals can be acquired wirelessly by the RSSI via Bluetooth. The RSSI range change was from -80 dBm to -72 dBm, -88 dBm to -79 dBm and -85 dBm to -80 dBm during expiration and inspiration for normal breathing, speaking and moving, respectively. The RSSI measurements were recorded for the participant at 1 m from the base station. Note that during movement, the participant maintains the physical distance between the receiver and transmitter. We can observe that the transmitted received signal strength oscillates as the participant breathes. The respiration signal is obtained with 11 breathing cycles in 60 s. Note that normal breathing rates for an adult person range from 11 to 16 breaths per minute according to the respiratory rate chart [25]. The expiration and the inspiration period are estimated to be 5 s, which is in a good agreement with the regular breathing cycle from 3 s to 6 s. An example of abnormal (apnea) breathing status is presented in Figure 7. No expiration and inspiration over a very short period imitates apnea (absence of breathing).
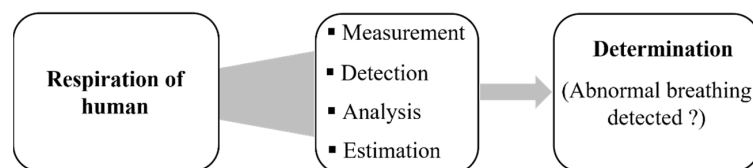

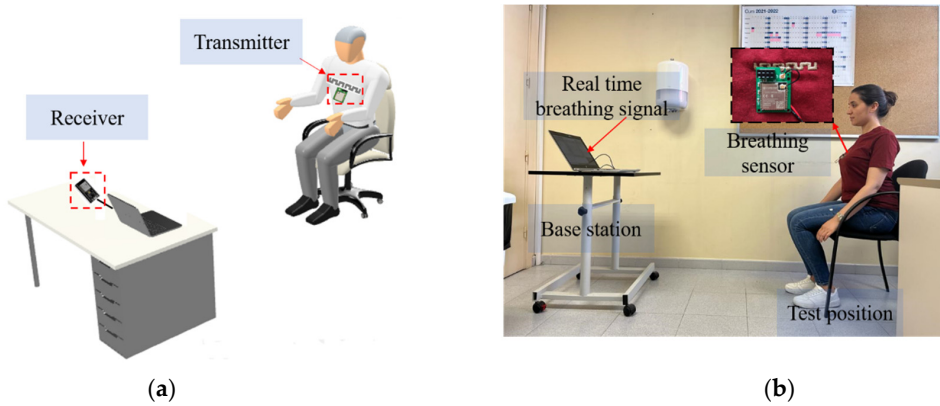**Figure 4.** Procedure to detect human breathing status.

Figure 5. Person under test wearing the e-textile for breathing monitoring: (**a**) experimental setup configuration and (**b**) photograph of experimental setup.
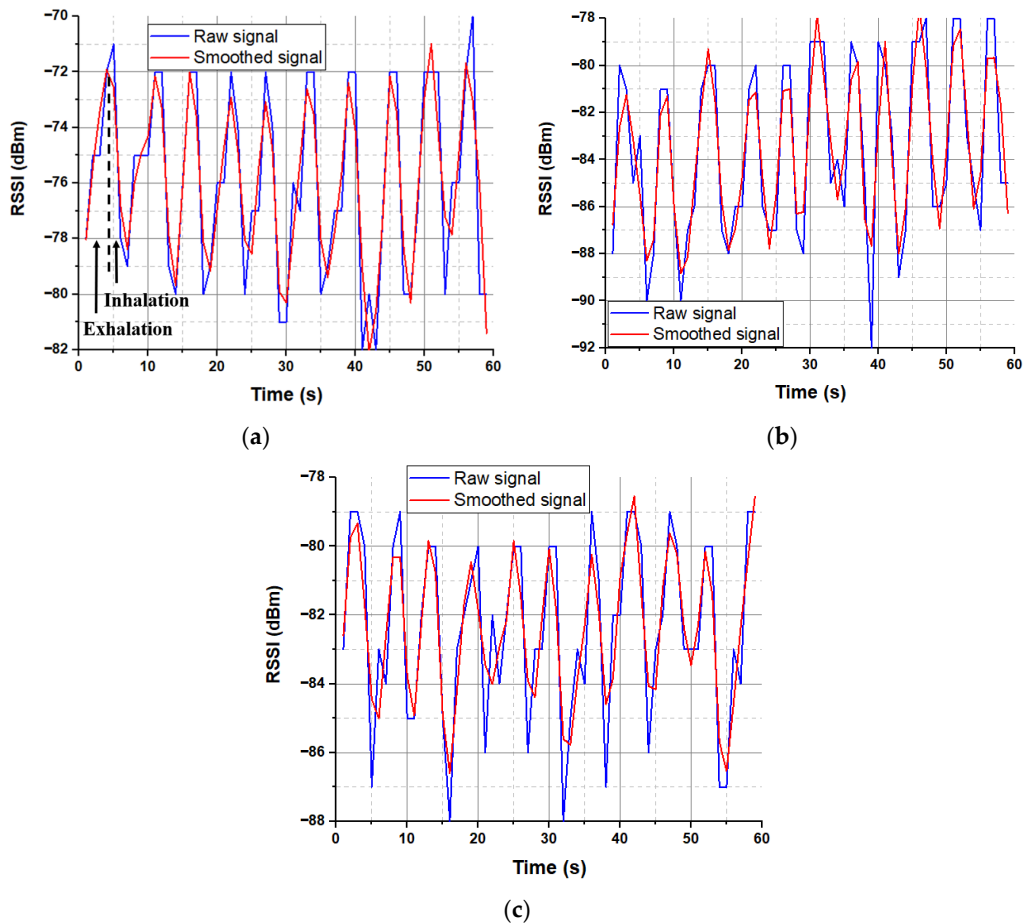

Figure 6. Examples of eupnea breathing signals: (**a**) normal breathing in stable position, (**b**) normal breathing while speaking and (**c**) normal breathing while moving.
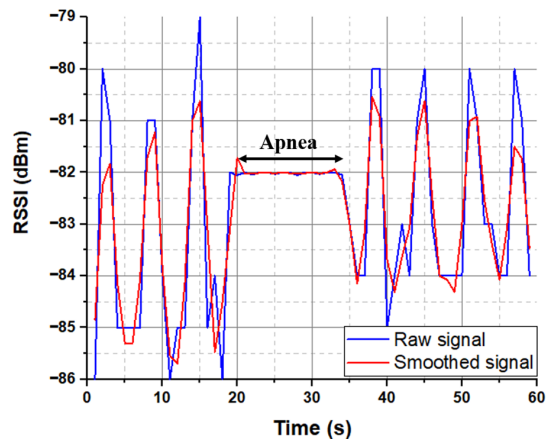
Figure 7. Example of abnormal breathing status.

4. Discussion

　　A novel, fully embroidered meander dipole antenna-based sensor integrated into a cotton T-shirt for real-time respiration monitoring using the technique based on chest wall movement analysis was developed in our group. This study demonstrated the capability of the embroidered antenna sensor to detect different breathing patterns [24]. However, this breathing monitoring technique is inconvenient because the breathing mechanism uses a connecting cable for VNA that restricts the use of the proposed system. To improve the user comfort, an e-textile T-shirt with wireless communication of an embroidered antenna-sensor for real-time breathing detection was developed in this work. The proposed system is composed of a contactless antenna-based sensor integrated into a cotton T-shirtthat is connected to a transmission integrated Bluetooth module and a laptop with a receiver Bluetooth module. The area of the proposed system is 4.5×0.48 cm^2, and the transmitter module is 2.36×3.17 cm^2. The breathing signal is recorded through the detection of the transmitted received signal strength indicator (RSSI) by means of a base station (laptop). Table 1 presents a comprehensive comparison between two proposed systems for breathing monitoring. The proposed work demonstrated the ability of the embroidered antenna-based sensor to detect the breathing signal in real time and communicate the data via a Bluetooth protocol at 2.4 GHz to a base station. Our breathing detection systems embedded into a commercially textile T-shirt are presented in Figure 8. The respiratory antenna sensor is placed on the middle of the chest position of the human body to monitor breathing in real time by means of the stretching deformation of the textile under the movement of the chest during breathing. The working principle is based on the resonant frequency shift using the vector network analyzer (VNA) (Figure 8a). This technique makes the user uncomfortable due to the connection cable of the VNA. Therefore, we proposed an e-textile T-shirt based on the received signal strength indicator (RSSI) detected wirelessly using a base station (Figure 8b) that presents a high level of comfort for the user. The reliability of the proposed system will be addressed in future work. Several studies on the durability and washability of textile antennas have been presented in the literature [26,27]. Different coating materials (latex, silicone and so on) are used to protect the antenna from detaching in the laundry. According to those studies, the effect of coating materials on antenna performance is far less significant than manufacturing tolerances. Table 2 provides a comparison of the proposed work with other studies that monitored breathing with different methods, and we can see that a few textile sensors were found in the literature. The main novelty of our research is the development of a new wireless communication platform for breathing monitoring using a fully embroidered antenna sensor embedded into a commercial T-shirt and connected

to a transmission Bluetooth module, which offers a compact size compared with reported works, provides a high level of comfort for the user and is comfortable for long-term use.

Table 1. Comparison between two systems for breathing monitoring.

| Breathing System	Sensor Type	Measuring Parameter	Technique	Advantages	Disadvantages
System 1 (our previous work)	Meander dipole antenna sensor connected to a SMA	Frequency shift of the S_{11}	Vector Network Analyzer (VNA)	• Wide frequency range operation. • No signal interference.	• Not comfortable for long term use. • Movement restriction • Requires a connection cable for VNA. • Not portable.
System 2 (our current work)	Meander dipole antenna sensor connected to a Bluetooth transmitter	Received Signal Strength Indicator (RSSI)	Wireless communication with a portable base station	• Portable. • Comfortable. • User friendly. • Low energy consumption.	• The signal strength depends on the distance between the transmitter and the detection base station. • Interference with another RF signal at 2.4 GHz.
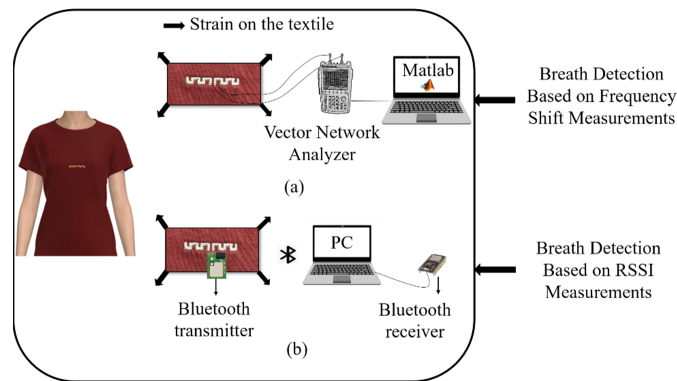
Figure 8. Breathing detection systems embedded into textile T-shirt: (**a**) system 1 (our previous work) based on the resonant frequency shift using VNA, (**b**) proposed system based on the RSSI detected wirelessly using a base station.

Table 2. Comparison with other breathing systems.

Ref	[28]	[29]	[30]	[31]	[32]	[33]	[34]	This Work
Sensor type	Microphone	Thermistor	Spiral antenna	Camera	Piezoelectric	Resistive	Multimodal Patch	**Dipole antenna**
[1] C.T	Mobile phone	[2] PAT	[3] BT	Wired	WatchPAT	wired	WIFI	[3]**BT**
Method	Recording sound	Nose airflow	RSSI	Image analysis	Raw signal	[4] RIP	Signal amplitude	**RSSI**
Real-time	Yes	Yes	Yes	Yes	Yes	No	Yes	**Yes**
Textile	No	No	Yes	No	No	No	No	**Yes**
Size (mm^2)	450×250	_	200×100	50×76	70×60	310×40	65.53×26.67	$\mathbf{45 \times 4.87}$

[1] C.T: Communication technology. [2] PAT: Portable analogue transmission. [3] BT: Bluetooth. [4] RIP: Respiratory Inductive Plethysmograph.

5. Conclusions

The feasibility of a contactless device for human breath detection based on a fully embroidered antenna-based sensor embedded into a commercial T-shirt has been presented and tested. An antenna sensor has been fully integrated into an e-textile T-shirt with wireless capability. We have demonstrated the ability of the wireless communicating portable system to monitor breathing in real time and communicate the data via a Bluetooth protocol at 2.4 GHz to a base station. The proposed wireless system demonstrated experimentally the breathing signal by means of the received signal strength indicator (RSSI) via standard Bluetooth protocol. The capability and accuracy of the proposed wearable device to detect in real time a breathing signal of a female volunteer has been demonstrated. The obtained results could make our proposed e-textile T-shirt a potential device for healthcare applications, such as in chronic obstructive pulmonary illness or sleep apnea and various respiration disorders in neonates, children and adults.

Author Contributions: M.E.G.: Conceptualization, methodology, investigation, software, data curation, formal analysis, writing—original draft. R.F.-G.: Writing—review and editing, supervision, visualization, project administration. I.G.: Writing—review and editing, supervision, validation, visualization, project administration. All authors have read and agreed to the published version of the manuscript.

Institutional Review Board Statement: Not applicable.

Informed Consent Statement: Not applicable.

Data Availability Statement: Not applicable.

Conflicts of Interest: The authors declare no conflict of interest.

References

1. Aroganam, G.; Manivannan, N.; Harrison, D. Review on wearable technology sensors used in consumer sport applications. *Sensors* **2019**, *19*, 1983. [CrossRef] [PubMed]
2. Rein, M.; Favrod, V.D.; Hou, C.; Khudiyev, T.; Stolyarov, A.; Cox, J.; Chung, C.-C.; Chhav, C.; Ellis, M.; Joannopoulos, J. Diode fibres for fabric-based optical communications. *Nature* **2018**, *560*, 214–218. [CrossRef]
3. Dagdeviren, C.; Yang, B.D.; Su, Y.; Tran, P.L.; Joe, P.; Anderson, E.; Xia, J.; Doraiswamy, V.; Dehdashti, B.; Feng, X.; et al. Conformal piezoelectric energy harvesting and storage from motions of the heart, lung, and diaphragm. *Proc. Natl. Acad. Sci. USA* **2014**, *111*, 1927–1932. [CrossRef] [PubMed]
4. Aliverti, A. Wearable technology: Role in respiratory health and disease. *Breathe* **2017**, *13*, e27–e36. [CrossRef] [PubMed]
5. Stoppa, M.; Chiolerio, A. Wearable electronics and smart textiles: A critical review. *Sensors* **2014**, *14*, 11957–11992. [CrossRef]
6. Cesareo, A.; Nido, S.A.; Biffi, E.; Gandossini, S.; D'Angelo, M.G.; Aliverti, A. A wearable device for breathing frequency monitoring: A pilot study on patients with muscular dystrophy. *Sensors* **2020**, *20*, 5346. [CrossRef]
7. Abbate, S.; Avvenuti, M.; Light, J. Usability study of a wireless monitoring system among Alzheimer's disease elderly population. *Int. J. Telemed. Appl.* **2014**, *2014*, 617495. [CrossRef]
8. Bates, J.H.T. Systems physiology of the airways in health and obstructive pulmonary disease. *Wiley Interdiscip. Rev. Syst. Biol. Med.* **2016**, *8*, 423–437. [CrossRef]
9. Gholamrezaei, A.; van Diest, I.; Aziz, Q.; Vlaeyen, J.W.S.; van Oudenhove, L. Psychophysiological responses to various slow, deep breathing techniques. *Psychophysiology* **2021**, *58*, e13712. [CrossRef]
10. Liu, H.; Allen, J.; Zheng, D.; Chen, F. Recent development of respiratory rate measurement technologies. *Physiol. Meas.* **2019**, *40*, 07TR01. [CrossRef]
11. Massaroni, C.; Nicolò, A.; Presti, D.L.; Sacchetti, M.; Silvestri, S.; Schena, E. Contact-based methods for measuring respiratory rate. *Sensors* **2019**, *19*, 908. [CrossRef] [PubMed]
12. Charlton, P.H.; Birrenkott, D.A.; Bonnici, T.; Pimentel, M.A.F.; Johnson, A.E.W.; Alastruey, J.; Tarassenko, L.; Watkinson, P.J.; Beale, R.; Clifton, D.A. Breathing rate estimation from the electrocardiogram and photoplethysmogram: A review. *IEEE Rev. Biomed. Eng.* **2017**, *11*, 2–20. [CrossRef] [PubMed]
13. Bricout, A.; Fontecave-Jallon, J.; Colas, D.; Gerard, G.; Pépin, J.-L.; Guméry, P.-Y. Adaptive accelerometry derived respiration: Comparison with respiratory inductance plethysmography during sleep. In Proceedings of the 2019 41st Annual International Conference of the IEEE Engineering in Medicine and Biology Society (EMBC), Berlin, Germany, 23–27 July 2019; IEEE: New York, NY, USA; pp. 6714–6717.

14. Satija, U.; Ramkumar, B.; Manikandan, M.S. A review of signal processing techniques for electrocardiogram signal quality assessment. *IEEE Rev. Biomed. Eng.* **2018**, *11*, 36–52. [CrossRef]

15. Wang, P.; Ma, Y.; Liang, F.; Zhang, Y.; Yu, X.; Li, Z.; An, Q.; Lv, H.; Wang, J. Non-contact vital signs monitoring of dog and cat using a UWB radar. *Animals* **2020**, *10*, 205. [CrossRef] [PubMed]

16. Mateu-Mateus, M.; Guede-Fernández, F.; Rodriguez-Ibáñez, N.; García-González, M.A.; Ramos-Castro, J.; Fernández-Chimeno, M. A non-contact camera-based method for respiratory rhythm extraction. *Biomed. Signal Process. Control* **2021**, *66*, 102443. [CrossRef]

17. Jakkaew, P.; Onoye, T. Non-contact respiration monitoring and body movements detection for sleep using thermal imaging. *Sensors* **2020**, *20*, 6307. [CrossRef]

18. Abbas, A.K.; Heimann, K.; Jergus, K.; Orlikowsky, T.; Leonhardt, S. Neonatal non-contact respiratory monitoring based on real-time infrared thermography. *Biomed. Eng. Online* **2011**, *10*, 93. [CrossRef]

19. Presti, D.L.; Massaroni, C.; Formica, D.; Saccomandi, P.; Giurazza, F.; Caponero, M.A.; Schena, E. Smart textile based on 12 fiber Bragg gratings array for vital signs monitoring. *IEEE Sens. J.* **2017**, *17*, 6037–6043. [CrossRef]

20. Milici, S.; Lázaro, A.; Villarino, R.; Girbau, D.; Magnarosa, M. Wireless wearable magnetometer-based sensor for sleep quality monitoring. *IEEE Sens. J.* **2018**, *18*, 2145–2152. [CrossRef]

21. Cesareo, A.; Previtali, Y.; Biffi, E.; Aliverti, A. Assessment of breathing parameters using an inertial measurement unit (IMU)-based system. *Sensors* **2018**, *19*, 88. [CrossRef]

22. Roudjane, M.; Bellemare-Rousseau, S.; Khalil, M.; Gorgutsa, S.; Miled, A.; Messaddeq, Y. A portable wireless communication platform based on a multi-material fiber sensor for real-time breath detection. *Sensors* **2018**, *18*, 973. [CrossRef] [PubMed]

23. Elias, N.A.; Samsuri, N.A.; Rahim, M.K.A.; Othman, N. The effects of human body and bending on dipole textile antenna performance and SAR. In Proceedings of the 2012 Asia-Pacific Conference on Microwave, Kaohsiung, Taiwan, 4–7 December 2012; IEEE: New York, NY, USA; pp. 34–36.

24. El Gharbi, M.; Fernández-García, R.; Gil, I. Embroidered Wearable Antenna-based Sensor for Real-Time Breath Monitoring. *Measurement* **2022**, *195*, 111080. [CrossRef]

25. Fleming, S.; Thompson, M.; Stevens, R.; Heneghan, C.; Plüddemann, A.; Maconochie, I.; Tarassenko, L.; Mant, D. Normal ranges of heart rate and respiratory rate in children from birth to 18 years of age: A systematic review of observational studies. *Lancet* **2011**, *377*, 1011–1018. [CrossRef]

26. Heikkinen, J.J.; Laine-Ma, T.T.; Kivikoski, M.A. Flexible fabric-base patch antenna with protective coating. In Proceedings of the 2007 IEEE Antennas and Propagation Society International Symposium, Honolulu, HI, USA, 9–15 June 2007; pp. 4168–4171.

27. Kellomäki, T.; Virkki, J.; Merilampi, S.; Ukkonen, L. Towards washable wearable antennas: A comparison of coating materials for screen-printed textile-based UHF RFID tags. *Int. J. Antennas Propag.* **2012**, *2012*, 476570. [CrossRef]

28. Watanabe, K.; Kurihara, Y.; Nakamura, T.; Tanaka, H. Design of a low-frequency microphone for mobile phones and its application to ubiquitous medical and healthcare monitoring. *IEEE Sens. J.* **2010**, *10*, 934–941. [CrossRef]

29. Milici, S.; Lorenzo, J.; Lazaro, A.; Villarino, R.; Girbau, D. Wireless breathing sensor based on wearable modulated frequency selective surface. *IEEE Sens. J.* **2016**, *17*, 1285–1292. [CrossRef]

30. Roudjane, M.; Bellemare-Rousseau, S.; Drouin, E.; Belanger-Huot, B.; Dugas, M.-A.; Miled, A.; Messaddeq, Y. Smart T-shirt based on wireless communication spiral fiber sensor array for real-time breath monitoring: Validation of the technology. *IEEE Sens. J.* **2020**, *20*, 10841–10850. [CrossRef]

31. Penne, J.; Schaller, C.; Hornegger, J.; Kuwert, T. Robust real-time 3D respiratory motion detection using time-of-flight cameras. *Int. J. Comput. Assist. Radiol. Surg.* **2008**, *3*, 427–431. [CrossRef]

32. Gunaratne, P.; Tamura, H.; Yoshida, C.; Sakurai, K.; Tanno, K.; Takahashi, N.; Nagata, J. A Study on breathing and heartbeat monitoring system during sleeping using multi-piezoelectric elements. In Proceedings of the 2019 Moratuwa Engineering Research Conference, Moratuwa, Sri Lanka, 3–5 July 2019; IEEE: New York, NY, USA; pp. 382–387.

33. Ramos-Garcia, R.I.; da Silva, F.; Kondi, Y.; Sazonov, E.; Dunne, L.E. Analysis of a coverstitched stretch sensor for monitoring of breathing. In Proceedings of the 2016 10th International Conference on Sensing Technology, Nanjing, China, 11–13 November 2016; IEEE: New York, NY, USA; pp. 1–6.

34. Elfaramawy, T.; Fall, C.L.; Arab, S.; Morissette, M.; Lellouche, F.; Gosselin, B. A wireless respiratory monitoring system using a wearable patch sensor network. *IEEE Sens. J.* **2018**, *19*, 650–657. [CrossRef]